

DISSERTATION

Titel der Dissertation

Development and Evaluation of Ion Exchange-type
Chiral Stationary Phases for Liquid Chromatography and
Subcritical Fluid Chromatography

Verfasser

Mag. Franz Reinhard Pell

angestrebter akademischer Grad

Doktor der Naturwissenschaften (Dr. rer. nat.)

Wien, Juni 2012

Studienkennzahl lt Studienblatt:

A 091 419

Studienrichtung lt Studienblatt:

Chemie

Betreuer:

Univ.-Prof. Dr. Wolfgang Lindner

Danksagung

Zuallererst möchte ich mich bei Prof. Wolfgang Lindner bedanken, der die Durchführung meiner Dissertation in einer tollen Arbeitsgruppe und über eine sehr interessante Themenstellung ermöglichte. Im Besonderen danke ich ihm für die motivierenden Gespräche, die oftmals in neuen Ideen endeten, für die Möglichkeit einer unabhängigen und eigenständigen Arbeitsweise und nicht zuletzt für den sehr wertvollen Auslandsaufenthalt bei AstraZeneca R&D in Mölndal, Schweden.

Ich danke Prof. Michael Lämmerhofer, der bei allfälligen Problemstellungen immer ein netter und äußerst kompetenter Ansprechpartner war. Peter Frühauf danke ich für das stets problemlose und schnelle Säulenpacken und für seine hilfsbereite Art und Weise beim Lösen von kleineren und größeren Problemen im Laboralltag. Ebenso danke ich Norbert Maier für das Korrekturlesen meiner Dissertation.

Weiters möchte ich meinen Arbeitskollegen danken, die für ein unterhaltsames Beisammensein, für lustige und lange Grillabende und allgemein für ein sehr angenehmes Arbeitsklima sorgten. Dieser Dank geht im Speziellen an Heli, Steffi, Georg, Andrea, Sissy, Michal, und zu guter Letzt an Roli, meinem Langzeit-Bürokollegen, der mit seinen lustigen Wortmeldungen so manchen Tag zu erheitern wusste. So werde ich die Gespräche über alle Bereiche des Lebens, jedoch meist übers Paragleiten, missen.

Ein ganz besonderer Dank, der sehr schwer in Worte zu fassen ist, geht an Edith. Ich danke dir für dein großes Entgegenkommen in manchen Lebenssituationen, für dein großes Einfühlungsvermögen und für die meist kurze, aber wunderschöne gemeinsame Zeit.

Abschließend möchte ich meinem Bruder, meiner Mutter und meinem Vater, der leider viel zu früh verstorben ist, ein herzliches Dankeschön aussprechen. Ihr wart mir stets ein starker familiärer Rückhalt und habt mich zu dem Menschen gemacht, der ich heute bin.

Table of Contents

1	Introduction	1
1.1	Enantioselective Liquid Chromatography	1
1.2	(Enantioselective) Supercritical Fluid Chromatography	2
1.3	Chiral Recognition in Chromatography and Related Thermodynamic Principles	3
1.4	Chiral Stationary Phases for HPLC and SFC	7
1.4.1	Overview and General Remarks	7
1.4.2	Protein-based CSPs	8
1.4.3	Polysaccharide-type CSPs	8
1.4.4	Macrocyclic Antibiotic CSPs	9
1.4.5	Crown Ether CSPs	10
1.4.6	Ligand Exchange CSPs	11
1.4.7	Ion Exchange-type CSPs	12
1.5	Retention Mechanisms in Chiral Ion Exchange Chromatography	15
2	Objectives	17
3	Results and Discussion	18
3.1	General Remarks	18
3.2	Anion Exchange-type CSPs	18
3.2.1	Application of Anion Exchanger CSPs for Indirect Chromatographic Absolute Configuration Assignment	18
3.2.2	Evaluation of Anion Exchange-type CSPs in SFC and HPLC for Separation of Chiral Carboxylic- and Sulfonic Acids	20
3.3	Zwitterionic CSPs: Preparation and Evaluation by HPLC	23
3.4	Unpublished Results: Zwitterionic CSPs in SFC-Mode for Separation of Chiral Acids	30
4	Concluding Remarks	33
5	References	35
6	List of Publications and Manuscripts	41

Appendix I – VI: Publications and Manuscripts

Abstract

Zusammenfassung

Curriculum Vitae

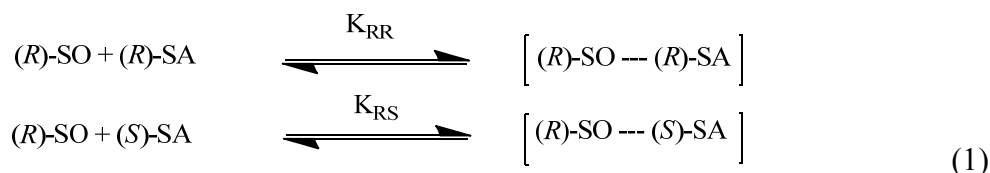
1 Introduction

1.1 Enantioselective Liquid Chromatography

Enantioselective high performance liquid chromatography (HPLC), often termed chiral HPLC, has evolved as a powerful tool for analysis and separation of enantiomers in both industry and academia [1-5]. In contrast to other enantioselective chromatographic techniques, such as gas chromatography (GC), supercritical fluid chromatography (SFC), thin-layer chromatography (TLC), or centrifugal partition chromatography (CPC), chiral HPLC exhibits the broadest applicability ranging from trace analysis of enantiomeric impurities to multi-kilogram-scale preparative enantioseparations [6, 7]. In fact, the need for optically pure compounds in the pharmaceutical and agrochemical industry has made chiral HPLC playing an important role in the drug development process. It enables facile and straightforward access to single enantiomers in the gram- to kilogram-scale, thereby avoiding potentially laborious and expensive stereoselective synthesis approaches. Indeed, owing to the implementation of cost-efficient preparative separation techniques, such as simulated moving bed chromatography (SMB) [8], chiral liquid chromatography is nowadays even applied in production-scale enantiomer separations [1, 9].

Since the emergence of HPLC in the early 1970s, two approaches have been applied for chromatographic resolution of enantiomers, namely the indirect and direct approach. The first one involves the formation of a covalent bond between an enantiomerically pure chiral derivatizing agent (CDA) and the racemate thus yielding two diastereomeric molecules. After chromatographic separation on an achiral stationary phase, the diastereomers can be cleaved to recover the CDA and the corresponding pure enantiomers. However, this method suffers from drawbacks like the need for CDAs of utmost enantiomeric purity (otherwise two pairs of enantiomers may be formed), the requirement of functional groups in the racemate being suitable for derivatization, or undesired kinetic resolution phenomena. Hence, the indirect method is of rather historic importance and not in widespread use anymore.

In the direct approach, a chiral selector (SO) is immobilized or adsorbed onto a chromatographic support material (mostly spherical silica gel) yielding a chiral stationary phase (CSP). Upon approaching of the analyte (selectand, SA) to the SO, transient and reversible SO-SA associates are formed (Eq. 1). The energetic difference in binding energy between the two diastereomeric associates, which is the manifestation of unequal equilibrium constants K_{RR} and K_{RS} , is responsible for and thus the fundamental basis of enantioseparation.



Nowadays, a plethora of CSPs is available on the market enabling successful HPLC resolution of enantiomers of broad structural diversity, thereby employing normal phase-, reversed phase- and polar organic mode as elution conditions. Finally, enantioselective chromatography has also advanced to the field of ultra (high) performance liquid chromatography (UPLC[®] or UHPLC) by immobilizing SOs on sub 3 μm particle size or superficially porous silica gel [10, 11].

1.2 (Enantioselective) Supercritical Fluid Chromatography

SFC is a chromatographic technique that mostly applies the same stationary phases like in HPLC, but employs a supercritical (sc) fluid as mobile phase. Usually, CO_2 is used as sc fluid due to its easily obtainable critical point (31.1°C and 73.8 bar), relatively low toxicity and inexpensiveness. However, the rather non-polar properties of neat sc CO_2 necessitates the addition of polar organic modifiers to enhance analyte solubility and elution strength of the mobile phase. The unique physicochemical properties of a supercritical mobile phase enable distinct advantages as compared to HPLC: (i) the reduced viscosity allows the use of higher mobile phase flow rates and thus shortens analysis time, (ii) the greater diffusion coefficient in SFC enables faster mass transfer often resulting in higher theoretical plate numbers and, also, shifts the Van-Deemter minimum to higher mobile phase flow rates.

It is noteworthy that most of the SFC applications are nowadays carried out using subcritical mobile phases, because either the applied temperature is below 31°C or the presence of organic modifier shifts the operation condition to the subcritical regime. However, no phase separation or any major chromatographic discontinuities are observed between the two states [12-14]. In literature, the abbreviation SFC is used synonymously for both subcritical and supercritical fluid chromatography, although some authors prefer the abbreviation SubFC for subcritical fluid chromatography.

SFC instruments for packed columns are nowadays similarly built to HPLC instruments using binary pumps (one for the organic modifier and a chilled pump with a high range of compressibility compensation for CO_2) and mainly the same columns like in HPLC. Two

differences in instrumentation are the use of an additional back pressure regulator (to keep the mobile phase in sub/supercritical state) and pressure resistant UV detector cells in SFC.

Since the first use of SFC as a form of supercritical GC by Klesper et al. in 1962, it was mainly applied in capillary or open-tubular formats with neat sc CO₂ in the following decades, thus limiting its application range to non-polar or moderately polar solutes [15]. Owing to a study which overestimated the polarity and thus elution strength of sc CO₂ [16], it was tried to improve elution strength and analyte solubility by density programming of neat sc CO₂ rather than by mixing polar organic co-solvents to the mobile phase. It took until the end of the 1990s, when packed column SFC displaced open-tubular SFC from the market, to reattract attention for a broader chromatographic community. Since the beginning of the 2000s, with the introduction of more robust and reliable instruments, SFC has emerged as a powerful chiral and achiral separation technique [13, 17-19]. It gained special popularity in the pharmaceutical industry for chiral screening, owing to its inherent speed, high efficiency and fast column equilibration times. Currently, SFC is in process of replacing HPLC for carrying out (chiral and achiral) normal phase separations, because of benefits in terms of faster column equilibration, tolerance to water in the mobile phase, and less environmental impact [15, 20]. Several companies have recently started to commercialize dedicated polar stationary phases for SFC to enable unique selectivity profiles [15]. Most recently, and similar to chiral HPLC, the first applications of sub 3 μm and/or superficially porous silica gels for CSPs in (chiral) SFC were reported [21, 22].

1.3 Chiral Recognition in Chromatography and Related Thermodynamic Principles

Several models were proposed to rationalize the basic requirements for successful chiral recognition at a molecular level. In 1933, Easson and Stedman proposed a “three-point attachment model” to explain stereoselective binding of chiral compounds to a protein receptor [23]. This model stipulated that a minimum of three configuration-dependent attractive contact points between a chiral receptor and a chiral substrate is required for chiral discrimination. However, the model neglected a fourth precondition, namely that the binding site had to be on a planar surface and that the receptor could not be approached from the interior. Nineteen years later in 1952, Dalglish adapted this model for chromatography (TLC) [24].

An extended and slightly modified definition of the three-point attachment model is known as the “three-point (interaction) rule”. It states that a minimum of three simultaneous

interactions between the selector and at least one of the selectands is required for chiral recognition, in which at least one of these interactions must be stereochemically dependent [25, 26]. The interactions can be of attractive or repulsive character. Even two interactions may be repulsive, as long as the third one is strong enough to facilitate at least one diastereomeric associate [25]. The “three-point rule” is nowadays commonly accepted, although intermittently challenged [27-29].

Furthermore, it is important to distinguish between single-point and multi-point interactions. Electrostatic forces, hydrogen bonding, or end-to-end dipole interactions are of single-point quality. In contrast, other interactions involving 2D-polarized functionalities, such as dipole-dipole stacking or aromatic interactions, are considered as two-point interactions. Concerning the three-point model, the combination of a single-point and a two-point interaction may already suffice to facilitate chiral recognition.

The three-point model is graphically illustrated in Fig. 1. In the course of the chromatographic process, the enantiomers (SAs) approach the SO which is bound or adsorbed onto the chromatographic support material. However, due to steric constraints, only one enantiomer is capable of forming three simultaneous interactions with the SO (ideal fit), thus being stronger retained than the other SA enantiomer.

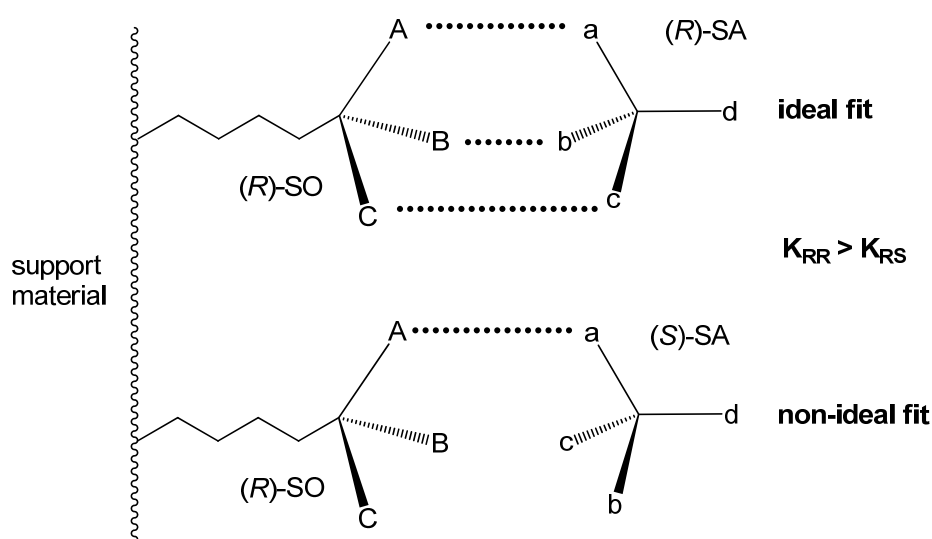


Figure 1. Graphical illustration of the three-point interaction model. With $\Delta G_{RR} = -RT \ln K_{RR}$ and $\Delta G_{RS} = -RT \ln K_{RS}$, it follows that $\Delta G_{RR} \neq \Delta G_{RS}$.

Taking Eq. 1 and Fig. 1 into account, it can be concluded that two conditions are required for enantiomers to be separated. Diastereomeric associates must be formed between the SO and at

least one of the enantiomers and, additionally, they must exhibit different Gibbs energies (ΔG) of formation. ΔG is related to the equilibrium constants as depicted in Eq. (2)

$$\Delta G = - RT \ln K \quad (2)$$

R denotes the universal gas constant ($8.3144 \text{ J mol}^{-1} \text{ K}^{-1}$) and T the absolute temperature in K. The retention factors k_R and k_S of the corresponding enantiomers are given by the product of their equilibrium constants for complex formation and the volume phase ratio Φ .

$$k_R = K_{RR} \cdot \Phi \quad k_S = K_{RS} \cdot \Phi \quad (3)$$

By convention, enantioselectivity α is defined as in Eq. (4), with $k_R > k_S$.

$$\alpha_{R,S} = k_R / k_S \quad (4)$$

Since retention factor k and enantioselectivity α are thermodynamically controlled, and different Gibbs energies of diastereomeric complex formation are required for enantiomer separation, Eq. (2) and Eq. (4) can be combined as follows (with $K_{RR} > K_{RS}$).

$$\Delta\Delta G_{R,S} = \Delta G_{RR} - \Delta G_{RS} = - RT \ln (K_{RR} / K_{RS}) = - RT \ln \alpha_{R,S} \quad (5)$$

For deconvolution of enthalpic and entropic increments to retention and enantioselectivity, respectively, one can rewrite Eq. (5) according to the Gibbs-Helmholtz equation ($\Delta G = \Delta H - T \Delta S$), resulting in the modified van't Hoff equations (6) and (7).

$$\ln \alpha_{R,S} = - \Delta\Delta H_{R,S} / RT + \Delta\Delta S_{R,S} / R \quad (6)$$

$$\ln k = - \Delta H / RT + \Delta S / R + \ln \Phi \quad (7)$$

As is evident from Eqs. 6 and 7, the enthalpic and entropic contributions can conveniently be extracted by measuring α - and k values over a certain temperature range. Then, graphical analysis is applied via plotting of $\ln k$ or $\ln \alpha_{R,S}$ against the reciprocal absolute temperature $1/T$ [K^{-1}]. Van't Hoff plots for $\ln \alpha$ normally give a linear relationship, from which $\Delta\Delta H$ and $\Delta\Delta S$ can be calculated from the slope ($-\Delta\Delta H / R$) and intercept ($\Delta\Delta S / R$), respectively.

Equations (5) to (7) pinpoint two salient points for discussion of thermodynamic influence on chromatographic enantioseparation. Owing to the nature of chromatography, even low $\Delta\Delta G_{R,S}$ values are sufficient for proper enantioseparation. For instance, 240 J mol^{-1} correspond to an $\alpha_{R,S} = 1.1$, which often enables baseline separation on many CSPs (with $5 \mu\text{m}$ particle size).

However, when carrying out mechanistic interpretations of thermodynamic contributions on a certain CSP-SA system, one has to be aware of enantioselective (es) and non-enantioselective (ns) interactions. Since CSPs are prepared via immobilization (adsorption) onto chromatographic support materials, there is the inherent possibility for the SA to undergo not only es interactions with the SO, but also ns interactions with, for instance, residual silanol groups of the silica gel. Strictly speaking, retention factors of the corresponding enantiomers should be displayed as $k_{\text{app,R}}$ and $k_{\text{app,S}}$.

$$k_{\text{app,R}} = k_{\text{ns}} + k_{\text{es,R}} \quad (8)$$

$$k_{\text{app,S}} = k_{\text{ns}} + k_{\text{es,S}} \quad (9)$$

Hence, the chromatographically observed (apparent) α_{app} is defined as

$$\alpha_{\text{app}} = k_{\text{app,R}} / k_{\text{app,S}} = (k_{\text{ns}} + k_{\text{es,R}}) / (k_{\text{ns}} + k_{\text{es,S}}) \quad (10)$$

$$\alpha_{\text{intr}} = k_{\text{es,R}} / k_{\text{es,S}} \quad (11)$$

Equations (6) and (7) illustrate that in case of present non-enantioselective interactions, the chromatographically observed enantioselectivity α_{app} is decreased compared to the intrinsic (“true”) enantioselectivity α_{intr} . Therefore, from a practical point of view, special care has to be taken for investigation of thermodynamic influences on chromatographic parameters. In such cases, the chromatographer has either to select CSPs with negligible k_{ns} values (e.g. cinchona alkaloid-based weak anion exchanger CSPs, as applied in this thesis) or to put effort on suppressing those non-selective interactions (e.g. by choosing a particular mobile phase system).

1.4 Chiral Stationary Phases for HPLC and SFC

1.4.1 Overview and General Remarks

In the following chapters only those CSPs are discussed which possess SOs with ionizable functionalities and thus are employed to address ionizable solutes. This is because the main objective of this thesis was to prepare and/or chromatographically evaluate ion exchange-type CSPs for separation of highly polar chiral acidic and zwitterionic compounds. Hence, the brief review presented herein aims at giving an overview of already established CSPs capable of resolving chiral acids and amphoteric compounds (viz. free amino acids and small peptides), including a discussion of their merits and limitations. Furthermore, it will be stated if the particular CSPs were also investigated in SFC.

A prevalent classification of CSPs and thus of their corresponding SOs divides them into three main categories:

- Polymeric selectors
 - Biopolymers: polysaccharide-derivatives, proteins
 - Synthetic polymers: poly(meth)acrylamides, polytartaramides
- Macrocyclic selectors
 - Macrocyclic antibiotics
 - Cyclodextrins
 - Cyclofructans
 - Chiral crown ethers
- Low molecular weight selectors
 - Pirkle-type (donor-acceptor-type) selectors
 - Ligand-exchange selectors
 - Chiral ion exchange-type selectors

1.4.2 Protein-based CSPs

With growing need for chiral separations of drug compounds by liquid chromatography in the 1970s, proteins immediately gained interest as SOs for liquid chromatography separations, mainly because they were easily accessible from nature and experienced continuous interest for pharmacological (drug-receptor) studies [30]. Protein families which are applied as SOs for CSPs include albumins, such as bovine serum albumin (BSA) and human serum albumin (HSA), glycoproteins (e.g. α_1 -acid glycoprotein, AGP, and ovomucoid, OMCHI) and enzymes (e.g. cellobiohydrolase I, CBH I) [31]. The proteins are covalently attached to the silica support material via their carboxylic or amino functions. The application of protein CSPs covers acidic, neutral and basic solutes for which AGP exhibits the broadest enantioseparation capability [30]. AGP and HSA are particularly useful for separation of acidic solutes, such as N-derivatized amino acids, but also for aromatic amino acids and sulfoxides [31, 32].

Numerous SO – SA interaction studies, including X-ray crystallography [33], molecular modelling [34] and thermodynamic studies by chromatography [35], state that chiral recognition is driven by electrostatic, hydrophobic and hydrogen bonding interactions. Furthermore, conformational changes occur by variation of mobile phase pH, modifier content and temperature, which can be visualized in obtaining non-linear van't Hoff plots [36].

Protein CSPs suffer from major drawback like low organic solvent tolerance and limited pH application range (e.g. <25 % and pH 3 – 7.5 for AGP), low efficiency (due to slow mass transfer kinetics) and poor sample loading capacity. Hence, they lost some popularity in industry but are still used in bioanalytical screening of chiral drugs. Apparently, protein CSPs cannot be employed in SFC due to their restriction to highly aqueous mobile phases.

1.4.3 Polysaccharide-type CSPs

Although these phases do not possess ionizable functionalities within their SOs, they should briefly be discussed here because of their widespread use in the field of enantioselective chromatography. In fact, amylose- and/or cellulose carbamate-type CSPs are extensively applied in the pharmaceutical industry in analytical and especially in preparative scale owing to their high column loadabilities [2, 9]. The SOs can either be coated or covalently bound to silica gel, whereas the immobilized CSPs are superior to their coated analogues with regard to their global solvent compatibility [30, 37]. However, both coated and immobilized CSPs,

even if identical polysaccharide derivatives are incorporated, can provide unique selectivity profiles [38, 39]. Polysaccharide-type columns exhibit the broadest scope of application, in resolving analytes of a broad structural diversity [40], and can interchangeably be used in HPLC and SFC [41]. Nevertheless, they are of limited use for resolving chiral amphoteric compounds (amino acids) and are restricted in enantioseparating primary amine containing analytes [42, 43], whereas separation of chiral acids has been reported in both HPLC and SFC [41, 44-46]. Also, the macromolecular SOs offer multiple interaction possibilities which complicates the understanding of the chiral recognition process [5]. For further reading on mechanistic studies on chiral recognition the reader is referred to dedicated reviews [5, 47].

1.4.4 Macrocyclic Antibiotic CSPs

Armstrong et al. introduced macrocyclic antibiotics as chiral selectors for HPLC [48]. The most popular representatives are those from the glycopeptide family, such as avoparcin, vancomycin, ristocetin A, teicoplanin (Fig. 2) and teicoplanin aglycon [49-55]. They have a rather broad scope of applicability, including separations of acidic, basic and zwitterionic enantiomers. Teicoplanin and its aglycone show the best ability for enantioseparation of underivatized α -, β -, and γ -amino acids and small peptides [49, 50, 56-58]. Overall, glycopeptide antibiotic CSPs show some complementarity in their enantioselectivity profiles, which means that if one solute cannot be separated on one particular column, there is a high chance for separation on another CSP. Macrocyclic antibiotic CSPs can be successfully operated in normal phase-, reversed phase and polar organic mode and were also applied in SFC [59, 60].

In the course of extensive investigations on their antibiotic properties [61], it was found that macrocyclic antibiotics bind to D-Ala-D-Ala terminating peptides to inhibit bacteria cell wall assembling. Thus, chromatographic enantioselectivity derives from the stronger binding of D-amino acids and peptides in the basket shaped aglycone cavity. Consequently, elution order for amino acids and peptides on all glycopeptide antibiotic CSPs is L before D with very few exceptions [56].

However, a detailed understanding of the chiral recognition mechanism is still lacking. Dominating SO-SA interactions were found to be hydrogen bonding, hydrophobic interactions and the steric fit into the aglycone cavity. Depending on the analyte structure, supporting interactions may be π - π interactions, electrostatic forces. The basket shaped aglycone plays a pivotal role for enantiorecognition of amino acids and peptides, as the carboxylate group binds to the aglycone in proximity to the ureido group via hydrogen

bonding [62]. This finding is further corroborated by studies on teicoplanin aglycon CSPs, which provide higher selectivity values for amino acids than teicoplanin due to the absence of the sugar moieties, which are hampering access for amino acid solutes to the aglycon cavity [54]. Usually, the acidic group is deprotonated under the applied mobile phase conditions giving the SO an overall negative net charge. Consequently, protonated basic compounds can be separated via a cation exchange mechanism. Interestingly, deprotonated chiral acids (e.g. N-Ac-amino acids) thus having the same charge as the SO can be separated via enantioselective ion-exclusion phenomena i.e. the L-enantiomer is repulsed from the column and the inherently stronger bound D-congener can enter the aglycone cavity and thus is retained [62, 63].

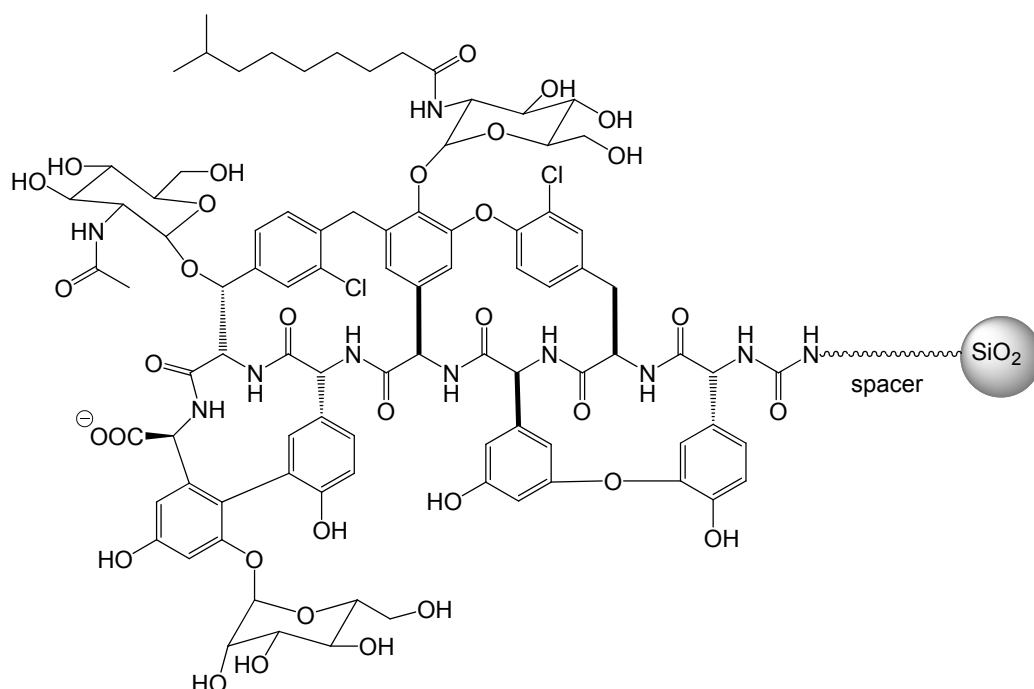


Figure 2. Structure of teicoplanin CSP

1.4.5 Crown Ether CSPs

Crown ether CSPs are restricted for enantioseparation of primary amine containing compounds, most importantly amino alcohols, primary amino acids, di- and tripeptides, and primary amine group containing bases. The chiral recognition mechanism is shown in Fig 3. It requires strongly acidic aqueous mobile phase conditions to protonate the primary amine of the solute, which then forms triple hydrogen bonding interactions with the selector to undergo inclusion complexation [64]. For this reason, chiral crown ether CSPs are not applicable SFC.

One of the most successful crown ether SOs is (18-crown-6)-2,3,11,12-tetracarboxylic acid, which is covalently bonded to aminopropyl-modified silica gel [65]. Since crown ethers are prepared by chemical synthesis rather than from chiral natural compounds, both enantiomeric forms of the SOs are available. Usually, enantiomer elution order can be conveniently reversed when switching from one SO to the opposite enantiomeric form.

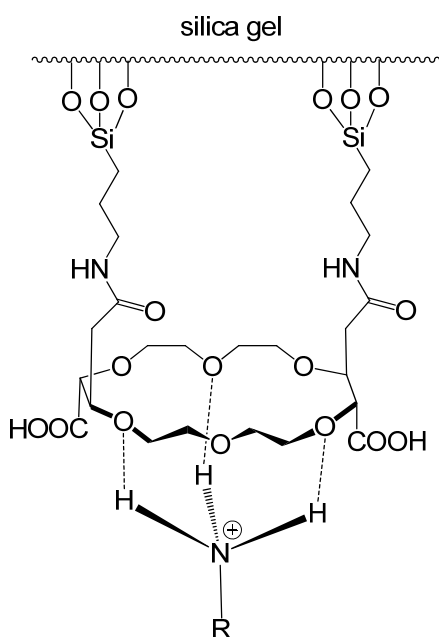


Figure 3. (18-crown-6)-2,3,11,12-tetracarboxylic acid crown ether CSP undergoing a triple hydrogen bond interaction with the protonated primary amine containing analyte

1.4.6 Ligand Exchange CSPs

Chiral ligand exchange chromatography (CLEC) was developed by Davankov in the late 1960s, which made them the first (and for a long time the only) option for direct enantiomer separation of free amino acids [66]. The separation principle of CLEC is based on formation of transient diastereomeric ternary complexes including a divalent metal-ion, a bidentate selector and the solute (Fig. 4). The SOs consists of a covalently bonded or adsorbed bidentate chiral ligand, such as proline, hydroxyproline or penicillamine, and a coordinated divalent metal ion like Cu(II), Ni(II) or Zn(II) [67, 68]. The particular stereochemical features of the analytes cause different thermodynamic stabilities and/or formation rates thus enabling separation of the enantiomers.

As mentioned above, CLEC is specifically addressed for enantiomer separation of α -amino acids, but also for other bidentate or tridentate compounds with electron donating groups, such as amino alcohols and α -hydroxy acids. During chromatography, the ternary reversible

complexes are continuously formed via adsorption/desorption of the corresponding solutes acting as ligands. In addition, solvent molecules (e.g. water) stabilize the complex via coordination to the metal ion in axial positions. Generally, metal-ions are added to the aqueous/organic mobile phase to compensate for metal-ion removal during elution.

Parameters for method optimization include temperature, type and amount of the organic modifier, buffer salts and metal-ions, respectively [67, 69, 70]. Generally, CLEC suffers from drawbacks such as slow exchange kinetics resulting in low column efficiency and the inherent problem of toxic and chelating metal-ions present in the chromatographic system. Consequently, CLEC has been largely replaced by more favorable alternatives for HPLC enantioseparation of amino acids.

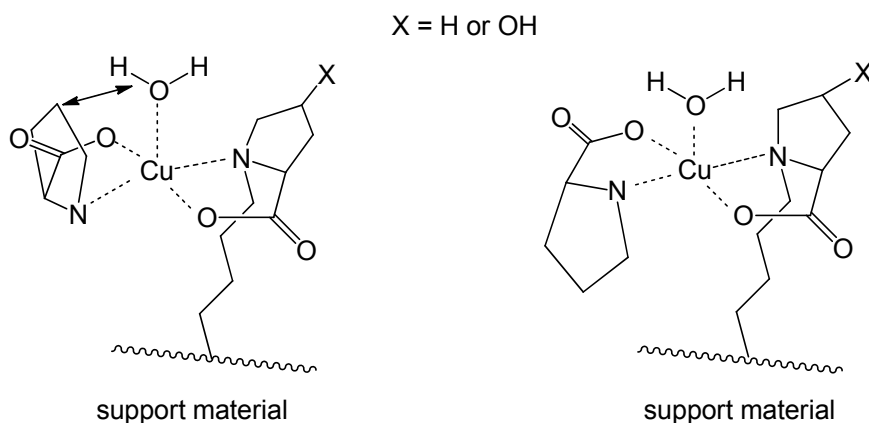


Figure 4. Chiral ligand exchange CSPs

1.4.7 Ion Exchange-type CSPs

Low molecular weight selectors which are dominated by ion exchange retention mechanisms have been reported for anion exchange (AX), cation exchange (CX) and zwitterion exchange (ZWIX) modes, respectively [5].

Most popular representatives are chiral anion exchangers derived from cinchona alkaloids quinine or quinidine, respectively, although anion exchange CSPs based on derivatized ergot alkaloids are also reported [71-74]. Salvadori and coworkers first investigated cinchona alkaloids as SOs for HPLC [75]. However, Lämmerhofer and Lindner significantly improved the enantiodiscrimination abilities by introduction of bulky substituents via a carbamate bond at the OH-group in C9 position [76]. Fig. 5 depicts tert-butylcarbamoyl-quinine and quinidine CSPs (QN-AX CSP and QD-AX CSP, respectively).

QN-AX and QD-AX CSPs are preferentially operated in weakly acidic hydro-organic or polar organic mobile phases, which enable a weak anion exchange (WAX) dominated

retention mechanism between the protonated quinuclidine tertiary amine and the deprotonated (negatively charged) acidic analyte. In these CSPs, the long range but non-directed electrostatic forces are supported by short range directing interactions, such as hydrogen bonding, π - π stacking, van der Waals or steric interactions [77], which in concert facilitate chiral discrimination of the acidic enantiomers. The carbamate motif in the SOs acts as a potent hydrogen donor and acceptor and is crucially involved in the chiral recognition process. The quinoline moiety can undergo charge transfer interactions (π - π) with aromatic solutes (Fig. 5) [77-80]. Moreover, different substitution patterns at the carbamoyl moiety also influence enantioselectivity, thereby confirming that van der Waals or steric interactions must play a supportive role [81, 82]

Due to their nature as chiral anion exchangers, QN-AX and QD-AX can resolve many classes of chiral acidic compounds with particularly high enantioselectivities for N-protected amino acids. Other enantioseparations of arylcarboxylic acids (profens), aryloxy-carboxylic acids, N-protected aminophosphinic and -phosphonic acids and few sulfonic acids are also reported [83].

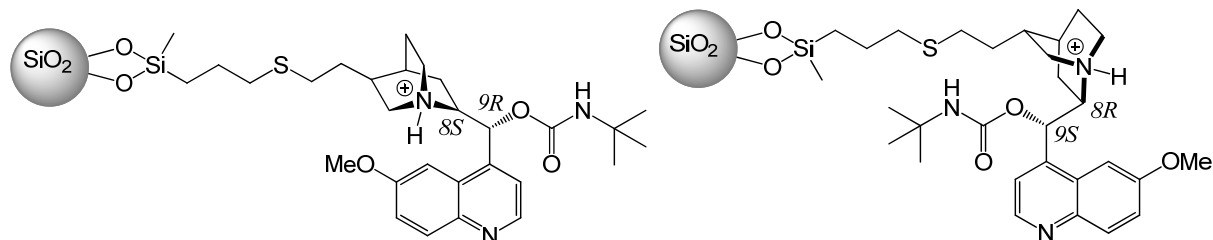


Figure 5. QN-AX (left) and QD-AX CSPs (right)

Recently, Lindner and co-workers introduced low molecular weight strong cation exchange-type (SCX) CSPs for HPLC. They were preferentially applied in buffered polar organic mobile phases and proved to be suitable for enantioselective and chemoselective separations of secondary and tertiary amines. Due to their nature as low molecular weight SCX CSPs, they also showed fast mass transfer kinetics resulting in high column efficiencies [84, 85].

With the aim to extend the limited applicability of the single anion and cation exchanger CSPs, cinchona alkaloids were merged with sulfonic acid moieties, thus creating a zwitterionic SO. After immobilization onto silica gel, the corresponding zwitterionic CSPs (ZWIX-CSPs) enabled all three modes of ion exchange and were therefore suitable for

resolving chiral acids, bases and amphoteric compounds (e.g. free amino acids and aminosulfonic acids) [86]. Fig. 6 exemplarily depicts a quinine-based ZWIX-CSP.

Due to their zwitterionic nature, the ZWIX CSPs exhibited unique properties as compared to their parent uni-ionic WAX or SCX-type SOs. The presence of an oppositely charged group on the SO molecule caused significantly reduced retention times for separation of acids in the anion-exchange mode or bases in the cation exchange mode, respectively. This was termed the “intra-molecular counterion (IMCI) effect” [86, 87]. Vice versa, compared to the WAX and SCX-type CSPs, the IMCI effect enables isoelution conditions in the AX and CX mode with reduced buffer amounts (ionic strength) in the mobile phase.

However, the preparation of ZWIX-CSPs was motivated by enabling separations of chiral zwitterionic (amphoteric) compounds, which are generally poorly or even not retained and thus not separated on uni-ionic WAX or SCX-type CSPs (although some examples exist [88]). Indeed, a broad range of structurally diverse free amino acids could be resolved. However, the chiral discrimination properties were strongly depending on the structure of the strong cation exchange subunit. The stereocenter in vicinity to the SCX moiety was found to enhance the enantioselectivity profile towards basic and zwitterionic solutes [86, 87] (Fig. 6). Moreover, enantiomer elution order could be inverted by switching from the quinine- to the pseudoenantiomeric quinidine-based CSP, which underlined that the cinchona alkaloid moiety played a pivotal role in the chiral recognition process.

Molecular recognition between the SO and the zwitterionic SA is assumed to be driven by a simultaneous double ion pairing process. Depending on the solute structure, additional intermolecular interactions can come into play, such as hydrogen bonding with the carbamate moiety of the SO, π - π stacking with the quinoline moiety, van der Waals or steric interactions.

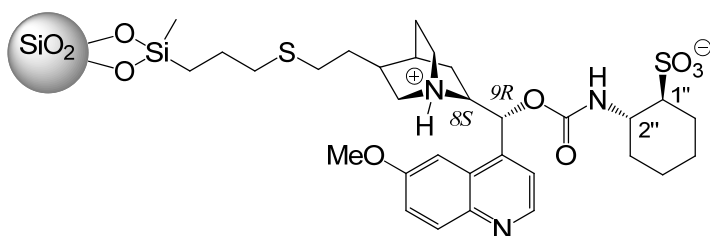


Figure 6. Quinine-based zwitterionic chiral stationary phase (ZWIX-CSP)

ZWIX-CSPs express most favorable enantioseparation profiles in all three ion exchange modes when applying weakly acidic mobile phase conditions with polar organic bulk solvents. Hydro-organic (reversed phase) conditions decreased retention due to strong

solvation effects of the charged sites of the ZWIX-SOs and the analytes, respectively. However, for amino acids with hydrophobic moieties, retention increased at high water content as supportive hydrophobic increments became active. Buffer concentration (ionic strength) had only moderate impact on retention and negligible influence on enantioselectivity, especially in the zwitterion exchange mode. This was particularly exemplified by separation of tryptophan without any buffer salts in the mobile phase (neat MeOH) [89].

1.5 Retention Mechanisms in Chiral Ion Exchange Chromatography

Several models exist for the description of the retention process in ion-exchange chromatography. Generally, models based on the diffuse double-layer theory are the most accurate ones but are very complex and require the solution of the Poisson-Boltzmann equation, a second order differential equation (e.g. the Gouy-Chapman model). Furthermore, they also rest on a number of assumptions that are in conflict with the physical realities (e.g. that ions are considered as point charges). A related, well-established physical concept is the Donnan model, a simplified version of the diffuse double-layer model [90].

A more practical and conceptually simpler approach is the often applied stoichiometric displacement model [83, 90-92], which states that counterions displace the solute ions from the oppositely charged selector site. According to this empirical model, ion exchange-based retention mechanisms show a linear relationship between the logarithm of the retention factor k and the logarithm of the molar counterion concentration $[C]$, as shown in Eq. 12.

$$\log k = \log K_z - Z \cdot \log [C] \quad (12)$$

Z is the slope of the linear regression line and is proportional to m/n , wherein m is the charge number of the analyte ion and n the charge number of the counterion. Thus, the slope Z indicates the number of charges being involved in the ion-exchange process.

The constant K_z , which can be calculated from the intercept, is defined by Eq. 13.

$$K_z = \frac{K \cdot S \cdot (q_x)^Z}{V_0} \quad (13)$$

K is the ion-exchange equilibrium constant (in L mol^{-1}), S is the surface area (in $\text{m}^2 \text{g}^{-1}$), q_x is the charge density on the surface (in mol m^{-2}) (i.e. the number of ion-exchange sites available for adsorption) and V_0 is the mobile phase volume (in L). Consequently, $\log K_Z$ can be seen as a system-specific constant and represents the $\log k$ value at a 1 mol/L counterion concentration.

Hence, the elution strength of a particular counterion can be deduced from the slope and intercept of the linear regression line. Generally, the ion-exchange mechanism is the same for both enantiomers following that enantioselectivity remains unaltered by changing the counterion concentration.

In the case of weak ion-exchange systems, acid-base equilibria are superimposed on the ion-exchange process (this is valid for both weak ion-exchanger CSPs and weakly acidic/basic solutes). The influence of the pH (or apparent proton activity pH_a , respectively) on retention in ion exchange chromatography was illustrated by Sellergren and co-workers [93], as shown in Eq. (14)

$$k = \Phi \cdot \frac{1}{[C]} \cdot K \cdot \alpha_{SA} \cdot \alpha_{SO} \cdot [SO]_{tot} \quad (14)$$

where α_{SA} and α_{SO} are the ionization states of the selectand and the selector, respectively, and $[SO]_{tot}$ is the total ion exchange capacity of the stationary phase (i.e. the surface concentration of SO which is tantamount to q_x). From Eq. 14 it follows that retention is strongest where the degree of ionization of both SO and SA is highest, which, in turn, can be controlled by the (apparent) pH of the mobile phase.

2 Objectives

The aim of the present dissertation was to design and prepare novel ion exchange-type CSPs, followed by their evaluation in HPLC and SFC towards their enantiodiscrimination capabilities for ionizable solutes. The field of research was mainly divided in two areas:

In the first part, the applicability of quinine- and quinidine-based chiral anion exchangers, which had already been extensively characterized in HPLC, should be further extended to SFC. First, it was planned to principally investigate the suitability of these anion exchange driven CSPs for enantiomer separation of chiral carboxylic acids in SFC. Second, a detailed analysis of the influence of particular parameters (e.g. buffer composition, temperature) on separation performance should be carried out. Overall, the merits and limitations of anion-exchange-type CSPs in SFC mode were to be discussed. In another study, the anion exchanger CSPs were evaluated for enantioseparation of sulfonic acids (or their sodium-salts, respectively) in HPLC and also SFC.

The second aim of the thesis included synthesis and chromatographic evaluation of zwitterionic CSPs. Following a semisynthetic approach, quinine and quinidine molecules should be modified with chiral strong cation exchange subunits, thus generating amphoteric chiral selectors. Due to their zwitterionic nature, the emerging CSPs can be operated in all three modes of ion exchange (i.e. anion, cation, and zwitterion exchange), but are specifically employed for enantioseparation of amphoteric compounds, such as free amino acids. Via systematic structural modifications of the strong cation exchange subunits, we aimed at (i) generating selectors with a broad scope of applicability for amino acid enantiomer separation and (ii) drawing conclusions on the involved chiral recognition mechanism between the zwitterionic selector and the amphoteric analyte.

3 Results and Discussion

3.1 General Remarks

This chapter primarily outlines those results that have already been published in peer-reviewed journals or have been included in manuscript drafts submitted for publication. Results that are closely related with the topic of the thesis, but have not yet been published are presented in 3.4.

Chapter 3 aims at putting the results of the individual publications and manuscript drafts in context. In order to allow straightforward reading and to avoid redundant information, the contents are only briefly summarized, and the abstracts of the corresponding articles are included within this chapter. For obtaining detailed information the reader is referred to the publications and manuscript drafts given in the appendix.

3.2 Anion Exchange-type CSPs

3.2.1 Application of Anion Exchanger CSPs for Indirect Chromatographic Absolute Configuration Assignment

Generally, determination of absolute configuration of individual enantiomers is commonly accomplished by X-ray diffraction analysis [94, 95], NMR [94, 96, 97], circular dichroism spectroscopy (CD) [98, 99] and vibrational circular dichroism spectroscopy (VCD) [100]. However, application of these methods can be laborious, be restricted to certain classes of compounds or may need considerable amounts of sample.

Indirect assignment of absolute configuration via chromatography can be a faster and more straightforward alternative to the above mentioned techniques and was frequently applied in the past [101]. It is carried out by comparison of the elution orders of the unknown enantiomer with those of a reference compound with known absolute configuration. Thus, the indirect chromatographic method implies several prerequisites to allow correct assignment of the absolute configuration (i) it requires a detailed understanding of the chiral recognition mechanism between the SO and the SA (ii) the sample compound must be structurally closely related to the reference compound in order avoid ambiguity due to potential changes in the chiral recognition mechanism [101] (iii) the applied CSP has to show consistent elution orders

for the investigated class of solutes, independently from changes in chromatographic conditions such as variation in mobile phase parameters.

Hence, among the numerous CSP available, only a few fulfil the above mentioned requirements. Tert-butylcarbamoyl quinine and its pseudoenantiomeric quinidine-based CSP belong to this class of CSPs, thereby exhibiting consistent enantiomer elution orders for certain classes of chiral acids (vide supra). We compared both anion exchanger phases with a polysaccharide-based CSP regarding their enantioseparation ability towards pirinixic acid derivatives and their potential for indirect absolute configuration assignment. The results are presented and discussed in the following publication (M. Lämmerhofer, R. Pell, M. Mahut, M. Richter, S. Schiesel, H. Zettl, M. Dittrich, M. Schubert-Zsilavecz, W. Lindner. *Journal of Chromatography A* 2010, 1217, p. 1033-1040; for the complete article see Appendix I)

Enantiomer separation and indirect chromatographic absolute configuration prediction of chiral pirinixic acid derivatives: Limitations of polysaccharide-type chiral stationary phases in comparison to chiral anion-exchangers

Michael Lämmerhofer ^{a, *}, Reinhard Pell ^a, Marek Mahut ^a, Martin Richter ^a, Simone Schiesel ^a, Heiko Zettl ^b, Michaela Dittrich ^b, Manfred Schubert-Zsilavecz ^b, Wolfgang Lindner ^a

^a Christian-Doppler Laboratory for Molecular Recognition Materials, University of Vienna, Department of Analytical Chemistry & Food Chemistry, Waehring Strasse 38, A-1090 Vienna, Austria

^b Institute of Pharmaceutical Chemistry/ZAFES/LiFF, Goethe-University Frankfurt, Max-von-Laue-Strasse 9, D-60348 Frankfurt/M., Germany

* Corresponding author

Abstract

Chiral α -arylthiocarboxylic acids with different substitution patterns, representing new pirinixic acid derivatives with dual PPAR α / γ agonistic activities, have been separated into enantiomers on tert-butylcarbamoylquinine and quinidine based chiral anion-exchangers and amylose tris(3,5-dimethylphenylcarbamate) coated silica on analytical and preparative scale. Absolute configurations of individual enantiomers were assigned chromatographically via elution orders on the chiral anion exchangers and were confirmed by stereoselective syntheses via Ewans auxiliaries that have lead to enantiomeric products with known absolute configurations. The results of both methods were in full agreement. Moreover, the receptor stereoselectivity in PPAR α transactivation activities was consistent within the test set of structurally related compounds. Limited correlation (between elution order and substitution) was observed within the set of α -arylthiocarboxylic acids on the amylose tris (3,5-dimethylphenylcarbamate) based chiral stationary phase (CSP), in particular the elution order changed with remote substitution. This clearly demonstrates the risks of chromatographic absolute configuration assignments by prediction from one structural analog to another one, especially with CSPs such as

polysaccharide CSPs that are recognized for their broad applicability due to multiple binding and chiral recognition modes. It is therefore of utmost importance that such chromatographic absolute configuration predictions by extrapolation to structural analogs are combined with orthogonal methods for verification of the results.

Keywords: Chiral stationary phase; Chiral anion-exchanger; Quinine and quinidine carbamates; Polysaccharide; Amylose tris (3,5-dimethylphenylcarbamate); Chiral separation; HPLC; Pirinixic acid derivatives; 2-Aryloxyalkanoic acids; 2-Arylthioalkanoic acids; Enantioselective synthesis; Peroxisome proliferator activated receptors (PPAR)

Received: 8 July, 2009; Available online: 21 October, 2009; <http://dx.doi.org/10.1016/j.chroma.2009.10.048>

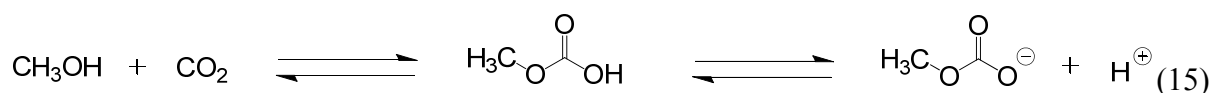
3.2.2 Evaluation of Anion Exchange-type CSPs in SFC and HPLC for Separation of Chiral Carboxylic- and Sulfonic Acids

As outlined in chapter 1.4.7, cinchona-alkaloid based weak anion exchangers were successfully employed in HPLC for enantioseparation of chiral acids in reversed phase-, polar organic- and normal phase mode. In an effort to further extending their application range, we evaluated tert-butylcarbamoyl quinine and –quinidine CSPs in another chromatographic separation technique, namely Subcritical Fluid Chromatography (SFC).

Supercritical CO₂ and a methanolic modifier with acidic and basic additives was employed to enantioseparate a broad set of N-protected amino acids and chiral arylcarboxylic acids. Actually, we applied a 25% modifier amount, a temperature of 40°C and a backpressure of 150 bars for the measurements, which results in a mobile phase of subcritical state.

A similar enantioselectivity profile for the investigated analytes was obtained which underlined the same chiral recognition mechanism as observed in HPLC. Moreover, retention also followed an ion exchange process, thereby exhibiting decreased retention times with increasing buffer concentrations in the mobile phase (at a constant acid to base ratio in the methanolic modifier). Interestingly, we could realize anion-exchange mediated chiral separations by merely applying sc CO₂ with neat MeOH (without any addition of acidic or basic additives to the modifier).

This phenomenon can be explained by the *in situ* formation of methylcarbonic acid in pressurized CO₂ - methanolic systems [66, 102]. The acid can then dissociate to methylcarbonate and a proton, as outlined in Eq. (15).



Hence, we could chromatographically confirm that the often coined “inherent acidity” of sc CO₂-methanolic systems is based on the *in situ* formation of methylcarbonate, which then acts as a counterion in the SFC mobile phase thus enabling elution of the acidic compounds. This finding enables high potential for preparative separations of chiral acids on cinchona-alkaloid based anion exchanger columns by avoiding potentially troublesome additives in the mobile phase, because after pressure release the acid disproportionates into CO₂ and methanol.

Detailed investigations on QN-AX and QD-AX CSPs in SFC mode are given in the following publication (R. Pell, W. Lindner, Journal of Chromatography A 2012, in press; Appendix II)

Potential of Chiral Anion-Exchangers Operated in Various Subcritical Fluid Chromatography Modes for Resolution of Chiral Acids

Reinhard Pell, Wolfgang Lindner*

Department of Analytical Chemistry, University of Vienna, Währingerstrasse 38, 1090 Vienna, Austria

* corresponding author

Abstract

Anion-exchange-type chiral stationary phases (CSPs) derived from quinine or quinidine were applied in subcritical fluid chromatography (SFC) for the direct separation of chiral acidic compounds. Employing subcritical (sc) mobile phase modes (CO₂ + methanol as co-solvent and acids and bases as additives) first the influence of type and amount of acidic and basic additives on separation performance was investigated. Secondly, water was tested as a neutral additive and the influence of temperature variation on enantioselectivity was studied. Thirdly, we could chromatographically confirm that the often verbalized “inherent acidity” of sc CO₂ + methanol is manifested by the *in situ* formation of methylcarbonic acids in the sc mobile phase and thus functioning as acidic additive. Accordingly the dissociated methylcarbonic acid, acting as a counterion, enables an anion exchange mechanism between the cationic CSP and the corresponding acidic analyte. In the absence of a dissociable acid in the mobile phase such an ion exchange mode would not work following a stoichiometric displacement model. This finding is further corroborated by the use of ammonia in methanol as co-solvent thus generating *in situ* the ammonium salt of methylcarbonic acid. In summary, we report on ion-exchange mediated chromatographic separations in SFC modes by merely using (i) sc CO₂ and MeOH, (ii) sc CO₂ and ammonia in MeOH, and (iii) sc CO₂ and MeOH plus acids and bases as additives. Comparisons to HPLC mode have been undertaken to evaluate merits and limitations. This mode exhibits high potential for preparative chromatography of chiral acids combining pronounced enantioselectivity with high column loadability and avoiding possibly

troublesome mobile phase additives, as the *in situ* formed methylcarbonic acid disintegrates to CO₂ and methanol upon pressure release.

Keywords: Enantiomer separation, Supercritical fluid chromatography, Subcritical mobile phase, Chiral Stationary phase, Chiral anion exchangers

Received: 16 March, 2012; accepted 5 May 2012; <http://dx.doi.org/10.1016/j.chroma.2012.05.023>

As already stated in the introduction, QN-AX and QD-AX columns proved to be suitable for retention and enantioseparation of all types of organic acids due to their nature as weak anion exchange-type CSPs. However, only a few chiral sulfonic acids or sulfonate salts, respectively, have been applied as analytes until now.

Hence, within the following publication QN-AX and QD-AX CSPs were applied to investigate the enantioseparation performance towards a set of sodium β -ketosulfonates in HPLC and subcritical fluid chromatography. The results have been published in the following paper (R. Pell, G. Schuster, M. Lämmerhofer, W. Lindner, Journal of Separation Science 2012, accepted; for the full article see Appendix III)

Enantioseparation of Chiral Sulfonates by Liquid Chromatography and Subcritical Fluid Chromatography

Reinhard Pell^a, Georg Schuster^a, Michael Lämmerhofer^{a,b}, Wolfgang Lindner^a

^aDepartment of Analytical Chemistry, University of Vienna, Währinger Strasse 38, 1090 Vienna, Austria

^bcurrent address: Institute of Pharmaceutical Sciences, Universität Tübingen, Auf der Morgenstelle 8, 72076 Tübingen, Germany

*corresponding author

Abstract

Tert-butylcarbamoyl-quinine and –quinidine weak anion exchange chiral stationary phases (Chiralpak® QN-AX and QD-AX) have been applied for the separation of sodium β -ketosulfonates, such as sodium chalconesulfonates and derivatives thereof. The influence of type and amount of co- and counterions on retention and enantioresolution was investigated using polar organic mobile phases. Both columns exhibited remarkable enantiodiscrimination properties for the investigated test solutes, in which the quinidine-based column showed better enantioselectivity and slightly stronger retention for all analytes compared to the quinine-derived chiral stationary phase. With an optimized mobile phase (MeOH, 50 mM HOAc, 25 mM NH₃) 12 out of 13 chiral sulfonates could be baseline separated within 8 minutes using the quinidine-derivatized column. Furthermore, subcritical fluid chromatography (SubFC) mode with a CO₂-based mobile phase using a buffered methanolic

modifier was compared to HPLC. Generally, SubFC exhibited slightly inferior enantioselectivities and lower elution power but also provided unique baseline resolution for one compound.

Keywords: chiral sulfonates, chiral separation, cinchona alkaloid, subcritical fluid chromatography, liquid chromatography

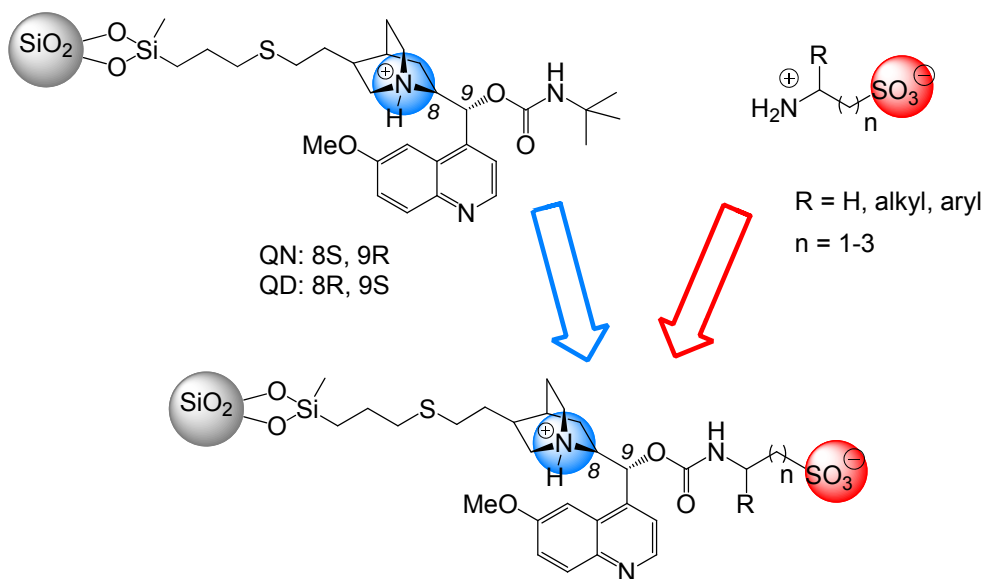
Received: 4 May 2012; accepted 25 May 2012

3.3 Zwitterionic CSPs: Preparation and Evaluation by HPLC

In 2008, Hoffmann et al. initially reported on preparation and HPLC-evaluation of novel zwitterion-exchange-type CSPs [86]. The remarkable enantiodiscrimination properties of these brush-type ZWIX-CSPs for resolving chiral acidic, basic and zwitterionic analytes prompted us to further develop this concept. The synthetic strategy focused on using cinchona alkaloids quinine or quinidine as weak anion exchange moieties and carrying out systematic variations of the sulfonic acid based strong cation exchange units (Scheme 1).

Hence, we synthesized aminosulfonic acid subunits and fused them with either QN or QD via a carbamate linkage to form novel zwitterionic low molecular weight selectors. Upon immobilization on mercaptopropyl-modified silica gel, the corresponding ZWIX-CSPs were chromatographically evaluated by HPLC in three different projects.

First, we investigated the impact of the intramolecular distance of the oppositely charged groups within the zwitterionic SO on the enantiodiscrimination properties. In doing so, ZWIX CSPs with increasing alkyl side chains at the SCX site were evaluated by HPLC for enantioseparation of chiral amines, acids and zwitterionic compounds, such as free amino acids and small peptides. The results were published in the following article (S. Wernisch, R. Pell, W. Lindner. *Journal of Separation Science* 2012, in press; for the full paper see Appendix IV)



Scheme 1. Synthetic concept of novel ZWIX-CSPs

Increments to chiral recognition facilitating enantiomer separations of chiral acids, bases, and ampholytes using *Cinchona*-based zwitterion exchanger chiral stationary phases

Stefanie Wernisch, Reinhard Pell, Wolfgang Lindner*

Institute of Analytical Chemistry, University of Vienna, Währinger Straße 38, 1090 Vienna, Austria

* corresponding author

Abstract

The intramolecular distances of anion and cation exchanger sites of zwitterionic chiral stationary phases represent potential tuning sites for enantiomer selectivity. In this contribution, we investigate the influence of alkanesulfonic acid chain length and flexibility on enantiomer separations of chiral acids, bases, and amphoteric molecules for six *Cinchona* alkaloid-based chiral stationary phases in comparison with structurally related anion and cation exchangers. Employing polar-organic elution conditions, we observed an intramolecular counterion effect for acidic analytes which led to reduced retention times but did not impair enantiomer selectivities. Retention of amphoteric analytes is based on simultaneous double ion pairing of their charged functional groups with the acidic and basic sites of the zwitterionic selectors. A chiral center in the vicinity of the strong cation exchanger site is vital for chiral separations of bases. Sterically demanding side chains are beneficial for separations of free amino acids. Enantioseparations of free (un-derivatized) peptides were particularly successful in stationary phases with straight-chain alkanesulfonic acid sites, pointing to a beneficial influence of more flexible moieties. In addition, we observed pseudo-enantiomeric behavior of quinine and quinidine-derived chiral stationary phases facilitating reversal of elution orders for all analytes.

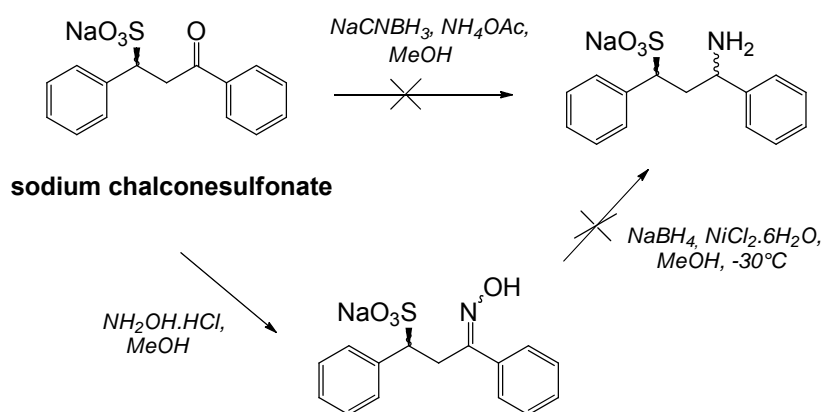
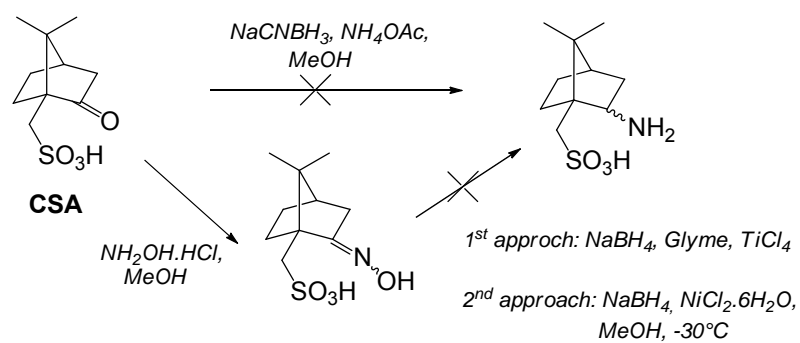
Keywords: Amino acid / Chiral stationary phase / Ion exchange / Liquid chromatography / Peptide / Zwitterion

Received January 31 2012, Accepted March 15, 2012; DOI 10.1002/jssc.201200103

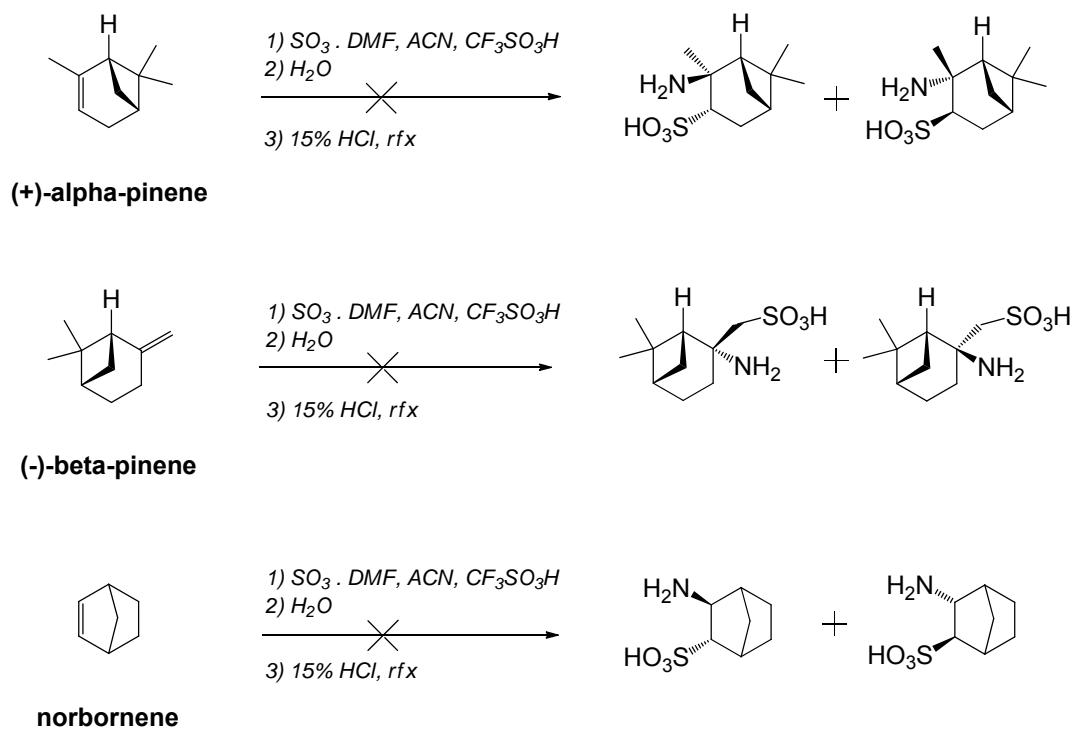
Amongst other issues, the article reported the necessity of a chiral center in the vicinity of the SCX moiety to successfully separate a broad range of chiral bases and free amino acids, thereby confirming earlier findings by Hoffmann et al. [86, 87].

Therefore, the focus was on design and synthesis of novel quinine- or quinidine-based ZWIX-SOs bearing a stereocenter close to the sulfonic acid group. A major effort was to synthesize chiral β -aminosulfonic acids, which were then used as synthons in the following step for ZWIX-SO preparation (for a general scheme on ZWIX-SO synthesis see Appendix IV or Appendix V in the Supporting information).

Briefly, three synthesis approaches were extracted from the rather limited amount of literature on synthesis of chiral β - or γ -aminosulfonic acids. First, reductive amination of (*1S*)-10-camphorsulfonic acid was applied to obtain diastereomeric endo/exo mixtures of the corresponding aminocamphorsulfonic acid (see Scheme 2) [103]. However, we could neither reproduce these results nor apply the reductive amination step for synthesis of γ -aminosulfonic acids from chalconesulfonic acid starting materials (Scheme 2). Consequently, it was tried to circumvent the reductive amination step via synthesis of stable ketoxim-intermediates and a subsequent reduction step to yield the corresponding aminosulfonic acid. However, whereas the synthesis of the ketoxim products worked straightforward, we failed in the following reduction step.



Scheme 2. Reductive amination strategy



Scheme 3. Aminosulfonation strategy

In the second approach, chiral trans-aminosulfonic acids were synthesized from their corresponding alkene-starting materials in a straightforward two-step conversion by Cordero et al. [104]. The reaction was applied to prepare trans-2-aminocyclohexanesulfonic acid required as a synthon for the preparation of SCX- and ZWIX-SOs [84, 86, 87, 105]. However, the reaction turned out to be not applicable for sterically hindered starting materials, such as α -pinene or just norbornene.

Third, the group of Xu and coworkers reported in several publications on synthesis of β -aminosulfonic acids (2-substituted taurines), thereby also exhibiting minor drawbacks such as multistep synthesis [106-108] or the tedious isolation of the zwitterionic product from inorganic salts [109, 110]. However recently, they reported on a smooth two-step synthesis, in which enantiomeric vicinal amino alcohols were transformed to thiazolidine-2-thione intermediates and subsequently oxidized with performic acid to the corresponding mono-substituted β -aminosulfonic acids [111].

We applied this rather cheap and salt-free method to synthesize a small library of enantiomerically pure 2-substituted taurine analogs, which were subsequently fused with quinine-or quinidine activated esters to obtain novel ZWIX-SOs with chiral subunits on the SCX site. After SO immobilization onto mercaptopropyl-modified silica gel, a set of novel ZWIX-CSPs with systematic structural variations at their SCX- or WAX subunits were obtained. In a following study, the ZWIX-CSPs were used for (i) deconvolution of the chiral recognition mechanism between ZWIX-SOs and zwitterionic analytes (ii) evaluation of the enantiodiscrimination properties of the particular CSPs for amino acid solutes and (iii) carrying out a systematic mobile phase optimization applying protic and aprotic bulk solvents in polar organic mode. The results are presented in the following manuscript (R. Pell, S. Sić, W. Lindner. Journal of Chromatography A 2012, submitted)

Mechanistic investigations of cinchona alkaloid-based zwitterionic chiral stationary phases

Reinhard Pell, Siniša Sić, Wolfgang Lindner*

Department of Analytical Chemistry, University of Vienna, Währinger Strasse 38, 1090 Vienna, Austria

* Corresponding author:

Abstract

Novel zwitterionic cinchona alkaloid-based chiral selectors (SOs) were synthesized and immobilized on silica gel. The corresponding brush-type chiral stationary phases (CSPs) were characterized as zwitterionic ion-

exchange-type materials and exhibited remarkable enantioselectivity for their zwitterionic target analytes, viz. underivatized amino acids and aminosulfonic acids. We rationally designed structural modifications on the strong cation exchange (SCX) subunit of the zwitterionic SO and investigated the influence on chiral recognition power for amphoteric solutes. SOs with chiral isopropyl- or cyclohexyl-moieties in vicinity to the SCX site showed broadest application range by baseline resolving 39 out of 53 test compounds, including α -, β -, and γ -amino acids with different substitution patterns. Furthermore, we introduced two pseudoenantiomeric zwitterionic CSPs which combined the unique features of providing comparable enantioselectivities but reversed enantiomer elution orders. By application of slightly acidic polar organic mobile phases as preferred elution mode, we found that certain amounts of aprotic acetonitrile in protic methanol substantially increased enantioselectivity and resolution of amino acids in a structure-dependent manner.

Keywords: enantioseparation, amino acid, aminosulfonic acid, chiral stationary phase, zwitterionic selector

Received 25 May, 2012

The reported results provide evidence that ZWIX-CSPs have a high potential for resolving amino acids and dipeptides of a broad structural diversity. In an attempt to further extend the application range towards larger amphoteric molecules, three ZWIX-CSPs were applied for enantioseparation of novel peptidomimetic drug candidates considered for antithrombotic therapy. Following a bioisosteric replacement approach, a research partner designed and synthesized structural analogs to the antiplatelet drug tirofiban, thereby introducing carboxylic-, phosphinic-, phosphonic and thiophosphonic acid moieties. However, as racemization occurred during synthesis, there was a need for chiral separations in the mg scale to enable biological tests with enantiomerically pure compounds.

Fig. 7 exemplarily outlines the broad applicability of particular ZWIX-CSPs by enantioseparating acidic and zwitterionic solutes of different acidic functionality on the same column under the same mobile phase conditions.

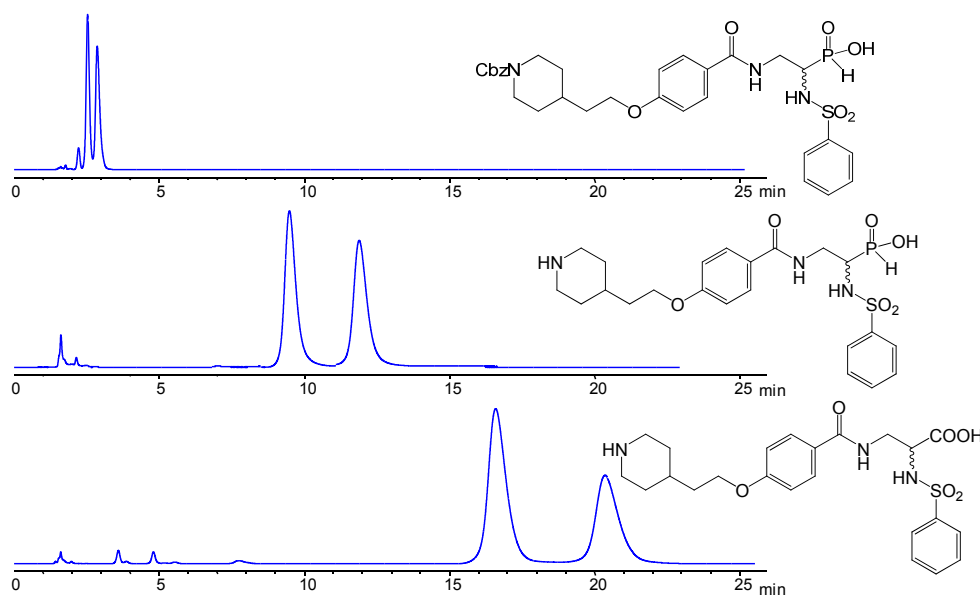


Figure 7. Conditions: CSP A185 (for CSP structure see Appendix VI, supporting info); MeOH, 50 mM HOAc, 25 mM NH₃; 25°C; flow 1.0 mL/min; UV detection; $t_0 = 1.51$ min

The analytical scale enantioseparations of four tirofiban analogs are shortly commented in the main article and described in detail in the supporting information in the following publication (M. Bollinger, F. Manzenrieder, R. Kolb, A. Bochen, S. Neubauer, L. Marinelli, V. Limongelli, E. Novellino, G. Moessmer, R. Pell, W. Lindner, J. Fanous, A. Hoffman, H. Kessler. *Journal of medicinal Chemistry*, 2012, 55, 871-88; for the full article see Appendix VI)

Tailoring of Integrin Ligands: Probing the Charge Capability of the Metal Ion-Dependent Adhesion Site

Markus Bollinger,[†] Florian Manzenrieder,[†] Roman Kolb,[†] Alexander Bochen,[†] Stefanie Neubauer,[†] Luciana Marinelli,[‡] Vittorio Limongelli,[‡] Ettore Novellino,[‡] Georg Moessmer,[§] Reinhard Pell,^{||} Wolfgang Lindner,^{||} Joseph Fanous,[⊥] Amnon Hoffman,[⊥] and Horst Kessler*,^{†,Ⓜ}

[†]Institute for Advanced Study and Center of Integrated Protein Science, Department Chemie, Technische Universität München, Lichtenbergstrasse 4, 85747 Garching, Germany

[‡]Dipartimento di Chimica Farmaceutica e Tossicologica, Università di Napoli "Federico II", Via D. Montesano, 49-80131 Napoli, Italy

[§]Institut für Klinische Chemie und Pathobiochemie, Klinikum rechts der Isar, Technische Universität München, Ismaninger Strasse 22, 81675 München, Germany

^{||}Institute of Analytical Chemistry, University of Vienna, Währinger Strasse 38, A-1090 Vienna, Austria

LSchool of Pharmacy, Faculty of Medicine, The Hebrew University of Jerusalem, P.O. Box 12065, Jerusalem 91120, Israel

@Chemistry Department, Faculty of Science, King Abdulaziz University, P.O. Box 80203, Jeddah 21589, Saudi Arabia

Abstract:

Intervention in integrin-mediated cell adhesion and integrin signaling pathways is an ongoing area of research in medicinal chemistry and drug development. One key element in integrin–ligand interaction is the coordination of the bivalent cation at the metal ion-dependent adhesion site (MIDAS) by a carboxylic acid function, a consistent feature of all integrin ligands. With the exception of the recently discovered hydroxamic acids, all bioisosteric attempts to replace the carboxylic acid of integrin ligands failed. We report that phosphinates as well as monomethyl phosphonates represent excellent isosters, when introduced into integrin antagonists for the platelet integrin α IIb β 3. The novel inhibitors exhibit *in vitro* and *ex vivo* activities in the low nanomolar range. Steric and charge requirements of the MIDAS region were unraveled, thus paving the way for an *in silico* prediction of ligand activity and in turn the rational design of the next generation of integrin antagonists.

Received: October 14, 2011; Accepted December 19, 2011

3.4 Unpublished Results: Zwitterionic CSPs in SFC-Mode for Separation of Chiral Acids

The successful application of cinchona alkaloid-based weak anion exchange CSPs in SFC (Appendix II, Appendix III) motivated to investigate a zwitterionic CSP in subcritical fluid chromatography.

Hence, we applied an already established quinine-based ZWIX-CSP (see Fig. 8; note that the SO is identical with the one of “CSP 4” in Appendix IV, but was immobilized onto 5 μ m silica gel packed into a 150 x 4 mm i.d. column) and investigated its chromatographic performance first in anion-exchange and second in zwitterion exchange operation mode.

Interestingly, despite its nature as a zwitterionic and thus highly polar SO, it proved to be perfectly applicable for SFC operation in anion exchange mode for enantioseparation of chiral acids. Higher plate numbers and substantially lower retention times were obtained compared to the parent weak anion exchange columns (QN-AX or QD-AX CSP, respectively). Consequently, the sulfonic acid moiety of the ZWIX-SO works as an intramolecular counterion (IMCI, see 1.x) thereby increasing the total amount of counterions in the mobile phase thus leading to decreased retention times according to a stoichiometric displacement model. Unfortunately, the benefits of shortened retention times are overshadowed by lower

enantioselectivity values obtained on the ZWIX-CSP compared to QN-AX (Fig. 9). However, this could be attributed to an inherently lower enantiodiscrimination ability of this particular ZWIX-SO, as alpha values could neither be enhanced in HPLC mode (data not shown).

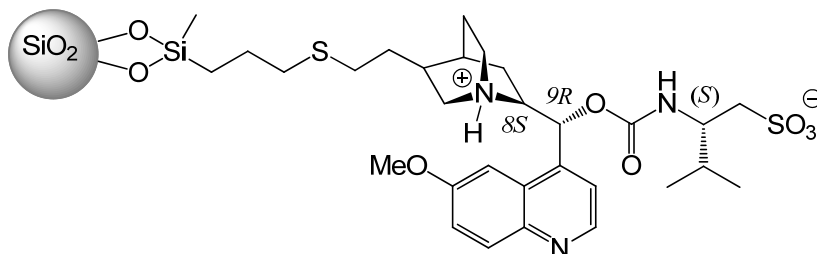


Figure 8. Applied ZWIX-CSP 4 for SFC study

Table 1. Enantioseparation of chiral acids on a ZWIX CSP in SFC mode^a

Analyte	ZWIX CSP 4					
	t_1 [min]	k_1	α	R_s	N_1 [m ⁻¹]	EO
Suprofen	3.01	4.90	1.00	0.0	12100	
Chromane-2-COOH	4.19	7.22	1.12	1.7	36500	n.d.
Naproxen	1.99	2.90	1.00	0.0	21100	
Fmoc-Abu	4.48	7.78	1.12	1.7	32900	D
Bz-Phe	4.41	7.65	1.15	2.0	35900	D
Boc-Tyr	5.36	9.51	1.00	0.0	11100	
Z-Ser	6.61	11.96	1.03	0.5	34400	D
DNB-Pro	3.52	5.90	1.14	1.9	38900	n.d.
Fmoc-Leu	3.80	6.45	1.10	1.3	34100	D
Bz-Leu	2.12	3.16	1.18	2.6	49000	D
DNB-N-Me-Leu	2.69	2.78	1.04	0.5	31700	D
Fmoc-Met	6.84	12.41	1.11	1.7	34200	n.d.

^aConditions: 25% modifier (MeOH, 100 mM HOAc, 50 mM NH₃); 4.0 mL/min, 40°C, 150 bar backpressure; detection 254 and 230 nm; $t_0 = 0.51$ min; for analyte structures see Appendix II

On the contrary, application of the ZWIX CSP in zwitterion exchange mode for enantioseparation of a few aromatic amino acids exhibited exceedingly long retention times (data not shown). We assume that the subcritical fluid mobile phase, which inherently exhibits lower dielectric constants and thus renders electrostatic interactions stronger, cannot properly balance the strong double ionic interaction between the zwitterionic SO and SA. It

seems that SFC has reached its limit of application in separation of zwitterionic compounds mediated by a double ion pairing process. However, it has to be stated that no dedicated modifier optimization was carried out (e.g. application of stronger co- and counterions) in order to potentially reduce retention times.

In conclusion, these initial studies of ZWIX CSPs in SFC mode yielded some promising results and encouraged to carry out further investigations in both anion exchange mode for separation of chiral acids and cation exchange mode for enantioseparation of chiral bases (amines). Especially, the IMCI feature of the zwitterionic selectors seems to be helpful in both ion exchange modes, thereby promoting significantly faster elution compared to their parent single-ionic WAX-type or SCX-type CSPs.

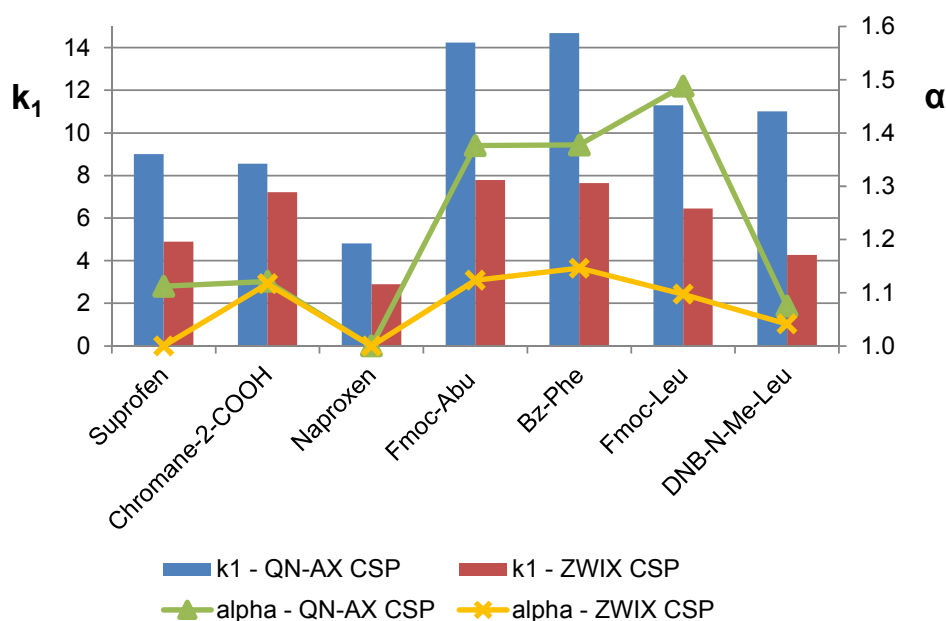


Figure 9. Retention factors of the first eluted enantiomer and alpha-values of 7 chiral acids on QN-AX- and ZWIX-CSP (column dimension 150 x 4 mm i.d., 5 μm particle size). Conditions: 25% modifier (MeOH, 100 mM HOAc, 50 mM NH₃), flow 4.0 mL/min; 40°C, 150 bar backpressure; UV detection

4 Concluding Remarks

The present dissertation describes the synthesis and chromatographic evaluation of low molecular weight ion exchange-type CSPs. The research carried out within this thesis can be categorized into two main areas:

In the first part, cinchona alkaloid-based WAX-type CSPs (QN-AX and QD-AX CSPs) were investigated in terms of (i) their chromatographic performance in SFC and (ii) their enantiodiscrimination properties for chiral sulfonic acids (or their sulfonate salts, respectively). QN-AX and QD-AX CSPs proved to be fully applicable in SFC which was manifested in similar enantioseparation properties for chiral carboxylic acids as compared to HPLC. Retention was found to be dominated by an anion-exchange mechanism and thermodynamic analysis confirmed an enthalpically controlled chiral recognition mechanism, thus resembling HPLC behavior. However, SFC exhibited the unique property of *in situ* formation of methylcarbonic acid in the sc CO₂-based methanolic mobile phase. The dissociated methylcarbonic acid functions as a counterion and thus enables elution of acidic solutes according to a stoichiometric displacement model. This finding opens up new possibilities for salt free anion exchange chromatography by application of sc CO₂ and MeOH, because the methylcarbonic acid disproportionates after pressure release.

Furthermore, QN-AX and QD-AX CSPs were applied to resolve novel chiral β -ketosulfonates in both HPLC and SFC. As enantioseparations of sulfonic acids (sulfonates) are scarcely reported in the literature, we could establish a novel straightforward method yielding high enantioselectivities and column efficiencies.

In an application study, QN-AX CSP was successfully applied for indirect chromatographic absolute configuration assignment of chiral acidic drug compounds of the pirinixic acid family. In this context, the merits and limitations of chiral chromatography for absolute configuration determination were discussed and exemplified.

In the second part of the thesis, novel zwitterionic CSPs were synthesized which were thus capable of exhibiting three modes of ion exchange, namely weak anion exchange (WAX), strong cation exchange (SCX) and, most importantly, zwitterion exchange mode (ZWIX). With the aim of carrying out detailed SO-structure – enantioselectivity relationships in the zwitterion exchange mode, structurally related zwitterionic CSPs were prepared and their enantiodiscrimination properties towards zwitterionic solutes (amino acids, small peptides) were chromatographically evaluated. In doing so, cinchona alkaloids quinine or

quinidine were derivatized at their C9 position via a carbamate bond for the introduction of structurally different sulfonic acid group comprising moieties.

Briefly, the following trends were observed: (i) an achiral side chain at the SCX site exhibited only a narrow application range for amino acids, whereas dipeptides were generally well resolved; (ii) elongation of the achiral alkyl side chain at the SCX site had only minor influence on the enantioselectivity profile of amphoteric compounds (amino acids, dipeptides); (iii) the introduction of a chiral moiety at the SCX side chain generally improved enantioselectivity for amino acids, however, in a structure dependent manner. For instance, most promising SOs incorporated 2-aminocyclohexanesulfonate or 2-isopropyl-aminoethanesulfonate moieties; (iv) elution orders of amino acid enantiomers could be inverted by switching from a quinine-based CSP to its pseudoenantiomeric quinidine-based CSP; (v) the applicability of ZWIX-CSPs is not restricted to amino acids and dipeptides, as peptidomimetics, such as tirofiban analogs, could also be baseline resolved.

Finally, apart from ZWIX-SO-structure optimization studies, also mobile phase optimization in terms of bulk solvent composition was carried out. Weakly acidic polar organic mobile phases were found to be the most favorable elution mode. Thereby, it was found that certain amounts of acetonitrile, as an aprotic co-modifier, in protic methanol substantially increased enantioselectivity and resolution of amino acids in a structure-dependent manner.

5 References

- [1] E. Francotte, in: E. Francotte, W. Lindner (Eds.) *Chirality in Drug Research*, Wiley-VCH, Weinheim, 2006, pp. 155-187.
- [2] E. Francotte, *Journal of Chromatography A*, 906 (2001) 379-397.
- [3] T.J. Ward, K.D. Ward, *Analytical Chemistry*, 82 (2010) 4712-4722.
- [4] N.M. Maier, P. Franco, W. Lindner, *Journal of Chromatography A*, 906 (2001) 3-33.
- [5] M. Lämmerhofer, *Journal of Chromatography A*, 1217 (2010) 814-856.
- [6] S. Andersson, in: G. Subramanian (Ed.) *Chiral Separation Techniques - A Practical Approach*, Wiley-VCH, Weinheim, 2007, pp. 585-599.
- [7] S. Andersson, S. Allenmark, *Journal of Biochemical and Biophysical Methods*, 54 (2002) 11-23.
- [8] A. Rajendran, G. Paredes, M. Mazzotti, *Journal of Chromatography A*, 1216 (2009) 709-738.
- [9] E. Francotte, *Chimia*, 63 (2009) 867-871.
- [10] G. Cancelliere, A. Ciogli, I. D'Acquarica, F. Gasparrini, J. Kocergin, D. Misiti, M. Pierini, H. Ritchie, P. Simone, C. Villani, *Journal of Chromatography A*, 1217 (2010) 990-999.
- [11] K. Lomsadze, G. Jibuti, T. Farkas, B. Chankvetadze, *Journal of Chromatography A*, 1234 (2012) 50-55.
- [12] L.T. Taylor, *Analytical Chemistry*, 82 (2010) 4925-4935.
- [13] L.T. Taylor, *The Journal of Supercritical Fluids*, 47 (2009) 566-573.
- [14] G. Guiochon, A. Tarafder, *Journal of Chromatography A*, 1218 (2011) 1037-1114.
- [15] T. Berger, B. Berger, R.E. Majors, *LC-GC North America*, (2010).
- [16] C.J. Giddings, M. Meyers, L.M. McLaren, R.A. Keller, *Science*, 162 (1968) 67-73.
- [17] K.W. Phinney, *Analytical and Bioanalytical Chemistry*, 382 (2005) 639-645.
- [18] D. Mangelings, Y. Vander Heyden, *Journal of Separation Science*, 31 (2008) 1252-1273.
- [19] G. Terfloth, *Journal of Chromatography A*, 906 (2001) 301-307.
- [20] L.T. Taylor, *Journal of Chromatography A*, DOI:10.1016/j.chroma.2012.02.037 (2012).
- [21] T.A. Berger, *Journal of Chromatography A*, 1218 (2011) 4559-4568.
- [22] T. Berger, *Chromatographia*, 72 (2010) 597-602.
- [23] L.H. Easson, E. Stedman, *Biochemistry Journal*, 27 (1933) 1257-1266.
- [24] C.E. Dalgliesh, *Journal of the Chemical Society (Resumed)*, (1952) 3940-3940.

- [25] V.A. Davankov, *Chirality*, 9 (1997) 99-102.
- [26] W.H. Pirkle, T.C. Pochapsky, *Chemical Reviews*, 89 (1989) 347-362.
- [27] S. Topiol, M. Sabio, *Journal of the American Chemical Society*, 111 (1989) 4109-4110.
- [28] T.D. Booth, D. Wahnon, I.W. Wainer, *Chirality*, 9 (1997) 96-98.
- [29] A.D. Mesecar, D.E. Koshland, *Nature*, 403 (2000) 614-615.
- [30] N.M. Maier, W. Lindner, in: E. Francotte, W. Lindner (Eds.) *Chirality in Drug Research*, Wiley-VCH, Weinheim, 2006, pp. 189-260.
- [31] J. Haginaka, *Journal of Chromatography A*, 906 (2001) 253-273.
- [32] S. Allenmark, *Journal of Liquid Chromatography*, 9 (1986) 425.
- [33] C. Divne, J. Ståhlberg, T. Reinikainen, L. Ruohonen, G. Pettersson, J. Knowles, T. Teeri, T.A. Jones, *Science*, 265 (1994) 524.
- [34] T.C. Pinkerton, W.J. Howe, E.L. Urlich, J.P. Comiskey, J. Haginaka, T. Murashima, W.F. Walkenhorst, W.M. Westler, J.L. Markley, *Analytical Chemistry*, 67 (1995) 2354.
- [35] T. Fornstedt, P. Sajonz, G. Guiochon, *Journal of the American Chemical Society*, 119 (1997) 1254-1264.
- [36] T. Fornstedt, G. Götmar, M. Andersson, G. Guiochon, *Journal of the American Chemical Society*, 121 (1999) 1164-1174.
- [37] P. Franco, A. Senso, L. Oliveros, C. Minguillón, *Journal of Chromatography A*, 906 (2001) 155-170.
- [38] L. Thunberg, J. Hashemi, S. Andersson, *Journal of Chromatography B*, 875 (2008) 72-80.
- [39] H. Nelander, S. Andersson, K. Öhlén, *Journal of Chromatography A*, 1218 (2011) 9397-9405.
- [40] F. Vögtle, A. Hünten, E. Vogel, S. Buschbeck, O. Safarowsky, J. Recker, A.H. Parham, M. Knott, W.M. Müller, U. Müller, Y. Okamoto, T. Kubota, W. Lindner, E. Francotte, S. Grimme, *Angewandte Chemie International Edition*, 40 (2001) 2468-2471.
- [41] P. Franco, T. Zhang, *Journal of Chromatography B*, 875 (2008) 48-56.
- [42] C. Wang, D.W. Armstrong, D.S. Risley, *Analytical Chemistry*, 79 (2007) 8125-8135.
- [43] P. Sun, D.W. Armstrong, *Journal of Chromatography A*, 1217 (2010) 4904-4918.
- [44] Y. Zhao, W. Pritts, S. Zhang, *Journal of Chromatography A*, 1189 (2008) 245-253.
- [45] A. Medvedovici, P. Sandra, L. Toribio, F. David, *Journal of Chromatography A*, 785 (1997) 159-171.
- [46] M. Johannsen, *Journal of Chromatography A*, 937 (2001) 135-138.

- [47] Y. Okamoto, E. Yashima, *Angewandte Chemie International Edition*, 37 (1998) 1020-1043.
- [48] D.W. Armstrong, Y. Tang, S. Chen, Y. Zhou, C. Bagwill, J.-R. Chen, *Analytical Chemistry*, 66 (1994) 1473-1484.
- [49] T.J. Ward, A.B. Farris Iii, *Journal of Chromatography A*, 906 (2001) 73-89.
- [50] A. Berthod, Y. Liu, C. Bagwill, D.W. Armstrong, *Journal of Chromatography A*, 731 (1996) 123-137.
- [51] D.W. Armstrong, Y. Liu, K.H. Ekborgott, *Chirality*, 7 (1995) 474-497.
- [52] K.H. Ekborg-Ott, Y. Liu, D.W. Armstrong, *Chirality*, 10 (1998) 434-483.
- [53] Berger, *Journal of Chromatography A*, 785 (1997) 3-33.
- [54] A. Berthod, X. Chen, J.P. Kullman, D.W. Armstrong, F. Gasparrini, I. D'Acquaric, C. Villani, A. Carotti, *Analytical Chemistry*, 72 (2000) 1767-1780.
- [55] S. Alcaro, I. D'Acquarica, F. Gasparrini, D. Misiti, M. Pierini, C. Villani, *Tetrahedron: Asymmetry*, 13 (2002) 69-75.
- [56] I. Ilisz, R. Berkecz, A. Péter, *Journal of Separation Science*, 29 (2006) 1305-1321.
- [57] Z. Pataj, I. Ilisz, A. Aranyi, E. Forró, F. Fülöp, D.W. Armstrong, A. Péter, *Chromatographia*, 71 (2010) 13-19.
- [58] I. D'Acquarica, F. Gasparrini, D. Misiti, C. Villani, A. Carotti, S. Cellamare, S. Muck, *Journal of Chromatography A*, 857 (1999) 145-155.
- [59] Y. Liu, A. Berthod, C.R. Mitchell, T.L. Xiao, B. Zhang, D.W. Armstrong, *Journal of Chromatography A*, 978 (2002) 185-204.
- [60] G. Lavison, D. Thiébaud, *Chirality*, 15 (2003) 630-636.
- [61] D.H. Williams, B. Bardsley, *Angewandte Chemie International Edition*, 38 (1999) 1172-1193.
- [62] A. Cavazzini, G. Nadalini, F. Dondi, F. Gasparrini, A. Ciogli, C. Villani, *Journal of Chromatography A*, 1031 (2004) 143-158.
- [63] R.J. Steffek, Y. Zelechok, *Journal of Chromatography A*, 983 (2003) 91-100.
- [64] M.H. Hyun, *Journal of Separation Science*, 26 (2003) 242-250.
- [65] M.H. Hyun, J.S. Jin, W. Lee, *Journal of Chromatography A*, 822 (1998) 155-161.
- [66] R.R. Weikel, J.P. Hallett, C.L. Liotta, C.A. Eckert, *Topics in Catalysis*, 37 (2006) 75.
- [67] V.A. Davankov, *Journal of Chromatography A*, 666 (1994) 55-76.
- [68] V.A. Davankov, *Journal of Chromatography A*, 1000 (2003) 891-915.
- [69] B. Natalini, R. Sardella, G. Carbone, A. Macchiarulo, R. Pellicciari, *Analytica Chimica Acta*, 638 (2009) 225-233.

- [70] N. Sanaie, C.A. Haynes, *Journal of Chromatography A*, 1104 (2006) 164-172.
- [71] M. Sinibaldi, M. Flieger, L. Cvak, A. Messina, A. Pichini, *Journal of Chromatography A*, 666 (1994) 471-478.
- [72] P. Padiglioni, C.M. Polcaro, S. Marchese, M. Sinibaldi, M. Flieger, *Journal of Chromatography A*, 756 (1996) 119-127.
- [73] A. Messina, A.M. Girelli, M. Flieger, M. Sinibaldi, P. Sedmera, L. Cvak, *Analytical Chemistry*, 68 (1996) 1191-1196.
- [74] J. Olšovská, M. Flieger, F. Bachechi, A. Messina, M. Sinibaldi, *Chirality*, 11 (1999) 291-300.
- [75] C. Rosini, C. Bertucci, D. Pini, P. Altemura, P. Salvadori, *Chromatographia*, 24 (1987) 671-676.
- [76] M. Lämmerhofer, W. Lindner, *Journal of Chromatography A*, 741 (1996) 33-48.
- [77] A. Mandl, L. Nicoletti, M. Lämmerhofer, W. Lindner, *Journal of Chromatography A*, 858 (1999) 1-11.
- [78] N.M. Maier, S. Schefzick, G.M. Lombardo, M. Feliz, K. Rissanen, W. Lindner, K.B. Lipkowitz, *Journal of the American Chemical Society*, 124 (2002) 8611-8629.
- [79] C. Hellriegel, U. Skogsberg, K. Albert, M. Lämmerhofer, N.M. Maier, W. Lindner, *Journal of the American Chemical Society*, 126 (2004) 3809-3816.
- [80] J. Lah, N.M. Maier, W. Lindner, G. Vesnaver, *The Journal of Physical Chemistry B*, 105 (2001) 1670-1678.
- [81] M. Lämmerhofer, P. Franco, W. Lindner, *Journal of Separation Science*, 29 (2006) 1486-1496.
- [82] W. Bicker, I. Chiorescu, V.B. Arion, M. Lämmerhofer, W. Lindner, *Tetrahedron: Asymmetry*, 19 (2008) 97-110.
- [83] M. Lämmerhofer, W. Lindner, *Liquid Chromatographic Enantiomer Separation and Chiral Recognition by Cinchona Alkaloid-Derived Enantioselective Separation Materials*, in: N. Grinberg, E. Grushka (Eds.) *Advances in Chromatography*, CRC Press, Boca Raton, FL, 2007.
- [84] C.V. Hoffmann, M. Lämmerhofer, W. Lindner, *Journal of Chromatography A*, 1161 (2007) 242-251.
- [85] C. Hoffmann, M. Lämmerhofer, W. Lindner, *Analytical and Bioanalytical Chemistry*, 393 (2009) 1257-1265.
- [86] C.V. Hoffmann, R. Pell, M. Lämmerhofer, W. Lindner, *Analytical Chemistry*, 80 (2008) 8780-8789.

- [87] C.V. Hoffmann, R. Reischl, N.M. Maier, M. Lämmerhofer, W. Lindner, *Journal of Chromatography A*, 1216 (2009) 1147-1156.
- [88] R. Sardella, M. Lämmerhofer, B. Natalini, W. Lindner, *Chirality*, 20 (2008) 571-576.
- [89] C.V. Hoffmann, R. Reischl, N.M. Maier, M. Lämmerhofer, W. Lindner, *Journal of Chromatography A*, 1216 (2009) 1157-1166.
- [90] J. Ståhlberg, *Journal of Chromatography A*, 855 (1999) 3-55.
- [91] W. Kopaciewicz, M.A. Rounds, J. Fausnaugh, F.E. Regnier, *Journal of Chromatography A*, 266 (1983) 3-21.
- [92] M.C. Millot, T. Debranche, A. Pantazaki, I. Gherghi, B. Sébille, C. Vidal-Madjar, *Chromatographia*, 58 (2003) 365-373.
- [93] B. Sellergren, K.J. Shea, *Journal of Chromatography A*, 654 (1993) 17-28.
- [94] N. Harada, *Chirality*, 20 (2008) 691-723.
- [95] H.D. Flack, G. Bernardinelli, *Chirality*, 20 (2008) 681-690.
- [96] D. Parker, *Chemical Reviews*, 91 (1991) 1441-1457.
- [97] J.M. Seco, E. Quiñoá, R. Riguera, *Chemical Reviews*, 104 (2004) 17-118.
- [98] W. Bicker, K. Kacprzak, M. Kwit, M. Lämmerhofer, J. Gawronski, W. Lindner, *Tetrahedron: Asymmetry*, 20 (2009) 1027-1035.
- [99] P.J. Stephens, F.J. Devlin, F. Gasparrini, A. Ciogli, D. Spinelli, B. Cosimelli, *The Journal of Organic Chemistry*, 72 (2007) 4707-4715.
- [100] T.B. Freedman, X. Cao, R.K. Dukor, L.A. Nafie, *Chirality*, 15 (2003) 743-758.
- [101] C. Roussel, A.D. Rio, J. Pierrot-Sanders, P. Piras, N. Vanthuyne, *Journal of Chromatography A*, 1037 (2004) 311-328.
- [102] J.P. Hallett, P. Pollet, C.L. Liotta, C.A. Eckert, *Accounts of Chemical Research*, 41 (2008) 458.
- [103] S.A. Ashraf, L.A.P. Kane-Maguire, S.G. Pyne, G.G. Wallace, *Macromolecules*, 31 (1998) 8737-8734.
- [104] F.M. Cordero, M. Cacciarini, F. Machetti, F. De Sarlo, *European Journal of Organic Chemistry*, (2002) 1407-1411.
- [105] B. Preinerstorfer, C. Hoffmann, D. Lubda, M. Lämmerhofer, W. Lindner, *Electrophoresis*, 29 (2008) 1626-1637.
- [106] J. Xu, S. Xu, *Synthesis*, (2004) 276-282.
- [107] L. Hu, H. Zhu, D.-M. Du, J. Xu, *The Journal of Organic Chemistry*, 72 (2007) 4543-4546.

- [108] B. Wang, W. Zhang, L. Zhang, D.-M. Du, G. Liu, J. Xu, *European Journal of Organic Chemistry*, (2008) 350-355.
- [109] J. Xu, *Tetrahedron: Asymmetry*, 13 (2002) 1129-1134.
- [110] W. Zhang, B. Wang, N. Chen, D.-M. Du, J. Xu, *Synthesis*, (2008) 0197-0200.
- [111] N. Chen, W. Jia, J. Xu, *European Journal of Organic Chemistry*, (2009) 5841-5846.

6 List of Publications and Manuscripts

Appendix I

M. Lämmerhofer, R. Pell, M. Mahut, M. Richter, S. Schiesel, H. Zettl, M. Dittrich, M. Schubert-Zsilavec, W. Lindner. *Enantiomer separation and indirect chromatographic absolute configuration prediction of chiral pirinixic acid derivatives: Limitations of polysaccharide-type chiral stationary phases in comparison to chiral anion-exchangers*
Journal of Chromatography A 2010, 1217, 1033-1040

Appendix II

R. Pell, W. Lindner. *Potential of Chiral Anion-Exchangers Operated in Various Subcritical Fluid Chromatography Modes for Resolution of Chiral Acids*
Journal of Chromatography A 2012, in press

Appendix III

R. Pell, G. Schuster, M. Lämmerhofer, W. Lindner. *Enantioseparation of Chiral Sulfonates by Liquid Chromatography and Subcritical Fluid Chromatography*
Journal of Separation Science, accepted 25th May 2012

Appendix IV

S. Wernisch, R. Pell, W. Lindner. *Increments to chiral recognition facilitating enantiomer separations of chiral acids, bases, and ampholytes using Cinchona-based zwitterion exchanger chiral stationary phases*
Journal of Separation Science 2012, in press

Appendix V

R. Pell, S. Sić, W. Lindner. *Mechanistic investigations of cinchona alkaloid-based zwitterionic chiral stationary phases*
Journal of Chromatography A, submitted

Appendix VI

M. Bollinger, F. Manzenrieder, R. Kolb, A. Bochen, S. Neubauer, L. Marinelli, V. Limongelli, E. Novellino, G. Moessmer, R. Pell, W. Lindner, J. Fanous, A. Hoffman, H. Kessler. *Tailoring of Integrin Ligands: Probing the Charge Capability of the Metal Ion-Dependent Adhesion Site*
Journal of Medicinal Chemistry 2012, 55, 871-882

APPENDIX I



Enantiomer separation and indirect chromatographic absolute configuration prediction of chiral pirinixic acid derivatives: Limitations of polysaccharide-type chiral stationary phases in comparison to chiral anion-exchangers

Michael Lämmerhofer^{a,*}, Reinhard Pell^a, Marek Mahut^a, Martin Richter^a, Simone Schiesel^a, Heiko Zettl^b, Michaela Dittrich^b, Manfred Schubert-Zsilavec^b, Wolfgang Lindner^a

^a Christian-Doppler Laboratory for Molecular Recognition Materials, University of Vienna, Department of Analytical Chemistry & Food Chemistry, Waehringer Strasse 38, A-1090 Vienna, Austria

^b Institute of Pharmaceutical Chemistry/ZAFES/LiFF, Goethe-University Frankfurt, Max-von-Laue-Strasse 9, D-60348 Frankfurt/M., Germany

ARTICLE INFO

Article history:

Available online 21 October 2009

Keywords:

Chiral stationary phase
Chiral anion-exchanger
Quinine and quinidine carbamates
Polysaccharide
Amylose
tris(3,5-dimethylphenylcarbamate)
Chiral separation
HPLC
Pirinixic acid derivatives
2-Aryloxyalkanoic acids
2-Arylthioalkanoic acids
Enantioselective synthesis
Peroxisome proliferator activated receptors (PPAR)

ABSTRACT

Chiral α -arylthiocarboxylic acids with different substitution patterns, representing new pirinixic acid derivatives with dual PPAR α/γ agonistic activities, have been separated into enantiomers on *tert*-butylcarbamoylquinine and quinidine based chiral anion-exchangers and amylose tris(3,5-dimethylphenylcarbamate) coated silica on analytical and preparative scale. Absolute configurations of individual enantiomers were assigned chromatographically via elution orders on the chiral anion-exchangers and were confirmed by stereoselective syntheses via Ewans auxiliaries that have lead to enantiomeric products with known absolute configurations. The results of both methods were in full agreement. Moreover, the receptor stereoselectivity in PPAR α transactivation activities was consistent within the test set of structurally related compounds. Limited correlation (between elution order and substitution) was observed within the set of α -arylthiocarboxylic acids on the amylose tris(3,5-dimethylphenylcarbamate) based chiral stationary phase (CSP), in particular the elution order changed with remote substitution. This clearly demonstrates the risks of chromatographic absolute configuration assignments by prediction from one structural analog to another one, especially with CSPs such as polysaccharide CSPs that are recognized for their broad applicability due to multiple binding and chiral recognition modes. It is therefore of utmost importance that such chromatographic absolute configuration predictions by extrapolation to structural analogs are combined with orthogonal methods for verification of the results.

© 2009 Elsevier B.V. All rights reserved.

1. Introduction

Pirinixic acid (Fig. 1) has been proposed as a moderate agonist of alpha and gamma peroxisome proliferator activated receptors (PPAR). It represents a potential lead structure for the development of new chemical entities for treatment of metabolic disorders such as dyslipidemia and type 2 diabetes. Alkyl substitution in α -position to the carboxylic acid group yields chiral pirinixic acid derivatives with enhanced PPAR alpha and gamma activities which can be further optimized by variation of the aryl-substitution pattern [1]. Through α -substitution chiral α -arylthio carboxylic acids are obtained for which enantioselectivities in terms of PPAR activation have to be considered.

Drug discovery of such chiral compounds involves the synthesis of individual enantiomers for biological activity tests and requires the determination of absolute configurations of the enantiomeric compounds as stereochemical descriptors to pinpoint their identity [2]. Preparative liquid chromatography is a viable route for straightforward and rapid access to both enantiomers with little efforts and minimal time for method development [3]. It provides the target enantiomers in high enantiomeric purities and yields. The most common methodologies for absolute configuration assignment nowadays [4–6] are NMR [5,7–13], X-ray diffraction analysis [5,9–11,14–22] and circular dichroism (CD) spectroscopy [19,23,24] (including VCD [4,17,23,25,26]). Single-crystal X-ray diffraction analysis is the most preferred direct method to determine absolute configurations. Yet, it is only amenable for enantiomeric compounds that provide crystals with adequate resonant scattering and has also some caveats especially for compounds which contain only light atoms (as critically reviewed recently by Flack and Bernardinelli [27]). It requires

* Corresponding author. Tel.: +43 1 4277 52323; fax: +43 1 4277 9523.
E-mail address: Michael.Laemmerhofer@univie.ac.at (M. Lämmerhofer).

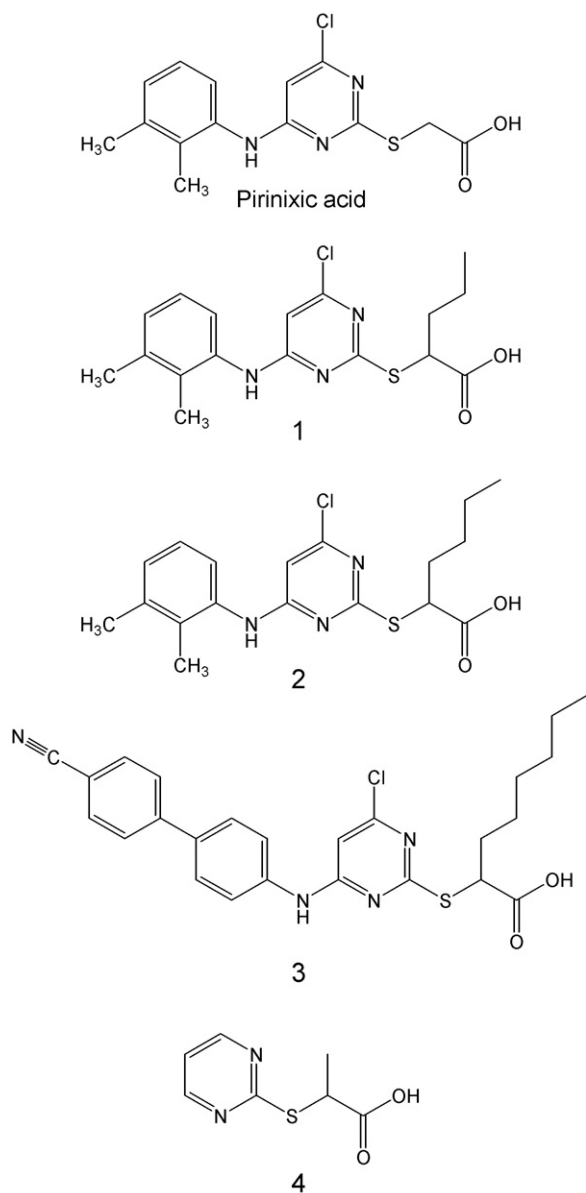


Fig. 1. Pirinixic acid and chiral α -arylthiocarboxylic acid analogs that have been investigated in the present study.

critical evaluation of characteristic parameters such as the Flack parameter which is sometimes not reported yet indicates satisfactory absolute-structure determination, in order to avoid erroneous results [27]. By means of CD and VCD absolute configurations can be determined by comparison of experimental CD or VCD spectra with those that have been calculated by quantum chemistry calculations. Agreement between calculated and experimental spectra is an indication for a correct absolute configuration assignment.

For sake of simplicity indirect methods such as assignment of absolute configurations by chromatographic elution orders have also been frequently employed [4,28–32]. It is based on the knowledge of the absolute configuration of a structurally related reference compound which follows the same chiral recognition mechanism in the chromatographic enantiomer separation process on a given chiral stationary phase [4]. It is a simple, straightforward and cheap methodology which can be employed for a larger set of structurally related compounds, yet requires some deeper understanding on how the chiral stationary phase recognizes and distinguishes enantiomers for a given class of test solutes featuring

more or less structural variability. Unfortunately, chiral recognition mechanisms on chiral stationary phases may be sensitive to even minor structural or conditional changes. This becomes clearly evident, for instance, by reversals of elution orders upon minor variations of experimental conditions such as changes of modifier type [33,34] or percentage [34,35]. It has also been reported that elution orders can be reversed upon deposition of polysaccharide selectors onto the silica surface from distinct solvents, i.e. with slightly altered preparation conditions, probably due to altered supramolecular structures of the polymeric selectors [36]. Last but not least, numerous examples can be found in the literature that showed reversals of elution orders on a given CSP with minute structural alterations within a homologous compound series, i.e. of structurally closely related compounds [37,38]. In particular the latter phenomenon poses some serious risks on the chromatographic absolute configuration assignment which is based on consistent elution orders within a series of structural homologs. Therefore, it exists consensus that verification of the chromatographic absolute configuration assignment must be performed by a second independent methodology in order to minimize the risk for false assignments.

Herein we report on a methodology for the chromatographic enantiomer separation of pirinixic acid analogs (Fig. 1) by enantioselective liquid chromatography as well as the absolute configuration assignment after preparative chromatographic resolution. Absolute configuration determinations were confirmed by independent methods such as chemical correlations via stereoselective synthesis and consistency in receptor subtype enantioselectivity. The risk of false assignments is illustrated by use of two distinct types of chiral stationary phases, low molecular brush-type chiral anion-exchangers (Chiralpak QD-AX and QN-AX) and polymeric type CSP based on a polysaccharide selector (Chiralpak AD-H), which differed in their consistencies of chiral recognition mechanisms within the set of investigated solutes, i.e. of chiral 2-arylthiocarboxylic acids.

2. Experimental

2.1. Materials

The pirinixic acid analogs **1–3** were synthesized as described elsewhere [1]. Enantiomers of **4** were synthesized as described below. The α -aryloxycarboxylic acid reference compounds **5–8** were research samples from former studies. Dichlorprop-, 2-(2,4-dichlorophenoxy)propionic acid **9**, was supplied by Aldrich (Sigma–Aldrich, Vienna, Austria).

For enantioselective HPLC 150 mm \times 4 mm I.D. Chiralpak QD-AX and QN-AX (5 μ m diameter particles) as well as a 250 mm \times 4 mm I.D. Chiralpak AD-H (5 μ m) from Chiral Technologies Europe (Illkirch, France) were employed as columns. (S)-(–)- and (R)-(+)-2-bromopropionic acid, caesium carbonate, and 2-mercaptopyrimidine were from Sigma–Aldrich (Vienna, Austria). Methanol (gradient grade), n-heptane and 2-propanol (both HPLC grade) were supplied by Merck (Darmstadt, Germany). Trifluoroacetic acid (TFA) was from Fluka. DMF (purum >99%, Fluka, Vienna, Austria), toluene (>99%, VWR, Vienna) and ethyl acetate (technical quality) were used as solvents for the synthesis.

2.2. Enantioselective HPLC experiments

Chromatographic measurements were carried out on a 1100 Series HPLC system from Agilent Technologies (Waldbronn, Germany) equipped with an autosampler, a binary pump, a degasser for the mobile phase, and a multiple wavelength detector (MWD). In some preliminary runs an optical rotation detector OR-990

Table 1
Chromatographic data.

Compound	Chiralpak QD-AX ^a				Chiralpak QN-AX ^a				Chiralpak AD-H ^b			
	<i>k</i> ₁	α	<i>R</i> _S	e.o.	<i>k</i> ₁	α	<i>R</i> _S	e.o.	<i>k</i> ₁	α	<i>R</i> _S	e.o.
1	2.53	1.33	2.4	(<i>R</i>)-(+)<(<i>S</i>)-(-)	2.66	1.21	1.8	(<i>S</i>)-(-)<(<i>R</i>)-(+)	0.49	1.23	1.8	<i>S</i> < <i>R</i>
2	1.98	1.30	2.3	(<i>R</i>)-(+)<(<i>S</i>)-(-)	2.52	1.20	1.7	(<i>S</i>)-(-)<(<i>R</i>)-(+)	0.47	1.25	1.9	<i>S</i> < <i>R</i>
3	5.04	1.77	6.5	<i>R</i> < <i>S</i>	5.31	1.83	7.2	<i>S</i> < <i>R</i>	2.14	1.68	6.4	<i>R</i> < <i>S</i>
4	8.70 ^c	1.03	0.6	<i>R</i> < <i>S</i>	1.96 ^d	1.06	1.0	<i>S</i> < <i>R</i>	1.25	1.12	1.7	<i>S</i> < <i>R</i>

^a Methanol–glacial acetic acid–ammonium acetate (98:2:0.5; v/v/w); 25 °C; 1 mL/min; 150 mm × 4 mm I.D.

^b Heptane–2-propanol–TFA (80:20:0.1; v/v/v); flow rate, 1 mL/min; temperature, ambient; 250 mm × 4 mm I.D.

^c Methanol–glacial acetic acid (98:2; v/v); flow rate, 0.25 mL/min; temperature, 25 °C.

^d Methanol–glacial acetic acid–ammonium acetate (98:2:0.5; v/v/w); 25 °C; flow 0.25 mL/min.

from Jasco (Gross-Umstadt, Germany) was coupled in series with a Corona charged aerosol detector (CAD) (ESA Analytical, Aylesbury, UK) to monitor the sign of optical rotation for the individual enantiomers. For analytical separations the sample was dissolved in methanol (Chiralpak QN-AX and QD-AX) and *n*-heptane/2-propanol (80:20; v/v) (Chiralpak AD-H), respectively, at a concentration of about 0.5 mg/mL and an aliquot of 2 μ L was injected. UV detection was performed at 250 nm. The column temperature was kept constant at 25 °C. The data analysis was performed with the Chemstation chromatographic data software from Agilent Technologies. The chromatographic results are summarized in Table 1.

Preparative chromatography runs were carried out on a VWR EliteChrom HPLC System equipped with a quaternary gradient pump, a UV detector, a manual injector from Rheodyne with a 500 μ L loop. The data were acquired and processed by EZ-Chrom software. The column was a 150 mm × 4 mm I.D. Chiralpak QD-AX. Separations were performed at ambient temperature employing an eluent consisting of a mixture of methanol–acetic acid–ammonium acetate (98:2:0.5; v/v/w) and a flow rate of 1 mL/min. The detection wavelength was 250 nm. For preparative scale separations on Chiralpak QD-AX, the sample was dissolved in methanol at a concentration of about 20 mg/mL. Depending on the type of solute and separation factor, about 5–10 mg sample masses per run were injected onto the analytical 150 mm × 4 mm I.D. column. Individual enantiomer fractions were collected separately and the combined fractions were evaporated to dryness. The obtained residues were extracted from slightly HCl-acidic saturated brine solution into ethyl acetate. The combined organic phases were dried over Na₂SO₄, filtrated and evaporated to dryness yielding the final enantiomeric products. Enantiomeric excess values of the obtained enantiomers are summarized in Table 2.

2.3. Synthesis of 2-(pyrimidin-2-ylthio)propionic acid (**4**) enantiomers

2.3.1. Synthesis

First, 0.50 g (4.5 mmol) of 2-mercaptopyrimidine was converted into its caesium salt by addition of 0.5 equiv. of Cs₂CO₃ (methanolic solution, 0.72 g, 2.25 mmol). After stirring for 1 h the solvent was evaporated and the residue dissolved in 40 mL of

DMF (turbid solution). 1 equiv. (0.40 mL, 4.5 mmol) of (*S*)- or (*R*)-2-bromopropionic acid was added with a Hamilton syringe. The reaction mixture was stirred at room temperature (r.t.) for 14 h under N₂-atmosphere. The reaction progress was controlled by TLC (eluent: ethyl acetate–methanol (9/1); *R*_f = 0.49).

After that DMF was evaporated, the residue suspended in toluene and again evaporated to remove all of the DMF. The crude product was extracted with an acidic (pH ~ 3–4), saturated NaCl-solution and ethyl acetate. The aqueous phase was washed with ethyl acetate (3 × 20 mL) and the combined organic phases were dried over MgSO₄. After evaporation of the solvent a yellowish or white powder was furnished.

(*R*)-2-(pyrimidin-2-ylthio)-propionic acid (from (*S*)-(+)-2-bromopropionic acid): yield: 88% of a yellowish powder; enantiomeric excess (ee), 57%.

(*S*)-2-(pyrimidin-2-ylthio)-propionic acid (from (*R*)-(+)-2-bromopropionic acid): yield: 95% of a white powder; ee, 89%.

2.3.2. Characterization

¹H NMR and ¹³C NMR were recorded at room temperature with a Bruker DRX400 spectrometer. Spectra were recorded in CD₃OD and the solvent signals were used as reference. Raw data were processed with SpinWorks Version 2.5.5. software. ESI-mass spectra were recorded on a PE Sciex API 365 spectrometer. Analytical thin-layer chromatography (TLC) was performed on Kieselgel 60 F₂₅₄ plates from Merck (Darmstadt, Germany).

NMR and MS spectra were identical for both enantiomers, as expected.

¹H NMR [CD₃OD]: δ = 1.60 (3H, d, *J* = 7.5 Hz), 4.49 (1H, q, *J* = 22.0 Hz), 7.13 (1H, t, *J* = 10.0 Hz), 8.56 (2H, d, *J* = 4.9 Hz); MS (ESI, negative): 182.8 [M–H][–].

3. Results and discussion

3.1. Analytical and preparative HPLC

Chiral pirinixic acid derivatives and analogs, respectively, are prime candidates to be separated into enantiomers on *O*-9-(*tert*-butylcarbamoyl)quinidine and corresponding quinine-based chiral stationary phases (Fig. 2) [30,31,39–41]. These acidic compounds are retained on such CSPs according to a primary anion-exchange

Table 2
Enantiomeric excess (%) and CSP employed for preparative scale separation of pirinixic acid analogs on Chiralpak QD-AX as well as their PPAR α activity [1].

	ee (%)	PPAR α activity, EC ₅₀ (μ M) \pm SD (rel. activation compared to control means \pm SD)
(<i>R</i>)- 1	94	2.2 \pm 0.1 (151 \pm 4%)
(<i>S</i>)- 1	93	9.7 \pm 0.3 (147 \pm 3%)
(<i>R</i>)- 2	91	0.5 \pm 0.2 (159 \pm 26%)
(<i>S</i>)- 2	93	5.61 \pm 0.7 (166 \pm 14%)
(<i>R</i>)- 3	99	0.03 \pm 0.005 (113 \pm 4%)
(<i>S</i>)- 3	97	2.2 \pm 0.4 (147 \pm 13%)

Table 3
Enantiomer separation data of reference aryloxy carboxylic acids^a.

Compound	R	Ar	Chiralpak QN-AX			Chiralpak QD-AX			Chiralpak AD-H		
			<i>k</i> ₁	α	e.o.	<i>k</i> ₁	α	e.o.	<i>k</i> ₁	α	e.o.
			Mobile phase, methanol–acetic acid–ammonium acetate (98:2:0.5; v/v/w)						Mobile phase, heptane–2-propanol (80:20; v/v)+0.1% (v/v) TFA		
5	CH ₃	2-Naphthyl	2.78	1.17	S<R	2.73	1.24	R<S	0.71	1.33	S<R
6	CH ₃	4-Chlorophenyl	1.93	1.08	S<R	1.90	1.18	R<S	0.57	1.50	S<R
7	C ₂ H ₅	4-Chlorophenyl	1.67	1.13	S<R	1.70	1.19	R<S	0.54	1.25	S<R
8	CH(CH ₃) ₂	4-Chlorophenyl	1.52	1.21	S<R	1.44	1.18	R<S	0.44	1.10	R<S
9 (Dichloroprop)	CH ₃	2,4-Dichlorophenyl	2.38	1.21	S<R	2.47	1.42	R<S	0.40	1.88	S<R
			Mobile phase, methanol–0.1 M ammonium acetate buffer (80:20; v/v) (pH=6.0)								
5	CH ₃	2-Naphthyl	11.10	1.11	S<R	1.61	1.18	R<S	–	–	–
6	CH ₃	4-Chlorophenyl	7.59	1.08	S<R	1.00	1.15	R<S	–	–	–
7	C ₂ H ₅	4-Chlorophenyl	7.09	1.09	S<R	n.d.	–	–	–	–	–
9 (Dichloroprop)	CH ₃	2,4-Dichlorophenyl	10.94	1.19	S<R	7.21	1.29	R<S	–	–	–

^a Experimental conditions: flow rate, 1 mL/min; temperature, 25 °C.

retention process. Hence, the eluent must contain a certain amount of chiral acids and counter-ions, respectively, that compete for binding at the ion-exchange site and allow the elution of solutes by their displacement from these primary interaction sites. A methanol-based mobile phase consisting of acetic acid and ammonium acetate providing counter- and co-ions was employed in the first instance for separation of the target solutes. The enantiomer separation results obtained with these two anion-exchangers are summarized in Table 1. It is obvious that arylthiocarboxylic acids with electron-withdrawing chlorine substitution (compounds **1**, **2**, and **3**) are much better separated than the analog which lacks such an electron-withdrawing group (**4**). These trends give rise to the conclusion that the aromatic moiety of the solutes is involved in π - π -interactions with the electron-rich quinoline moiety of cinchona alkaloid derived selectors. This points towards a chiral recognition mechanism resembling that of aryloxy carboxylic acids of the type Ar–X–CH(R₁)–COOH with X being –O– for which the enantioselectivity factor α increased with the electron-withdrawing effect of the aromatic substituents (Table 3) [42]. Fig. 3 depicts chromatograms of separations obtained for **1** and **2** on quinidine and quinine carbamate-based anion-exchangers with charged aerosol detector (CAD) along with optical rotation detector (ORD) traces (corrected for delay times between detectors). It is worth noting that elution orders are reversed when the quinidine based CSP is exchanged for its quinine-based counterpart (Fig. 3). This “pseudo-enantiomeric” behaviour of quinidine- and quinine-derived CSPs which possess opposite configurations at the stereogenic centers of C8 and C9 (Fig. 1), but equal configurations in positions 1, 3, and 4 is also in agreement with what is known from corresponding α -aryloxy carboxylic acid type herbi-

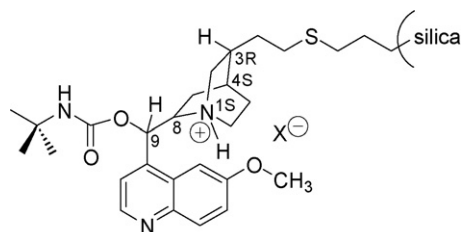


Fig. 2. Quinine and quinidine carbamate-based chiral stationary phases. Chiralpak QN-AX: (8S,9R), quinine derived; Chiralpak QD-AX: (8R,9S), quinidine derived.

cides. Fig. 4 shows the enantiomer separation of compound **3** on the quinine carbamate CSP.

Chromatographic separations of compounds **1**, **2**, and **3** were finally performed preparatively in 20–100 mg scale employing the quinidine carbamate-based CSP to produce single enantiomers for *in vitro* activity tests on PPAR α and PPAR γ receptor subtypes [1]. Table 2 summarizes the results in terms of enantiomeric excess that was measured for each enantiomer along with information on employed column type. Throughout single enantiomers with a high enantiomeric excess could be obtained (typically between 90% and 99% ee). Such ee-values are certainly good enough for supporting unambiguous *in vitro* tests to elucidate the receptor subtype stereoselectivities (Table 2).

3.2. Absolute configuration assignment

3.2.1. By correlation with aryloxy carboxylic acids as reference system

Prior information on chromatographic enantiomer separation data and on preferred binding affinities of quinidine and quinine carbamate selectors existed for a wider set of aryloxy carboxylic acids of the type Ar–X–CH(R₁)–COOH with X being –O– as mentioned above [42]. A selection of such data is shown in Table 3. The quinidine CSP displays slightly better enantioselectivities than the quinine CSP which showed reversed elution order. Most importantly, *R*-enantiomers exhibit throughout higher affinities to quinine carbamate selectors, while *S*-enantiomers show consistently higher binding strength to quinidine carbamate selectors.

The thio ether group is isosteric to the ether group. Thus the chiral recognition mechanism is supposed to be identical for these two sets of chiral acids Ar–X–CH(R₁)–COOH with X being –O– and –S–. Enantiomers of 2-aryloxy carboxylic acids eluting first from the quinidine carbamate CSP should therefore have *R*-configuration and the second eluted enantiomers *S*-configuration.

3.2.2. Via chemical correlation

No single enantiomer standards with known absolute configuration were available from the thioether subset to validate that the substitution of the oxygen by a sulphur as well as replacement of the phenyl ring by a pyrimidine ring does not perturb the molecular recognition mechanism of cinchonane carbamate selectors. Thus, we considered to synthesize single enantiomers of

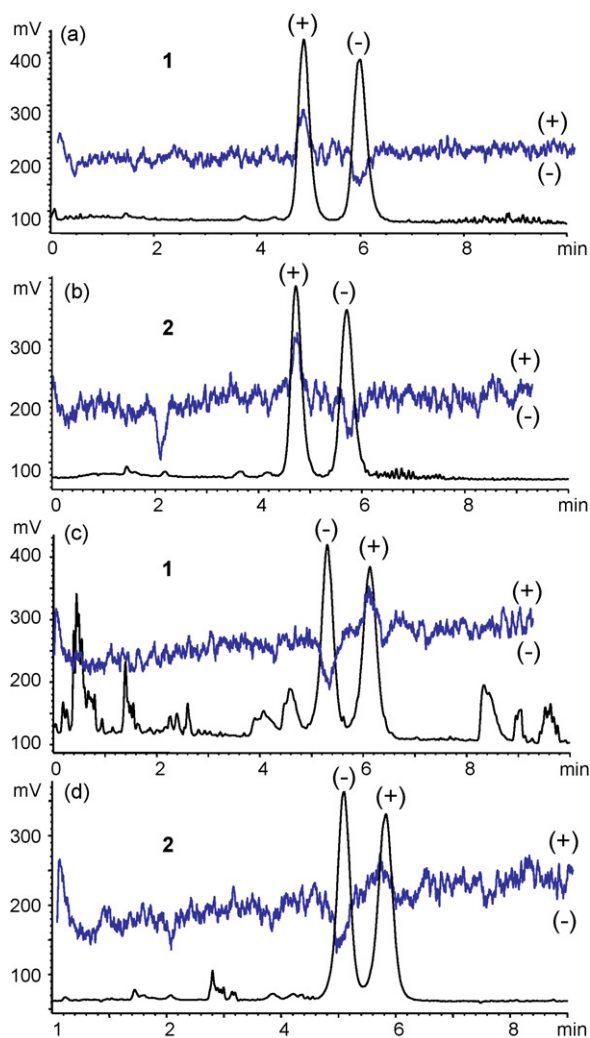


Fig. 3. HPLC-CAD chromatograms with overlaid ORD traces of compounds **1** (a and c) and **2** (b and d) on *O*-9-(*tert*-butylcarbamoyl) quinidine (a and b) and quinine (c and d) based CSPs. Experimental conditions: eluent, methanol–glacial acetic acid–ammonium acetate (98:2:0.5; v/v/w); flow rate, 1 mL/min; temperature, 25 °C. (Note, the extra peaks in chromatogram c represent detector noise/spikes! The ORD traces were shifted for the delay time between the detectors to align the corresponding chromatograms!).

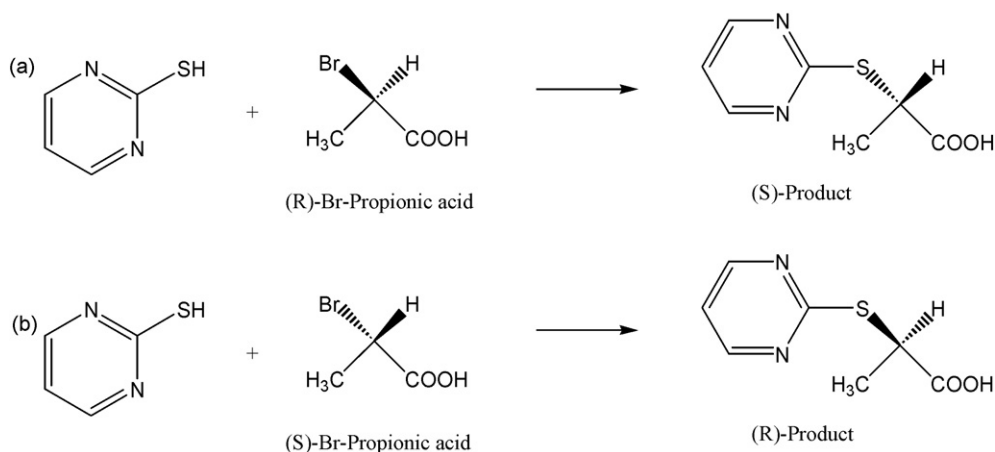


Fig. 5. Reaction scheme for the preparation of 2-(pyrimidin-2-ylthio)propionic acid (**4**) enantiomers. (a) *S*-product from (*R*)-bromopropionic acid, and (b) *R*-product from (*S*)-bromopropionic acid.

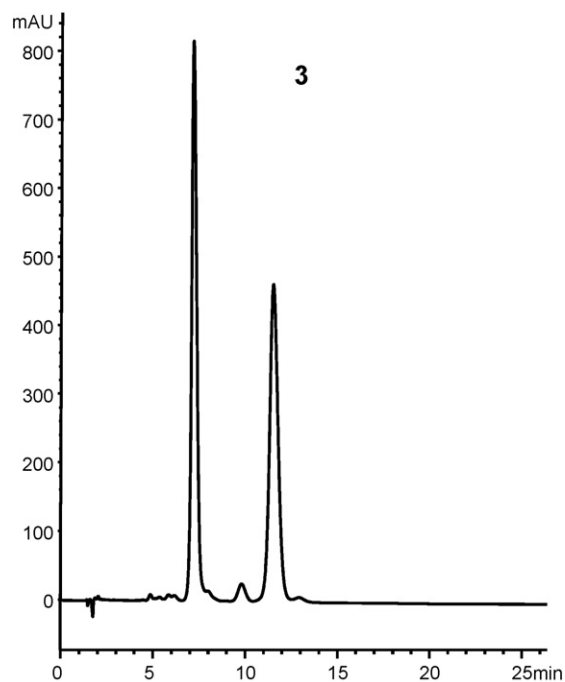


Fig. 4. HPLC enantiomer separations of **3** on *O*-9-(*tert*-butylcarbamoyl) quinine-based CSP. Experimental conditions: Eluent, methanol–glacial acetic acid–ammonium acetate (98:2:0.5; v/v/w); flow rate, 1 mL/min; temperature, 25 °C.

2-(2-pyrimidinylthio)propionic acid. They were readily accessible from (*R*)- and (*S*)-2-bromopropionic acid by nucleophilic substitution (S_N2) with pyrimidine-2-thiol (Fig. 5). Due to inversion of the stereoconfiguration in the course of S_N2, the *S*-enantiomer of the 2-(2-pyrimidinylthio)propionic acid should be obtained from (*R*)-bromopropionic acid and the *R*-enantiomer of the product from (*S*)-bromopropionic acid. It turned out that high enantiomeric excess values of the products are solely afforded if the reaction is carried out with caesium thiolate as nucleophile while nearly racemic products were obtained with thiol as reagent [43]. As can be seen from Fig. 6, relatively high ee values of 57% and 89% for *R*- and *S*-products, respectively, resulted when caesium thiolate was employed for the nucleophilic substitution reaction (vs. ~10% ee with thiol). Moreover, on the quinine carbamate CSP the *S*-enantiomer eluted prior to the *R*-enantiomer (Fig. 6a and b) while the elution order is reversed on the quinidine carbamate CSP (not shown). These results confirm the above chromatographic absolute

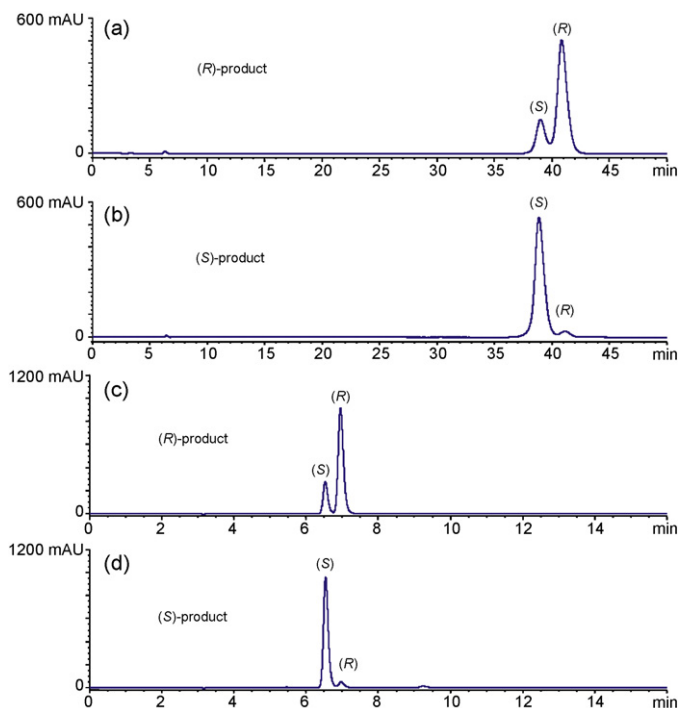


Fig. 6. Analytical quality control of the synthesized enantiomers of 2-(pyrimidin-2-ylthio)propionic acid (**4**) on a *O*-9-(*tert*-butylcarbamoyl) quinine-based CSP (a and b) and an amylose tris(3,5-dimethylphenylcarbamate) type CSP (c and d). Conditions: (a and b) mobile phase, methanol-acetic acid (98:2; v/v); flow rate, 0.25 mL/min; ambient temperature; (c and d) mobile phase, heptane-2-propanol-TFA (80:20:0.1; v/v/v); flow rate, 1.0 mL/min; ambient temperature; UV detection at 254 nm.

configuration assignment on basis of elution orders of α -aryloxy alkanic acids as reference compounds.

3.2.3. Via stereoselective synthesis employing Evan's auxiliary

The above chromatographic absolute configuration assignment represents an indirect method that makes use of reference compound(s) with known configuration and assumes consistencies of chiral recognition mechanisms between reference and sample compounds. Since this is not necessarily always the case, verification by an independent method is of utmost importance. In the present study, an enantioselective synthesis method has been devised for preparation of α -substituted carboxylic acid enantiomers employing the established method of Evan's auxiliary [44] (Fig. 7). It starts from the *R*- or *S*-enantiomer of benzyloxazolidinone

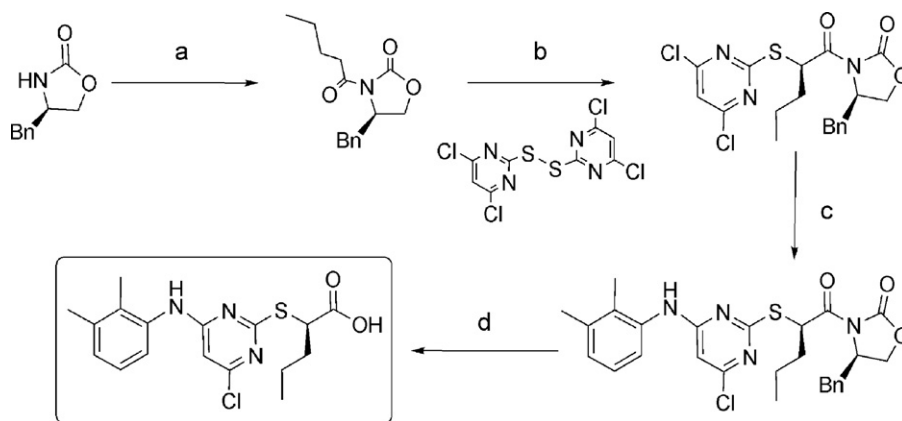


Fig. 7. Reaction scheme for stereoselective synthesis of (*R*)-**1** via Evan's auxiliary (*R*)-benzyloxazolidinone (corresponding (*S*)-**1** can be obtained by starting with (*S*)-benzyloxazolidinone). Reagents and conditions: (a) potassium-*tert*-butoxide, pentanoyl chloride, abs. THF, 0 °C, 1 h (b) LDA, abs. THF, -78 °C, 3 h; (c) 2,3-dimethylaniline, *N*-ethyl isopropyl amine, THF, reflux, 3.5 d; (d) LiOH, THF, H₂O, 0 °C → r.t., 3 h. Experimental details have been described elsewhere [1].

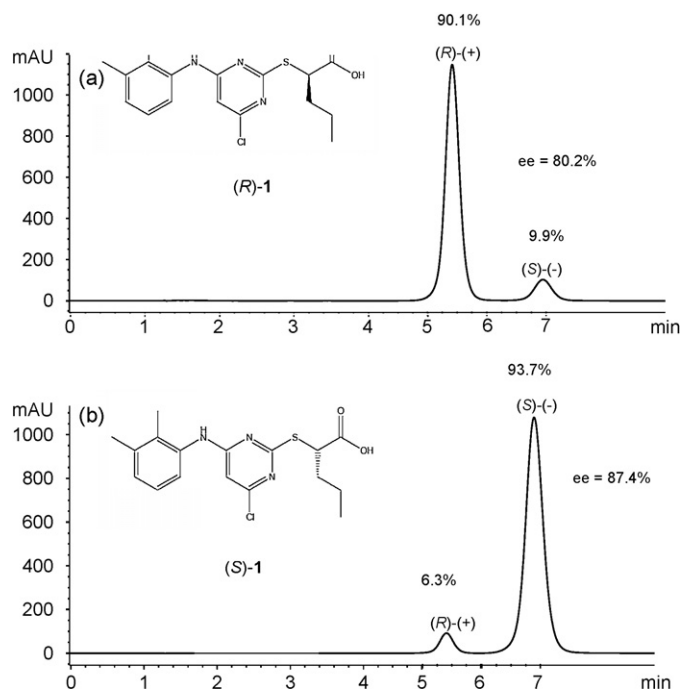


Fig. 8. Enantiomeric purity determination of (*R*)-**1** (a) and (*S*)-**1** (b) obtained from enantioselective synthesis via Evan's auxiliary. Chiral stationary phase, Chiralpak QD-AX; column dimension, 150 mm × 4 mm I.D.; Eluent, methanol-glacial acetic acid-ammonium acetate (98:2:0.5; v/v/w); flow rate, 1 mL/min; temperature, 25 °C; sample, (*R*)-**1** (2.56 mg/0.5 mL in methanol); sample, (*S*)-**1** (2.86 mg/0.5 mL in methanol); injection volume, 1 μ L; detection, UV 254 nm.

lidinone which was first converted into its *N*-alkanoyl derivative. The following α -substitution reaction involves an intermediary metal-chelated (*Z*)-enolate in which the C₄-substituent of the oxazolidinone ring dictates the diastereoface selection of nucleophilic reagent [44]. By starting from (*R*)-4-benzyloxazolidinone primarily *R*-configured intermediates and end products, respectively, are expected to be obtained (Fig. 7). In fact, (*R*)-**1** could be obtained from (*R*)-benzyloxazolidinone with an ee of about 80% and the resultant enantiomeric product showed the expected elution order on the quinidine carbamate CSP as predicted by above described considerations (Fig. 8a). The corresponding (*S*)-4-benzyloxazolidinone starting material gives rise to formation of the *S*-enantiomers of the target α -arythio carboxylic acids as demonstrated by the chromatogram for (*S*)-**1** in Fig. 8b (ee = 87%). Similar results could be achieved for **2** (e.g. 90% ee for *S*-enantiomer) with the elution order

being fully in agreement with predictions of the indirect chromatographic assignment.

3.3. Changes in molecular recognition mechanisms as risks for false assignments exemplified by polysaccharide CSP

Enantioselective liquid chromatography is probably the most important method for absolute configuration assignment of enantiomers via their elution order if it has been previously proven for the same pair of enantiomers under the same conditions. Any CSP can be safely applied for this purpose provided that the enantioselectivity of the CSP is good enough and the elution order has been validated before.

A frequent important task in drug discovery is to determine the absolute configurations of a set of structural congeners synthesized for sake of lead optimization. X-ray and CD spectroscopy may be too time consuming to apply them for all individual members of a test set. Hence, some sort of correlations such as chromatographic assignments may be put in place instead for sake of simplicity. However, one must bear in mind that the prediction of absolute configurations of structural analogs based on elution orders that have been established with a reference system of the same lead structure, but distinct substitution patterns (like herein) is by far more critical. Considerable precaution is of utmost importance as variations in molecular recognition within a congeneric set of compounds may easily occur upon different substitutions of a lead structure. In principle, this holds for all type of CSPs, yet polysaccharide CSPs may be particularly prone to such perturbations and alterations in chiral recognition mechanisms and elution orders in dependence of substitution patterns. This may be attributed to the multiple binding modes that may exist for such polymeric selectors (as opposed to more well-defined receptor-like brush-type selectors). It is also obvious that the risk for perturbations in the chiral recognition mechanism within a congeneric series increases with decreasing similarity of the substitutions around the stereogenic center. The problem will be illustrated hereafter for the current test set with a polysaccharide CSP.

The target test compounds **1–4** were also injected on an amylose tris(3,5-dimethylphenylcarbamate) coated polysaccharide-type CSP. This CSP exhibited good enantioselectivities for the target solutes as pointed out above (Table 1). However, it is striking that the elution orders within the test set of α -arylthiocarboxylic acids are less consistent than with quinidine and quinine carbamate CSPs. Most notably, the elution order was reversed for 2-(pyrimidin-2-ylthio)propionic acid derivative **3** as compared to the other α -arylthiocarboxylic acids. A similar observation is found for the α -aryloxycarboxylic acid **8** (see Table 3). Such reversals of elution order with minor structural changes have been frequently reported in the literature for polysaccharide type CSPs (e.g. Ref. [35]). They constitute a serious problem limiting polysaccharide CSPs for the purpose of chromatographic absolute configuration predictions of structural analogs. For example, if the synthesized 2-(pyrimidin-2-ylthio)propionic acid enantiomers were taken as reference compounds to chromatographically assign configurations of pirinixic acid analogs **1–3**, one would have run into problems with false absolute configuration assignments for **3**.

Polysaccharide CSPs are widely applicable for enantiomer separations of various types of solutes. However, the molecular recognition mechanisms with which they distinguish between enantiomers remains mostly concealed because of the structural complexity of polymeric selectors. Understanding of interaction mechanisms, though, would be helpful or even necessary for unequivocal indirect chromatographic absolute configuration assignments. Current knowledge states that hydrogen bonding, dipole–dipole interaction as well as π – π –interactions are driving forces for inclusion complexation into the grooves formed by the

pendant aryl carbamate residues of the polysaccharide selectors [35,45]. Steric factors may play a major role which enantiomer is the stronger bound one. Such mechanisms are sensitive to structure-induced binding mode alterations, even within a congeneric series. This has been demonstrated, for example, in a recent paper by Ma et al. in which they described the reversal of the elution order for two structural analogs that differed solely in π -acidity/basicity of an aromatic group [35]. Even minor variations of steric factors, π -electron density and substitution patterns may easily lead to perturbation of molecular recognition mechanisms within a series of structural analogs on polysaccharide CSPs leading to altered elution orders. While this may provide the basis for the broad applicability, it makes polysaccharide CSPs virtually useless for chromatographic absolute configuration assignments of structural analogs for which elution orders have not been validated before. In the given case, the reversal of elution order for compound **3** as compared to the other arylthiocarboxylic acids could be triggered by the additional aromatic substitutions on the arylthio ring system (“remote effects”), while the change in elution order of compound **8** in comparison to the remaining set of aryloxycarboxylic acids may have been induced by the steric bulkiness of the R-substituent (see Table 3).

In contrast, on quinine and quinidine carbamate CSPs elution orders were found to be more consistent [39–41,46,47], and this seems to be valid for aryloxy carboxylic acids [42] and arylthiocarboxylic acids likewise. The primary driving force for interaction of acidic solutes with the selectors is an ionic hydrogen bond at the fixed anion-exchange site. Thus, all test analytes are equally oriented towards the quinuclidine ring. They are similarly aligned in the active binding and chiral distinction site of the selector which is spanned by moieties arranged around the C9-stereogenic center [18,46]. Short-range secondary interactions that only become activated if steric dispositions are spatially favorable are then deciding on the preferentially established chiral recognition mechanism and the elution order. For the present aryloxy- and arylthio carboxylic acids π – π -interaction of the α -aryl group with quinoline is tentatively driving enantioselectivity and elution order on the cinchona alkaloid CSPs. The degree of enantioselectivity usually increases significantly with π -acidity, yet also π -basic solutes are separated. The elution order does not change with π -acidity/basicity (see Table 3). Thus, the chiral recognition mechanism is more consistent facilitating the application for absolute configuration assignment. Substitutions farther away from the stereogenic center such as structural decorations at the α -arylthio moiety have usually less effect on the principal chiral recognition mechanism and the elution order, as they are exposed to unoccupied open space of the chiral selector's binding site (see X-ray crystal structures in Refs. [18,46,48]). Scrambling of the enantioselective mechanism might be envisaged by acidic groups in the alkyl side chain of the solutes which are, however, not present in the current solute set. Being aware of mechanistic fundamentals on such low molecular anion-exchangers, its use for predictions of absolute configurations of structural analogs is feasible with high confidence, unlike with polymeric polysaccharide CSPs.

4. Conclusion

Enantiomers of pirinixic acid analogs were obtained by preparative chromatography and enantioselective synthesis. Absolute configuration assignments were based, in the first instance, on chromatographic elution orders on cinchona alkaloid derived CSPs taking a set of α -aryloxycarboxylic acids with known absolute configurations as reference system. Since this methodology bears some considerable risks for false assignments, several attempts for verification of the absolute configuration predictions were undertaken. First, 2-(pyrimidin-2-ylthio)propionic acid enantiomers

with established configurations were synthesized stereoselectively. Second, enantiomers of two pirinixic acid derivatives were synthesized by enantioselective synthesis via Evan's auxiliary. Both approaches confirmed the assigned configurations. Moreover, receptor stereoselectivity in terms of preferential activity was consistent within the tested series with significantly lower EC₅₀ values at the PPAR α receptor for the *R*-enantiomers (more active) of **1**, **2**, and **3** being a further indication for a correct assignment [1].

In general, it turned out that the chiral recognition mechanism is more consistent within the test set of α -arylthiocarboxylic acids on the cinchonan carbamate-based CSPs while limited correlation (between elution order and substitution) was observed with the polysaccharide type CSP. This finding suggests that chromatographic absolute configuration assignments based on elution orders which have been validated for a pair of enantiomers with known configuration is always safely possible for this pair of enantiomers, while predictions for structural analogs assuming an identical chiral recognition mechanism bears a considerable risk for false assignments if the molecular recognition mechanism is unknown. Confirmations by an orthogonal methodology are therefore absolutely required. Yet, configuration predictions of structural analogs based on elution orders on polysaccharide CSPs are strongly discouraged because of the high susceptibility to alterations of the chiral recognition mechanisms even with minute structural changes. CD and X-ray diffraction methodologies appear to be better choices if such technologies are readily available, but are more laborious and time consuming. They are therefore usually applied for one or two members of a congeneric series. For the rest of the molecules indirect assignments are still frequently employed.

Acknowledgements

The financial support by the Austrian Christian-Doppler Research Society and the industry partners AstraZeneca (Mölnadal, Sweden) and Merck KGaA (Darmstadt, Germany) is gratefully acknowledged.

References

- [1] H. Zettl, M. Dittrich, R. Steri, E. Proschak, O. Rau, D. Steinhilber, G. Schneider, M. Lämmerhofer, M. Schubert-Zsilavecz, *QSAR Comb. Sci.* 28 (2009) 576.
- [2] H.Y. Aboul-Enein, I.W. Wainer (Eds.), *The Impact of Stereochemistry on Drug Development and Use*, John Wiley, New York, 1997.
- [3] E.R. Francotte, *J. Chromatogr. A* 906 (2001) 379.
- [4] C. Roussel, A. Del Rio, J. Pierrot-Sanders, P. Piras, N. Vanthuyne, *J. Chromatogr. A* 1037 (2004) 311.
- [5] N. Harada, *Chirality* 20 (2008) 691.
- [6] S. Allenmark, J. Gawronski, *Chirality* 20 (2008) 606.
- [7] W.H. Pirkle, *J. Chem. Soc. [Sect.] D: Chem. Commun.* (1970) 1525.
- [8] W.H. Pirkle, K.A. Simmons, *J. Org. Chem.* 46 (1981) 3239.
- [9] J.K. Rugutt, H.H. Yarabe, S.A. Shamsi, D.R. Billodeaux, F.R. Fronczek, I.M. Warner, *Anal. Chem.* 72 (2000) 3887.
- [10] M. Kosaka, T. Sugito, Y. Kasai, S. Kuwahara, M. Watanabe, N. Harada, G.E. Job, A. Shvet, W.H. Pirkle, *Chirality* 15 (2003) 324.
- [11] J. Naito, M. Kosaka, T. Sugito, M. Watanabe, N. Harada, W.H. Pirkle, *Chirality* 16 (2004) 22.
- [12] G.E. Job, A. Shvets, W.H. Pirkle, S. Kuwahara, M. Kosaka, Y. Kasai, H. Taji, K. Fujita, M. Watanabe, N. Harada, *J. Chromatogr. A* 1055 (2004) 41.
- [13] M. Kurosu, K. Li, *Org. Lett.* 11 (2009) 911.
- [14] D. Casarini, L. Lunazzi, F. Gasparrini, C. Villani, M. Cirilli, E. Gavuzzo, *J. Org. Chem.* 60 (1995) 97.
- [15] C. Roberto, F. Rosella, G. Bruno, T. Luciana, B. Adriana, S. Daniela, C. Paola, P. Marco, F. Vincenzo, B. Olivia, L.T. Francesco, *Chirality* 16 (2004) 625.
- [16] C. Danel, C. Foulon, A. Guelzim, C.H.A. Park, J.-P. Bonte, C. Vaccher, *Chirality* 17 (2005) 600.
- [17] J.-V. Naubron, L. Giordano, F. Fotiadu, T. Buergi, N. Vanthuyne, C. Roussel, G. Buono, *J. Org. Chem.* 2006 (2006) 5586.
- [18] W. Bicker, I. Chiorescu, V.B. Arion, M. Lämmerhofer, W. Lindner, *Tetrahedron Asymm.* 19 (2008) 97.
- [19] U. Kiehne, T. Bruhn, G. Schnakenburg, R. Frohlich, G. Bringmann, A. Luetzen, *Chem. Eur. J.* 14 (2008) 4246.
- [20] Y. Zhang, B. Song, P.S. Bhadury, D. Hu, S. Yang, X. Shi, D. Liu, L. Jin, *J. Sep. Sci.* 31 (2008) 2946.
- [21] M.-P. Vaccher, J. Charton, A. Guelzim, D.-H. Caignard, J.-P. Bonte, C. Vaccher, *J. Pharm. Biomed. Anal.* 46 (2008) 920.
- [22] C. Roberto, F. Rosella, L.T. Francesco, B. Anna, F. Vincenzo, C. Mercedes, F. Cristina, R. Dante, M. Antonello, *Chirality* 21 (2009) 604.
- [23] P.J. Stephens, F.J. Devlin, F. Gasparrini, A. Ciogli, D. Spinelli, B. Cosimelli, *J. Org. Chem.* 72 (2007) 4707.
- [24] W. Bicker, K. Kacprzak, M. Kwit, M. Lämmerhofer, J. Gawronski, W. Lindner, *Tetrahedron Asymm.* 20 (2009) 1027.
- [25] S. Abbate, G. Longhi, E. Castiglioni, F. Lebon, P.M. Wood, L.W.L. Woo, B.V.L. Potter, *Chirality* 21 (2009) 802.
- [26] S. Abbate, L.F. Burgi, E. Castiglioni, F. Lebon, G. Longhi, E. Toscano, S. Caccamese, *Chirality* 21 (2009) 436.
- [27] H.D. Flack, G. Bernardinelli, *Chirality* 20 (2008) 681.
- [28] W.H. Pirkle, A. Tsipouras, M.H. Hyun, D.J. Hart, C.S. Lee, *J. Chromatogr.* 358 (1986) 377.
- [29] W. Pirkle, H.L.J. Brice, T.S. Widlanski, J. Roestamadji, *Tetrahedron Asymm.* 7 (1996) 2173.
- [30] E. Zarbl, M. Lämmerhofer, F. Hammerschmidt, F. Wuggenig, M. Hanbauer, N.M. Maier, L. Sajovic, W. Lindner, *Anal. Chim. Acta* 404 (2000) 169.
- [31] M. Lämmerhofer, D. Hebenstreit, E. Gavioli, W. Lindner, A. Mucha, P. Kafarski, P. Wieczorek, *Tetrahedron Asymm.* 14 (2003) 2557.
- [32] S. Coles, D. Davies, M. Hursthouse, S. Yesilot, B. Cosut, A. Kilic, *Acta Crystallogr. Sect. B: Struct. Sci.* B65 (2009) 355.
- [33] K. Balmér, B.-A. Persson, P.-O. Lagerström, *J. Chromatogr. A* 660 (1994) 269.
- [34] B.-A. Persson, S. Andersson, *J. Chromatogr. A* 906 (2001) 195.
- [35] S. Ma, S. Shen, H. Lee, M. Eriksson, X. Zeng, K. Fandrick, N. Yee, C. Senanayake, N. Grinberg, *J. Chromatogr. A* 1216 (2009) 3784.
- [36] E. Francotte, T. Zhang, *J. Chromatogr. A* 718 (1995) 257.
- [37] G. Massolini, G. Fracchiolla, E. Calleri, G. Carbonara, C. Temporini, A. Lavecchia, S. Cosconati, E. Novellino, F. Loiodice, *Chirality* 18 (2006) 633.
- [38] A. Ghanem, *J. Chromatogr. A* 1132 (2006) 329.
- [39] M. Lämmerhofer, W. Lindner, *J. Chromatogr. A* 741 (1996) 33.
- [40] N.M. Maier, L. Nicoletti, M. Lämmerhofer, W. Lindner, *Chirality* 11 (1999) 522.
- [41] A. Mandl, L. Nicoletti, M. Lämmerhofer, W. Lindner, *J. Chromatogr. A* 858 (1999) 1.
- [42] M. Lämmerhofer, PhD thesis, Karl-Franzens University Graz, 1996.
- [43] B. Strijtveen, R.M. Kellogg, *J. Org. Chem.* 51 (1986) 3664.
- [44] D.A. Evans, M.D. Ennis, D.J. Mathre, *J. Am. Chem. Soc.* 104 (1982) 1737.
- [45] T.D. Booth, I.W. Wainer, *J. Chromatogr. A* 737 (1996) 157.
- [46] C. Czerwenka, M. Lämmerhofer, N.M. Maier, K. Rissanen, W. Lindner, *Anal. Chem.* 74 (2002) 5658.
- [47] C. Czerwenka, M. Lämmerhofer, W. Lindner, *J. Sep. Sci.* 26 (2003) 1499.
- [48] K. Akasaka, K. Gyimesi-Forras, M. Lämmerhofer, T. Fujita, M. Watanabe, N. Harada, W. Lindner, *Chirality* 17 (2005) 544.

APPENDIX II



Contents lists available at [SciVerse ScienceDirect](http://www.sciencedirect.com)

Journal of Chromatography A

journal homepage: www.elsevier.com/locate/chroma



Potential of chiral anion-exchangers operated in various subcritical fluid chromatography modes for resolution of chiral acids

Reinhard Pell, Wolfgang Lindner*

Department of Analytical Chemistry, University of Vienna, Währingerstrasse 38, 1090 Vienna, Austria

ARTICLE INFO

Article history:

Received 16 March 2012
Received in revised form 3 May 2012
Accepted 5 May 2012
Available online xxx

Keywords:

Enantiomer separation
Supercritical fluid chromatography
Subcritical mobile phase
Chiral stationary phase
Chiral anion exchangers

ABSTRACT

Anion-exchange-type chiral stationary phases (CSPs) derived from quinine or quinidine were applied in subcritical fluid chromatography (SFC) for the direct separation of chiral acidic compounds. Employing subcritical (sc) mobile phase modes (CO₂ + methanol as co-solvent and acids and bases as additives) first the influence of type and amount of acidic and basic additives on separation performance was investigated. Secondly, water was tested as a neutral additive and the influence of temperature variation on enantioselectivity was studied. Thirdly, we could chromatographically confirm that the often verbalized “inherent acidity” of sc CO₂ + methanol is manifested by the in situ formation of methylcarbonic acids in the sc mobile phase and thus functioning as acidic additive. Accordingly the dissociated methylcarbonic acid, acting as a counterion, enables an anion exchange mechanism between the cationic CSP and the corresponding acidic analyte. In the absence of a dissociable acid in the mobile phase such an ion exchange mode would not work following a stoichiometric displacement model. This finding is further corroborated by the use of ammonia in methanol as co-solvent thus generating in situ the ammonium salt of methylcarbonic acid. In summary, we report on ion-exchange mediated chromatographic separations in SFC modes by merely using (i) sc CO₂ and MeOH, (ii) sc CO₂ and ammonia in MeOH, and (iii) sc CO₂ and MeOH plus acids and bases as additives. Comparisons to HPLC mode have been undertaken to evaluate merits and limitations. This mode exhibits high potential for preparative chromatography of chiral acids combining pronounced enantioselectivity with high column loadability and avoiding possibly troublesome mobile phase additives, as the in situ formed methylcarbonic acid disintegrates to CO₂ and methanol upon pressure release.

© 2012 Elsevier B.V. All rights reserved.

1. Introduction

The first use of a CO₂-based supercritical fluid as a mobile phase in chromatography dates back to 1962 [1]. During the following decades, instrumental development of CO₂-type supercritical fluid chromatography (SFC) focused on capillary SFC as a form of extended gas chromatography (GC), thereby limiting its application range compared to high performance liquid chromatography (HPLC). Therefore, the breakthrough of SFC from a niche chromatographic technique began with the use of packed columns as stationary phases in combination with the development of more broadly applicable SFC instruments in the 1990s [2]. Nowadays, SFC is established as a flourishing separation technique on both analytical and preparative scale, especially in the pharmaceutical industry [3,4].

Carbon dioxide became the fluid of choice in SFC mainly because of its moderate critical pressure and temperature (31 °C and 74 bars), its low toxicity and low detector response. However, the limited polarity of supercritical CO₂ necessitates certain amounts of polar (mostly protic) organic solvents as modifiers or co-solvents to enhance the overall elution strength, thereby increasing the critical conditions and thus transforming the supercritical fluid into a subcritical (sc) fluid. In fact, most of the SFC separations nowadays are carried out in the subcritical range (but phase separation was not observed chromatographically) [5]. Often, the addition of an acidic or basic compound to the dominantly used protic co-solvent facilitates efficient elution of ionizable compounds, thus occasionally enhancing also (enanti)selectivity and improving peak shape [6,7]. Especially basic additives reduce peak tailing in chiral and achiral SFC due to their masking effects of residual silanol groups, thus suppressing interactions with basic compounds [8,9].

For enantiomer separations under SFC conditions a plethora of chiral stationary phases (CSPs) has been used [10–12], in particular polysaccharide-type CSPs [13], but also glycopeptide antibiotic-based CSPs [14], cyclodextrin-based CSPs [15] or Pirkle-type CSPs [16]. Until now, SFC-enantioseparations of highly polar

* Corresponding author. Tel.: +43 1427752300; fax: +43 142779523.
E-mail addresses: Reinhard.Pell@univie.ac.at (R. Pell),
Wolfgang.Lindner@univie.ac.at (W. Lindner).

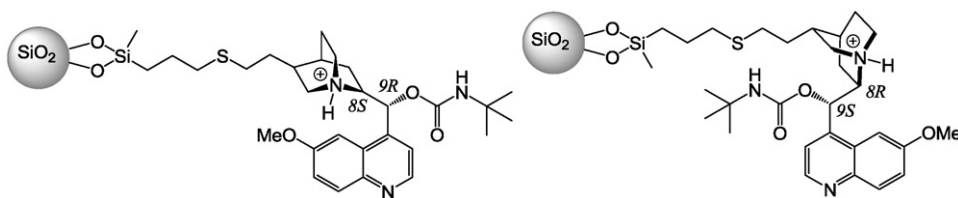


Fig. 1. Structures of weak anion exchangers QN-AX (left) and QD-AX (right).

(ionizable) compounds, such as chiral acids, were carried out on synthetic polymeric chiral phases [17,18], on derivatized amylose and cellulose-based CSPs [19] and on macrocyclic glycopeptide-type stationary phases [20].

Hence, this work presents the application of weak anion exchange (WAX)-type CSPs under various SFC conditions for the enantioseparation of chiral acidic compounds. The chiral selectors (SOs), which are immobilized onto porous silica gel, are tert-butyl-carbamoyl-derivatives of quinine and quinidine, respectively (QN-AX and QD-AX, Fig. 1). We show that an anion-exchange (AX) process as primary interaction force is maintained under SFC conditions. The influence of different types and amounts of additives (acids, bases and water, each in MeOH as a co-solvent) and of temperature on chromatographic performance is described. In addition, a detailed study on the so-called “inherent acidity” of the sc CO₂-methanol mobile phases is undertaken.

2. Experimental

2.1. General information and materials

The preparation of QN-AX- and QD-AX-CSPs was reported previously [21]. The columns were made in house but are identical in terms of selector structure and silica gel endcapping with the commercially available columns CHIRALPAK®-QN-AX and CHIRALPAK®-QD-AX from Chiral Technologies (Illkirch, France). The SO loading of both columns was around 390 μmol/g, unless otherwise stated. Column dimensions were 150 mm × 4 mm I.D. The silica gel used had a particle size of 5 μm, a pore size of 120 Å, a surface area of 300 m²/g and was obtained from Daiso Chemicals (Osaka, Japan). Methanol (MeOH) was purchased in HPLC grade quality from VWR (Vienna, Austria). Water was double distilled in house. Liquid carbon dioxide was purchased from Air Liquide Austria (Schwechat, Austria). Modifier additives ammonium acetate (NH₄OAc), ammonium formate (NH₄FA), acetic acid (HOAc), formic acid (FA), diethylamine (DEA) and NH₃ (7 N solution in MeOH) were purchased in analytical grade quality from Sigma-Aldrich. The chiral solutes were either commercially available or kind gifts of research partners.

2.2. Instrumentation and chromatography

Supercritical fluid chromatography studies were performed on a Thar Discovery system from Thar Technologies Inc., equipped with a combined CO₂ and modifier pump, a combined column oven and column selector valve for 6 columns, an automated back pressure regulator, a water bath and a Gilson UV variable wavelength detector. Instrument control and data acquisition were carried out with Thar SuperChrome software and Thar ChromScope software, respectively. Elution was performed in isocratic mode with 25% co-solvent (modifier) content at a flow rate of 4.0 mL/min. Unless otherwise stated, column temperature was 40 °C and the backpressure was adjusted to 150 bars. UV detection was used in a range from 220 to 280 nm. The analytes were dissolved in MeOH

in concentrations between 3 and 5 mg/mL. The injection volume was between 5 and 20 μL. The elution order of selected analytes was determined by injecting single enantiomers of known configuration. Column equilibration times were at least 20 min and each run was carried out twice. HPLC measurements were carried out on an 1100 Series HPLC system from Agilent Technologies (Waldbronn, Germany) consisting of a solvent degasser, a quaternary pump, an autosampler, a column thermostat and a diode array UV-vis detector. Data acquisition and instrument control were accomplished with ChemStation software from Agilent Technologies. Elution was carried out at a flow rate of 1.0 mL/min and at a temperature of 40 °C. The HPLC mobile phase consisted of MeOH with acidic and basic additives in a 2:1 ratio. The solutes were applied as methanolic solutions of 1.0–1.5 mg/mL. Injection volumes were in the range of 5–10 μL. The void volume was determined by injecting a solution of acetone in MeOH (for both HPLC and SFC measurements).

3. Results and discussion

3.1. General aspects

Experimental conditions were chosen to facilitate high enantioresolution values with reasonably fast solute elution times. Therefore, the mobile phase composition throughout the studies consisted of 25% methanol as co-solvent to ensure high elutropic strength for the elution of the very polar (ionized) analytes. The temperature was set to 40 °C (unless otherwise stated) and a backpressure of 150 bars was used. Applying these parameters, the mobile phase is no longer a supercritical fluid but is considered as subcritical (sc). However, numerous studies demonstrated that there are no discontinuities in chromatographic properties between the subcritical and supercritical range, which was also confirmed within this work. QN-AX CSP and QD-AX CSP exhibit remarkable separation performance towards chiral acidic compounds in HPLC using buffered polar organic (methanolic) or buffered reversed phase conditions [22–26]. The chiral recognition mechanism is driven by a non-directed or directed ion-exchange process between the protonated quinuclidine-tertiary amine (the positively charged ionic interaction site of the SO) and the dissociated (anionic) analyte (selectand, SA) depending on the overall interaction model. Ion-pair formation is supported by additional SO-SA interactions such as hydrogen bonding, π-π stacking, van der Waals and steric interactions, thus enabling chiral discrimination [21,27–30]. Consequently, analyte retention is mainly controlled by the concentration of the salt- and acidic additives without compromising enantioselectivity following the stoichiometric displacement model. Both retention and enantioselectivity can be adjusted by the mobile phase pH, the nature and content of the organic additives and the temperature. Based on these investigations in HPLC mode, the impact of the aforementioned parameters on the chromatographic behavior was now scrutinized for SFC conditions.

Table 1
SFC enantiomer separation of chiral acidic analytes on QN-AX- and QD-AX CSP.^a

Racemic solutes	QN-AX				QD-AX			
	EO	<i>t</i> ₁ [min] ^b	α	<i>R</i> _s	EO	<i>t</i> ₁ [min] ^b	α	<i>R</i> _s
1, Suprofen	n.d.	3.80	1.12	1.8	n.d.	4.08	1.11	1.7
2, Chromane-2-carb. acid	n.d.	3.15	1.13	1.9	n.d.	2.85	1.00	0.0
3, Flurbiprofen	n.d.	2.16	1.05	0.7	n.d.	2.40	1.06	0.8
4, Ibuprofen		1.08	1.00	0.0		1.16	1.00	0.0
5, Naproxen		2.18	1.00	0.0	R	2.45	1.08	1.2
6, Carprofen	n.d.	8.05	1.13	2.0	n.d.	9.70	1.13	2.2
7, Dichlorprop	n.d.	2.98	1.19	2.8	n.d.	3.10	1.36	4.1
8, Tropic acid	n.d.	2.65	1.03	0.5	n.d.	2.75	1.06	0.8
9, 2-Phenylbutyric acid		1.15	1.00	0.0		1.22	1.00	0.0
10, Fmoc-Abu	n.d.	4.84	1.48	5.5	n.d.	4.79	1.46	4.8
11, Bz-Phe	D	4.75	1.47	5.1	L	4.44	1.58	5.5
12, Ac-Phe	D	2.84	1.31	3.6	L	2.60	1.37	4.4
13, Cbz-Phe	D	4.48	1.13	1.8	L	4.59	1.18	2.5
14, Cbz-beta-Phe	n.d.	3.05	1.13	1.9	n.d.	3.17	1.23	3.1
15, Boc-Phe	D	2.33	1.10	1.7	L	2.37	1.16	2.3
16, Ac-Trp	D	8.86	1.52	5.3	L	8.40	1.50	5.6
17, Boc-Tyr	D	5.08	1.13	1.7	L	5.44	1.19	2.7
18, Cbz-Ser	D	4.28	1.16	2.1	L	4.27	1.27	3.6
19, Cbz-Arg	D	5.41	1.13	1.5	L	4.65	1.13	1.4
20, DNB-Pro		3.85	1.00	0.0		4.36	1.00	0.0
21, Fmoc-Pro		3.70	1.00	0.0	L	3.70	1.10	1.6
22, Fmoc-Aze		4.28	1.00	0.0	L	4.20	1.08	1.3
23, Fmoc-Leu	D	3.95	1.56	5.7	L	4.13	1.52	5.3
24, Bz-Leu	D	2.38	1.97	7.6	L	2.25	1.95	7.3
25, DNB-Leu	D	3.97	12.51	14.4	L	4.43	9.30	10.5
26, DNB-N-Methyl-Leu	n.d.	3.39	1.08	1.4	n.d.	4.34	1.07	1.3
27, Fmoc-Ile	D	4.28	1.61	6.3	L	4.30	1.63	6.0
28, Fmoc-Asn	D	7.98	1.17	2.4	L	7.69	1.23	3.2
29, Fmoc-Gln	D	8.80	1.24	3.2	L	8.24	1.28	3.8
30, Fmoc-Met	n.d.	7.81	1.40	4.9	n.d.	7.32	1.48	5.2
31, Ac-Tyr	D	6.10	1.36	3.7	L	4.88	1.37	4.0

^a Conditions: column dimensions 150 mm × 4 mm I.D.; 25% modifier (MeOH, 200 mM HOAc, 100 mM NH₃); 40 °C, 150 bar, flow rate 4.0 mL/min; EO, elution order (configuration of the first eluted enantiomer); n.d., not determined.

^b *t*₁ [min], retention time of first eluted peak; void times on both columns: 0.49 min.

3.2. General performance and molecular recognition of QN-AX and QD-AX CSPs in SFC mode

Retention of chiral acids on QN-AX and QD-AX CSPs is primarily driven by long-range electrostatic interactions. Thus, the ion exchange process is strongly dependent on the ionization state of SO and SAs and on the ionic strength (equal to buffer salt content) in the mobile phase. The mobile phase was optimized concerning the amounts of acidic and basic additives in the methanolic modifier: The applied acid to base ratios of 20:1 to 2:1 (190 mM HOAc/10 mM NH₄OAc to 10 mM HOAc/10 mM NH₄OAc) revealed that with increasing amounts of acidic additives (without increasing the total salt concentration) retention decreased only marginally, whereas selectivity remained unaltered (data not shown). Thus, an acid to base ratio of 2:1 (e.g. 100 mM NH₄OAc and 100 mM HOAc in MeOH) was used to investigate the separation performance of QN-AX and QD-AX CSPs for chiral acidic test solutes such as propionic acid derivatives and N-protected amino acids (see Fig. 2).

Table 1 summarizes the results obtained on both QN-AX and QD-AX CSPs. In general, enantioselectivities in SFC mode equal those obtained in HPLC-polar organic mode using MeOH with acid and salt additives. For the sake of clarity, the test solutes were also measured by HPLC using a mobile phase of the same type as the modifier in SFC measurements. Differences in enantioselectivity values were negligible while plate numbers (and thus resolutions) slightly exceeded the values observed in HPLC (data not shown). Additionally, measuring a Van Deemter curve revealed that the applied SFC flow rate of 4.0 mL/min exceeds the Van Deemter minimum, however, it is common practice

to accept this for the sake of shorter elution times (data not shown).

Although QN-AX SO and QD-AX SO are diastereomers to each other (2 out of the five stereogenic centers are of opposite configuration), they possess “pseudo-enantiomeric” attributes. This relies on the fact that enantioselectivity of the solutes is mainly controlled by the configuration of the C8 and C9 stereocenters of the binding pocket of this chiral selector family (see Fig. 1) [21]. The “pseudo-enantiomeric” behavior is chromatographically reflected in a switch of elution orders of the enantiomers on a quinine- and quinidine-based CSP. A change of elution orders for all tested compounds was also observed in SFC mode between the QN-AX and QD-AX columns (Table 1 and Fig. 3) which is in full agreement with HPLC data. A unique feature in SFC is the ability of the QD-AX CSP to baseline resolve N-protected, cyclic amino acids such as Fmoc-Pro, **21** or Fmoc-Aze, **22**. These types of amino acids could only be partially separated on QN- or QD-AX CSPs in HPLC mode [31] whereas the majority of their α -substituted derivatives can be resolved. Furthermore, both columns show “complementary enantioselectivity” regarding some compounds like chromane-2-carboxylic acid, **2**. To conclude, the observed selectivities and separation characteristics are to a large extent comparable to those in HPLC, which suggests that molecular interaction and thus chiral recognition is of the same mechanism as in HPLC. Using QN-AX and QD-AX CSPs in SFC mode can therefore be regarded as a useful alternative to HPLC, additionally taking advantage of SFC conditions leading, e.g. to shorter column equilibration times compared to HPLC, etc. However, since the separations are based on ion exchange mechanisms the SFC modus cannot significantly speed up such type processes. This has to be accepted.

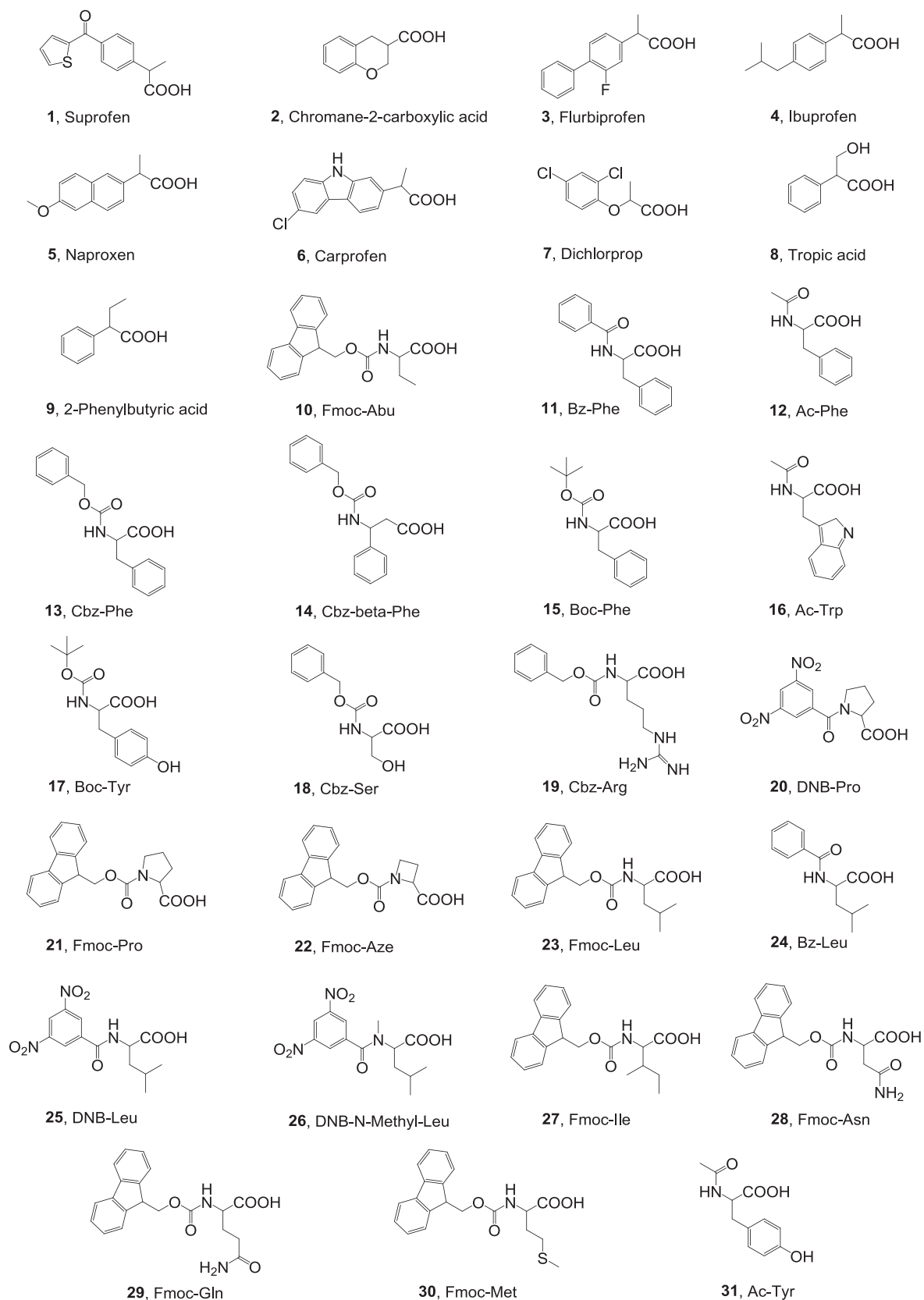


Fig. 2. Structural formulas of the chiral test analytes.

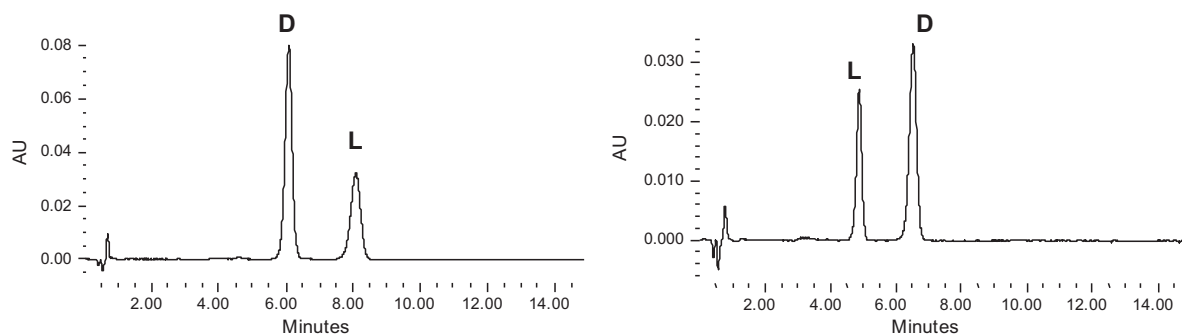


Fig. 3. Enantioseparation of Ac-Tyr, **31** on QN-AX (left) and QD-AX CSP (right). 25% modifier: (MeOH, 200 mM HOAc, 100 mM NH₃); 40 °C, 150 bar, 4.0 mL/min; d-enantiomer enriched sample.

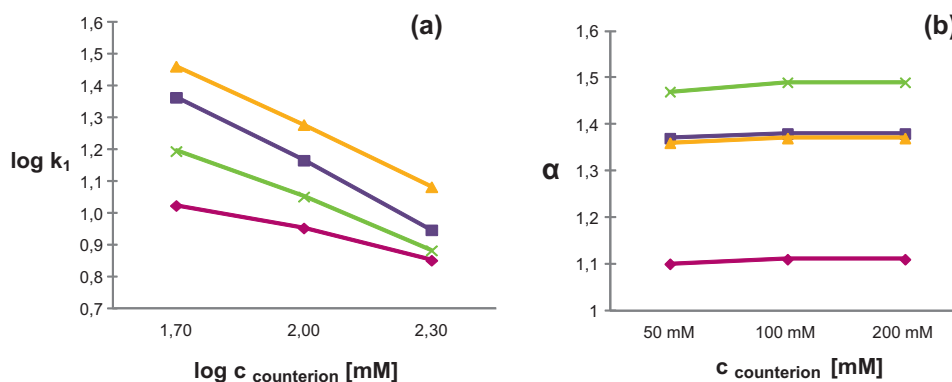


Fig. 4. Influence of counterion concentration on (a) retention of the first eluted enantiomer and (b) selectivity. (●) Suprofen (■) Bz-Phe (▲) Ac-Tyr (×) Fmoc-Leu. CSP: QN-AX; 25% modifier (MeOH, HOAc, NH₄OAc, acid to base ratio 2:1), 40 °C, 150 bar, 4.0 mL/min.

3.3. Influence of type and amount of methanolic SFC mobile phase additives

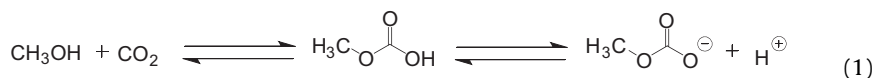
As previously discussed, an ion pairing process between the SO and the SA dominates retention of the WAX-type CSPs in HPLC mode. In practice, this means that run times can be adjusted by the amount of co- and counterions in the mobile phase. To ascertain whether the anion-exchange mechanism also controls retention in sc CO₂ based mobile phases, the counterion concentration in the modifier was varied in the range of 50–200 mM of acid (the acid to base ratio was kept constant to ensure identical ionization states of SO and SA). Increasing acid and thus counterion concentrations led to a decrease in retention along with a linear relationship between $\log k$ and $\log c$ (Fig. 4). This clearly indicates that also in SFC we follow an ion exchange mechanism according to a stoichiometric displacement model as primary interaction force. Moreover, both enantiomers of the respective solute exhibit very similar slopes which confirms that the ion exchange process is “of the same quality” for both enantiomers (data not shown). This in turn means that enantioselectivity is mainly unaffected by a change of the counterion concentration enabling the unique feature of adjusting retention times without compromising enantioselectivity (Fig. 4).

In a following study the effect of the additive-type was investigated. At a constant acid to base ratio of 100 mM acid and 50 mM base in the methanolic co-solvent the HOAc/NH₄OAc additives were replaced by stronger acids and bases such as FA and DEA. The data revealed rather analyte specific but no general effect of the additive type on retention. Enantioselectivity almost remained

unaltered whereas the combination of FA/DEA in the methanolic solvent modifier achieved best peak shapes and thus highest resolution for the investigated analytes (Fig. 5). However, the effect of the different additive combinations on chromatographic performance remained to be marginal and the use of a specific co- or counterion is incumbent to the chromatographer. Additionally, the combination of FA/NH₄FA was also tested (200 mM acid/100 mM base) and revealed similar chromatographic performance to the already mentioned additive combinations. Generally, in terms of high salt volatility and suitability for a potential SFC-MS hyphenation HOAc/NH₄OAc or FA/NH₄FA are recommended as additives for SFC enantioseparations on QN-AX or QD-AX columns.

3.4. Acidity of methanol-carbon dioxide subcritical fluids and their benefit for the operation of weak anion exchange (QN-AX and QD-AX) CSPs

As extracted from literature, although in a different context, sc CO₂-MeOH mixtures exhibit distinct acidity due to the in situ formation of methylcarbonic acid [32,33]. Formally, this is based on the addition reaction of MeOH to liquid CO₂ for which we need pressurized conditions. By this finding it becomes evident that the often verbalized “slight acidity of CO₂” is actually caused by the pressurized methanolic CO₂ and thus the formed methylcarbonic acid in the SFC mobile phase (reaction Eq. (1)). The in situ generated and dissociated acid could then act as a co- or counterionic additive for the operation of WAX-type CSPs such as QN-AX or QD-AX following again the stoichiometric displacement model.



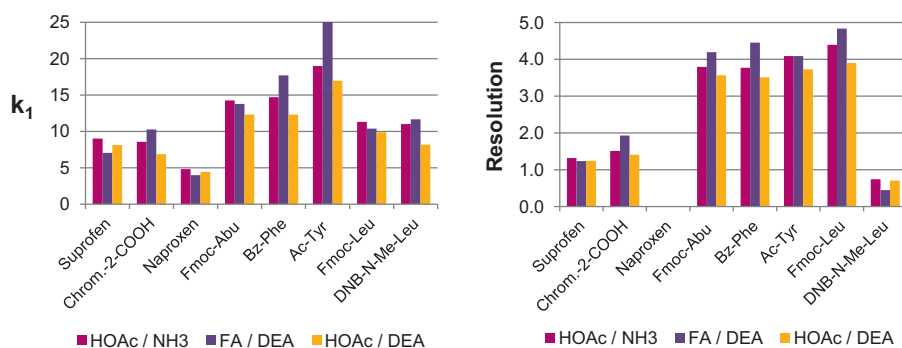


Fig. 5. Change of retention factor of the first eluted enantiomer (k_1 , left) and resolution (right) by applying different types and combinations of additives: HOAc/NH₃, FA/DEA and HOAc/DEA; conditions: QN-AX CSP; 25% modifier (MeOH, 100 mM acid, 50 mM base); 40 °C, 150 bar, 4.0 mL/min; Chrom.-2-COOH = chromane-2-carboxylic acid, **2**.

To examine this concept which apparently is less of an issue for e.g. neutral polysaccharide-type CSPs and columns, we applied additive free sc CO₂-MeOH as mobile phase for SFC operation of QN-AX and QD-AX columns. The data summarized in Table 2 demonstrate convincingly the proposed SFC operational mode as one reaches similar enantioselectivity- and resolution values of selected analytes matching those measured with SFC mobile phases containing acidic and basic additives (for instance, compare data of Tables 1 and 2). With these results the “proof of principle” could be demonstrated although the plate numbers were in the average slightly lower than with the “benchmark” modifier (MeOH, 200 mM HOAc, 100 mM NH₃) in combination with unfavorably high retention times. Therefore, we applied a QN-AX column with a lower SO coverage (140 μmol SO/g silica instead of “standard” 390 μmol SO/g) applying again only sc CO₂-MeOH (25%) in order to check the validity of the stoichiometric displacement model also for these conditions. As prognosticated, the retention times were significantly reduced while maintaining enantioselectivity (Table 2, right column).

The data demonstrate that the “inherent acidity” of CO₂-MeOH subcritical fluids has to be traced back to the in situ formation of methylcarbonic acid. As a consequence, it supports an ion-exchange mechanism between the SO and the SA thus allowing salt additive-free mobile phase conditions for the elution of chiral acids on anion exchangers in general and on QN-AX and QD-AX CSPs in particular. Such a phenomenon can only be explained by the dissociation of the in situ formed methylcarbonic acid into the methylcarbonate anion and the proton. The methylcarbonate acts as a counterion and the hydron guarantees protonation of the SO-tertiary amine thus enabling the ion-exchange mechanism. The unique feature of the common methanolic SFC conditions open up new possibilities also for preparative enantioseparations of chiral acids on chiral anion exchangers without the use of acidic or basic additives in the SFC mobile phase. The ingenious thing about it is

that the methylcarbonic acid disproportionate into CO₂ and MeOH when the pressurized mobile phase medium gets released.

3.5. Ammonia in methanol used as additive and co-solvent

To further corroborate our hypothesis, a control experiment was carried out in both HPLC and SFC. A basic methanolic solution containing 25 mM NH₃ was applied as a mobile phase or modifier, respectively. In the case of HPLC the alkaline mobile phase led to a “breakdown” of the chromatographic performance. First, the acidic analytes are not eluted from the anion exchanger (infinite retention times) as the ion pairing process between the SO and the SA is taking place but elution cannot be enforced as there is no salt in the mobile phase acting as a displacer. On the contrary, in SFC mode the ammonia containing methanolic co-solvent (25% in sc CO₂) yielded proper enantioselectivity, peak shape and strongly reduced retention times compared to the pure methanolic modifier (Fig. 6). The results are consistent with the hypothesis of the in situ formation of methylcarbonic acid which then forms with ammonia its ammonium salt. Following the stoichiometric displacement model, this salt dissolved in the SFC mobile phase leads then to significantly shortened retention times. This finding opens up an extended use of sc methanolic CO₂ as a mobile phase in chromatography as via the addition of an amine easily ammonium salts can be generated in situ. Conceptual, this is a significant extension of the recently published work of Ventura et al. describing the value of ammonia as additive to methanol and respective SFC resolution of enantiomers on polysaccharide-type chiral columns [9].

3.6. Water as additive in sc CO₂-MeOH mobile phases

In the late 1980s water was first used as a modifier in packed column SFC [34,35]. Due to its low solubility in pure sc CO₂ (<0.5%, w/w) water only gained some importance as neutral additive in

Table 2
Enantioseparations on QN-AX CSPs with different SO coverages using a sc CO₂ + MeOH mobile phase.^a

Racemic solutes	QN-AX (390 μmol SO/g)				QN-AX (140 μmol SO/g)			
	t_1 [min] ^b	α	R_s	N_1 [m ⁻¹] ^c	t_1 [min] ^b	α	R_s	N_1 [m ⁻¹] ^c
1, Suprofen	6.62	1.13	1.7	32,000	3.28	1.11	1.6	39,800
2, Chromane-2-carb. acid	15.38	1.16	2.2	30,700	7.51	1.17	2.1	24,500
7, Dichlorprop	28.32	1.25	3.2	29,600	14.29	1.27	2.4	26,500
11, Bz-Phe	32.79	1.49	5.3	30,000	15.25	1.42	4.0	20,500
16, Ac-Trp	41.53	1.56	5.4	21,200	14.41	1.61	5.8	30,700
17, Boc-Tyr	18.11	1.15	1.7	20,600	7.63	1.14	1.7	26,800
23, Fmoc-Leu	12.87	1.59	5.1	31,300	7.17	1.55	4.6	23,700
30, Fmoc-Met	36.25	1.48	5.5	32,300	18.13	1.43	3.7	19,400

^a Conditions: column dimension 150 mm × 4 mm I.D.; 25% modifier (neat MeOH), 40 °C, 150 bar, 4.0 mL/min.

^b t_1 [min] retention time of first eluted peak.

^c N_1 [m⁻¹] plate number/meter of first eluted peak.

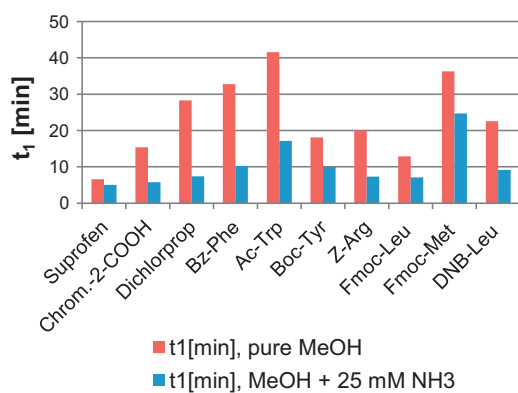


Fig. 6. Comparison of retention times of the first eluted peaks by using either pure methanol or methanolic ammonia (25 mM) as modifier in the sc CO₂-based mobile phase. Conditions: QN-AX-CSP; 25% modifier; 40 °C, 150 bar, 4.0 mL/min; Chrom.-2-COOH: Chromane-2-carboxylic acid.

sc CO₂-alcohol mobile phases. However, in the limited amount of publications available, water was used either to facilitate elution of highly polar compounds on polar stationary phases or to improve peak shapes due to enhanced analyte solubility in the mobile phase [36–38].

In our study, water was used as a neutral additive in the sc CO₂-MeOH mobile phase. Increasing amounts of water in the modifier (1–8%, v/v, equates 0.25–2% in the mobile phase) led to a decrease in retention times and an increase in plate numbers (Fig. 7). However, the use of 10% water in the methanolic modifier caused already potential phase separation in the SFC system (no meaningful chromatograms could be obtained even after several repetitions) confirming an earlier study by Li and Thurbird [36]. The decrease in retention times can be explained by an increased formation of counterions in the sc hydroorganic mobile phase via reaction of CO₂ with water yielding carbonic acid dissociating to hydrogen carbonate and a proton. Moreover, the use of small amounts of water can be used to enhance solubility of highly hydrophilic compounds in the sc mobile phase and thus leading to improved peak shapes (e.g. for Cbz-Arginine, being inherently zwitterionic in sc CO₂-MeOH mobile phases, fourfold higher plate numbers were achieved when increasing the water content from 0% to 8% in the modifier). In other words, the addition of a limited amount of water to an alcoholic SFC mobile phase can cause beneficial effects. However, more investigations are needed to deconvolute also the extended water adsorption on the silica based stationary phase.

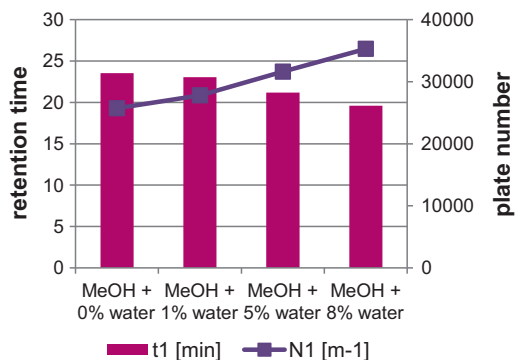


Fig. 7. Average retention times and plate numbers of the first eluted peak of 9 tested solutes (Suprofen, Chromane-2-carboxylic acid, Dichlorprop, Bz-Phe, Ac-Trp, Boc-Tyr, Cbz-Arg, Fmoc-Leu, Fmoc-Met). Conditions: QN-AX CSP; 25% modifier (MeOH + water); 40 °C, 150 bar, 4.0 mL/min.

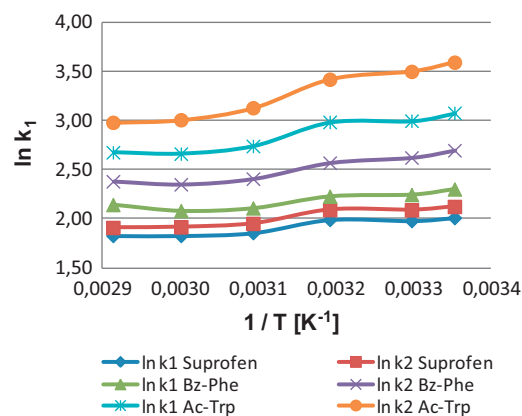


Fig. 8. Van't Hoff plot displaying $\ln k_1$ vs. $1/T$. Conditions: CSP: QN-AX; 25% modifier (MeOH, 200 mM HOAc, 100 mM NH₃); 150 bar, 4.0 mL/min.

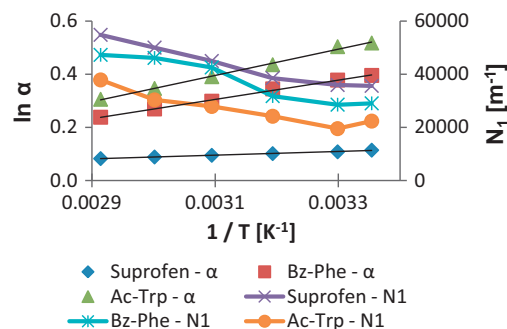


Fig. 9. Van't Hoff plot showing the relationship of $\ln \alpha$ and N_1 vs. $1/T$. Conditions: CSP: QN-AX; 25% modifier (MeOH, 200 mM HOAc, 100 mM NH₃); 150 bar, 4.0 mL/min; N_1 [m⁻¹], plate numbers per meter for first eluted peak.

3.7. Influence of temperature on the chromatographic performance

Dependence of retention on temperature variations is known to be more complex in SFC than in HPLC. Supercritical fluid mobile phases tend to possess a “retention minimum”, i.e. with increasing temperature retention is first decreased and then starts to increase due to lower fluid density (and thus decreased elution strength). In contrast, in a subcritical fluid retention is reduced with increasing temperature (and thus resembles liquid behavior like in HPLC). Van't Hoff analysis (Fig. 8), logarithm of the retention factor versus $1/T$ gave non-linear plots showing a decrease in retention with increasing temperature. On the other hand, a linear relationship was obtained for Van't Hoff plots of $\ln \alpha$ vs. $1/T$, thereby confirming that enantioselectivity is enthalpically controlled (Fig. 9). Moreover, temperature dependence of retention and enantioselectivity follows the same rules as observed in HPLC studies [39]. As expected, plate numbers (efficiencies) are increasing with increasing temperature (Fig. 9) due to enhanced mass transfer between the mobile and stationary phase. As a practical aspect, a change in temperature can be a powerful tool for challenging enantioseparations. Ambient column temperatures up to 40 °C turned out to be promising in terms of separation performance, because reduced enantioselectivity at higher temperature gets outperformed by higher column efficiency thus providing the highest resolution values.

4. Conclusions

Weak anion-exchange-type chiral stationary phases were investigated in SFC mode exhibiting a separation performance

comparable to HPLC mode: (1) Enantioselectivity followed the same pattern as observed in HPLC which indicates the same chiral recognition mechanism. (2) As ion exchange is the driving interaction force between the SO and SA, retention can be tuned by the amounts and types of co- and counterions (salts) in the modifier while enantioselectivity remains almost unaltered. (3) Temperature changes offer potential for improving enantioselectivity, which is increased at decreasing temperature, manifesting an enthalpically controlled chiral recognition mechanism. Moreover, a temperature increase led to significantly enhanced peak efficiencies and to better resolution combined with shortened retention times. (4) The early findings of Eckert and co-workers [32,33] describing the phenomenon of in situ formation of methylcarbonic acid (and its dissociated species methylcarbonate, respectively) in pressurized methanolic CO₂ solutions could be confirmed indirectly. (5) Due to this reaction scheme it is possible to use chiral anion exchangers QN-AX and QD-AX with only pressurized methanolic CO₂. (6) Given the existence of methylcarbonic acid the addition of ammonia to methanol as co-solvent and modifier for CO₂ leads to the in situ formation of ammonium methylcarbonate which acts as a salt in the mobile phase. It supports again the stoichiometric displacement model of action in the use of anion exchangers. (7) QN-AX and QD-AX CSPs operated in SFC mode have a high potential for preparative chromatography due to their high column loading capacity (data not shown).

To conclude, (chiral) anion exchange columns can equally well be operated in HPLC and SFC mode, whereby the latter mode opens up the use of salt-free mobile phase conditions due to the in situ generation of volatile acid and salt components.

Acknowledgements

The authors gratefully thank AstraZeneca (Möln dal, Sweden) for providing a stay to carry out SFC-measurements. R.P. thanks particularly Hanna Nelander and Tomas Leek for fruitful discussions and support during the stay. Finally, the authors thank Peter Frühauf for packing the columns.

References

- [1] E. Klesper, A.H. Corwin, D.A. Turner, *J. Org. Chem.* 27 (1962) 700.
- [2] L.T. Taylor, *J. Supercrit. Fluids* 47 (2009) 566–573.
- [3] L.T. Taylor, *Anal. Chem.* 82 (2010) 4925–4935.
- [4] E. Abbott, T.D. Veenstra, H.J. Issaq, *J. Sep. Sci.* 31 (2008) 1223.
- [5] E. Lesellier, *J. Sep. Sci.* 31 (2008) 1238.
- [6] K.W. Phinney, L.C. Sander, *Chirality* 15 (2003) 287.
- [7] J.A. Blackwell, R.W. Stringham, J.D. Weckwerth, *Anal. Chem.* 69 (1997) 409.
- [8] Y.K. Ye, K.G. Lynam, R.W. Stringham, *J. Chromatogr. A* 1041 (2004) 211.
- [9] M. Ventura, B. Murphy, W. Goetzinger, *J. Chromatogr. A* 1220 (2012) 147.
- [10] D. Mangelings, Y. Vander Heyden, *J. Sep. Sci.* 31 (2008) 1252.
- [11] K.W. Phinney, *Anal. Bioanal. Chem.* 382 (2005) 639.
- [12] G. Terfloth, *J. Chromatogr. A* 906 (2001) 301.
- [13] H. Nelander, S. Andersson, K. Öhlén, *J. Chromatogr. A* 1218 (2011) 9397.
- [14] G.T. Lavison, *Chirality* 15 (2003) 630.
- [15] R. Duval, H. Lévêque, Y. Prigent, H.Y. Aboul-Enein, *Biomed. Chromatogr.* 15 (2001) 202.
- [16] C.M. Kraml, D. Zhou, N. Byrne, O. McConnell, *J. Chromatogr. A* 1100 (2005) 108.
- [17] X. Han, A. Berthod, C. Wang, K. Huang, D.W. Armstrong, *Chromatographia* 65 (2007) 381.
- [18] M. Johannsen, *J. Chromatogr. A* 937 (2001) 135.
- [19] Y. Zhao, W.A. Pritts, S. Zhang, *J. Chromatogr. A* 1189 (2008) 245.
- [20] Y. Liu, A. Berthod, C.R. Mitchell, T.L. Xiao, B. Zhang, D.W. Armstrong, *J. Chromatogr. A* 978 (2002) 185.
- [21] N.M. Maier, L. Nicoletti, M. Lämmerhofer, W. Lindner, *Chirality* 11 (1999) 522.
- [22] M. Lämmerhofer, W. Lindner, *J. Chromatogr. A* 741 (1996) 33.
- [23] E. Zarbl, M. Lämmerhofer, F. Hammerschmidt, F. Wuggenig, M. Hanbauer, N.M. Maier, L. Sajovic, W. Lindner, *Anal. Chim. Acta* 404 (2000) 169.
- [24] W. Bicker, M. Lämmerhofer, W. Lindner, *J. Chromatogr. A* 1035 (2004) 37.
- [25] M. Lämmerhofer, P. Imming, W. Lindner, *Chromatographia* 60 (2004).
- [26] C. Czerwenka, M. Lämmerhofer, W. Lindner, *J. Pharm. Biomed. Anal.* 30 (2003) 1789.
- [27] A. Mandl, L. Nicoletti, M. Lämmerhofer, W. Lindner, *J. Chromatogr. A* 858 (1999) 1.
- [28] J. Lah, N.M. Maier, W. Lindner, G. Vesnaver, *J. Phys. Chem. B* 105 (2001) 1670.
- [29] C. Hellriegel, U. Skogsberg, K. Albert, M. Lämmerhofer, N.M. Maier, W. Lindner, *J. Am. Chem. Soc.* 126 (2004) 3809.
- [30] W. Bicker, I. Chiorescu, V.B. Arion, M. Lämmerhofer, W. Lindner, *Tetrahedron: Asymmetry* 19 (2008) 97.
- [31] Y. Tojo, K. Hamase, M. Nakata, A. Morikawa, M. Mita, Y. Ashida, W. Lindner, K. Zaitso, *J. Chromatogr. B* 875 (2008) 174.
- [32] R.R. Weikel, J.P. Hallett, C.L. Liotta, C.A. Eckert, *Top. Catal.* 37 (2006) 75.
- [33] J.P. Hallett, P. Pollet, C.L. Liotta, C.A. Eckert, *Acc. Chem. Res.* 41 (2008) 458.
- [34] F.O. Geiser, S.G. Yocklovich, S.M. Lurcott, J.W. Guthrie, E.J. Levy, *J. Chromatogr.* 459 (1988) 173.
- [35] H. Engelhardt, A. Gross, R. Mertens, M. Petersen, *J. Chromatogr.* 477 (1989) 169.
- [36] J. Li, K.B. Thurvide, *Can. J. Anal. Sci. Spectrosc.* 53 (2008) 59.
- [37] M. Ashraf-Khorassani, L.T. Taylor, *J. Sep. Sci.* 33 (2010) 1682.
- [38] A. dos Santos Pereira, A.J. Girón, E. Admasu, P. Sandra, *J. Sep. Sci.* 33 (2010) 834.
- [39] W.R. Oberleitner, N.M. Maier, W. Lindner, *J. Chromatogr. A* 960 (2002) 97.

APPENDIX III

Enantioseparation of Chiral Sulfonates by Liquid Chromatography and Subcritical Fluid Chromatography

Reinhard Pell^a, Georg Schuster^a, Michael Lämmerhofer^{a,b}, Wolfgang Lindner^a

^aDepartment of Analytical Chemistry, University of Vienna, Währinger Strasse 38, 1090 Vienna, Austria

^bcurrent address: Institute of Pharmaceutical Sciences, Universität Tübingen, Auf der Morgenstelle 8, 72076 Tübingen, Germany

*Author for correspondence:

e-mail: wolfgang.lindner@univie.ac.at

Tel.: +43 1 4277 52300 Fax: +43 1 42779523

Abstract:

Tert-butylcarbamoyl-quinine and –quinidine weak anion exchange chiral stationary phases (Chiralpak® QN-AX and QD-AX) have been applied for the separation of sodium β -ketosulfonates, such as sodium chalconesulfonates and derivatives thereof. The influence of type and amount of co- and counterions on retention and enantioresolution was investigated using polar organic mobile phases. Both columns exhibited remarkable enantiodiscrimination properties for the investigated test solutes, in which the quinidine-based column showed better enantioselectivity and slightly stronger retention for all analytes compared to the quinine-derived chiral stationary phase. With an optimized mobile phase (MeOH, 50 mM HOAc, 25 mM NH₃) 12 out of 13 chiral sulfonates could be baseline separated within 8 minutes using the quinidine-derivatized column. Furthermore, subcritical fluid chromatography (SubFC) mode with a CO₂-based mobile phase using a buffered methanolic modifier was compared to HPLC. Generally, SubFC exhibited slightly inferior enantioselectivities and lower elution power but also provided unique baseline resolution for one compound.

27 **Keywords:** chiral sulfonates, chiral separation, cinchona alkaloid, subcritical fluid
28 chromatography, liquid chromatography

29 **Abbreviations:** CSP, chiral stationary phase; QN-AX, tert-butylcarbamoyl-quinine anion
30 exchanger; QD-AX, tert-butylcarbamoyl-quinidine anion exchanger; SO, chiral selector; SA,
31 selectand; FA, formic acid; HOAc, acetic acid; CitOH, citric acid; MalOH, malonic acid;
32 SucOH, succinic acid; DEA, diethylamine; TEA, triethylamine; MeOH, methanol;

33 **1. Introduction:**

34 Liquid chromatography using chiral stationary phases (CSPs) is nowadays routinely used for
35 direct separation of enantiomers in both analytical and preparative scale [1]. Among the vast
36 number of commercially available CSPs, tert-butylcarbamoyl-quinine- and -quinidine (Figure
37 1) exhibit remarkable enantiodiscrimination properties towards chiral acids, such as N-protected
38 amino acids, aryl carboxylic acids, N-protected aminophosphonic and -phosphinic acids [2-5].
39 The CSPs are preferentially operated with slightly acidic polar organic or hydro organic
40 mobile phases, which protonates the quinuclidine tertiary amine of the chiral selector (SO)
41 and deprotonates the acidic selectand (SA) thus enabling a weak anion exchange retention
42 mechanism. Additional interactions between the SO and SA, such as hydrogen bonding, $\pi - \pi$
43 stacking, van der Waals or steric interactions working in concert with each other, may support
44 the ion pairing process and thus facilitate enantiodiscrimination [6, 7].

45 Chiral sulfonic acids (or their sulfonate salts, respectively) gained distinct importance as
46 resolving agents. For instance, camphor sulfonic acid, 3-bromocamphorsulfonic acid and 1-
47 phenylethanesulfonic acid were successfully employed for resolving racemic amines and
48 amino acids via diastereomeric salt formation [8]. Chalconesulfonic acid and derivatives
49 thereof were used in the “Dutch Resolution” process, a smooth variation of the classical

50 Pasteur resolution, where mixtures of resolving agents are used instead of one single resolving
51 agent [9]. Since sulfonic acids are isosteric to carboxylates, they show potential for
52 pharmaceutical applications. For example, 6-gingesulfonic acid, a 1,3-ketosulfonic acid
53 derivative found in ginger (*zingiberis rhizoma*), shows anti-ulcer activity [10, 11]. (R)-
54 saclofen, the sulfonic acid analogue of baclofen, is a potent GABA_A receptor antagonist [12].

55 Acquiring enantiomerically pure sulfonic acids was either achieved by asymmetric
56 synthesis or synthesis of the racemate following a resolution via diastereomeric salt
57 formation. For example, the preparation of enantiopure chalconesulfonic acid was
58 accomplished via homogenous catalysis using a quinine-or quinidine-modified catalyst [13]
59 or via Dutch Resolution with (R)-4-methylphenylglycinol [14]. However, enantioresolution of
60 a broad set of free (unprotected) sulfonic acids via chromatography has not been reported so
61 far. Only camphorsulfonic acid, three N-protected aminosulfonic acids and alpha-
62 perfluoromethyl branched perfluorooctane sulfonate (*1m*-PFOS) were separated in their
63 enantiomers on a quinine-carbamate type weak anion exchange CSP [2, 3, 15]. Furthermore,
64 camphorsulfonic acid was resolved by indirect enantioseparation using an achiral diol
65 stationary phase with quinine as chiral mobile phase additive [16].

66 Hence, we herein report the application of tert-butylcarbamoyl-quinine and –quinidine
67 CSPs (Figure 1) for enantioseparation of β -ketosulfonic acids (applied as their sodium salts)
68 by HPLC and SubFC. Employing a polar organic mobile phase, the influence of type and
69 amounts of acidic and basic additives was investigated. Additionally, the separation
70 performance of subcritical fluid chromatography (SubFC) for the same analyte set was also
71 examined.

72 <insert Figure 1>

73

74

<insert Figure 2>

75

76 **2. Experimental:**

77 **2.1 Materials**

78 Compounds **1-4** were kind gifts of Syncom (Groningen, Netherlands). 2,4-
79 dichlorobenzaldehyde, acetophenone, benzaldehyde, 2',4'-dichloroacetophenone, 2,4-
80 dimethoxybenzaldehyde, 2',4'-dimethoxyacetophenone, 2-methoxybenzaldehyde, 2'-
81 methoxyacetophenone, coumarin, phenalen-1-one, NaHSO₃ and NaOH were purchased from
82 Sigma-Aldrich (Vienna, Austria) in reagent grade or higher quality. Ethanol (96%), CH₂Cl₂
83 and methanol (MeOH) was purchased from VWR (Vienna, Austria) and water was bidistilled
84 in house. Mobile phases for HPLC (or modifiers for SubFC, respectively) were prepared with
85 HPLC-grade solvents and analytical grade reagents and were degassed in the ultrasonication
86 bath prior to use. Mobile phases containing HOAC/NH₃ buffers were prepared by combining
87 ammonium acetate with acetic acid.

88

89 **2.2 Synthesis of sodium β -ketosulfonate test compounds**

90 The synthesis of chalconesulfonate derivatives **6-12** was accomplished by 1,4-addition (Thia-
91 Michael addition) of sodium bisulfite to the corresponding chalcone derivatives, which were
92 synthesized via aldol condensation. The synthetic protocol followed the published procedure
93 by Kellogg et al [14]. Accordingly, sodium β -ketosulfonates **5** and **13** were also prepared via
94 1,4 - addition of NaHSO₃ to the α,β unsaturated carbonyl compound starting materials: 20.0

95 mmol of coumarin (2.93 g, for synthesis of **5**) or phenalen-1-one (3.61 g, for synthesis of **13**)
96 were suspended in 20 mL 96% ethanol. 2.08 g (20.0 mmol, 1 eq.) NaHSO₃ were dissolved in
97 10 mL water and added to the ethanolic solution. The mixture was heated and refluxed
98 overnight. After cooling to r.t. and evaporation of solvent crude **5** or **13** were obtained, which
99 were then purified by flash chromatography (CH₂Cl₂ : MeOH 10:1, then 1:1; v/v).

100 **5**, yield 45%, white powder; ¹H-NMR [CD₃OD]: δ = 3.22 (m, 2H), 4.34 (dd, 1H), 6.87 (m,
101 2H), 7.17 (m, 2H). ¹³C-NMR [CD₃OD]: δ = 31.2 (CH₂), 56.3 (CH), 116.6 (C_{ar}H), 121.0
102 (C_{ar}H), 122.7 (C_{ar}), 125.4 (C_{ar}H), 130.7 (C_{ar}H), 154.8 (C_{ar}), 170.5 (C=O). MS (ESI, negative):
103 227.1 [M-Na]⁻

104 **6**, yield 33%, white crystals; ¹H-NMR [D₂O]: δ = 3.72 (dd, 1H), 3.82 (dd, 1H), 5.14 (dd, 1H),
105 7.05 (dd, 1H), 7.26 (t, 2H), 7.32 (t, 2H), 7.41 (t, 1H), 7.66 (d, 2H). ¹³C-NMR [D₂O]: δ = 40.7
106 (CH₂), 57.0 (CH), 127.7 (C_{ar}H), 128.5 (C_{ar}H), 129.2 (C_{ar}H), 129.6 (C_{ar}H), 129.9 (C_{ar}H), 132.5
107 (C_{ar}), 134.2 (C_{ar}), 134.6 (C_{ar}H), 135.9 (C_{ar}), 136.2 (C_{ar}), 200.3 (C=O). MS (ESI, negative):
108 357.0 [M-Na]⁻

109 **7**, yield 34%, white powder; ¹H-NMR [D₂O]: δ = 3.68 (dd, 1H), 3.81 (dd, 1H), 4.48 (dd, 1H),
110 7.11 (dd, 1H), 7.17-7.31 (m, 7H). ¹³C-NMR [D₂O]: δ = 44.2 (CH₂), 62.2 (CH), 127.8 (C_{ar}H),
111 128.8 (C_{ar}H), 129.0 (C_{ar}H), 129.6 (C_{ar}H), 130.7 (C_{ar}H), 130.9 (C_{ar}H), 132.0 (C_{ar}), 135.2 (C_{ar}),
112 135.8 (C_{ar}), 138.0 (C_{ar}), 201.8 (C=O). MS (ESI, negative): 357.0 [M-Na]⁻

113 **8**, yield 50%, white powder; ¹H-NMR [D₂O]: δ = 3.60 (s, 6H), 3.63-3.78 (m, 2H), 5.02 (dd,
114 1H), 6.37 (d, 2H), 7.21 (d, 1H), 7.29 (t, 2H), 7.45 (t, 1H), 7.67 (d, 2H). ¹³C-NMR [D₂O]: δ =
115 40.7 (CH₂), 53.9 (CH), 55.7 (OCH₃), 56.4 (OCH₃), 99.2 (C_{ar}H), 105.9 (C_{ar}H), 116.8 (C_{ar}H),
116 128.5 (C_{ar}H), 129.2 (C_{ar}H), 129.4 (C_{ar}H), 134.4 (C_{ar}H), 136.3 (C_{ar}), 159.0 (C_{ar}), 160.3 (C_{ar}),
117 201.7 (C=O). MS (ESI, negative): 349.1 [M-Na]⁻

118 **9**, yield 66%, white powder; $^1\text{H-NMR}$ [D_2O]: $\delta = 3.68$ (d, 6H), 3.72 (d, 2H), 4.45 (dd, 1H),
119 6.31 (m, 2H), 7.26 (m, 6H). $^{13}\text{C-NMR}$ [D_2O]: $\delta = 44.5$ (CH_2), 55.9 (OCH_3), 56.0 (OCH_3),
120 62.8 (CH), 98.7 (C_{arH}), 106.4 (C_{arH}), 119.7 (C_{ar}), 128.6 (C_{arH}), 128.9 (C_{arH}), 129.5 (C_{arH}),
121 132.9 (C_{arH}), 135.7 (C_{ar}), 161.4 (C_{ar}), 165.2 (C_{ar}), 200.7 ($\text{C}=\text{O}$). MS (ESI, negative): 349.1
122 $[\text{M-Na}]^-$

123 **10**, yield 97%, yellowish powder; $^1\text{H-NMR}$ [D_2O]: $\delta = 3.66$ (s, 3H), 3.69-3.85 (m, 2H), 5.14
124 (dd, 1H), 6.87 (dd, 2H), 7.20 (t, 1H), 7.36 (t, 3H), 7.51 (t, 1H), 7.73 (d, 2H). $^{13}\text{C-NMR}$ [D_2O]:
125 $\delta = 40.7$ (CH_2), 54.2 (CH), 56.5 (OCH_3), 112.4 (C_{arH}), 121.3 (C_{arH}), 124.1 (C_{arH}), 128.5
126 (C_{arH}), 128.6 (C_{arH}), 129.2 (C_{arH}), 129.9 (C_{arH}), 134.5 (C_{arH}), 136.3 (C_{ar}), 157.9 (C_{ar}), 201.8
127 ($\text{C}=\text{O}$). MS (ESI, negative): 319.0 $[\text{M-Na}]^-$

128 **11**, yield 74%, white powder; $^1\text{H-NMR}$ [D_2O]: $\delta = 3.72$ (s, 3H), 3.73-3.85 (m, 2H), 4.45 (dd,
129 1H), 6.84 (t, 1H), 6.96 (d, 1H), 7.24 (m, 6H), 7.41 (t, 1H). $^{13}\text{C-NMR}$ [D_2O]: $\delta = 44.8$ (CH_2),
130 56.0 (CH), 62.7 (OCH_3), 112.9 (C_{arH}), 121.1 (C_{arH}), 127.0 (C_{ar}), 128.7 (C_{arH}), 128.9 (C_{arH}),
131 129.6 (C_{arH}), 130.2 (C_{arH}), 135.2 (C_{arH}), 135.5 (C_{ar}), 158.6 (C_{ar}), 203.7 ($\text{C}=\text{O}$). MS (ESI,
132 negative): 319.1 $[\text{M-Na}]^-$

133 **12**, yield 60%, yellowish powder; $^1\text{H-NMR}$ [D_2O]: $\delta = 3.64$ (dd, 2H), 4.50 (dd, 1H), 6.58 (d,
134 2H), 7.17 (d, 2H), 7.25 (d, 2H), 7.57 (d, 2H). $^{13}\text{C-NMR}$ [D_2O]: $\delta = 39.8$ (CH_2), 61.2 (CH),
135 115.7 (C_{arH}), 126.1 (C_{arH}), 126.8 (C_{arH}), 126.9 (C_{ar}), 128.4 (C_{ar}), 128.9 (C_{arH}), 130.6 (C_{arH}),
136 131.0 (C_{ar}), 133.4 (C_{ar}), 135.7 (C_{arH}), 200.2 ($\text{C}=\text{O}$). MS (ESI, negative): 338.1 $[\text{M-Na}]^-$

137 **13**, yield 65%, yellow powder; $^1\text{H-NMR}$ [D_2O]: $\delta = 3.04$ (dd, 1H), 3.27 (dd, 1H), 4.63 (m,
138 1H), 7.47 (m, 2H), 7.57 (d, 1H), 7.82 (d, 1H), 7.92 (d, 1H), 8.01 (d, 1H). $^{13}\text{C-NMR}$ [D_2O]: $\delta =$
139 39.2 (CH_2), 62.2 (CH), 114.9 (C_{arH}), 126.3 (C_{ar}), 128.9 (C_{arH}), 130.9 (C_{arH}), 131.5 (C_{arH}),
140 133.8 (C_{ar}), 134.4 (C_{ar}), 153.6 (C_{ar}), 198.8 ($\text{C}=\text{O}$). MS (ESI, negative): 261.1 $[\text{M-Na}]^-$

141 **2.3 Instrumentation and Chromatography**

142 All HPLC experiments were conducted on a 1200 series HPLC systems from Agilent
143 Technologies (Waldbronn, Germany) consisting of a solvent degasser, a quaternary pump, an
144 autosampler, a column thermostat and a diode array detector. Chemstation software version
145 Rev. B.01.03 was used for data acquisition and analysis. The mobile phase flow rate was 1.0
146 mL/min using a 5 μ m particle size, 150 x 4 mm i.d. column. The test compounds were
147 dissolved in MeOH in a concentration of 1.0-2.0 mg/mL. The injection volume varied
148 between 5 and 10 μ L and column temperature was 25°C. The void volume was determined by
149 injecting a solution of acetone in MeOH. Before switching from stronger to weaker acid as
150 mobile phase counter ion, the CSP was washed with MeOH containing 1% (v/v) TEA with a
151 flow of 2 ml/min for about 10 minutes followed by plain MeOH with 2 ml/min for 10
152 minutes, in order to remove the high-affinity counter-ion and achieve reproducible retention
153 times with subsequent additive.

154 SubFC experiments were carried out on a Thar Discovery system from Thar
155 Technologies Inc., equipped with a combined CO₂ and modifier pump, a combined column
156 oven and column selector valve for 6 columns, an automated back pressure regulator, a water
157 bath and a Gilson UV variable wavelength detector. Instrument control and data acquisition
158 were carried out with Thar SuperChrome software and Thar ChromScope software,
159 respectively. The runs were performed in isocratic mode with 25% modifier content at a flow
160 rate of 4.0 mL/min, 40°C and 150 bar backpressure. The analytes were dissolved in MeOH in
161 a concentration of 3-5 mg/mL and the void time was determined by injecting a methanolic
162 solution of acetone.

163

164 3. Results and Discussion

166 3.1 General remarks

167 First, the sulfonic acid test compounds were applied as their sodium salts. However, no
168 differences in chromatographic separation properties are observed between sulfonic acid- and
169 sodium sulfonate analytes, as sulfonic acids are strong acids and thus fully dissociated under
170 the applied mobile phase conditions. Second, polar organic mode with MeOH as bulk solvent
171 was chosen for the HPLC studies. The sulfonate analytes **1-13** show high solubility in MeOH
172 which is advantageous for potential preparative separations. Taking analyte solubility into
173 account, also reversed phase mode could have been chosen. However, operation of QN-AX or
174 QD-AX CSPs with hydro organic mobile phases cause prolonged retention and eventually
175 decreased enantioselectivity due to the activation of nonspecific hydrophobic interactions [2].
176 Moreover, regarding preparative separations, one tries to avoid water in the mobile phase due
177 to higher energy costs in the evaporation process.

178 3.2 Influence of counterion type and strength

179 The interaction, and thus retention and separation, between the quinine carbamate type SOs
180 and the SAs is dominated by long range electrostatic forces [6, 7]. Hence, under slightly
181 acidic mobile phase conditions the protonated tertiary amine in the quinuclidine moiety (see
182 Figure 1) undergoes an ionic interaction with the corresponding deprotonated (ionized) acidic
183 analyte. The anion exchange retention mechanism following a stoichiometric displacement
184 model is strongly dependent on the type and amount of counterions in the mobile phase.

185 The counterion effect was systematically studied by Gyimesi-Forrás et al [17] for
186 carboxylic acid analytes. Sulfonic acids have not yet been explored in this regard. We
187 therefore investigated five different mono-, bi, and trivalent acids as acidic additives
188 (counterions) using MeOH as bulk solvent (the apparent pH was adjusted to 6.1 with

189 triethylamine, TEA). An increase of competitor acid (counterion) concentration in the mobile
190 phase led to a decrease of retention times for all sulfonate test compounds **1-13**. Plots of the
191 logarithm of the retention factor ($\log k_1$) versus the logarithm of the counterion concentration
192 ($\log [C]$) gave a linear relationship which clearly indicates an anion exchange mechanism
193 following the stoichiometric displacement model (Equation 1) [2, 18].

$$194 \quad \log k = \log K_z - Z \cdot \log [C] \quad (1)$$

195 wherein k is the retention factor, $[C]$ the molar concentration of the counterion in the eluent, Z
196 is the slope of the linear regression line, and $\log K_z$ the intercept with the system-specific
197 constant K_z being defined by equation 2.

$$198 \quad K_z = \frac{K \cdot S \cdot (q_x)^Z}{V_0} \quad (2)$$

199 wherein K is the ion-exchange equilibrium constant, S the surface area, q_x the charge density
200 on the surface i.e. the number of ion-exchange sites available for adsorption and V_0 the mobile
201 phase volume. Hence, the intercept $\log K_z$ can be regarded as measure for the affinity of the
202 solute towards the ion-exchanger under given conditions and represents the $\log k$ -value at 1M
203 concentration of counterion. The slope Z in eq. 1 is indicative for the charges involved in the
204 ion-exchange process and is directly proportionally depending on the ratio of the effective
205 charge numbers of solute ($z_{eff,S}$) and counterion ($z_{eff,C}$) [19, 20].

206 Thus, both intercept and slope are characteristic for the given ion-exchange process and
207 can be used for retention prediction. Table 1 depicts the values of slopes and intercepts of the
208 linear relationship for compounds **9** and **11**. They can also be used to illustrate the elution
209 strength of different counterions.

210 As can be seen from Table 1, the strongest acids within this study, citric acid and
211 malonic acid, exhibited the lowest values for the intercept (-1.19 and -1.92, respectively). On
212 the contrary, for acetic acid as the weakest acid investigated, the value was 0.55. Hence, the
213 more competitive the counterion (the stronger and polyprotic the acid) the lesser amount is
214 needed to achieve isoeluotropic conditions. This findings corroborate earlier investigations
215 made for carboxylic acid analytes [17], but the effect is more pronounced for the sulfonate
216 compounds. For instance, to adjust k_1 to 4.5 for compound **9**, only 2 mM of citric acid are
217 needed compared to 214 mM of acetic acid (Table 1). However, employing such low
218 concentrations of counterions may be detrimental for the peak shapes or for the
219 reproducibility of retention times (especially in preparative chromatography under high
220 sample loads). Thus, citric acid or malonic acid may be avoided as counterions, unless
221 analytes are extremely strongly retained like polyprotic acids.

222 In sharp contrast, a variation of the counterion concentration showed insignificant
223 effects on enantioselectivity. Moreover, the type of counterion (acidic additive) exhibited also
224 only a minor influence on α (note: the pH_a was always adjusted to 6.1 with TEA). For
225 instance, the α -value for **9** varied from 1.31 to 1.36 using different types of acidic additives
226 (data not shown).

227 To summarize, separation of sodium β -ketosulfonates on quinine- and quinidine derived
228 CSPs follows an ion-exchange mechanism as it was observed for other acidic (anionic)
229 analytes such as carboxylic-, phosphonic- and phosphinic acids. This means in practical terms
230 that retention can easily be adjusted by the amount or type of acidic additive without
231 significantly changing enantioselectivity.

232 <insert Table 1>

233 **3.3 Influence of the co-ion**

234 Basic additives act as co-ions in the anion-exchange dominated retention process and can also
235 be influential for separation of chiral acids on cinchona alkaloid derived CSPs. Primarily, they
236 are utilized to adjust the pH of the eluent. Since cinchona carbamate type SOs are weak anion
237 exchangers and are operated with weak acids as mobile phase additives, the apparent pH (and
238 thus the ionization state of SOs and SAs) plays a decisive role for retention and
239 enantioselectivity [21]. Typically, small amounts of organic amines are only needed to
240 establish weakly acidic conditions, which also favours repeatability, shortens retention times
241 and improves peak shape (compared to the sole addition of acidic additives) [22]. Under the
242 given slightly acidic mobile phase conditions, the decreased retention can be explained by the
243 competition between the protonated quinuclidinium moiety of the SO and the protonated
244 amine additive to form ion pairs with the deprotonated acidic analyte. It seems that the
245 competitive effect is necessary to balance the electrostatic interaction between the SO and SA.

246 In this study, three amines with differing alkyl substitution degree, namely NH_3 , DEA
247 and TEA, were chosen as basic additives. In previous studies for carboxylic acid solutes they
248 showed increasing elution strength on QN-AX or QD-AX CSPs in the following order:
249 $\text{NH}_3 < \text{DEA} < \text{TEA}$ [22]. First, the mobile phase acid to base ratio (i.e. the pH_a of the mobile
250 phase being responsible for the protonation state of the SO and dissociation state of the SA)
251 was optimized in matters of short retention times with adequate resolution of the chiral
252 compounds (data not shown). Hence, an acid to base ratio of 2:1 was chosen with HOAc as
253 acidic additive. Figure 3 depicts the influence of the various amine additives on
254 chromatographic parameters (retention k_1 , enantioselectivity α , plate number N_1 and
255 resolution R_s). Unlike for the acidic counterions, the type of the basic co-ions showed
256 negligible influence on separation performance (note that the pH_a for all three additive

257 combinations was almost constant, namely 6.8 for HOAc/NH₃, 6.9 for HOAc/DEA and 6.9
258 for HOAc/TEA, each 50 mM acid and 25 mM base).

259 On the contrary, employing a different combination of acidic and basic additives, such
260 as FA and DEA, yielded strongly differing results (see right bars in Figure 3). Compared to
261 HOAc/DEA, the use of FA/DEA led to a 6-fold increased retention, but also to a better
262 separation performance. The higher retention times may be related to the lower p*H*_a of
263 FA/DEA (p*H*_a = 5.6 for 50 mM FA and 25 mM DEA in MeOH) and may be a combined
264 effect of altered ionization states, in particular reduced counterion dissociation. Therefore, the
265 observed overall ionic interaction of the analytes with the SOs is strengthened because of less
266 counterion competition.

267 <insert Figure 3>

268 **3.4 Separation Performance of QN-AX and QD-AX CSP**

269 A set of 13 sodium β-ketosulfonates was chosen to investigate the separation performance of
270 QN-AX and QD-AX CSP towards chiral sulfonate compounds. Analytes **2-4** and **6-12** are
271 derivatives of chalconesulfonate **1**. They comprise either electron donating or electron
272 withdrawing groups on their phenyl-rings turning them π-basic or π-acidic. Besides,
273 compounds **5** and **13** possess a more rigid molecular structure compared to the
274 conformationally more flexible chalconesulfonates (and derivatives thereof).

275 MeOH with 50 mM HOAc and 25 mM NH₃ was employed as mobile phase which was
276 a good compromise between fast analyte elution, good separation performance and high
277 buffer volatility for a potential LC-MS hyphenation. As summarized in Table 2, QD-AX CSP
278 outperformed the QN-AX column in terms of enantioselectivity and resolution values, and
279 yielded baseline resolution for 12 out of the 13 test compounds. Nevertheless, also the

280 quinine-based column achieved at least partial separation of 11 sodium β -ketosulfonates with
281 8 of them being baseline resolved with the given conditions.

282 Regarding the structure-enantioselectivity relationship, some trends became evident:
283 disubstituted chalconesulfonates derivatives with their substituents at the phenyl ring next to
284 the carbonyl group were better resolved on both columns than their constitutional isomers
285 having the phenyl-substitution in vicinity of the sulfonate group (for instance, **7** and **9** showed
286 higher α -values than **6** and **8**). Ortho-substitution at the sulfonate-group containing aromatic
287 ring seems to be detrimental for the enantiodiscrimination properties , as α -values for **10** are
288 lower than for its para-substituted isomer **4** (Figure 4).

289 Furthermore, pronounced retention characteristics were not observed. Both electron
290 donating and electron withdrawing substituents caused slightly increased retention for the
291 chalconesulfonate derivatives compared to the unsubstituted chalconesulfonate. Furthermore,
292 naphthyl-group containing compounds **3** and **13** were retained strongest.

293

294 <insert Table 2>

295 <insert Figure 4>

296

297 **3.5 SubFC Enantioseparation of sodium β -ketosulfonates**

298 Recently, we reported on separation of chiral carboxylic acids on QN-AX and QD-AX CSPs
299 by subcritical fluid chromatography [23]. By applying supercritical (sc) CO₂ and a methanolic
300 modifier (containing buffer salts) we achieved separation performance similar to HPLC
301 experiments using polar organic mobile phases. Although SubFC does not appear to be the
302 first choice technique for separation of such polar compounds like sulfonic acids (sulfonates),

303 it was examined herein for SubFC enantioseparation of the sulfonate analytes on QN-AX and
304 QD-AX CSP, respectively (Figure 5).

305 Table 3 summarizes the data obtained for both columns in SubFC mode using sc CO₂
306 with 25% modifier content (MeOH, 200 mM HOAc, 100 mM NH₃). Generally,
307 enantioselectivity and plate numbers are slightly lower than in HPLC mode using MeOH, 50
308 mM HOAc, 25 mM NH₃ as mobile phase (compare Table 2 and 3). However, compound **6**
309 could only be baseline separated when applying QD-AX CSP in SubFC mode. Moreover, the
310 “separation profile” for all analytes on both CSPs is similar for SubFC and HPLC, which
311 implies the same chiral recognition mechanism in both modes.

312 Elution strength is lower in SubFC due to a lower dielectric constant of the eluent which
313 renders electrostatic interactions stronger and is reflected in roughly fivefold higher k_1 values.
314 However, due to the low viscosity of the sc CO₂-methanolic mobile phase, this disadvantage
315 can almost be compensated by application of a fourfold higher mobile phase flow rate.
316 Additionally, the higher temperature for SubFC measurements (40°C compared to 25°C in
317 HPLC) caused slightly decreased selectivity according to the enthalpically controlled chiral
318 recognition mechanism observed on cinchona carbamate type CSPs [23, 24].

319 <insert Table 3>

320 <insert Figure 5>

321 **4. Concluding remarks**

322 Chiral sodium β -ketosulfonates, such as chalconesulfonates and derivatives thereof, were
323 successfully separated on cinchona-alkaloid derivatized CSPs using HPLC and SubFC. It was
324 demonstrated that also for sulfonic acid compounds anion-exchange is the dominating

325 retention mechanism. Hence, retention can be adjusted by using different counterion
326 concentrations without affecting enantioselectivity. However, acid-base equilibria are
327 superimposed to the ion exchange-process, as the protonation state of both weak anion-
328 exchange-type SO and weak competitor acid is dependent on the apparent pH. From a
329 practical point of view this means that the ratio or type of the acidic and basic additives,
330 respectively, cause pronounced influence not only on retention but also on enantioselectivity
331 and peak shape.

332 HPLC turned out to be superior to SubFC in terms of faster solute elution but
333 employing the same co- and counterion strength in the mobile phase. However, for some
334 analytes SubFC afforded the highest magnitude of resolution values. Moreover, SubFC could
335 be considered a valuable alternative for preparative applications due to ease of solvent
336 evaporation.

337

338 **Acknowledgements**

339 The authors thank Dario Bianchi for synthesizing test compounds **12** and **13** and Peter
340 Frühauf for packing the columns.

341

342 **5. References**

343

- 344 [1] Francotte, E., Lindner, W., *Chirality in Drug Research*, Wiley-VCH, Weinheim 2006.
345 [2] Lämmerhofer, M., Lindner, W., in: Grinberg, N., Grushka, E. (Eds.), *Advances in Chromatography*,
346 CRC Press, Boca Raton, FL 2007.
347 [3] Lämmerhofer, M., Lindner, W., *J. Chromatogr. A* 1996, *741*, 33-48.
348 [4] Zarbl, E., Lämmerhofer, M., Hammerschmidt, F., Wuggenig, F., Hanbauer, M., Maier, N. M.,
349 Sajovic, L., Lindner, W., *Anal. Chim. Acta* 2000, *404*, 169-177.
350 [5] Lämmerhofer, M., Hebenstreit, D., Gavioli, E., Lindner, W., Mucha, A., Kafarski, P., Wieczorek, P.,
351 *Tetrahedron: Asymmetry* 2003, *14*, 2557-2565.
352 [6] Mandl, A., Nicoletti, L., Lämmerhofer, M., Lindner, W., *J. Chromatogr. A* 1999, *858*, 1-11.

- 353 [7] Maier, N. M., Schefzick, S., Lombardo, G. M., Feliz, M., Rissanen, K., Lindner, W., Lipkowitz, K. B., *J.*
354 *Am. Chem. Soc.* 2002, *124*, 8611-8629.
- 355 [8] Newman, P., *Optical Resolution Procedures for Chemical Compounds: Amines and Related*
356 *Compounds*, Optical Resolution Information Center, Riverdale, N.Y. 1978.
- 357 [9] Sluis, S. v. d., Hulshof, L., Kooistra, J., Vries, T., Wynberg, H., Echten, E. v., Koek, J., Hoeve, W. t.,
358 Kellogg, R. M., Broxterman, Q. B., Minnaard, A., Kaptein, B., *Angew. Chem. Int. Ed.* 1998, *37*, 2349-
359 2354.
- 360 [10] Macchiarulo, A., Pellicciari, R., *J. Mol. Graphics Modell.* 2007, *26*, 728-739.
- 361 [11] Yoshikawa, M., Yamaguchi, S., Kunimi, K., Matsuda, H., Okuno, Y., Yamahara, J., Murakami, N.,
362 *Chem. Pharm. Bull.* 1994, *42*, 1226-1230.
- 363 [12] Kerr, D. I. B., Ong, J., Vaccher, C., Berthelot, P., Flouquet, N., Vaccher, M.-P., Debaert, M., *Eur. J.*
364 *Pharmacol.* 1996, *308*, R1-R2-R1-R2.
- 365 [13] Moccia, M., Fini, F., Scagnetti, M., Adamo, M. F. A., *Angew. Chem. Int. Ed.* 2011, *50*, 6893-6895.
- 366 [14] Kellogg, R. M., Nieuwenhuijzen, J. W., Pouwer, K., Vries, T. R., Broxterman, Q. B., Grimbergen, R.
367 F. P., Kaptein, B., Crois, R. M., de Wever, E., Zwaagstra, K., van der Laan, A. C., *Synthesis* 2003, 1626-
368 1638.
- 369 [15] Wang, Y., Beeson, S., Benskin, J. P., De Silva, A. O., Genuis, S. J., Martin, J. W., *Environ. Sci.*
370 *Technol.* 2011, *45*, 8907-8914.
- 371 [16] Pettersson, C., No, K., *J. Chromatogr. A* 1983, *282*, 671-684.
- 372 [17] Gyimesi-Forrás, K., Akasaka, K., Lämmerhofer, M., Maier, N. M., Fujita, T., Watanabe, M.,
373 Harada, N., Lindner, W., *Chirality* 2005, *17*, S134-S142-S134-S142.
- 374 [18] Ståhlberg, J., *J. Chromatogr. A* 1999, *855*, 3-55.
- 375 [19] Hinterwirth, H., Lämmerhofer, M., Preinerstorfer, B., Gargano, A., Reischl, R., Bicker, W., Trapp,
376 O., Brecker, L., Lindner, W., *J. Sep. Sci.* 2010, *33*, 3273-3282.
- 377 [20] Millot, M. C., Debranche, T., Pantazaki, A., Gherghi, I., Sébille, B., Vidal-Madjar, C.,
378 *Chromatographia* 2003, *58*, 365-373.
- 379 [21] Lämmerhofer, M., Maier, N. M., Lindner, W., *Am. Lab.* 1998, *30*.
- 380 [22] Xiong, X., Baeyens, W. R. G., Aboul-Enein, H. Y., Delanghe, J. R., Tu, T., Ouyang, J., *Talanta* 2007,
381 *71*, 573-581.
- 382 [23] Pell, R., Lindner, W., *J. Chromatogr. A* 1012, *in press*. DOI: 10.1016/j.chroma.2012.05.023
- 383 [24] Oberleitner, W. R., Maier, N. M., Lindner, W., *J. Chromatogr. A* 2002, *960*, 97-108.

384

385

386

387

388

389

390

391 **Table 1.** Influence of counterion concentration on retention of first eluted enantiomers of **9** and **11** on
 392 **CSP 2^a** according to eq. 1.

Acid (counter-ion)	compound 9				compound 11			
	c [mM] ^b	slope	intercept	c _{iso} [M] ^c	c [mM] ^b	slope	intercept	c _{iso} [M] ^c
HOAc	25-100	-0.33	0.43	0.214	25-100	-0.33	0.39	0.166
FA	25-100	-0.70	-0.23	0.055	25-100	-0.71	-0.28	0.048
CitOH	2-10	-0.70	-1.19	0.002	2-10	-0.76	-1.36	0.002
SucOH	25-100	-0.64	-0.16	0.053	25-100	-0.64	-0.20	0.048
MalOH	2-10	-1.22	-1.92	0.008	2-10	-1.28	-2.01	0.008

393 ^a pH_a of methanolic mobile phase was adjusted with TEA to 6.1; ^b employed concentration range of
 394 acid in MP; ^c calculated concentrations for isoelutropic conditions (k₁ = 4.5)

395

396

397

398 **Table 2.** Enantiomer separation of compounds **1-13** on QN-AX and QD-AX CSP in HPLC mode^a

Analyte	QN-AX CSP				QD-AX CSP			
	k ₁	α	R _s	N ₁ [m ⁻¹]	k ₁	α	R _s	N ₁ [m ⁻¹]
1	1.75	1.21	2.5	47700	2.14	1.23	2.8	47800
2	1.86	1.21	2.3	38000	2.27	1.24	2.9	46300
3	2.86	1.16	2.0	38400	3.74	1.17	2.4	45200
4	1.94	1.22	2.4	40200	2.63	1.27	3.2	42100
5	1.88	1.10	1.2	12900	2.12	1.24	3.0	45200
6	1.90	1.00	0.0	18000	2.33	1.05	0.7	36200
7	2.09	1.14	1.8	43200	2.64	1.15	2.0	44900
8	1.92	1.07	0.8	21600	2.39	1.24	2.8	39800
9	1.88	1.29	3.2	44200	2.37	1.32	3.6	42900
10	1.90	1.00	0.0	20800	2.16	1.19	2.4	45300
11	1.77	1.23	2.6	40800	2.21	1.26	3.0	44400
12	1.88	1.19	2.0	35700	2.33	1.26	2.9	38500
13	2.96	1.05	0.6	35500	3.26	1.28	3.5	44000

399 ^a Conditions: mobile phase: MeOH, 50 mM HOAc, 25 mM NH₃; 1.0 mL/min, 25°C, detection 254 and
 400 230 nm; t₀ = 1.51 min

401

402

403

404

405 **Table 3.** Enantioseparation of analytes **1-13** on QN-AX and QD-AX CSP in SubFC mode^a

Analyte	QN-AX CSP				QD-AX CSP			
	k_1	α	R_s	$N_1[m^{-1}]$	k_1	α	R_s	$N_1[m^{-1}]$
1	10.35	1.16	2.2	31100	10.27	1.25	3.3	36800
2	9.37	1.08	1.2	34400	9.61	1.21	2.9	35900
3	21.29	1.10	1.5	33700	21.98	1.15	2.3	36500
4	10.31	1.18	2.5	30900	11.04	1.24	3.2	38200
5	10.59	1.12	1.7	35400	9.98	1.18	2.8	42600
6	14.37	1.05	0.7	23300	13.82	1.09	1.5	41400
7	12.02	1.11	1.7	34700	12.16	1.15	2.2	38400
8	8.96	1.05	0.7	20200	9.12	1.16	2.3	36300
9	10.73	1.26	3.1	36300	11.22	1.29	3.6	39400
10	9.76	1.00	0.0	27900	9.22	1.15	2.3	37100
11	10.49	1.21	2.7	29300	10.90	1.23	3.1	37400
12	38.22	1.13	1.7	26600	35.08	1.20	3.3	35900
13	14.69	1.00	0.0	25700	13.71	1.19	2.9	40900

406 ^aConditions: 25% modifier (MeOH, 200 mM HOAc, 100 mM NH₃); 4.0 mL/min, 40°C, 150 bar
407 backpressure; detection 254 and 230 nm; $t_0 = 0.49$ min
408

409

410

411

412

413

414

415

416

417

418

419

420

421

422

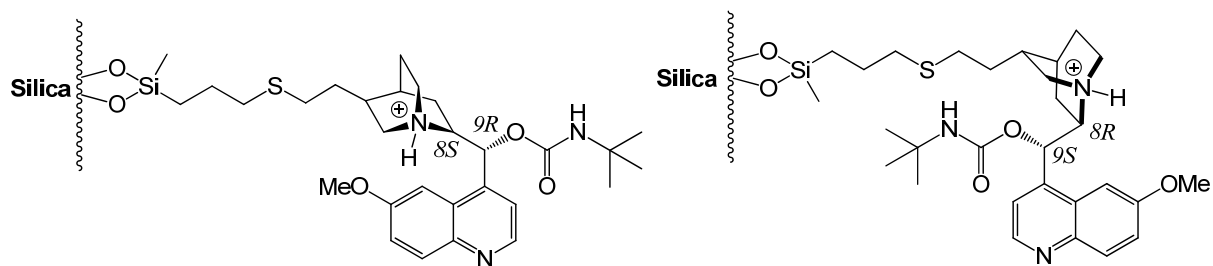
423

424

425

426

427



428

429 **Figure 1.** Structures of weak anion exchangers QN-AX (left) and QD-AX (right)

430

431

432

433

434

435

436

437

438

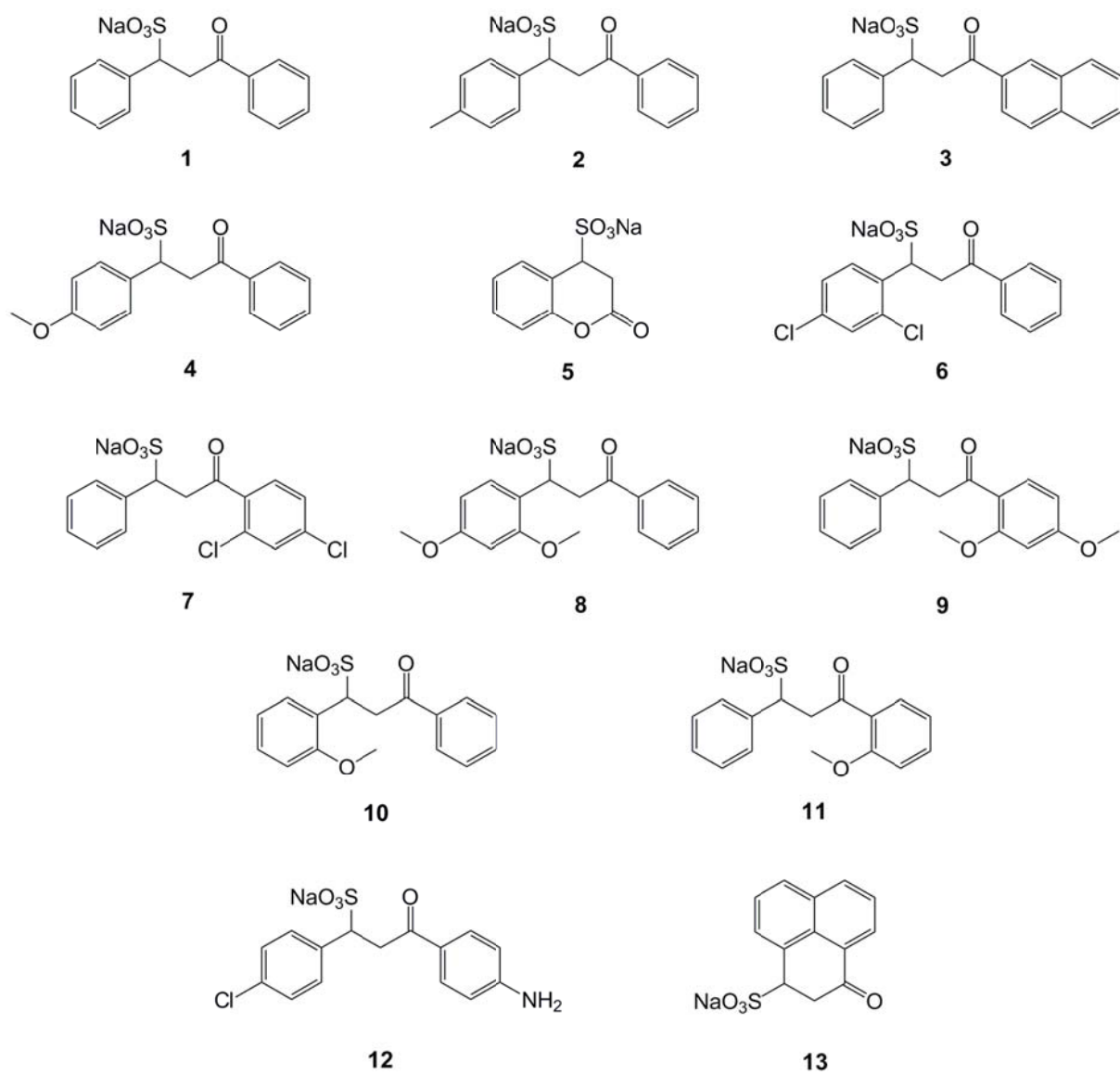
439

440

441

442

443



445

446 **Figure 2.** Structural formulas of the investigated analytes

447

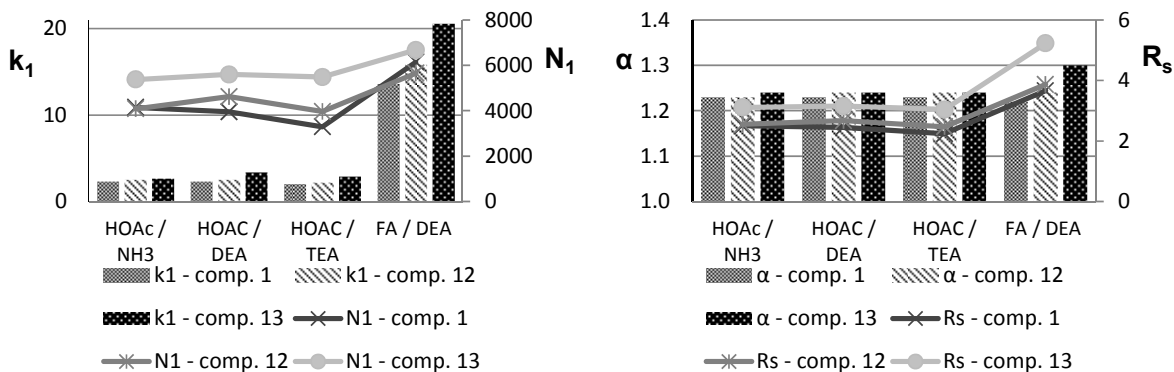
448

449

450

451

452



453

454

455 **Figure 3.** Effect of acidic and basic additives on chromatographic behavior of compounds **1**, **12** and **13**

456 on QD-AX CSP. Left diagram: retention factors and plate numbers of the first eluted peak. Right

457 diagram: enantioselectivity and resolution. Mobile phases: MeOH, 50 mM acid and 25 mM base;

458

459

460

461

462

463

464

465

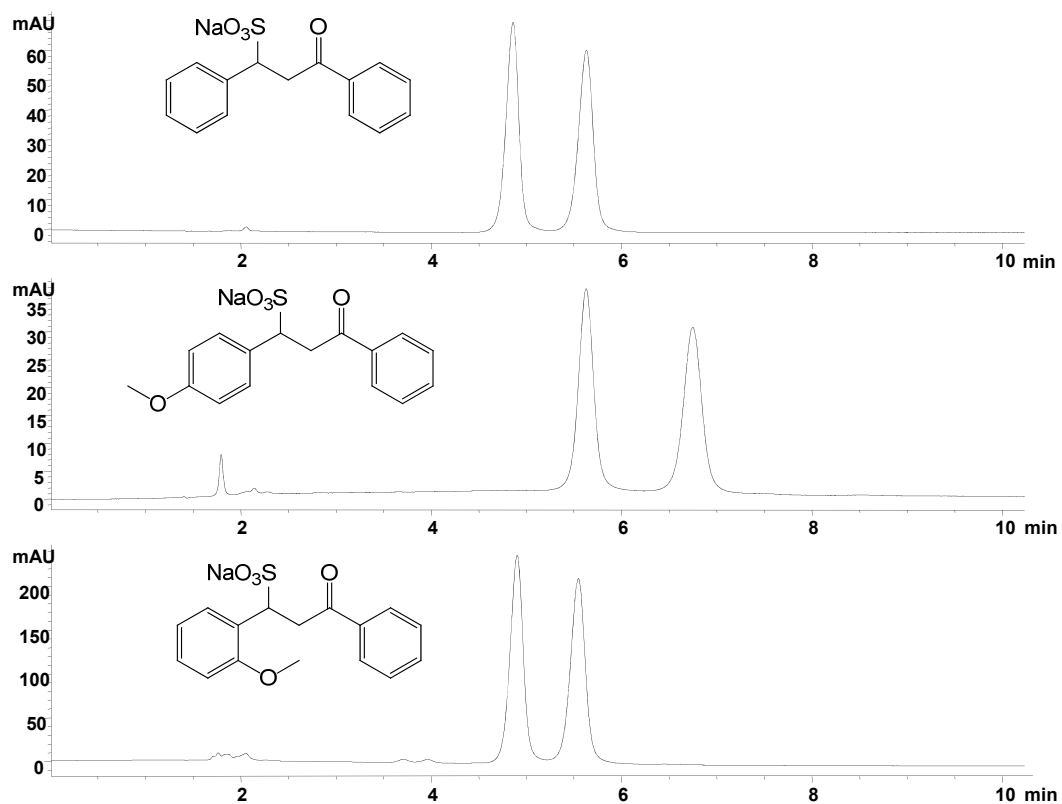
466

467

468

469

470



471

472 **Figure 4.** HPLC enantioseparations of **1** (top), **4** (middle) and **10** (bottom) on QD-AX CSP. Mobile

473 Phase: MeOH, 50 mM HOAc, 25 mM NH₃; 1.0 mL/min, 25°C UV detection at 280 nm.

474

475

476

477

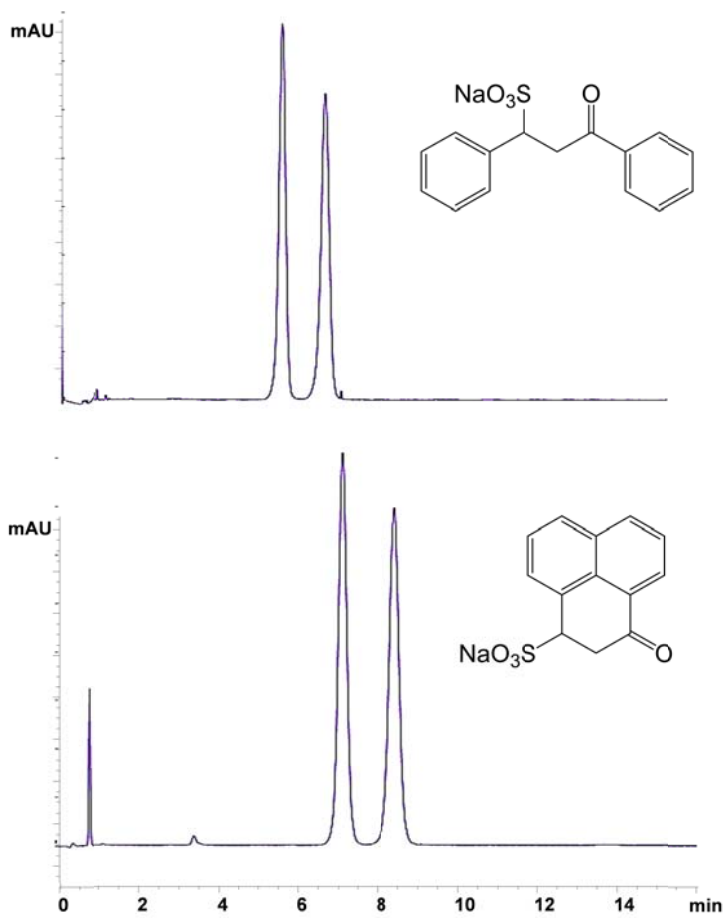
478

479

480

481

482



483

484 **Figure 5.** SubFC enantioseparations of 1 (top) and 13 (bottom) on QD-AX CSP. Conditions: 25 %
485 modifier (MeOH, 200 mM HOAc, 100 mM NH₃; 4.0 mL/min, 40°C, 150 bar; UV detection at 254 nm.

486

APPENDIX IV

Stefanie Wernisch
Reinhard Pell
Wolfgang Lindner

Institute for Analytical Chemistry,
University of Vienna, Währinger
Straße 38, Vienna, Austria

Received January 31, 2012

Revised March 12, 2012

Accepted March 15, 2012

Research Article

Increments to chiral recognition facilitating enantiomer separations of chiral acids, bases, and ampholytes using *Cinchona*-based zwitterion exchanger chiral stationary phases

The intramolecular distances of anion and cation exchanger sites of zwitterionic chiral stationary phases represent potential tuning sites for enantiomer selectivity. In this contribution, we investigate the influence of alkanesulfonic acid chain length and flexibility on enantiomer separations of chiral acids, bases, and amphoteric molecules for six *Cinchona* alkaloid-based chiral stationary phases in comparison with structurally related anion and cation exchangers. Employing polar-organic elution conditions, we observed an intramolecular counterion effect for acidic analytes which led to reduced retention times but did not impair enantiomer selectivities. Retention of amphoteric analytes is based on simultaneous double ion pairing of their charged functional groups with the acidic and basic sites of the zwitterionic selectors. A chiral center in the vicinity of the strong cation exchanger site is vital for chiral separations of bases. Sterically demanding side chains are beneficial for separations of free amino acids. Enantioseparations of free (un-derivatized) peptides were particularly successful in stationary phases with straight-chain alkanesulfonic acid sites, pointing to a beneficial influence of more flexible moieties. In addition, we observed pseudo-enantiomeric behavior of quinine and quinidine-derived chiral stationary phases facilitating reversal of elution orders for all analytes.

Keywords: Amino acid / Chiral stationary phase / Ion exchange / Liquid chromatography / Peptide / Zwitterion
DOI 10.1002/jssc.201200103

1 Introduction

1.1 Structural properties of *Cinchona* alkaloids

Quinine (QN) and its pseudo-enantiomer quinidine (QD) are the most prominent representatives of *Cinchona* alkaloids, a group of molecules with anti-malarial properties isolated in multi-ton scale from the bark of *Cinchona ladgeriana*. These natural chiral compounds comprise several interesting structural features: a vinyl group attached to a sterically demanding

1-azabicyclo[2.2.2]octane (quinuclidine) moiety, a secondary hydroxyl group, a π -basic quinoline ring system, two nitrogen atoms with different basicity, and a total of five stereogenic centers including the tertiary amino group (Fig. 1).

Investigations regarding the structure [1] and (total) synthesis [2–5] of quinine as well as modifications of the alkaloid scaffold [6–10] have led to a huge number of publications since the middle of the 19th century. Among chemists, *Cinchona* alkaloids enjoy a reputation as powerful chiral catalysts.

1.2 Application of *Cinchona* alkaloid-based chiral stationary phases for high-performance liquid chromatography (HPLC)

Today, chiral stationary phase (CSP)-mode HPLC is considered a very elegant way to achieve analytical and preparative enantiomer separations. The surface of a solid support material (e.g. highly porous spherical silica) is modified with an enantiomerically pure selector (SO) either by covalent bonding or adsorption (coating). The separation of the “selectand” (SA) enantiomers is facilitated by the formation of intermediate diastereomeric SO–SA complexes on the stationary phase. For charged solutes, the ion pairing/ion exchange principles

Correspondence: Prof. Dr. Wolfgang Lindner, Institute for Analytical Chemistry, University of Vienna, Währinger Straße 38, A-1090 Vienna, Austria

E-mail: wolfgang.lindner@univie.ac.at

Fax: +43 1 4277 9523

Abbreviations: AIBN, *N,N*-azobisisobutyronitrile; AX, anion exchanger; BSA, *N,O*-bis(trimethylsilyl)acetamide; CAD, charged aerosol detector; CSP, chiral stationary phase; CX, cation exchanger; DAD, diode array detector; DCM, dichloromethane; DNB, 3,5-dinitrobenzoyl; DNP, 2,4-dinitrophenyl; Htau, homotaurine; IMCI, intramolecular counterion; MFQ, mefloquine; MWD, multiple wavelength detector; QD, quinidine; QN, quinine; Tau, taurine; SO, selector; ZWIX, zwitterion exchanger

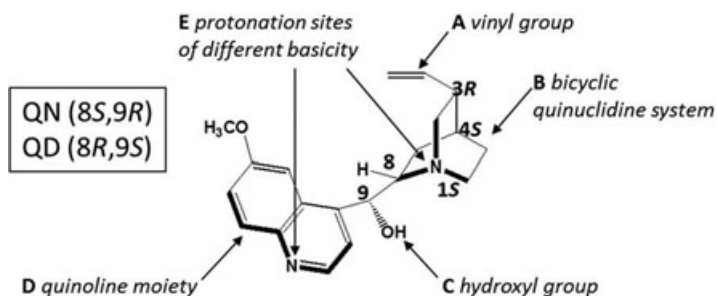


Figure 1. Structural features of cinchona alkaloids. Quinine (QN) and quinidine (QD) are pseudo-enantiomers with opposite configuration of two out of their five stereocenters. The vinyl group (A) is often used for immobilization. The bulky quinuclidine system (B) contains a basic nitrogen atom (E) that engages in protonation and, subsequently, ionic interactions. Due to its fixed conformation, it cannot flip and therefore represents a chiral center. The secondary OH group at C-9 (C) can act as H-bond donor or metal coordination site or can be the target of derivatization procedures carried out under inversion or retention of configuration. The quinoline moiety (D) is capable of π - π stacking and steric interaction and contains a methoxy group sometimes used for immobilization. (Adapted from [20].)

that rely on comparatively strong long-range electrostatic interactions can serve to establish the close contact between a charged selector and the analyte that gives rise to chiral recognition. Besides the *Cinchona*-based chiral ion exchangers discussed in [9], a large number of commercially available CSPs allow chemists to choose from a legion of elution conditions to address diverse separation problems. The most popular ones employ polysaccharides, proteins, crown ethers, macrocyclic antibiotics, or low-molecular weight selectors [10].

The first report of a *Cinchona* alkaloid derivative as chiral selector in a brush-type silica-supported CSP dates back to the 1980s [11] and was followed by various structural modifications that failed to achieve substantial improvements on the mediocre enantiomer selectivities and low chromatographic resolution values obtained with these early weak anion exchanger (WAX)-type CSPs. In the 1990s, Lindner and coworkers reported a carbamoyl modification of the secondary hydroxyl group at C-9. It significantly enhanced the enantioselectivities of a native QN-based WAX CSP toward diverse chiral acids [10, 12], especially when combined with a sterically demanding residue [13].

In 2008, Hoffmann et al. reported the fusion of the *Cinchona* alkaloid WAX motif with sulfonic acid-based SCX structures via a carbamate bond that yielded zwitterion exchanger (ZWIX)-type chiral selectors [14]. Employing a non-aqueous, polar-organic mobile phase with low concentrations of ionic additives, they managed to overcome the limited applicability inherent to single-charge ion exchangers and achieved reasonable to excellent results in separations of chiral acids and bases. In addition, the novel CSPs facilitated the retention and enantioselective separation of amphoteric analytes such as free amino acids and peptides based on simultaneous double ion pairing. This challenge cannot be met by the corresponding SCX or WAX-type CSPs due to the electrostatic repulsion exerted on the second charge of the zwitterionic analyte which compromises retention and leads to a complete loss of enantioselectivity.

1.3 *Cinchona* alkaloid-based ZWIX-type CSPs with non-chiral homologous alkanesulfonic acid SCX motifs

From the results of Hoffmann et al. [14], the existence of chiral centers in the vicinity of the cyclic SCX site (CSP 10

in Fig. 2) seemed essential for enantiomer separations of free amino acids. As an extension of the studies conducted by Hoffmann et al., we synthesized two pseudo-enantiomeric series of ZWIX-type CSPs by fusion of *Cinchona* alkaloids QN and QD with straight-chain aminoalkanesulfonic acids of different chain lengths (CSPs 1–6 in Fig. 2). Our objectives were (a) the systematic evaluation of the influence of intramolecular distances between anion and cation exchanger sites on the separation of enantiomers and (b) the elucidation of the role of a chiral element or a flexible alkyl chain close to the SCX site.

2 Materials and methods

2.1 CSP synthesis

2.1.1 General information and materials

Reactions were carried out under exclusion of moisture (nitrogen atmosphere) and with oven-dried glassware. Technical grade solvents were obtained from Merck (via VWR, Vienna, Austria) and HPLC grade solvents and mobile phase additives (diethylamine, ammonium acetate, formic, and acetic acid) from Merck, Carl Roth GmbH (Karlsruhe, Germany) or Sigma-Aldrich (Vienna, Austria). Dichloromethane was distilled over CaCl_2 and water was removed from toluene by azeotropic distillation before use.

Bulk chemicals and reagents (synthesis grade or higher purity, from Sigma-Aldrich) were used without further purification. Quinine (QN) and quinidine (QD) were from Buchler (Braunschweig, Germany), taurine from EGA Chemie Gesellschaft (Steinheim, Germany) and 1,4-butanediol from Tokyo Chemical Industries (Eschborn, Germany). Silica gel 60 (40–63 μm) for flash chromatography and *N,N'*-azobisisobutyronitrile (AIBN) for selector immobilization were from Merck. Silica for selector immobilization (Daisogel 120-5P, particle size: 5 μm , pore diameter: 120 Å, surface area: 300 m^2/g) was obtained from Daiso Co., Ltd. (Düsseldorf, Germany) and mercaptopropyl-modified and end-capped in-house (SH content: 680 $\mu\text{mol}/\text{g}$ silica). Reactions were monitored by thin-layer chromatography (TLC).

Nuclear magnetic resonance (NMR) solvents were from Deutero GmbH (Kastellaun, Germany). NMR experiments were carried out using a Bruker DRX 400 MHz NMR

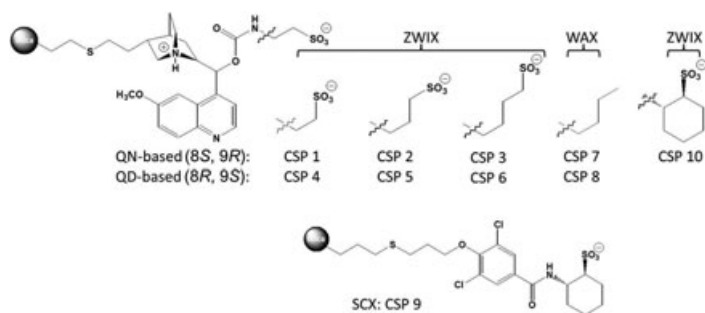


Figure 2. Chemical structures of chiral stationary phases (CSPs) 1–10. CSPs 1–6 and CSP 10: zwitterion exchanger-type (ZWIX); CSPs 7–8: weak anion exchanger-type (WAX); CSP 9: strong cation exchanger-type (SCX).

spectrometer (Bruker Austria GmbH, Vienna, Austria). Spectra were recorded in CD₃OD or CDCl₃ and chemical shifts are stated in ppm with tetramethylsilane as internal standard. Solvent signals were used as reference signals. NMR spectra were processed with SpinWorks 2.2.5 software.

MS experiments were performed using a PE Sciex API 365 triple-quadrupole mass spectrometer equipped with an electrospray ion source and an Agilent 1100 Series CL/MSD Trap ion-trap MS system.

Surface coverages (μmol selector/g silica gel) of the CSPs were determined by elemental analysis (CHNS) of the modified silica gel using an EA 1108 CHNS-O Element Analyser (Carlo Erba, ~~now Thermo Scientific~~). Selector coverage of the silica was calculated from the nitrogen content (accuracy according to manufacturer specifications: ±8%).

The modified silica CSPs were slurry-packed into 150 mm × 4 mm i.d. stainless steel columns (Bischoff, Leonberg, Germany) in-house.

2.1.2 Synthesis of ZWIX CSPs based on aminoalkanesulfonic acids and *Cinchona* alkaloids

Aminopropane- and aminobutanesulfonic acid were prepared from commercially available 1,3-propanesultone and 1,4-butanesultone according to [15] and [16]. The respective sultone was filled into a reaction flask and cooled with a 3:1 mixture of ice and NaCl. A three-fold excess of NH₃ (as a 7N solution in MeOH) was added slowly while stirring and cooling was continued for 2 h. The ice was allowed to melt and the mixture was stirred at ambient temperature overnight. The internal salts of the aminosulfonic acids precipitated as white solids and were recrystallized from water/ethanol 1:1 (v/v). They were obtained in good yields (>80%) and excellent purities.

For the fusion of aminosulfonic acids with activated 4-nitrophenyl ester hydrochlorides of quinine and quinidine we followed the procedure reported previously by Hoffmann et al. [14] and illustrated in Fig. 3. The zwitterionic selectors were purified by flash chromatography on silica gel employing a stepwise elution with a mixture of dichloromethane and methanol. The side-product *para*-nitrophenol was eluted with dichloromethane (DCM)/MeOH 9:1 (v/v) followed by a switch to DCM/MeOH 5:1 for the elution of unwanted

alkaloid derivatives. Eventually, the selector was eluted with DCM/MeOH 1:1 and the fractions containing the main product were pooled and concentrated *in vacuo*. The last eluting fractions were discarded because they contained the silylation by-product acetamide which adversely affects the immobilization of the selectors.

Product identification was achieved by MS and NMR. Exemplary NMR data are reported for novel selectors “*Aminobutanesulfonic acid-QN*” (CSP 3) and “*Homotaurine-QD*” (CSP 5).

The selectors were immobilized onto mercaptopropyl-modified silica via a radical addition reaction (radical initiator: AIBN) in boiling MeOH [14] employing the “thio-click” concept.

The synthetic routes toward weak anion exchanger-type CSPs 7 and 8 were carried out in analogy to the published procedure for the preparation of carbamoylated derivatives of *Cinchona* alkaloids [13]. The synthesis procedures for the strong cation exchanger-type CSP 9 and the reference zwitterion exchanger-type CSP 10 were reported previously [14, 17].

CSP 1—based on selector *N*-[[[(8*S*,9*R*)-6-methoxycinchonan-9-yl]oxy]carbonyl]-aminoethanesulfonic acid (“*Tau-QN*”):

Light yellow crystals, 86% yield.

MS (ESI, positive): 476.4 [M + H]⁺, 498.4 [M + Na]⁺. MS (ESI, negative): 474.2 [M – H].

Elemental analysis of modified silica gel: 250 μmol SO/g silica.

CSP 2—based on selector *N*-[[[(8*S*,9*R*)-6-methoxycinchonan-9-yl]oxy]carbonyl]-aminopropanesulfonic acid (“*Homotau-QN*”):

Light yellow crystals, 70% yield.

MS (ESI, positive): 490.2 [M + H]⁺; MS (ESI, negative): 488.0 [M – H].

Elemental analysis of modified silica gel: 280 μmol SO/g silica.

CSP 3—based on selector *N*-[[[(8*S*,9*R*)-6-methoxycinchonan-9-yl]oxy]carbonyl]-aminobutanesulfonic acid (“*Aminobutanesulfonic acid-QN*”):

Light yellow crystals, 40% yield.

¹H-NMR [CD₃OD]: δ = 7.88 (d, 1H), 7.48 (d, 1H), 7.39 (m, 2H), 6.69 (s, 1H), 5.74–5.62 (m, 1H), 5.04–4.98 (d, 1H), 4.95–4.90 (d, 1H), 3.93 (s, 3H), 3.62–3.57 (s, 1H), 3.54–3.48 (s, 1H), 3.15–3.04 (m, 3H), 3.04–2.98 (m, 1H), 2.87–2.83 (d, 1H),

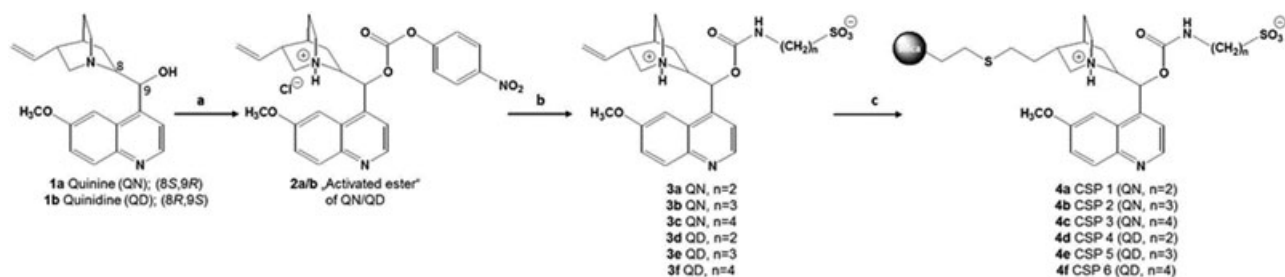


Figure 3. Synthetic route to CSPs 1–6. Conditions: (A) 4-nitrophenyl chloroformate, toluene(dest), r.t., 24 h. (B) Aminoalkanesulfonic acid, BSA, CH_2Cl_2 dest, reflux, 24 h. (c) AIBN, mercaptopropylsilane-modified silica gel, $\text{MeOH}_{\text{HPLC}}$, reflux, 5 h.

2.78–2.68 (m, 3H), 2.61 (s, 1H), 2.10–1.90 (m, 3H), 1.83–1.48 (m, 6H).

MS (ESI, negative): 502.8 $[\text{M} - \text{H}]^-$.

Elemental analysis of modified silica gel: 254 $\mu\text{mol SO/g}$ silica.

CSP 4—based on selector *N*-[[[(8*R*,9*S*)-6'-methoxycinchonan-9-yl]oxy]carbonyl]-aminoethanesulfonic acid ("Tau-QD"):

Yellow crystals, 58% yield.

MS (ESI, positive): 476.2 $[\text{M} + \text{H}]^+$, 498.2 $[\text{M} + \text{Na}]^+$, 951.4 $[2\text{M} + \text{H}]^+$, 973.4 $[2\text{M} + \text{Na}]^+$.

Elemental analysis of modified silica gel: 150 $\mu\text{mol SO/g}$ silica.

CSP 5—based on selector *N*-[[[(8*R*,9*S*)-6'-methoxycinchonan-9-yl]oxy]carbonyl]-aminopropanesulfonic acid ("Homotau-QD"):

Yellow crystals, 50% yield.

$^1\text{H-NMR}$ [CD_3OD]: δ = 8.79 (d, 1H), 7.88 (d, 1H), 7.81 (d, 1H), 7.55 (m, 2H), 7.00 (s, 1H), 6.11–6.0 (m, 1H), 5.2–5.1 (m, 2H), 3.94 (s, 3H), 3.76 (m, 1H), 3.49 (m, 3H), 3.27 (s, 1H), 3.13 (m, 2H), 2.84–2.61 (m, 3H), 2.31 (m, 1H), 2.08–1.70 (m, 5H), 1.36 (m, 1H).

MS (ESI, negative): 488.1 $[\text{M} - \text{H}]^-$.

Elemental analysis of modified silica gel: 188 $\mu\text{mol SO/g}$ silica.

CSP 6—based on selector *N*-[[[(8*R*,9*S*)-6'-methoxycinchonan-9-yl]oxy]carbonyl]-aminobutanesulfonic acid ("Aminobutane-sulfonic acid-QD"):

Yellow crystals, 20 % yield.

MS (ESI, negative): 502.6 $[\text{M} - \text{H}]^-$.

Elemental analysis of modified silica gel: 187 $\mu\text{mol SO/g}$ silica.

CSP 7—based on selector *O*9-*N*-butyl carbamoylated quinine ("*N*-Bu-CQN"):

White crystals, 55 % yield.

MS (ESI, positive): 424.8 $[\text{M} + \text{H}]^+$.

Elemental analysis of modified silica gel: 281 $\mu\text{mol SO/g}$ silica.

CSP 8—based on selector *O*9-*N*-butyl carbamoylated quinidine ("*N*-Bu-CQD"):

Off-white solid, 80 % yield.

MS (ESI, positive): 424.6 $[\text{M} + \text{H}]^+$.

Elemental analysis of modified silica gel: 252 $\mu\text{mol SO/g}$ silica.

2.2 CSP evaluation

2.2.1 Instrumentation

HPLC experiments were performed at 25°C using an Agilent 1100 HPLC system equipped with a binary pump and a multiple wavelength detector (MWD) and an Agilent 1200 HPLC system (Agilent, Waldbronn, Germany) with a quaternary pump and a diode array detector (DAD) with detection wavelength set to 254 nm for aromatic analytes. Non-UV active compounds were detected using a Corona Charged Aerosol Detector (ESA Biosciences, Inc., now a part of Dionex, Sunnyvale, CA, USA).

Void times were determined by the injection of 10 μL of acetone (MWD, DAD) or toluene (CAD) diluted with methanol (1:1, v/v).

2.2.2 Analytes

Acidic (Table 2) and basic analytes (Table 3) used in this study were either commercially available or synthesized in-house according to established procedures (amino acid derivatives, modified mefloquine). Zwitterionic analytes (Table 4) were commercially available (Bachem, Weil am Rhein, Germany), custom synthesized (PiChem, Graz, Austria and Genecust Europe, Dudelange, Luxembourg), or gifts from research partners.

Analytes were dissolved in methanol at concentrations of ca. 1 mg/mL. If available, single enantiomers were injected to determine elution orders. Injection volumes were between 5 (CAD detection) and 20 μL . Elution was performed in isocratic mode with methanol as the bulk solvent and 50 mM formic acid and 25 mM diethylamine as mobile phase additives corresponding to an apparent pH of 5.6.

Data acquisition and processing were achieved with Agilent ChemStation software and evaluation was carried out using Microsoft Excel.

Table 1. Aminosulfonic acid-*Cinchona* ZWIX-type CSPs and reference WAX-type and SCX-type CSPs

Q5

CSP #	Abbreviation	SCX site	WAX site	S0 loading ($\mu\text{mol S0/g silica}$)
1	Tau-QN	Taurine	Quinine	219
2	Htau-QN	Homotaurine (aminopropanesulfonic acid)	Quinine	280
3	ABSA-QN	Aminobutanesulfonic acid	Quinine	254
4	Tau-QD	Taurine	Quinidine	150
5	Htau-QD	Homotaurine (aminopropanesulfonic acid)	Quinidine	188
6	ABSA-QD	Aminobutanesulfonic acid	Quinidine	187
7	N-Bu-CQN	–	<i>N</i> -Butyl carbamoylated QN	281
8	N-Bu-CQD	–	<i>N</i> -Butyl carbamoylated QD	252
9	ACHSA-SCX	(<i>S,S</i>)- <i>trans</i> -2-(<i>N</i> -4-allyloxy-3,5-dichlorobenzoyl)-ACHSA	–	200
10	ACHSA-QN	(1 <i>S</i> ,2 <i>S</i>)-ACHSA	Quinine	215

ACHSA, aminocyclohexanesulfonic acid.

Table 2. Acidic analytes

Q6

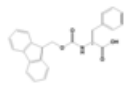
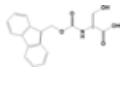
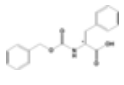
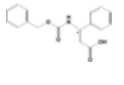
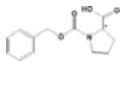
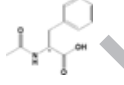
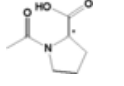
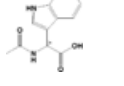
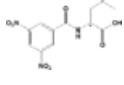
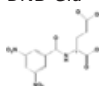
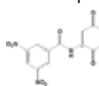
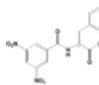
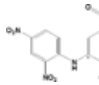
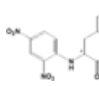
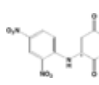
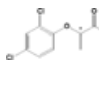
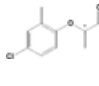
Analyte	CSP #	k_2	α	R_S	CSP #	k_2	α	R_S
	CSP 1	1.08	1.31	1.69	CSP 4	0.54	1.33	1.52
	CSP 2	1.79	1.30	2.80	CSP 5	0.71	1.28	1.52
	CSP 3	1.86	1.33	2.74	CSP 6	0.59	1.34	1.50
	CSP 7	3.99	1.47	5.34	CSP 8	5.88	1.42	5.11
	CSP 1	0.98	1.35	1.86	CSP 4	0.55	1.54	1.89
	CSP 2	1.69	1.30	2.81	CSP 5	0.66	1.34	1.5
	CSP 3	1.77	1.31	2.39	CSP 6	0.54	1.38	1.36
	CSP 7	3.24	1.37	4.35	CSP 8	4.55	1.35	3.47
	CSP 1	0.56	1.16	0.62	CSP 4	0.28	1.23	0.65
	CSP 2	0.99	1.14	1.17	CSP 5	0.39	1.19	0.60
	CSP 3	1.07	1.15	1.22	CSP 6	0.31	1.25	0.69
	CSP 7	2.38	1.30	3.40	CSP 8	3.25	1.21	2.70
	CSP 1	0.28	1.48	1.28	CSP 4	0.15	1.00	0.00
	CSP 2	0.76	1.90	3.99	CSP 5	0.20	1.62	1.20
	CSP 3	0.41	1.34	1.52	CSP 6	0.17	1.59	1.03
	CSP 7				CSP 8			
	CSP 1	0.25	1.00	0.00	CSP 4			
	CSP 2	0.41	1.00	0.00	CSP 5			
	CSP 3	0.48	1.00	0.00	CSP 6			
	CSP 7	1.06	1.00	0.00	CSP 8			
	CSP 1	0.30	1.45	1.40	CSP 4			
	CSP 2	0.54	1.40	2.29	CSP 5			
	CSP 3	0.65	1.39	2.12	CSP 6			
	CSP 7	1.49	1.53	4.65	CSP 8			
	CSP 1	0.15	1.16	0.32	CSP 4			
	CSP 2	1.88	1.87	6.77	CSP 5			
	CSP 3	0.36	1.00	0.00	CSP 6			
	CSP 7				CSP 8			
	CSP 1	0.93	1.75	3.48	CSP 4	0.52	1.96	3.53
	CSP 2	0.77	1.37	2.14	CSP 5	0.69	1.87	3.76
	CSP 3	1.70	1.65	4.86	CSP 6	0.49	1.64	2.28
	CSP 7	2.41	1.44	4.54	CSP 8	3.95	1.64	6.69
	CSP 1				CSP 4	1.33	6.00	10.08
	CSP 2				CSP 5	2.14	5.71	13.01
	CSP 3				CSP 6	1.62	5.78	11.39
	CSP 7				CSP 8	23.25	9.45	26.08

Table 2. Continued

Analyte	CSP #	k_2	α	R_S	CSP #	k_2	α	R_S
DNB-Glu 	CSP 1	4.20	3.95	8.44	CSP 4	1.73	3.93	10.39
	CSP 2	11.48	4.70	16.91	CSP 5	3.48	3.99	11.77
	CSP 3	10.71	4.10	15.07	CSP 6	2.53	4.23	11.71
	CSP 7				CSP 8			
DNB-Asp 	CSP 1	4.90	1.88	4.41	CSP 4	2.18	1.34	2.99
	CSP 2	12.00	1.62	n.d.	CSP 5	4.01	1.23	1.98
	CSP 3	11.87	1.40	3.66	CSP 6	2.74	1.32	2.73
	CSP 7				CSP 8			
DNB-Phe 	CSP 1	7.62	5.36	9.55	CSP 4	4.13	6.61	16.31
	CSP 2	15.29	5.67	18.29	CSP 5	5.09	4.87	15.19
	CSP 3	12.95	4.73	n.d.	CSP 6	4.22	5.49	12.79
	CSP 7				CSP 8			
DNP-Glu 	CSP 1	2.48	1.31	1.83	CSP 4	1.01	1.25	1.85
	CSP 2	6.14	1.25	2.78	CSP 5	1.81	1.13	1.11
	CSP 3	6.53	1.17	1.90	CSP 6	1.37	1.14	1.17
	CSP 7				CSP 8			
DNP-Phe 	CSP 1				CSP 4	1.13	1.35	2.75
	CSP 2				CSP 5	1.69	1.24	2.36
	CSP 3				CSP 6	1.35	1.27	2.20
	CSP 7				CSP 8			
DNP-Asp 	CSP 1	3.62	1.43	2.44	CSP 4	1.33	1.34	2.74
	CSP 2	10.04	1.47	5.19	CSP 5	2.67	1.23	1.87
	CSP 3	11.57	1.38	3.88	CSP 6	1.87	1.25	2.11
	CSP 7				CSP 8			
Dichlorprop 	CSP 1	0.56	1.36	1.34	CSP 4	0.32	1.96	2.49
	CSP 2	1.08	1.25	2.21	CSP 5	0.49	1.64	2.56
	CSP 3	1.26	1.21	1.77	CSP 6	0.37	1.65	1.95
	CSP 7	2.97	1.33	3.95	CSP 8	3.55	1.22	3.08
Mecoprop 	CSP 1	0.33	1.28	0.87	CSP 4	0.18	1.68	1.34
	CSP 2	0.64	1.20	1.44	CSP 5	0.28	1.44	1.25
	CSP 3	0.78	1.16	1.14	CSP 6	0.21	1.43	0.89
	CSP 7	1.93	1.19	2.06	CSP 8	2.49	1.14	1.85

Conditions: CSPs 1–8: 150 mm × 4 mm i.d., 5 μm material, selector coverage = 150–280 μmol SO/g silica. Mobile phase: methanol, 50 mM formic acid, 25 mM diethylamine, 1 mL/min, 25°C. Detection: UV @ 254 nm, CAD (non-UV active analytes). k_2 : retention factor of second eluting enantiomer.

3 Results and discussion

In this contribution, we present the synthesis of six chiral zwitterion exchange (ZWIX) selectors and the comprehensive evaluation of the corresponding brush-type chiral stationary phases (CSPs) for their enantioseparation performance toward chiral acids, bases, and ampholytes (Tables 2–4).

Figure 2 depicts all CSPs used in this study: ZWIX CSPs 1–3 are based on quinine (QN); CSPs 4–6 represent their *pseudo*-enantiomeric quinidine (QD) analogs. The two series of selectors are homologous with regard to their alkanesulfonic acid side chains.

WAX-type CSPs 7 (QN-based) and 8 (QD-based) were synthesized as control phases to evaluate the performance of ZWIX CSPs in the enantioseparations of acids and to verify

the necessity of the presence of the sulfonic acid SCX moiety for separations of bases and ampholytes. SCX-type CSP 9 was used as a reference CSP for chiral separations of basic analytes. ZWIX-type CSP 10, which incorporates as SCX site (1*S*,2*S*)-aminocyclohexanesulfonic acid—a chiral cyclic analog of taurine—was expected to aid the elucidation of interaction increments contributing to the overall chiral recognition concept of SCX-WAX (ZWIX)-type selectors and CSPs.

3.1 Synthesis of SCX-WAX (ZWIX)-type selectors by fusion of aminoalkanesulfonic acids and *Cinchona* alkaloids

CSPs 1 and 4 have been described briefly before [14] but it was reasonable to expect a systematic evaluation of CSPs 1–6

1
2
3
4
5
6
7
8
9
10
11
12
13
14
15
16
17
18
19
20
21
22
23
24
25
26
27
28
29
30
31
32
33
34
35
36
37
38
39
40
41
42
43
44
45
46
47
48
49
50
51
52
53
54
55
56
57
58

Table 3. Basic analytes

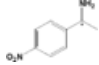
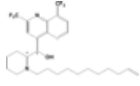
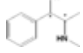
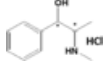
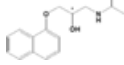
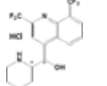
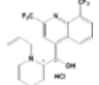
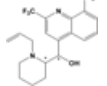
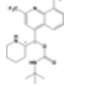
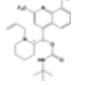
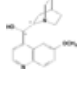
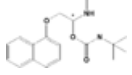
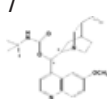
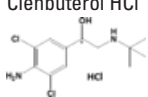
Analyte	CSP #	k_2	α	R_S	CSP #	k_2	α	R_S
Nitroresolve 	CSP 1	1.61	1.01	n.d.	CSP 4	1.17	1.00	0.00
	CSP 2	1.77	1.01	n.d.	CSP 5	1.26	1.00	0.00
	CSP 3	0.73	1.00	n.d.	CSP 6	1.47	1.00	0.00
	CSP 9	11.36	1.02	n.d.				
1 	CSP 1	1.01	1.24	1.98	CSP 4	0.69	1.20	1.38
	CSP 2	1.09	1.23	2.24	CSP 5	0.70	1.18	1.05
	CSP 3	0.45	1.15	0.66	CSP 6	0.78	1.06	0.47
	CSP 9	7.43	1.16	2.85				
(+/–) Ephedrin 	CSP 1	0.85	1.08	n.d.	CSP 4	0.59	1.06	n.d.
	CSP 2	0.93	1.00	n.d.	CSP 5	0.63	1.06	n.d.
	CSP 3	0.42	1.11	n.d.	CSP 6	0.81	1.09	n.d.
	CSP 9	5.58	1.23	n.d.				
Ephedrin HCl 	CSP 1	0.85	1.00	0.00	CSP 4	0.61	1.00	0.00
	CSP 2	0.95	1.00	0.00	CSP 5	0.65	1.00	0.00
	CSP 3	0.42	1.00	0.00	CSP 6	0.81	1.00	0.00
	CSP 9	5.61	1.05	1.16				
Propranolol 	CSP 1	1.29	1.00	0.00	CSP 4	0.95	1.00	0.00
	CSP 2	1.44	1.00	0.00	CSP 5	1.02	1.00	0.00
	CSP 3	0.65	1.00	0.00	CSP 6	1.21	1.00	0.00
	CSP 9	8.68	1.00	0.00				
2 	CSP 1	1.83	1.34	3.12	CSP 4	1.57	1.50	4.17
	CSP 2	1.76	1.11	1.42	CSP 5	1.32	1.09	0.68
	CSP 3	0.75	1.00	0.00	CSP 6	1.42	1.00	0.00
	CSP 9	15.33	1.27	5.17				
3 	CSP 1	0.20	1.00	0.00	CSP 4	0.11	1.00	0.00
	CSP 2	0.30	1.00	0.00	CSP 5	0.13	1.00	0.00
	CSP 3	0.28	1.00	0.00	CSP 6	0.10	1.00	0.00
	CSP 9	0.02	1.00	0.00				
4 	CSP 1	1.09	1.20	1.72	CSP 4	0.79	1.23	1.82
	CSP 2	1.20	1.17	1.86	CSP 5	0.79	1.15	1.00
	CSP 3	0.52	1.10	0.57	CSP 6	0.92	1.09	0.65
	CSP 9	7.15	1.10	2.07				
5 	CSP 1	1.36	1.04	0.44	CSP 4	0.98	1.00	0.00
	CSP 2	1.53	1.09	1.04	CSP 5	1.06	1.00	0.00
	CSP 3	0.69	1.00	0.00	CSP 6	1.23	1.00	0.00
	CSP 9	17.53	1.61	9.77				
6 	CSP 1	0.51	1.00	0.00	CSP 4	0.41	1.00	0.00
	CSP 2	0.57	1.19	0.86	CSP 5	0.41	1.00	0.00
	CSP 3	0.23	1.00	0.00	CSP 6	0.49	1.00	0.00
	CSP 9	4.77	1.08	1.25				
QN/QD 	CSP 1	1.88	1.11	n.d.	CSP 4	1.84	1.11	n.d.
	CSP 2	2.06	1.04	n.d.	CSP 5	1.64	1.02	n.d.
	CSP 3	1.02	1.04	n.d.	CSP 6	1.88	1.03	n.d.
	CSP 9	23.38	4.30	n.d.				
tBu-Propranolol 	CSP 1	1.18	1.00	0.00	CSP 4	0.88	1.00	0.00
	CSP 2	1.33	1.00	0.00	CSP 5	0.95	1.00	0.00
	CSP 3	0.61	1.00	0.00	CSP 6	1.12	1.00	0.00
	CSP 9	7.96	1.03	0.59				

Table 3. Continued

Analyte	CSP #	k_2	α	R_S	CSP #	k_2	α	R_S
	CSP 1	1.45	1.18	n.d.	CSP 4	1.07	1.07	n.d.
	CSP 2	1.43	1.07	n.d.	CSP 5			
	CSP 3	0.77	1.07	n.d.	CSP 6	1.14	1.02	n.d.
	CSP 9	48.39	5.02	n.d.				
	CSP 1	0.94	1.00	0.00	CSP 4	0.65	1.00	0.00
	CSP 2	1.09	1.00	0.00	CSP 5	0.73	1.00	0.00
	CSP 3	0.50	1.00	0.00	CSP 6	0.89	1.00	0.00
	CSP 9	6.65	1.16	3.11				

Analytes: 1: (*R,S*)/(*S,R*)-*N*-undecenoyl-MFQ; 2: (*R,S*)/(*S,R*)-MFQ HCl, 3: (*R,S*)/(*S,R*)-*N*-allyl-MFQ HCl, 4: (*R,S*)/(*S,R*)-*N*-allyl-MFQ, 5: (*R,S*)/(*S,R*)-*tert*-butyl-carbamoylated MFQ, 6: (*R,S*)/(*S,R*)-*N*-allyl-MFQ carbamate, and 7: O9-*tert*-butyl carbamoylated QN/QD.

Conditions: CSPs 1–9: 150 mm × 4 mm i.d., 5 μm material, selector coverage = 150–280 μmol SO/g silica. Mobile phase: methanol, 50 mM formic acid, 25 mM diethylamine, 1 mL/min, 25°C. Detection: UV @ 254 nm. k_2 : retention factor of second eluting enantiomer.

to help our understanding of the underlying chiral recognition mechanism. Indisputably, the intramolecular distances of anion and cation exchanger sites of the zwitterionic selectors and the conformational flexibilities residing in the alkyl spacer represent increments modifying the selector motif and its conformational preferences and, thereby, potentially, enantiomer distinction on ZWIX CSPs.

While taurine is available commercially, aminopropanesulfonic acid and aminobutanesulfonic acid had to be prepared from 1,3-propanesultone and 1,4-butanedisultone via ring opening with NH_3 according to [15] and [16].

To increase solubility and thereby optimize the yield of the crucial fusion step, the aminosulfonic acids were silylated with *N,O*-bis(trimethylsilyl)acetamide (BSA) in dried boiling dichloromethane. Fusion with the respective activated *Cinchona* alkaloid 4-nitrophenyl ester hydrochlorides as described by Hoffmann et al. [14] yielded the carbamoylated zwitterionic selectors (Fig. 3).

Yields decreased from taurine- to aminobutanesulfonic acid-based selectors even though the solubility of the longer aminoalkanesulfonic acids in the reaction solvent is higher. We believe that the explanation is to be found in the increasing basicity of the NH_2 group in the order taurine < homotaurine < aminobutanesulfonic acid. It encourages a higher level of internal salt formation; it decreases nucleophilicity and thus affects the nucleophilic attack on the activated alkaloid ester.

Figure 3 also illustrates the preparation of CSPs 1–6 by immobilization of the selectors onto mercaptopropyl-modified silica in a radical reaction. The covalent anchoring strategy is used to ensure the compatibility of the CSPs with a broad range of commonly used chromatographic conditions.

We applied exactly the same synthesis procedure for the two series of pseudo-enantiomeric CSPs but product yields and surface coverages were found to be higher for QN-based selectors. In this context it must be noted again that, strictly speaking, the QN and QD intermediates are diastereomers (*not* enantiomers). Due to different steric effects arising in the course of the selector synthesis and the thio-click immo-

bilization, the reactive center and the vinyl group of the QD intermediate are less accessible compared to those of the QN intermediate.

3.2 CSP evaluation

3.2.1 General remarks

As summarized in Table 1, selector coverages of CSPs 1–6 range from 150 to 280 μmol/g silica. Such a broad distribution could be suspected to compromise a comparative CSP study. However, our results demonstrate clearly that while retention (reflected in the retention factor k) is strongly dependent on the number of interaction sites available, lower selector loading does not impair the main parameter of interest of this study, the enantioselectivity (α value).

We used a previously optimized polar-organic mobile phase with methanol as the bulk solvent and a 2:1 ratio of acidic and basic additives (50 mM formic acid, 25 mM diethylamine) [18] corresponding to slightly acidic conditions (apparent pH 5.6). It facilitates protonation of the quinuclidine nitrogen (WAX site) while providing sufficient elution power for isocratic elution and permitting both UV and CAD detection. The polar aprotic solvent acetonitrile can be of value in method development on ZWIX CSPs but the use of water is not advisable due to an increased solvation effect on the SCX and WAX sites compared to methanol that leads to decreasing retention factors and ultimately to complete loss of enantioselectivity.

Overall enantioselectivity of *Cinchona* alkaloid-based CSPs originates from multiple intermolecular interactions occurring simultaneously between the respective functional groups of selector and selectand. Among them are electrostatic, H bond-type, polar, aromatic (π – π) and steric as well as Van der Waals (dispersive) interactions [13]. Eventually, chiral recognition is achieved by the fixed arrangement of the interaction sites in the selector.

2

Table 4. Amphoteric (zwitterionic) analytes

3

4

5

6

7

8

9

10

11

12

13

14

15

16

17

18

19

20

21

22

23

24

25

26

27

28

29

30

31

32

33

34

35

36

37

38

39

40

41

42

43

44

45

46

47

48

49

50

51

52

53

54

55

56

57

58

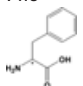
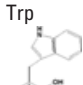
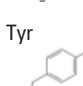
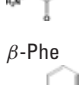
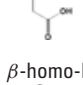
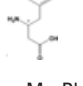
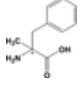
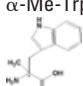
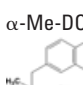
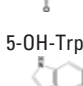
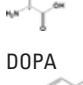
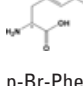
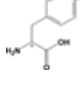
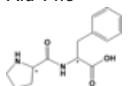
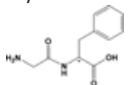
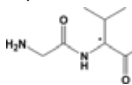
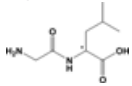
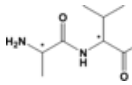
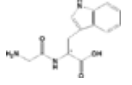
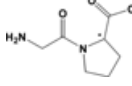
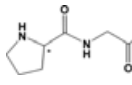
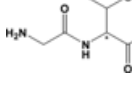
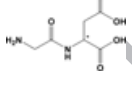
Analyte	CSP #	k_2	α	R_S	CSP #	k_2	α	R_S
Phe 	CSP 1	0.76	1.04	0.42	CSP 4	0.46	1.00	0.00
	CSP 2	1.00	1.12	1.14	CSP 5	0.45	1.00	0.00
	CSP 3	0.62	1.11	0.63	CSP 6	0.44	1.00	0.00
	CSP 10	1.47	1.18	1.36				
Trp 	CSP 1	2.18	1.53	4.31	CSP 4	1.10	1.39	3.01
	CSP 2	3.55	1.86	7.95	CSP 5	1.25	1.50	3.41
	CSP 3	1.98	1.67	5.04	CSP 6	1.06	1.27	1.75
	CSP 10	4.12	1.66	6.12				
Tyr 	CSP 1	0.97	1.07	0.46	CSP 4	0.50	1.00	0.00
	CSP 2	1.34	1.16	1.35	CSP 5	0.63	1.00	0.00
	CSP 3	0.87	1.15	0.77	CSP 6	0.55	1.00	0.00
	CSP 10	1.82	1.10	0.79				
β -Phe 	CSP 1	1.35	1.00	0.00	CSP 4	1.01	1.09	0.78
	CSP 2	1.50	1.00	0.00	CSP 5	0.75	1.00	0.00
	CSP 3	0.93	1.07	0.55	CSP 6	0.85	1.00	0.00
	CSP 10							
β -homo-Phe 	CSP 1	1.53	1.00	0.00	CSP 4			
	CSP 2	1.68	1.00	0.00	CSP 5			
	CSP 3	1.00	1.00	0.00	CSP 6			
	CSP 10							
α -Me-Phe 	CSP 1	0.03	1.00	0.00	CSP 4	0.47	1.25	1.37
	CSP 2	1.05	1.32	2.50	CSP 5	0.48	1.28	1.31
	CSP 3	0.63	1.32	1.78	CSP 6	0.46	1.23	1.02
	CSP 10	1.09	1.12	0.59				
α -Me-Trp 	CSP 1	3.22	2.42	10.34	CSP 4	1.68	2.35	8.38
	CSP 2	6.73	2.90	8.79	CSP 5	2.30	2.38	5.17
	CSP 3	3.20	2.30	5.21	CSP 6	1.80	1.83	3.28
	CSP 10	6.34	3.13	10.03				
α -Me-DOPA 	CSP 1	1.57	1.44	3.36	CSP 4	0.88	1.57	3.51
	CSP 2	2.28	1.54	4.84	CSP 5	0.85	1.42	2.39
	CSP 3	1.44	1.53	3.28	CSP 6	0.84	1.36	1.84
	CSP 10							
5-OH-Trp 	CSP 1				CSP 4	1.33	1.32	2.71
	CSP 2				CSP 5	1.51	1.47	3.46
	CSP 3				CSP 6	1.35	1.29	1.95
	CSP 10							
DOPA 	CSP 1	1.46	1.00	0.00	CSP 4	0.72	1.00	0.00
	CSP 2	1.96	1.21	2.03	CSP 5	0.73	1.10	0.56
	CSP 3	1.21	1.21	1.50	CSP 6	0.74	1.00	0.00
	CSP 10	2.26	2.42	1.07				
p-Br-Phe 	CSP 1	1.02	1.00	0.00	CSP 4	0.66	1.00	0.00
	CSP 2	1.35	1.08	0.71	CSP 5	0.62	1.00	0.00
	CSP 3	0.83	1.09	0.61	CSP 6	0.59	1.00	0.00
	CSP 10	2.14	1.11	0.63				
p-Cl-Phe 	CSP 1	0.90	1.00	0.00	CSP 4	0.58	1.00	0.00
	CSP 2	1.18	1.08	0.67	CSP 5	0.55	1.00	0.00
	CSP 3	0.74	1.09	0.58	CSP 6	0.53	1.00	0.00
	CSP 10	1.87	1.13	0.92				
Pro-Phe 	CSP 1	3.52	1.89	8.31	CSP 4	2.00	2.37	9.24
	CSP 2	4.22	2.01	9.63	CSP 5	2.54	3.10	10.63
	CSP 3	2.32	2.08	7.55	CSP 6	1.86	2.26	7.42
	CSP 10							

Table 4. Continued

Analyte	CSP #	k_2	α	R_S	CSP #	k_2	α	R_S
Ala-Phe 	CSP 1	2.71	1.75	7.15	CSP 4	1.45	2.34	8.13
	CSP 2	3.27	1.77	7.65	CSP 5	1.67	2.60	8.33
	CSP 3	1.88	1.95	6.52	CSP 6	1.38	2.09	6.14
	CSP 10	2.39	1.28	2.08				
Gly-Phe 	CSP 1	2.54	1.33	3.47	CSP 4	1.29	1.68	5.11
	CSP 2	3.00	1.35	4.07	CSP 5	1.35	1.76	4.67
	CSP 3	1.65	1.49	3.93	CSP 6	1.18	1.60	3.69
	CSP 10	3.43	1.11	0.72				
Gly-Val 	CSP 1	1.81	1.13	0.95	CSP 4	1.20	1.20	0.48
	CSP 2	2.05	1.17	1.94	CSP 5	0.86	1.30	1.03
	CSP 3	1.27	1.27	1.60	CSP 6	0.93	1.27	1.21
	CSP 10	2.49	1.17	0.98				
Gly-Leu 	CSP 1	1.68	1.00	0.00	CSP 4	1.13	1.00	0.00
	CSP 2	1.84	1.00	0.00	CSP 5	0.77	1.19	0.51
	CSP 3	1.12	1.00	0.00	CSP 6	0.83	1.13	0.58
	CSP 10	2.37	1.00	0.00				
Ala-Val 	CSP 1	1.69	1.28	1.67	CSP 4	1.17	1.29	0.74
	CSP 2	1.99	1.36	2.85	CSP 5	0.80	1.60	1.06
	CSP 3	1.28	1.45	2.25	CSP 6	0.90	1.37	1.41
	CSP 10	1.72	1.26	1.71				
Gly-Trp 	CSP 1	4.18	1.00	0.00	CSP 4			
	CSP 2	5.16	2.13	7.21	CSP 5			
	CSP 3	6.88	2.52	7.98	CSP 6			
	CSP 10							
Gly-Pro 	CSP 1	1.93	1.07	0.31	CSP 4			
	CSP 2	1.91	1.47	1.09	CSP 5			
	CSP 3	1.15	1.73	1.47	CSP 6			
	CSP 10	4.46	1.63	2.44				
Pro-Gly 	CSP 1	2.21	1.08	0.74	CSP 4			
	CSP 2	2.56	1.09	0.86	CSP 5			
	CSP 3	1.57	1.10	0.68	CSP 6			
	CSP 10							
Gly-Thr 	CSP 1	2.42	1.30	2.37	CSP 4			
	CSP 2	2.85	1.30	2.45	CSP 5			
	CSP 3	1.81	1.40	2.13	CSP 6			
	CSP 10	4.24	1.56	3.55				
Gly-Asp 	CSP 1	3.74	1.18	2.13	CSP 4			
	CSP 2	5.33	1.20	2.00	CSP 5			
	CSP 3	3.16	1.21	1.80	CSP 6			
	CSP 10	4.48	1.00	0.00				

Conditions: CSPs 1–6, CSP 10: 150 mm × 4 mm i.d., 5 μm material, selector coverage = 150–280 μmol SO/g silica. Mobile phase: methanol, 50 mM formic acid, 25 mM diethylamine, 1 mL/min, 25°C. Detection: UV @ 254 nm, CAD (non-UV active analytes). k_2 : retention factor of second eluting enantiomer.

To study the influence of the homologous aminosulfonic acid side chains and the effect of the pseudo-enantiomeric alkaloid scaffolds of CSPs 1–6, we evaluated the enantiomer separations of acids (Table 2), bases (Table 3), and ampholytes (Table 4):

For a large number of acidic analytes, enantiomer selectivities (α) of ZWIX CSPs were comparable and in some cases even superior to those of dedicated anion exchanger-

type CSPs 7 and 8 (Table 2 and Fig. 2). The ZWIX CSPs showed the particularly high enantiomer recognition capabilities toward DNB-protected amino acids that have been recognized before in structurally related WAX-type CSPs [13]. This is understandable because they also comprise the well-established carbamate moiety that engages in H bond donor–acceptor interactions with the amide group of this analyte class.

In contrast to this, their overall performance in the separation of basic analytes was rather weak and did not match that of the dedicated strong cation exchanger-type CSP 9 (Table 3). The reasons for this are most likely the lack of (a) a chiral element in the vicinity of the cation exchanger site and (b) a π -acidic aryl system near the amide group of CSPs 1–6. However, more successful separation performance with regard to basic analytes might be feasible after mobile phase optimization (type of bulk solvent and additives, pH adjustment) but this was outside the scope of this study.

Generally, retention factors for single-charge analytes were significantly lower on ZWIX CSPs than on the reference WAX or SCX CSPs. This can be attributed to an intramolecular counterion (IMCI) effect which is exerted on the analyte by the functional group of the selector that bears a charge of the same name and leads to shortened retention times of acidic and basic analytes due to partial repulsion.

As can be deduced from Table 4, the enantiomers of amphoteric molecules—the main conceptual target analytes of ZWIX CSPs—could be separated especially well if they comprised aromatic systems which are capable of engaging in π - π interactions with the aromatic quinoline system of the selectors. Un-derivatized Phe, Tyr, and Trp were typical examples for successful enantiomer separations of proteinogenic amino acids on ZWIX CSPs 1–6, while the enantiomers of aliphatic ones such as Ala, Leu, or Val eluted unresolved (data not shown). Strikingly, enantiomer distinction of α -methyl substituted amino acids was more eminent than that of their un-substituted analogs on all aminosulfonic acid-*Cinchona* ZWIX-type CSPs.

3.2.2 Influence of the distance of SCX and WAX sites on enantioselectivity

The two pseudo-enantiomeric series of CSPs (CSPs 1–3 and 4–6) are characterized by a “non-chiral” variation of the alkyl chain connecting the sulfonic acid SCX site to the alkaloid WAX part of the selector molecule (Fig. 2). The number of carbon atoms in the side chain increases from 2 (taurine) via 3 (aminopropanesulfonic acid) to 4 (aminobutanesulfonic acid), corresponding to increasing distances between the anionic and cationic sites of the chiral selectors.

Obviously, this structural modification does not introduce an additional chiral center into the selector but modifies its flexibility and capacity for Van der Waals interactions. It can therefore be expected to influence the quality of enantioseparations reflected in the selectivity coefficient α while the underlying chiral recognition mechanism remains essentially unchanged (no reversal of elution orders).

Evaluation of the enantioseparation characteristics revealed that the effect of the alkyl chain length is of minor importance for acids, bases and un-protected (free) amino acids. For acidic and basic analytes we observed only irregular or slightly decreasing selectivities in the order

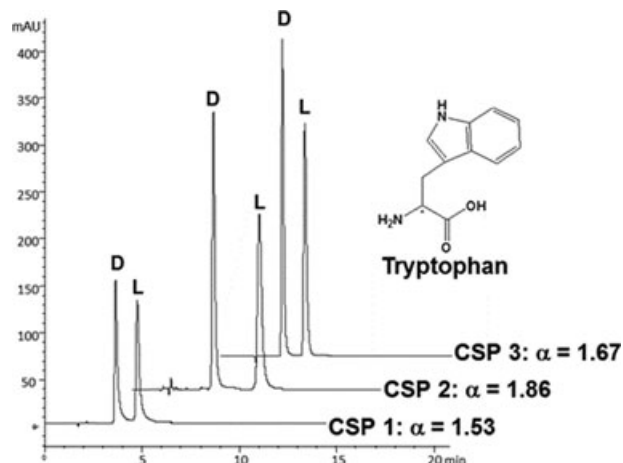


Figure 4. Separation of free amino acid Trp on ZWIX-type CSPs. On quinine-based CSPs 1–3, the D enantiomers of tryptophan elute before their L counterparts, while on quinidine-based CSPs 4–6, the D enantiomers elute first (not shown). The enhanced flexibility of the aminosulfonic acid side chains of CSPs 2/3 compared to CSP 1 is reflected in higher enantioselectivity values. Chromatographic conditions: CSPs 1–3: 150 mm \times 4 mm i.d., 5 μ m material. Mobile phase: methanol (50 mM formic acid, 25 mM diethylamine), 1 mL/min, 25°C. Detection: UV (254 nm).

taurine-QN > homotaurine-QN > aminobutanesulfonic acid-QN while for amphoteric solutes we found either irregular or slightly increasing selectivities. In most cases however, no significant difference in enantioselectivity was observed between CSPs 1–3 and 4–6 and no general connection between the number of bonds separating the SCX and WAX interactions sites of the ZWIX selector and its enantiomer separation capabilities could be established. As an example, Fig. 4 depicts the separation of Trp on CSPs 1–3. In addition, conflicting trends were observed for individual analytes on QN- and QD-based CSPs. This confirmed our presupposition that the increase in non-polar interaction areas provided by the longer alkyl chains of CSPs 2/4 and 3/6 does not suffice to induce a significant change in enantiomer selectivity because the most influential structural features contributing to chiral recognition—the polar carbamate moiety, the aromatic quinoline residue, and the highly asymmetric, spatially demanding quinuclidine ring system—reside within the alkaloid scaffold.

In contrast to the statement made above, for all-L and all-D peptide enantiomers we found an increase in enantiomer selectivities of >10% when comparing the selectivities of CSP 1 and CSP 3. Also for QD-based selectors, at least one of the CSPs with longer aminosulfonic acid chains always performed better than CSP 4. These results suggest that a more flexible alkyl spacer and its potential to engage in Van der Waals interactions with the amino acid side chains are of advantage for successful separations of small peptides. Recent experiments with homologous series of oligopeptides revealed the versatility of CSPs 1–6 not only for enantiomer separations but also for separations of sequential

and conformational stereoisomers of peptides (publication in preparation).

3.2.3 Variations of the SCX motif (straight chain and cyclic SCX sites)

The chiral selectors of CSPs 1 and 10 represent structural analogs (Fig. 2). While CSP 1 is prepared by the fusion of QN with achiral taurine, CSP 10 is derived from its chiral cyclic relative (1*S*,2*S*)-*trans*-aminocyclohexanesulfonic acid. The higher enantiomer selectivities achieved with CSP 10 for chiral acids (Table 2) and bases (Table 3) compared to CSP 1 led to the conclusion that the sterically demanding, rigid side chain of CSP 10 contributes strongly to the overall chiral recognition. In addition, we found that a chiral center in the vicinity (α and/or β position) of the sulfonic acid SCX site is essential for successful separation of most free (un-derivatized) proteinogenic amino acids: Of the 20 proteinogenic amino acids, only Phe, Tyr, and Trp could be separated on one or more of the CSPs 1–6, albeit with comparatively low enantiomer selectivities and chromatographic resolutions (Table 4). The ZWIX reference CSP 10 performed better in separations of free amino acids than any of the CSPs 1–6. Our findings suggest that rigid SCX side chains comprising at least one chiral element are also beneficial for chiral separations of *N*-protected amino acids and bases on *Cinchona*-based ZWIX CSPs.

However, we found that ZWIX CSPs with achiral side chains were more successful in achieving enantiomer separations

of small non-protected peptides with selectivity values typically above 1.2 (Table 4). These separations benefit from a higher level of conformational flexibility offered by the straight-chain aminosulfonic acids in CSPs 1–6 compared to CSP 10. The additional steric/chiral discrimination increments provided by a rigid, chiral SCX site are of minor influence for small peptide analytes.

3.2.4 Variation of the WAX moiety (quinine- and quinidine-based CSPs)

Due to their status as pseudo-enantiomers (different configurations of two out of five stereocenters), quinine (8*S*,9*R*) and quinidine (8*R*,9*S*) are known to give rise to comparable chromatographic results (in particular selectivities and resolutions) but reversed elution orders when used as selector scaffolds in CSPs [12]. We therefore compared the chromatographic performance of CSPs 1–3 to that of their pseudo-enantiomeric analogs and were able to show that, indeed, similar enantiomer selectivities and resolutions were achieved on CSPs 1 and 4, CSPs 2 and 5, and CSPs 3 and 6, respectively. We observed reversal of elution orders in all cases under investigation. With the exception of DNP derivatives, the *D* enantiomers of (α -*N*-acyl-type derivatives of) amino acids were eluted first from QN-based CSPs while the respective *L* enantiomers were eluted first from QD-based CSPs. This further supports earlier findings stating that chiral recognition on *Cinchona*-based CSPs is governed by the configuration of C-9 (QN: 9*R*, QD: 9*S*) of the alkaloid scaffold [19].

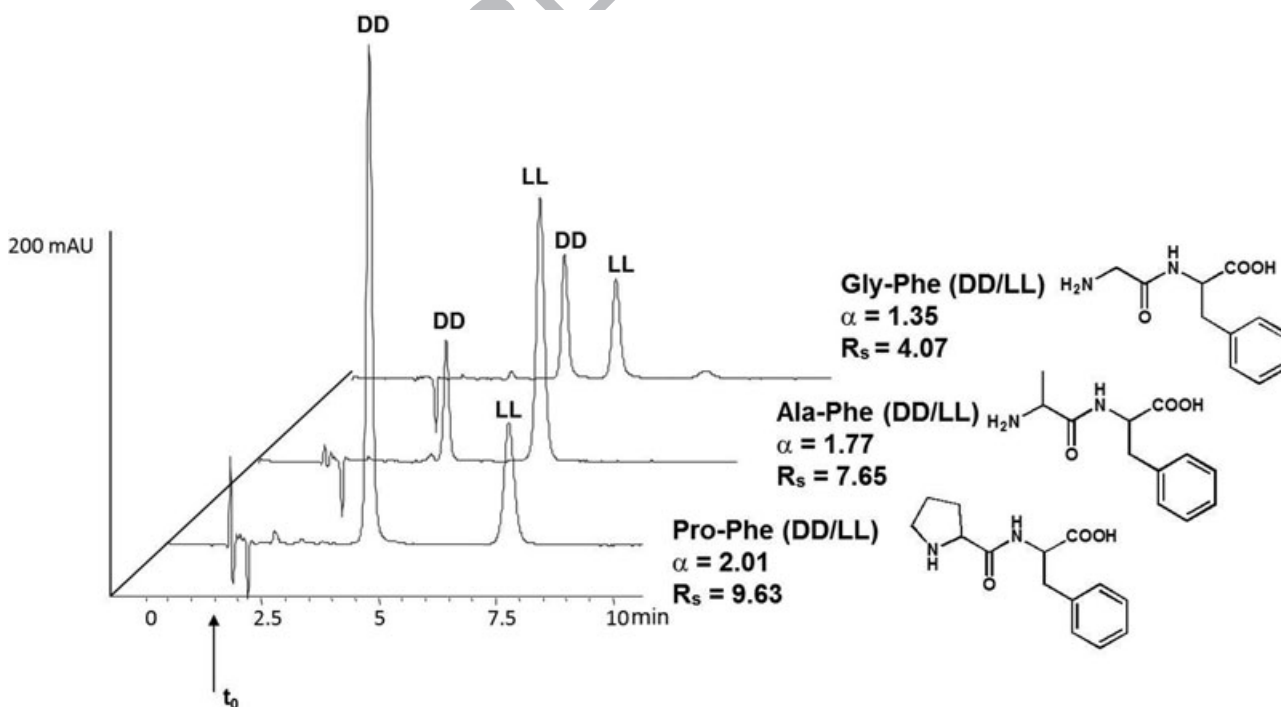


Figure 5. Dipeptide enantioseparations on CSP 6. Bulky and rigid amino acid side chains increase enantioselectivity. Elution order: DD before LL (QN-based CSP). Chromatographic conditions: CSP 3: 150 mm \times 4 mm i.d., 5 μ m material. Mobile phase: methanol (50 mM formic acid, 25 mM diethylamine), 1 mL/min, 25°C. Detection: UV (254 nm).

Due to their different selector coverages, QN- and QD-based CSPs gave rise to strikingly different retention factors especially for single-charge analytes. For example, for acids they were almost twice as high on CSP 1 (219 $\mu\text{mol SO/g silica}$) as they were on CSP 4 (150 $\mu\text{mol SO/g silica}$). Still, α and R_S values were found to be within a very close range of ± 10 –20%.

It is worth mentioning that the QD-based CSPs seem better suited for the enantiomer separation of small underivatized peptides such as the ones resolved on CSP 6 in Fig. 5.

These separations also illustrated the statement made before about there being no significant influence of SO loading on enantiomer selectivity. The QN-based CSPs have higher coverage but their separation performance was inferior to that of the QD-based CSPs. Selectivities and chromatographic resolution were higher on QD-based CSPs than on their QN analogs, pointing to the fact that they are, strictly speaking, not enantiomers, but of diastereomeric nature. As with other analytes, the reversal of elution orders of peptides was feasible by switching from a QD-based (all-L enantiomers elute first) to a QN-based (all-D enantiomers elute first) CSP.

4 Concluding remarks

By synthesizing and evaluating a total of six novel aminosulfonic acid-*Cinchona*-based SCX-WAX/ZWIX-type CSPs, we were able to show that such media can be successfully employed for enantiomer separations of chiral acids, bases, and ampholytes in many cases. Retention times of single-charge analytes on zwitterion exchangers were significantly shorter than on structurally related dedicated anion or cation exchangers while equally high selectivities and resolutions were achieved. The CSPs, which were run in non-aqueous, polar-organic mobile phase mode, exhibited especially favorable separation characteristics toward the enantiomers of small peptides. It is appropriate to mention the added benefits of straightforward applicability and easily accomplished reversal of elution orders by switching from QN-based to QD-based CSPs. We found that numerous challenging chiral separations are feasible with the ZWIX CSPs introduced in this publication, but the correlation of enantiomer selectivity with the number of carbon atoms in the alkanesulfonic acid-carbamoyl motif of the selector is not universal. It can vary strongly from one analyte to the other, making predictions of the separation performance very difficult.

The ZWIX CSPs are currently the subject of a study regarding stereoselective separations of small, non-enantiomeric peptides.

S.W. gratefully acknowledges the financial support of the interdisciplinary Ph.D. program "Initiativkolleg Functional Molecules" within the University of Vienna (Grant No. 1401-N). Furthermore, the authors wish to thank Peter Frühauf for column packing and Denise Wolrab and Michal Kohout for the preparation of mefloquine derivatives.

The authors have declared no conflict of interest.

5 References

- [1] Pasteur, L., *Compt. Rend.* 1858, XXXVII, 110.
- [2] Kaufman, T. S., Rúveda, E. A., *Angew. Chem. Int. Ed.* 2005, 44, 854–885.
- [3] Stork, G., Niu, D., Fujimoto, A., Koft, E. R., et al., *J. Am. Chem. Soc.* 2001, 123, 3239–3242.
- [4] Seeman, J. I., *Angew. Chem. Int. Ed.* 2007, 46, 1378–1413.
- [5] Smith, A. C., Williams, R. M., *Angew. Chem. Int. Ed.* 2008, 47, 1736–1740.
- [6] Christensen, B., *J. Prak. Chem.* 1904, 193–227.
- [7] Hoffmann, H. M. R., Frackenhohl, J., *Cinchona Alkaloids in Synthesis and Catalysis*, Wiley-VCH Verlag GmbH & Co. KGaA 2009, pp. 359–418.
- [8] Brajč, W. M., Holzgrebe, J., Wartchow, R., Hoffmann, H. M. R., *Angew. Chem. Int. Ed.* 2000, 39, 2085–2087.
- [9] Lämmerhofer, M., Lindner, W., *Adv. Chromatogr.* 2008, 46, 1–107.
- [10] Lämmerhofer, M., *J. Chromatogr. A* 2010, 1217, 814–856.
- [11] Rosini, C., Bertucci, C., Pini, D., Altemura, P., Salvadori, P., *Tetrahedron Lett.* 1985, 26, 3361–3364.
- [12] Lämmerhofer, M., Lindner, W., *J. Chromatogr. A* 1996, 741, 33–48.
- [13] Mandl, A., Nicoletti, L., Lämmerhofer, M., Lindner, W., *J. Chromatogr. A* 1999, 858, 1–11.
- [14] Hoffmann, C. V., Pell, R., Lämmerhofer, M., Lindner, W., *Anal. Chem.* 2008, 80, 8780–8789.
- [15] Helberger, J. H., Manecke, G., Heyden, R., *Justus Liebigs Ann. Chem.* 1949, 565, 22–35.
- [16] Helberger, J. H., Lantermann, H., *Justus Liebigs Ann. Chem.* 1954, 586, 158–164.
- [17] Hoffmann, C. V., Lämmerhofer, M., Lindner, W., *J. Chromatogr. A* 2007, 1161, 242–251.
- [18] Hoffmann, C. V., Reischl, R., Maier, N. M., Lämmerhofer, M., Lindner, W., *J. Chromatogr. A* 2009, 1216, 1157–1166.
- [19] Maier, N. M., Nicoletti, L., Lämmerhofer, M., Lindner, W., *Chirality* 1999, 11, 522–528.
- [20] Kacprzak, K., Gawronski, J., *Cinchona Alkaloids in Synthesis and Catalysis*, Wiley-VCH Verlag GmbH & Co. KGaA 2009, pp. 419–469.

APPENDIX V

Mechanistic investigations of cinchona alkaloid-based zwitterionic chiral stationary phases

Reinhard Pell, Siniša Sić, Wolfgang Lindner*

Department of Analytical Chemistry, University of Vienna, Währinger Strasse 38, 1090 Vienna, Austria

*Author for correspondence:

e-mail: Wolfgang.Lindner@univie.ac.at

Tel.: ++43-1-4277-52300

Fax: ++43-1-4277-9523

Abstract:

Novel zwitterionic cinchona alkaloid-based chiral selectors (SOs) were synthesized and immobilized on silica gel. The corresponding brush-type chiral stationary phases (CSPs) were characterized as zwitterionic ion-exchange-type materials and exhibited remarkable enantioselectivity for their zwitterionic target analytes, viz. underivatized amino acids and aminosulfonic acids. We rationally designed structural modifications on the strong cation exchange (SCX) subunit of the zwitterionic SO and investigated the influence on chiral recognition power for amphoteric solutes. SOs with chiral isopropyl- or cyclohexyl-moieties in vicinity to the SCX site showed broadest application range by baseline resolving 39 out of 53 test compounds, including α -, β -, and γ -amino acids with different substitution patterns. Furthermore, we introduced two pseudoenantiomeric zwitterionic CSPs which combined the unique features of providing comparable enantioselectivities but reversed enantiomer elution orders. By application of slightly acidic polar organic mobile phases as preferred elution mode, we found that certain amounts of aprotic acetonitrile in protic methanol substantially increased enantioselectivity and resolution of amino acids in a structure-dependent manner.

26 **Keywords:** enantioseparation, amino acid, aminosulfonic acid, chiral stationary phase,
27 zwitterionic selector

28 **1. Introduction:**

29 The biological and pharmacological properties of amino acids strongly depend on their
30 stereochemistry. Whereas it was long believed that mammalian organisms exclusively consist
31 of L-amino acids, several D-amino acids were found in higher animals and humans over the
32 last two decades [1, 2]. For instance, D-serine was identified to play an eminent role as a
33 neuromodulator and concentrations of up to one third of those of its L-enantiomer were
34 quantified in the human central nervous system [3, 4]. D-aspartate, being produced in
35 mammalian brain and concentrated in endocrine glands, is involved in hormone regulation [5,
36 6] Furthermore, amino acids have significant importance as chiral building blocks for
37 synthetic therapeutic peptides, one class of drugs which regained importance in the
38 pharmaceutical industry [7]. Consequently, the enantiomeric purity of amino acids is of
39 utmost importance to avoid diastereomeric impurities in the final peptidic drug.

40 Hence, there is a need for straightforward and robust techniques to either analyse minute
41 enantiomeric impurities or separate amino acid enantiomers, or both. Several approaches for
42 resolving underivatized amino acids have been successfully applied, such as resolution via
43 preferential crystallization [8] or diastereomeric salt formation [9], or enantioseparation by
44 gas-chromatography [10], thin-layer chromatography [11] and capillary electrophoresis [12].
45 However, high performance liquid chromatography (HPLC) employing chiral stationary
46 phases (CSPs) often evolved as method of choice, as it combines the capability for both chiral
47 analysis and preparative separation of enantiomers. Among the limited number of CSPs
48 available for separation of free (native) amino acids and small peptides, crown ether- [13-16],
49 protein-[17, 18], glycopeptide-[19-23]- and ligand-exchange-type CSPs [24, 25] exhibit the

50 broadest application range. However, ligand exchange-type and crown ether phases require
51 the use of transition metal ions or strong mineral acids, respectively, in the mobile phase,
52 which makes them practically unsuitable for preparative separations or hyphenation with mass
53 spectrometry. On the other hand, protein based CSPs suffer from drawbacks such as
54 denaturation in nonaqueous organic solvents and a low loading capacity [26].

55 Recently, we reported on cinchona alkaloid-based zwitterionic ion exchange-type chiral
56 selectors (SOs) which were immobilized onto silica gel yielding brush-type CSPs [27-30].
57 The columns were preferentially operated in slightly acidic polar organic mobile phases
58 enabling three modes of ion-exchange: anion-exchange mode for separation of chiral acids,
59 cation exchange mode for resolving chiral amines and, most importantly, zwitterion exchange
60 for enantioseparation of amphoteric compounds such as native amino acids and small
61 peptides. The type and chiral environment of the single cation and anion-exchange sites had a
62 strong impact on enantioselectivity for the target analytes in all three ion-exchange modi.

63 Based on these initial findings, we herein present the synthesis and HPLC evaluation of
64 novel zwitterionic ion exchange-type chiral stationary phases (ZWIX-CSPs). Rationally
65 designed structural modifications at both the strong cation exchange site (SCX) and weak
66 anion exchange moiety (WAX) will be presented and their impact on the chiral recognition
67 power for zwitterionic analytes will be discussed. Using nonaqueous mobile phases, we
68 investigated the influence of protic and aprotic solvent compositions on the separation
69 performance.

70

71 2. Experimental:

72 2.1 General Information and Materials

73 The preparation of CSPs 1 and 3 (see Figure 1) was reported previously [27]. The synthesis of
74 CSPs 2 and 4-8, including a general synthetic scheme (Figure S-1) and spectroscopic data of
75 the corresponding SOs, is described in detail in the supporting information. The SO loadings
76 of CSPs 1-8 were 190, 255, 232, 203, 265, 186, 260 and 274 $\mu\text{mol SO / g}$ totally porous silica
77 (12 nm pore size), respectively. CSPs 1-6 and 8 were prepared with 3 μm particle size silica
78 gel and packed into 250 x 3 mm i.d. stainless steel columns, whereas CSP 7 was made with 5
79 μm particle size silica and packed in house into a stainless steel column with a dimension of
80 150 x 4 mm i.d.

81 HPLC solvents Methanol (MeOH) and Acetonitril (ACN) were of HPLC-grade quality from
82 Carl-Roth GmbH (Karlsruhe, Germany). Mobile phase additives formic acid (FA) and
83 diethylamine (DEA) were of analytical grade from Sigma-Aldrich (Vienna, Austria). The
84 amino acid test solutes were either commercially available or kind gifts of research partners.

85 2.2 HPLC method

86 All experiments were conducted on a 1200 series HPLC system from Agilent Technologies
87 (Waldbronn, Germany) consisting of a solvent degasser, a quaternary pump, an autosampler,
88 a column thermostat and a variable wavelength UV detector (VWD) for the detection of
89 aromatic test solutes. Non UV-active compounds were detected on a corona charged aerosol
90 detector (CAD) from Dionex (Sunnyvale, CA, USA). Chemstation software version Rev.
91 B.01.03 was used for data acquisition and analysis. The mobile phase flow rate was 0.4
92 mL/min for the 3 μm , 250 x 3mm i.d. columns and 1.0 mL/min for the 5 μm , 150 x 4 mm i.d.
93 column. The test compounds were dissolved in MeOH or MeOH-water mixtures in a
94 concentration of 1.0-1.5 mg/mL. The injection volume varied between 5 and 15 μL and
95 column temperature was set to 25°C. The void volume was determined by injecting a solution

96 of acetone in MeOH. For determination of the elution order the single enantiomer, if
97 available, was injected.

98

99 **3. Results and Discussion**

100 Figure 1 displays the chemical structures of CSPs 1-8. The corresponding chiral selectors are
101 based on the cinchona alkaloids quinine (CSPs 1-7) and quinidine (CSP 8) which are linked to
102 chiral or achiral sulfonic acid moieties via a carbamate bond. The corresponding chiral SOs,
103 being of zwitterionic character under the applied mobile phase conditions, were immobilized
104 onto mercaptopropyl-modified spherical silica yielding brush type CSPs. Mechanistically
105 speaking, molecular interaction between the SOs and the amphoteric selectands (SAs) is
106 dominated by a double ionic attraction i.e. the protonated amine and the dissociated acid of
107 the zwitterionic SA are recognized simultaneously by both charged sites of the zwitterionic
108 SO. The simultaneous double ion pairing process may be supported by additional interactions
109 such as hydrogen bonding, $\pi - \pi$ -, dipole dipole - or van der Waals (dispersive) interactions
110 which then can lead to chiral discrimination of one enantiomeric analyte.

111 The analyte portfolio comprised 48 free (underivatized) amino acids and five
112 aminosulfonic acids possessing chiral centers in α -, β - or γ - position. Furthermore, the
113 solutes contained different substitution patterns, as α -methyl-, halogen atom- and hydroxyl-
114 substituted amino acids were employed in this study (for structures also see Table 1).

115 <insert Figure 1>

116 <insert Table 1>

117 *3.1 Overall CSP enantioselectivity and separation performance*

118 Previous studies revealed that CSP 3, which comprises two chiral centers in the vicinity of the
119 SCX site, exhibited remarkable enantioselectivity towards a broad spectrum of amino acid
120 analytes [27, 28]. In order to further improve the enantiodiscrimination capability for chiral
121 amino acids, we designed and synthesized novel zwitterionic SOs with chiral moieties close
122 to their SCX binding site. Another goal of the study was to gain more insights on the chiral
123 recognition mechanism between the zwitterionic SOs and SAs by making a systematic
124 variation of the ZWIX-SOs structural motifs and to evaluate chromatographically their
125 influence on enantioselectivity. For instance, quinine-based CSP 4 and quinidine-based CSP 8
126 each possess chiral isopropyl residues of different absolute configuration in β -position to their
127 sulfonic acid groups. Other SOs (and their corresponding CSPs, respectively) consist of more
128 spatially demanding substituents of the same or opposite absolute configuration, such as (*S*)-
129 isobutyl (CSP 5), (*S*)-phenyl (CSP 6) or (*R*)-phenyl (CSP 7) substituents.

130 Table 1 lists comprehensively the chromatographic data for all tested amino acids using
131 MeOH and MeOH-ACN mixtures as mobile phase bulk solvents. Regarding overall
132 enantioseparation performance, some trends became visible: first, a chiral moiety at the SCX
133 binding site is highly beneficial for the chiral recognition power, as CSP 1 and CSP 2 both
134 comprising achiral SCX subunits, were outperformed by all other investigated CSPs in the
135 study, thereby confirming earlier findings [27, 30]. Neither the presence of a more bulky
136 achiral side chain (CSP 2), which could theoretically display stronger stereodirecting
137 properties, improved enantiodiscrimination capability compared to CSP 1.

138 Generally, highest alpha- and resolution values were achieved on CSPs 4 and 8. The
139 isopropyl-moiety on the SCX site seemed to favour chiral recognition, as both the quinine-
140 based and quinidine-based CSP yielded highest alpha values for all classes of investigated
141 amino acids. For instance, 38 out of 53 solutes could be baseline separated ($R_s \geq 1.5$) and 14

142 compounds were at least partially separated ($0.4 \leq R_s \leq 1.5$). Only for serine (entry A11) no
143 separation was observed, however, serine could not be resolved on any of the presented CSPs.
144 We found a similar separation profile for CSP 8, which baseline resolved 39 of the amino
145 acids and additionally yielded highest overall resolution values for 25 analytes. CSP 3, the
146 only ZWIX-SO comprising two stereogenic centers in vicinity to the sulfonic acid group, but
147 being conformationally less flexible than the SOs of the other CSPs, performed roughly equal
148 to CSP 4 and baseline resolved 39 compounds. Additionally, the column showed some
149 complementary separation behaviour to CSPs 4 and 8 which was manifested in baseline
150 resolving those compounds which were only partially separated on the other columns and vice
151 versa.

152 Interestingly, for CSP 4 and CSP 5, which have close structural similarity and differ only
153 in one methylene group at the SCX binding site, we encountered a profoundly different
154 separation behaviour. Enantioselectivity was inferior on CSP 5 for the majority of the solutes
155 and even when similar α -values were obtained, we observed lower resolution due to bad peak
156 shapes. The low efficiency may also originate from a badly packed column as ascertained via
157 injection of neutral nonpolar test compounds such as toluene.

158 In order to trace the influence of a more rigid and spatially demanding SCX side chain, we
159 prepared CSPs 6 and 7 which both comprise phenyl residues of opposite absolute
160 configuration. The bulky and rigid aromatic groups proved to be detrimental for chiral
161 recognition, as both columns showed a limited separation capabilities (Table 2 lists
162 compounds which could be resolved on both columns) comparable to those of CSPs 1 and 2
163 (which comprise achiral SCX units only). We hypothesize that the flat but spatially
164 demanding phenyl ring hampers accessibility to the cleft-like binding pocket and thus causes
165 diminished enantiodiscrimination.

166 Regarding the trends among the different classes of amino acid structures, tryptophan and
167 its derivatives were exceptionally well separated on all CSPs. Moreover, halogen atom
168 substituted aromatic amino acids could be equally well resolved independently from their
169 substitution patterns. Generally, β -amino (carboxylic and sulfonic) acids exhibited higher
170 enantioselectivity values than most of the corresponding α -amino acids whereas some of the
171 hydroxyl-substituted AAs, such as serine or DOPA, were not or only partially resolved.
172 Interestingly, high enantioseparation factors were observed for trans-hydroxy-proline (entry
173 C3) on all CSPs, while cis-hydroxy-proline (C4) was only partially resolved. Finally, the
174 ZWIX-CSPs exhibited better enantiodiscrimination properties for amino(sulfonic) acids with
175 bulkier substituents than with smaller ones. For instance, *tert*-leucine (F6) and 2-*tert*-
176 butyltaurine (H4) were better resolved than alanine (A1) or 2-methyltaurine (H1). These
177 findings suggest that steric and van der Waal interactions must support the ion-exchange
178 dominated chiral recognition process.

179

180 *3.2 Mobile phase aspects*

181 Nonaqueous polar organic solvents in combination with acidic and basic additives (often
182 referred to as polar organic mode) turned out to be the preferential mobile phase for
183 separation of zwitterionic solutes on ZWIX CSPs [29]. Polar organic mode proved to be
184 superior to reversed phase mode due to potential inactivation of nonspecific hydrophobic
185 interactions with the stationary phase and thus enhancing enantioselectivity [29, 31]. We
186 assume that in aqueous mobile phases a strong solvation of both zwitterionic SAs and SOs
187 takes place thus reducing on the one side the strength of the ion pairing process and on the
188 other side hydrogen bonding effects, if possible. Additionally, the solvation must hamper non-
189 ionic, but stereodiscriminating interactions, as a decrease of enantioselectivity was observed
190 with increasing water content in the mobile phase.

191 Hence, polar organic mode was chosen for the mobile phase optimization study. We used
192 MeOH as a protic solvent (which can suppress H-bonding interactions) and additionally
193 selected acetonitrile, being an aprotic solvent known to support ionic interactions but to
194 interfere with aromatic (π - π) interactions [32]. We scrutinized the impact of protic and aprotic
195 bulk solvent composition on the chromatographic parameters, thereby increasing the amount
196 of ACN in MeOH (0%, 25%, 50% and 75% v/v; the acid to base ratio was kept constant at
197 2:1).

198 The use of high acetonitrile contents in the mobile phase (such as 75% in MeOH) is not
199 recommended because of the limited solubility of the very polar zwitterionic solutes. This
200 leads to a disrupted mass transfer between the stationary and the mobile phase resulting in bad
201 peak shapes (severe tailing). However, application of 25 % or 50% acetonitrile content could
202 substantially increase enantioselectivity and resolution. Figure 2 exemplarily depicts
203 chromatographic behaviour of 4 representative analytes in presence of different MeOH-ACN
204 mixtures as mobile phase bulk solvents. For tryptophan and its derivatives, such as 5-HTP
205 (C2), both selectivity and resolution were decreasing with increasing ACN content which
206 corroborates the effect of ACN on weakening π - π interactions.

207 However, especially for non-aromatic (aliphatic) amino acids, a certain amount of aprotic
208 acetonitrile most often enhanced enantioselectivity in special and separation performance in
209 general (Figure 2 and Figure 3). The stronger tailing observed at higher ACN content was
210 outbalanced by the gain in selectivity and thus resolution was often improved by application
211 of up to 50% ACN in the mobile phase (Figure 3). For instance, β -homo-Phe (D2) only
212 yielded a single peak using a methanolic mobile phase but was baseline separated upon using
213 50% acetonitrile. Generally, for all β -amino acids a marked increase in separation
214 performance was observed at 50% ACN content on every CSP (Table 1). Without exception,

215 retention increased with increasing acetonitrile percentage for all amino (carboxylic) acid
216 solutes.

217 Mechanistically, the observed chromatographic behaviour can be summarized in the
218 following way: (i) acetonitrile deficient mobile phases enabled better analyte solubility and
219 therefore enhanced mass transfer, which was chromatographically manifested in reduced
220 tailing and higher efficiency. Additionally, high percentage of (protic) MeOH causes stronger
221 solvation of the zwitterionic solutes, thereby weakening the electrostatic SO-SA interactions
222 and thus shortening retention times. (ii) The trend in selectivity enhancement for ACN rich
223 mobile phases can be explained by promotion of electrostatic and hydrogen-bonding
224 interactions which seem to substantially support the chiral recognition process. With
225 increasing methanol content analyte solvation is more pronounced than in aprotic acetonitrile.
226 We conclude that augmented solvation by protic metanol can distract chiral recognition by
227 potentially blocking accessibility between the SO and SA.

228 From a practical point of view, recommended mobile phase optimization for separation of
229 zwitterionic compounds on ZWIX-CSPs is carried out by a mobile phase screening
230 employing both neat methanol and an equal mixture of MeOH and ACN as bulk solvents.

231 <insert Figure 2>

232 <insert Figure 3>

233 *3.3 Considerations on the chiral recognition mechanism*

234 A tentative chiral recognition model between amphoteric compounds and zwitterionic
235 cinchona alkaloid-based SOs was described by Hoffmann et al. [27]. It stated that SO-SA
236 interaction is dominated by a simultaneous double-ion pairing process which mainly controls
237 solute retention. The non-stereodirecting electrostatic forces must be accompanied by
238 additional interactions (of single-point or multipoint quality according to the three-point-rule

239 [33]) to enable chiral recognition and thus facilitate separation of enantiomers. Depending on
240 the analyte structure, such interactions can be hydrogen bonding with the SOs carbamate
241 group, π - π interactions with the π -basic quinoline ring, and steric / van der Waals interactions
242 with hydrophobic moieties of the SO (Figure 1).

243 Generally, deductions from elution orders of single enantiomers on CSPs may provide
244 useful information about molecular interaction between the SO and the SA. In the case of the
245 present quinine- or quinidine-based ZWIX-SOs, either the cinchona alkaloid WAX unit or the
246 sulfonic acid-based SCX moiety unit may exhibit stereodiscriminating properties.

247 As can be extracted from Table 1, quinine-based CSPs 1-7 exhibit reversed elution orders
248 compared to quinidine-derived CSP 8 for almost all resolved amino acids (however, there are
249 few exceptions). These findings corroborate our previously established hypothesis of the
250 cinchona alkaloid playing the dominant role in the chiral recognition process and of the chiral
251 sulfonic acid subunit exhibiting rather supporting than stereodirecting character. More
252 strikingly, CSPs 4 and CSP 8, which SOs can be referred to as pseudoenantiomeric, show
253 inverted elution orders for all but two analytes. In a chromatographic context, the term
254 pseudoenantiomeric means that two diastereomeric SOs behave like enantiomers, which is
255 expressed in a switch of elution order of the single enantiomers but preserving
256 enantioselectivity upon interchanging the (pseudoenantiomeric) CSP. Indeed, as can be seen
257 on the selectivity plot in Figure 4, CSP 4 and CSP 8 exhibit similar enantioselectivities for
258 most of the investigated amino acid analytes, thereby confirming their pseudoenantiomeric
259 properties.

260 <insert Figure 4>

261 In a further control experiment we compared elution orders of CSP 6 and CSP 7 (Table 2),
262 which comprise the same quinine-based SOs but with opposite absolute configuration at the

263 chiral center at the SCX site. Hence, if the sulfonic acid cation exchange unit played a
264 dominant role in chiral recognition of amino acid analytes, we would expect inverted elution
265 orders between both CSPs. However, as expected, no inversion was observed with one single
266 exception.

267 To summarize, we could chromatographically confirm the importance of the cinchona-
268 alkaloid WAX subunits for chiral recognition of amphoteric compounds. The corresponding
269 chiral SCX moieties are substantially important for yielding proper enantioselectivities but
270 play a rather supportive role in chiral recognition. Hence, this also means that elution orders
271 of amphoteric compounds can, in most cases, easily be inverted by simply exchanging the
272 pseudoenantiomeric CSP.

273 <insert Table 2>

274 **4. Conclusion**

275 Novel zwitterionic low molecular weight selectors were prepared by combining cinchona
276 alkaloid weak anion exchange motifs with sulfonic acid-based strong cation exchange
277 moieties. The corresponding brush-type zwitterion exchange chiral stationary phases were
278 evaluated by HPLC. Due to their zwitterionic nature these CSPs are primarily suited for
279 enantioseparation of amphoteric analytes, such as free amino acids, via a simultaneous double
280 ion pairing process. Chiral recognition of amino acids was dominated by the cinchona
281 alkaloid anion exchange subunit, whereas the chiral substitution pattern in vicinity to the
282 cation exchanger site exhibited marked influence on enhancing enantioselectivity. Hence, via
283 a systematic structure variation of the sulfonic acid moiety we could identify zwitterionic
284 selectors with remarkable enantiodiscrimination properties for underivatized amino acids,
285 namely CSP 3, 4 and 8. Further enhancement of enantioseparation performance was realized
286 by application of polar organic mobile phases using acetonitrile-methanol mixtures as bulk

287 solvents. A beneficial feature of the presented CSPs is their ability to systematically switch
288 elution orders of single amino acid enantiomers when changing from a quinine- to a
289 quinidine-based CSP. Finally, the inherently high loading capacities of ion-exchange-type
290 CSPs make them ideally suited for preparative enantioseparations.

291 **Acknowledgements**

292 The authors thank Peter Frühauf for packing the columns.

293

294 **References**

- 295 [1] K. Hamase, A. Morikawa, S. Etoh, Y. Tojo, Y. Miyoshi, K. Zaitso, *Anal. Sci.*, 25 (2009) 961.
296 [2] D.L. Kirschner, T.K. Green, *J. Sep. Sci.*, 32 (2009) 2305-2318.
297 [3] A. Hashimoto, S. Kumashiro, T. Nishikawa, T. Oka, K. Takahashi, T. Mito, S. Takashima, N. Doi,
298 Y. Mizutani, T. Yamazaki, T. Kaneko, E. Ootomo, *J. Neurochem.*, 61 (1993) 348-351.
299 [4] A. Hashimoto, T. Nishikawa, T. Oka, K. Takahashi, *J. Neurochem.*, 60 (1993) 783-786.
300 [5] M.J. Schell, O.B. Cooper, S.H. Snyder, *Proc. Natl. Ac. Sci.*, 94 (1997) 2013-2018.
301 [6] D.S. Dunlop, A. Neidle, D. McHale, D.M. Dunlop, A. Lajtha, *Biochem. Biophys. Res. Commun.*,
302 141 (1986) 27-32.
303 [7] P. Vlieghe, V. Lisowski, J. Martinez, M. Khrestchatsky, *Drug Discovery Today*, 15 (2010) 40-56.
304 [8] M. Naomasa, H. Minoru, I. Kenkichi, A. Takekazu, O. KO., K. Jiro, in: K.K. Ajinomoto (Ed.) *US*
305 *Pat.* 3266871, United States, 1966.
306 [9] M.S. Hoekstra, D.M. Sobieray, M.A. Schwindt, T.A. Mulhern, T.M. Grote, B.K. Huckabee, V.S.
307 Hendrickson, L.C. Franklin, E.J. Granger, G.L. Karrick, *Org. Process. Res. Dev.*, 1 (1997) 26-38.
308 [10] S. Volker, *J. Chromatogr. B*, 879 (2011) 3122-3140.
309 [11] R. Bhushan, J. Martens, *Biomed. Chromatogr.*, 15 (2001) 155-165.
310 [12] F. Kitagawa, K. Otsuka, *J. Chromatogr. B*, 879 (2011) 3078-3095.
311 [13] M.H. Hyun, J.S. Jin, W. Lee, *J. Chromatogr. A*, 822 (1998) 155-161.
312 [14] M.H. Hyun, *J. Sep. Sci.*, 26 (2003) 242-250.
313 [15] M.H. Hyun, Y.J. Cho, Y. Song, H.J. Choi, B.S. Kang, *Chirality*, 19 (2006) 74-81.
314 [16] R. Berkecz, I. Ilisz, F. Fülöp, Z. Pataj, M.H. Hyun, A. Péter, *J. Chromatogr. A*, 1189 (2008) 285-
315 291.
316 [17] J. Haginaka, *J. Chromatogr. A*, 906 (2001) 253-273.
317 [18] E.J. Franco, H. Hofstetter, O. Hofstetter, *J. Sep. Sci.*, 29 (2006) 1458-1469.
318 [19] A. Berthod, Y. Liu, C. Bagwill, D.W. Armstrong, *J. Chromatogr. A*, 731 (1996) 123-137.
319 [20] K.H. Ekborg-Ott, Y. Liu, D.W. Armstrong, *Chirality*, 10 (1998) 434-483.
320 [21] A. Péter, G. Török, D.W. Armstrong, *J. Chromatogr. A*, 793 (1998) 283-296.
321 [22] A. Berthod, X. Chen, J.P. Kullman, D.W. Armstrong, F. Gasparrini, I. D'Acquaric, C. Villani, A.
322 Carotti, *Anal. Chem.*, 72 (2000) 1767-1780.
323 [23] T.J. Ward, A.B. Farris Iii, *J. Chromatogr. A*, 906 (2001) 73-89.
324 [24] V.A. Davankov, *J. Chromatogr. A*, 666 (1994) 55-76.
325 [25] B. Natalini, R. Sardella, G. Carbone, A. Macchiarulo, R. Pellicciari, *Anal. Chim. Acta*, 638
326 (2009) 225-233.
327 [26] E. Francotte, *J. Chromatogr. A*, 906 (2001) 379-397.
328 [27] C.V. Hoffmann, R. Pell, M. Lämmerhofer, W. Lindner, *Anal. Chem.*, 80 (2008) 8780-8789.

- 329 [28] C.V. Hoffmann, R. Reischl, N.M. Maier, M. Lämmerhofer, W. Lindner, *J. Chromatogr. A*, 1216
330 (2009) 1147-1156.
- 331 [29] C.V. Hoffmann, R. Reischl, N.M. Maier, M. Lämmerhofer, W. Lindner, *J. Chromatogr. A*, 1216
332 (2009) 1157-1166.
- 333 [30] S. Wernisch, R. Pell, W. Lindner, *J. Sep. Sci.*, accepted (2012).
- 334 [31] M. Lämmerhofer, W. Lindner, in: N. Grinberg, E. Grushka (Eds.) *Advances in Chromatography,*
335 *Liquid Chromatographic Enantiomer Separation and Chiral Recognition by Cinchona Alkaloid-*
336 *Derived Enantioselective Separation Materials*, CRC Press, Boca Raton, FL, 2007.
- 337 [32] C.A. Hunter, K.R. Lawson, J. Perkins, C.J. Urch, *J. Chem. Soc., Perkin Trans. 2*, (2001) 651-669.
- 338 [33] W.H. Pirkle, T.C. Pochapsky, *Chem. Rev.*, 89 (1989) 347-362.

339

340

341

342

343

344

345

346

347

348

349

350

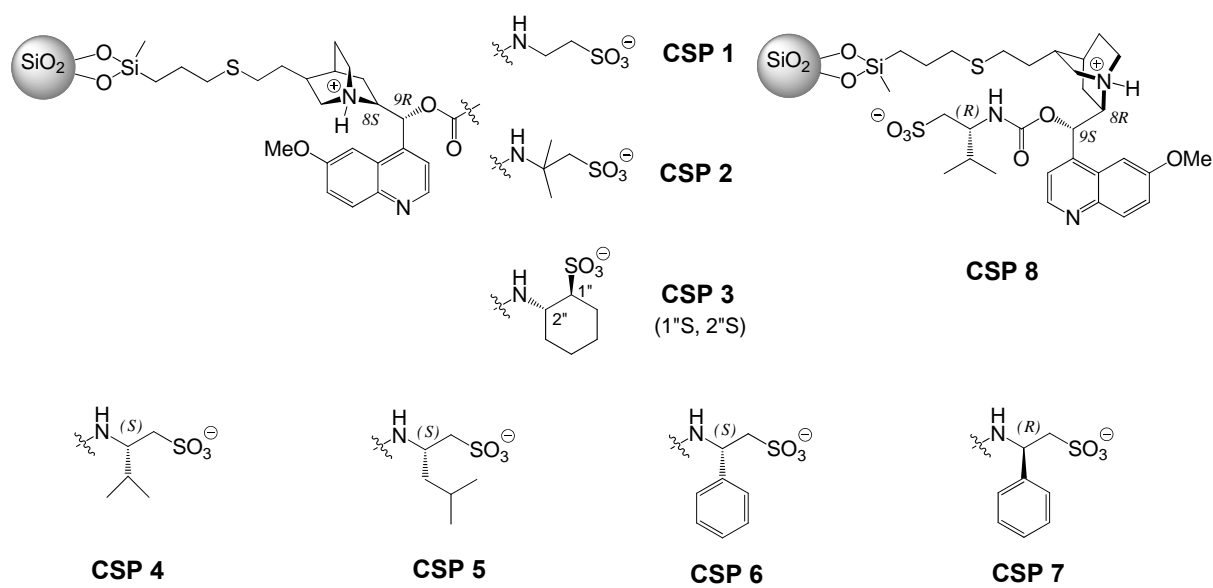
351

352

353

354

355



356

357

358 **Figure 1.** Chemical structures of quinine-based CSPs 1-7 and quinidine based CSP 8

359

360

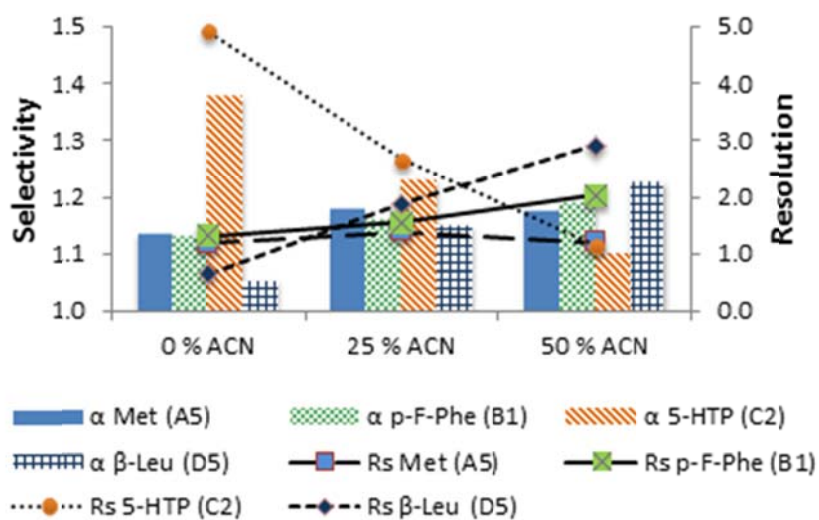
361

362

363

364

365



366

367

368 **Figure 2.** Influence of acetonitrile and methanol as bulk solvents on enantioselectivity and resolution
 369 for methionine (entry A5), para-fluoro-phenylalanine (B1), 5-hydroxy-tryptophan (C2) and β -leucine
 370 (D5). Conditions: CSP 3, mobile phase: ACN-MeOH mixture, 50 mM FA, 25 mM DEA; flow rate 0.4
 371 mL/min, 25°C;

372

373

374

375

376

377

378

379

380

381

382
383
384
385
386
387
388
389
390
391
392
393
394
395
396
397
398
399
400
401
402

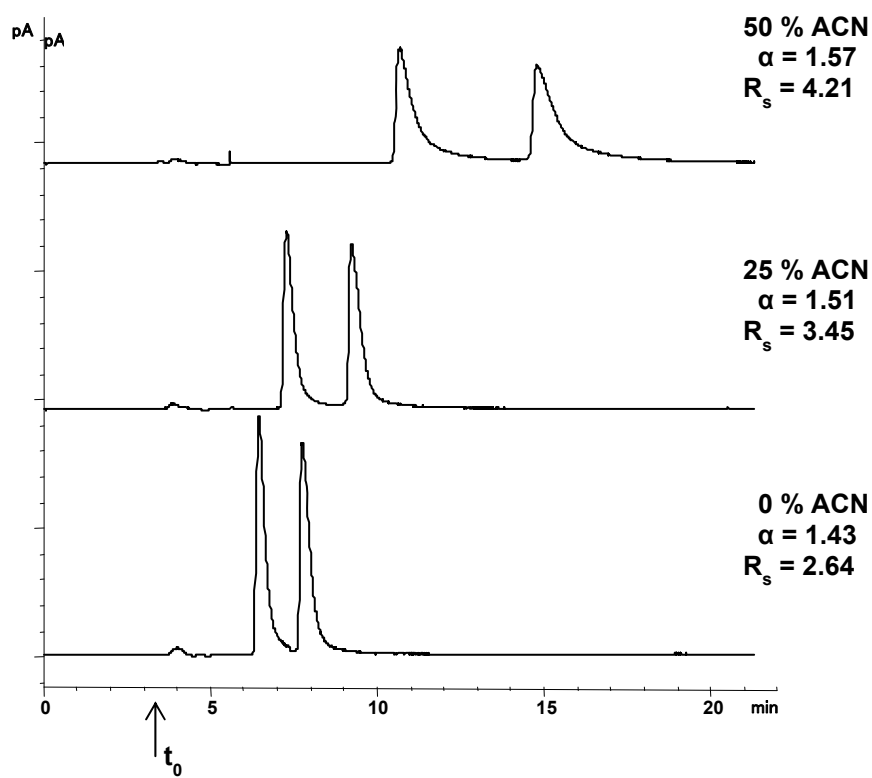


Figure 3. Enantioseparation of *tert*-leucine (F6) on CSP 3. Mobile phase: ACN-MeOH mixtures, 50 mM FA, 25 mM DEA; flow rate 0.4 mL/min, 25°C; $t_0 = 3.68$ min;

403
404
405
406
407
408
409
410
411
412
413
414
415
416
417
418
419
420
421
422
423

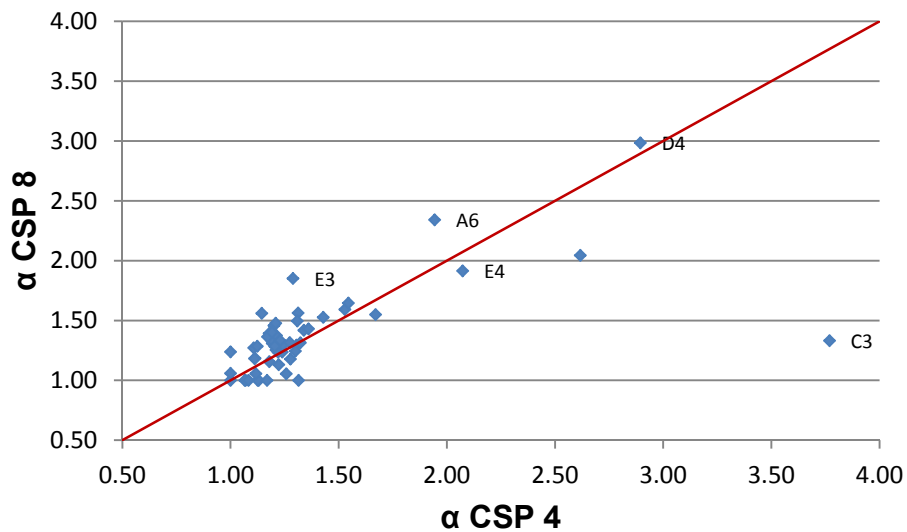
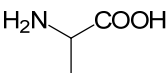
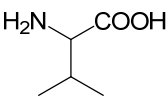
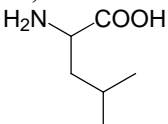
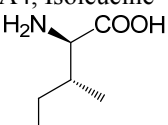
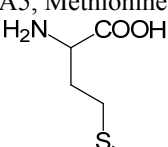
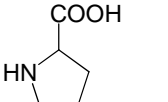
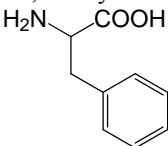
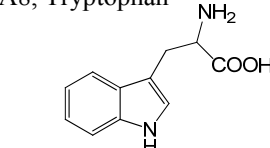
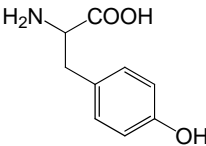
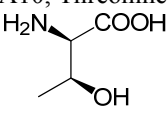
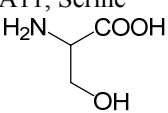
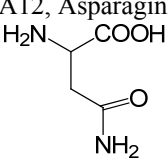
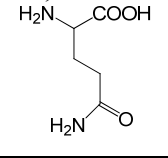
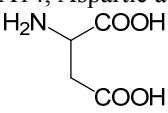
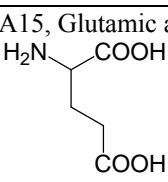


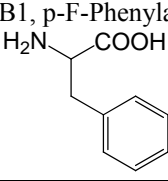
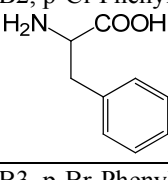
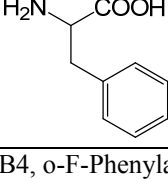
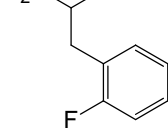
Figure 4. Selectivity plots of CSP 4 versus CSP 8 for all 53 analytes. Mobile phase: ACN-MeOH 50-50 v/v, 50 mM FA, 25 mM DEA; flow rate 0.4 mL/min, 25°C; the red line denotes the 1th median

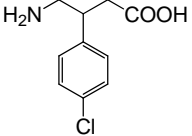
Table 1. Enantioseparation of zwitterionic analytes on CSP 1-5 and CSP 8^a

Class A, proteinogenic amino acids	100 % MeOH				MeOH/ACN 50/50 v/v				
		k_1	α	R_s	EO ^b	k_1	α	R_s	EO ^b
A1, Alanine 	CSP 1	0.34	1.00	0.0	-	0.85	1.04	0.5	L
	CSP 2	0.45	1.00	0.0	-	1.01	1.00	0.0	-
	CSP 3	1.05	1.15	0.5	L	2.46	1.17	0.6	L
	CSP 4	0.89	1.13	0.5	L	2.38	1.11	0.6	L
	CSP 5	0.98	1.00	0.0	-	2.77	1.00	0.0	-
	CSP 8	0.70	1.22	1.6	D	2.28	1.18	1.8	D
A2, Valine 	CSP 1	0.42	1.00	0.0	-	0.80	1.04	0.5	L
	CSP 2	0.40	1.00	0.0	-	0.91	1.00	0.0	-
	CSP 3	0.93	1.26	1.7	L	2.27	1.33	2.4	L
	CSP 4	0.74	1.22	1.5	L	2.12	1.22	1.9	L
	CSP 5	0.85	1.25	1.2	L	2.24	1.27	0.9	L
	CSP 8	0.60	1.35	2.1	D	2.06	1.27	2.4	D
A3, Leucine 	CSP 1	0.43	1.05	0.5	L	0.83	1.07	0.7	L
	CSP 2	0.42	1.13	0.6	L	0.92	1.11	0.6	L
	CSP 3	1.05	1.22	1.7	L	2.44	1.27	2.2	L
	CSP 4	0.86	1.22	1.6	L	2.35	1.19	2.0	L
	CSP 5	0.98	1.23	1.1	L	2.53	1.21	0.6	L
	CSP 8	0.74	1.34	3.1	D	2.41	1.31	4.0	D
A4, Isoleucine 	CSP 1	0.43	1.00	0.0	-	0.83	1.05	0.5	L
	CSP 2	0.37	1.00	0.0	-	0.85	1.00	0.0	-
	CSP 3	0.98	1.26	2.0	L	2.35	1.33	2.4	L
	CSP 4	0.80	1.24	2.0	L	2.25	1.24	2.6	L
	CSP 5	0.88	1.28	1.3	L	2.39	1.28	0.8	L
	CSP 8	0.65	1.33	1.9	D	2.27	1.24	2.3	D
A5, Methionine 	CSP 1	0.59	1.00	0.0	-	1.01	1.05	0.5	L
	CSP 2	0.60	1.00	0.0	-	1.16	1.00	0.0	-
	CSP 3	1.47	1.14	1.2	L	3.18	1.17	1.2	L
	CSP 4	1.24	1.10	1.0	L	3.01	1.11	1.0	L
	CSP 5	1.34	1.07	0.3	L	3.53	1.00	0.0	-
	CSP 8	0.99	1.24	1.6	D	3.02	1.27	1.9	D
A6, Proline 	CSP 1	0.54	1.15	1.3	L	0.68	1.19	1.9	L
	CSP 2	0.61	1.00	0.0	-	0.90	1.00	0.0	-
	CSP 3	1.15	1.57	4.0	L	1.55	1.86	5.9	L
	CSP 4	1.07	1.56	4.3	L	1.44	1.94	6.0	L
	CSP 5	1.14	1.52	2.3	L	1.54	1.81	3.3	L
	CSP 8	0.94	1.80	6.7	D	1.43	2.34	10.2	D
A7, Phenylalanine 	CSP 1	0.54	1.06	0.5	D	0.88	1.00	0.0	-
	CSP 2	0.58	1.00	0.0	-	1.04	1.00	0.0	-
	CSP 3	1.03	1.15	1.0	L	2.25	1.21	1.6	-
	CSP 4	1.03	1.16	1.1	L	2.50	1.19	1.2	L
	CSP 5	0.91	1.21	1.2	L	2.09	1.23	0.9	L
	CSP 8	0.80	1.34	3.5	D	2.21	1.34	4.3	D
A8, Tryptophan 	CSP 1	0.98	1.58	6.3	D	1.41	1.37	4.2	D
	CSP 2	1.02	1.68	5.8	D	1.69	1.34	2.3	-
	CSP 3	2.18	1.57	7.1	D	4.02	1.25	3.1	D
	CSP 4	1.98	1.61	7.6	D	3.93	1.26	3.2	D
	CSP 5	1.79	1.44	3.0	D	3.55	1.15	0.8	D
	CSP 8	1.45	1.26	2.9	L	3.27	1.05	0.6	L
A9, Tyrosine 	CSP 1	0.67	1.00	0.0	-	1.17	1.00	0.0	-
	CSP 2	0.68	1.00	0.0	-	1.36	1.00	0.0	-
	CSP 3	1.30	1.15	1.1	L	2.89	1.30	1.8	L
	CSP 4	1.20	1.13	0.9	L	2.89	1.24	1.6	L
	CSP 5	1.11	1.15	0.6	L	2.73	1.21	0.6	L
	CSP 8	0.86	1.28	2.1	D	2.42	1.30	2.3	D

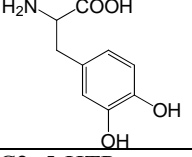
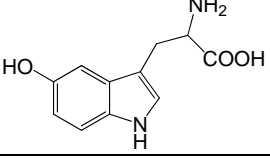
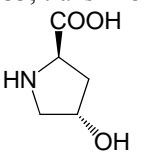
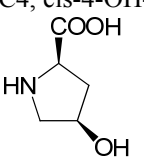
A10, Threonine 	CSP 1	0.55	1.00	0.0	-	0.97	1.06	0.5	L
	CSP 2	0.56	1.00	0.0	-	1.13	1.00	0.0	-
	CSP 3	1.33	1.23	1.3	L	3.14	1.30	2.0	L
	CSP 4	1.03	1.25	1.3	L	2.67	1.30	1.5	L
	CSP 5	1.15	1.21	0.5	L	3.05	1.20	0.4	L
	CSP 8	0.77	1.26	0.8	D	2.37	1.29	1.2	D
A11, Serine 	CSP 1	0.61	1.00	0.0	-	1.11	1.00	0.0	-
	CSP 2	0.63	1.00	0.0	-	1.38	1.00	0.0	-
	CSP 3	1.68	1.00	0.0	-	4.24	1.00	0.0	-
	CSP 4	1.26	1.00	0.0	-	3.80	1.00	0.0	-
	CSP 5	1.40	1.00	0.0	-	3.68	1.00	0.0	-
	CSP 8	1.05	1.00	0.0	-	3.42	1.00	0.0	-
A12, Asparagine 	CSP 1	0.72	1.00	0.0	-	1.08	1.03	0.3	L
	CSP 2	0.72	1.00	0.0	-	1.36	1.00	0.0	-
	CSP 3	2.17	1.00	0.0	-	3.38	1.33	1.6	L
	CSP 4	3.44	1.87	1.5	L	4.96	1.30	2.8	L
	CSP 5	1.60	1.12	0.4	n.d.	3.90	1.00	0.0	-
	CSP 8	1.20	1.15	1.3	D	2.74	1.24	2.4	D
A13, Glutamine 	CSP 1	0.58	1.00	0.0	-	0.89	1.15	0.6	L
	CSP 2	0.59	1.00	0.0	-	1.03	1.00	0.0	-
	CSP 3	1.50	1.16	0.7	L	2.94	1.27	0.9	L
	CSP 4	2.09	1.12	1.0	n.d.	3.38	1.21	2.2	n.d.
	CSP 5	1.26	1.00	0.0	-	2.40	1.00	0.0	-
	CSP 8	0.86	1.26	0.7	D	2.22	1.25	0.8	D
A14, Aspartic acid 	CSP 1	1.45	1.00	0.0	-	2.36	1.00	0.0	-
	CSP 2	1.71	1.05	0.4	L	3.18	1.00	0.0	-
	CSP 3	6.00	1.00	0.0	-	11.40	1.00	0.0	-
	CSP 4	6.19	1.07	0.7	D	12.69	1.07	0.6	D
	CSP 5	7.52	1.00	0.0	-	5.60	1.00	0.0	-
	CSP 8	2.53	1.00	0.0	-	6.56	1.00	0.0	-
A15, Glutamic acid 	CSP 1	0.90	1.00	0.0	-	1.49	1.09	0.6	D
	CSP 2	0.99	1.00	0.0	-	2.14	1.00	0.0	-
	CSP 3	2.57	1.06	0.5	n.d.	6.56	1.15	1.0	D
	CSP 4	3.12	1.08	0.7	D	7.74	1.13	1.3	D
	CSP 5	3.07	1.12	0.6	D	4.67	1.86	0.5	D
	CSP 8	1.38	1.00	0.0	-	4.20	1.00	0.0	-

Class B, halogen atom-substituted amino acids

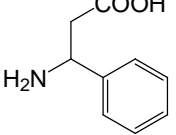
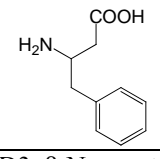
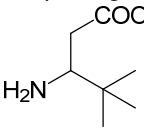
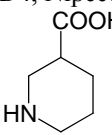
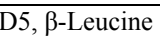
		k_1	α	R_s	EO	k_1	α	R_s	EO
B1, p-F-Phenylalanine 	CSP 1	0.53	1.00	0.0	-	0.87	1.00	0.0	-
	CSP 2	0.55	1.00	0.0	-	1.07	1.00	0.0	-
	CSP 3	1.10	1.13	1.3	L	2.38	1.19	2.0	L
	CSP 4	1.10	1.11	1.1	L	2.60	1.18	2.1	L
	CSP 5	0.98	1.13	0.7	L	2.32	1.18	0.7	L
	CSP 8	0.84	1.33	1.9	D	2.38	1.39	2.4	D
B2, p-Cl-Phenylalanine 	CSP 1	0.57	1.11	0.5	D	1.04	1.00	0.0	-
	CSP 2	0.66	1.00	0.0	-	1.28	1.00	0.0	-
	CSP 3	1.36	1.14	1.5	L	2.97	1.19	1.3	L
	CSP 4	1.34	1.12	1.5	L	3.14	1.20	2.5	L
	CSP 5	1.20	1.14	0.7	L	2.85	1.18	0.7	L
	CSP 8	1.05	1.39	3.3	D	2.94	1.46	3.6	D
B3, p-Br-Phenylalanine 	CSP 1	0.67	1.04	0.4	-	1.14	1.00	0.0	-
	CSP 2	0.74	1.00	0.0	-	1.41	1.00	0.0	-
	CSP 3	1.53	1.14	1.8	n.d.	3.29	1.18	2.1	n.d.
	CSP 4	1.48	1.13	1.6	n.d.	3.40	1.21	2.7	n.d.
	CSP 5	1.34	1.14	0.7	n.d.	3.16	1.18	0.7	n.d.
	CSP 8	1.16	1.42	4.4	n.d.	3.22	1.48	5.1	n.d.
B4, o-F-Phenylalanine 	CSP 1	0.56	1.00	0.0	-	0.91	1.00	0.0	-
	CSP 2	0.55	1.00	0.0	-	1.01	1.13	0.6	n.d.
	CSP 3	1.03	1.16	1.8	n.d.	2.08	1.21	2.8	n.d.
	CSP 4	1.00	1.16	1.1	n.d.	2.29	1.21	1.6	n.d.
	CSP 5	0.91	1.17	0.7	n.d.	2.10	1.21	0.7	n.d.

	CSP 8	0.78	1.35	3.6	n.d.	2.18	1.37	5.1	n.d.
B5, Baclofen 	CSP 1	1.13	1.09	1.1	n.d.	1.70	1.11	1.6	n.d.
	CSP 2	0.83	1.00	0.0	-	1.53	1.00	0.0	-
	CSP 3	4.01	1.25	3.4	n.d.	9.55	1.32	4.0	n.d.
	CSP 4	4.63	1.28	5.4	n.d.	11.92	1.34	7.0	n.d.
	CSP 5	3.48	1.33	3.3	n.d.	7.35	1.41	3.8	n.d.
	CSP 8	2.72	1.32	2.3	n.d.	8.96	1.42	3.9	n.d.

Class C, hydroxy-substituted amino acids

		k_1	α	R_s	EO	k_1	α	R_s	EO
C1, DOPA 	CSP 1	0.80	1.14	0.9	D	1.43	1.00	0.0	-
	CSP 2	0.86	1.00	0.0	-	1.81	1.00	0.0	-
	CSP 3	1.91	1.07	0.6	L	4.10	1.16	0.8	L
	CSP 4	1.71	1.00	0.0	-	4.30	1.07	0.4	L
	CSP 5	1.84	1.00	0.0	-	2.86	1.51	1.0	L
	CSP 8	1.36	1.00	0.0	-	3.68	1.00	0.0	-
C2, 5-HTP 	CSP 1	1.16	1.58	5.8	D	1.60	1.37	3.1	D
	CSP 2	1.14	1.67	5.3	D	1.75	1.33	1.8	D
	CSP 3	2.63	1.38	4.9	D	4.67	1.10	1.2	D
	CSP 4	2.24	1.43	5.2	D	4.48	1.13	1.3	D
	CSP 5	2.06	1.38	2.5	D	3.82	1.11	0.6	D
	CSP 8	1.78	1.14	1.5	L	3.66	1.00	0.0	-
C3, trans-4-OH-Proline 	CSP 1	0.57	1.73	1.5	L	0.71	1.83	2.0	L
	CSP 2	0.50	1.99	1.8	L	0.89	1.61	1.1	L
	CSP 3	1.07	3.90	6.5	L	1.77	3.78	5.9	L
	CSP 4	0.95	3.88	6.0	L	1.58	3.77	6.7	L
	CSP 5	1.05	3.42	3.5	L	1.77	3.08	3.1	L
	CSP 8	1.24	2.37	2.7	L	3.22	1.33	0.8	L
C4, cis-4-OH-Proline 	CSP 1	0.99	1.00	0.0	-	1.24	1.00	0.0	-
	CSP 2	1.00	1.13	0.6	D	1.46	1.00	0.0	-
	CSP 3	4.16	1.00	0.0	-	6.36	1.05	0.4	L
	CSP 4	3.66	1.20	1.1	D	5.89	1.00	0.0	-
	CSP 5	3.56	1.00	0.0	-	5.43	1.00	0.0	-
	CSP 8	2.93	1.00	0.0	-	4.27	1.24	0.7	D

Class D, beta-amino acids

		k_1	α	R_s	EO	k_1	α	R_s	EO
D1, β -Phenylalanine 	CSP 1	0.96	1.00	0.0	-	1.43	1.11	1.2	n.d.
	CSP 2	0.85	1.16	0.8	n.d.	1.55	1.16	0.8	n.d.
	CSP 3	3.28	1.11	1.2	n.d.	6.71	1.26	2.7	n.d.
	CSP 4	3.22	1.15	2.0	n.d.	7.09	1.31	5.8	n.d.
	CSP 5	2.84	1.08	0.8	n.d.	5.81	1.28	1.8	n.d.
	CSP 8	2.36	1.26	2.1	n.d.	5.89	1.56	4.3	n.d.
D2, β -homo-Phenylalanine 	CSP 1	1.10	1.00	0.0	-	1.59	1.03	0.5	n.d.
	CSP 2	0.95	1.11	1.2	n.d.	1.59	1.06	0.6	n.d.
	CSP 3	4.20	1.03	0.5	n.d.	7.55	1.10	1.9	n.d.
	CSP 4	4.16	1.00	0.0	-	7.77	1.11	1.8	n.d.
	CSP 5	3.32	1.06	0.7	n.d.	6.21	1.08	1.0	n.d.
	CSP 8	3.18	1.00	0.0	-	7.05	1.18	3.2	n.d.
D3, β -Neopentylglycine 	CSP 1	0.66	1.12	0.8	n.d.	0.99	1.16	1.6	n.d.
	CSP 2	0.51	1.00	0.0	-	1.04	1.12	0.4	n.d.
	CSP 3	2.10	1.33	2.0	n.d.	3.87	1.50	3.2	n.d.
	CSP 4	2.01	1.35	2.6	n.d.	3.98	1.53	4.4	n.d.
	CSP 5	2.03	1.33	1.9	n.d.	3.89	1.49	2.7	n.d.
	CSP 8	1.88	1.36	3.4	n.d.	4.29	1.59	6.2	n.d.
D4, Nipicotic acid 	CSP 1	1.00	1.17	1.8	R	1.38	1.22	2.5	R
	CSP 2	0.92	1.00	0.0	-	1.56	1.00	0.0	-
	CSP 3	2.19	1.99	4.1	R	3.68	2.40	5.7	R
	CSP 4	2.22	2.23	5.7	R	3.82	2.89	10.0	R
	CSP 5	2.02	2.04	3.2	R	8.22	1.10	0.7	R
	CSP 8	1.23	2.52	9.0	S	2.72	2.99	11.8	S
D5, β -Leucine 	CSP 1	0.76	1.04	0.5	n.d.	1.17	1.11	1.3	n.d.
	CSP 2	0.58	1.14	0.5	n.d.	1.03	1.16	1.3	n.d.

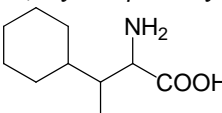
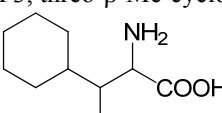
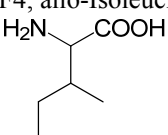
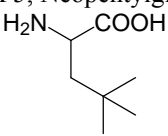
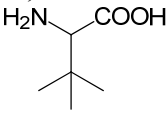
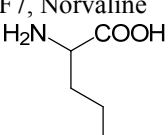
	CSP 3	2.62	1.06	0.6	n.d.	5.14	1.23	2.9	n.d.
	CSP 4	2.40	1.06	0.6	n.d.	5.13	1.23	3.6	n.d.
	CSP 5	2.42	1.04	0.5	n.d.	4.76	1.22	2.8	n.d.
	CSP 8	2.06	1.11	1.4	n.d.	5.05	1.33	4.7	n.d.

Class E, alpha- and N-methylated amino acids

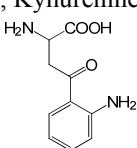
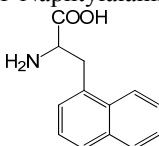
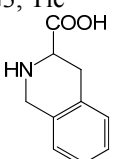
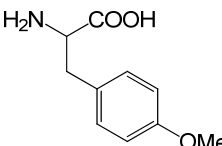
		k_1	α	R_s	EO	k_1	α	R_s	EO
E1, α -Me-Phenylalanine 	CSP 1	0.44	1.31	2.6	D	0.80	1.19	2.2	D
	CSP 2	0.47	1.00	0.0	-	0.96	1.08	0.5	D
	CSP 3	0.72	1.13	0.5	D	1.58	1.00	0.0	-
	CSP 4	0.66	1.18	0.6	D	1.68	1.00	0.0	-
	CSP 5	0.64	1.10	0.5	D	1.53	1.00	0.0	-
	CSP 8	0.49	1.08	0.6	L	1.44	1.06	0.7	L
E2, α -Me-m-Tyrosine 	CSP 1	0.58	1.48	4.6	n.d.	1.02	1.31	4.0	n.d.
	CSP 2	0.57	1.45	1.5	n.d.	1.10	1.24	1.4	n.d.
	CSP 3	0.93	1.42	2.7	n.d.	2.04	1.29	2.0	n.d.
	CSP 4	0.83	1.42	2.5	n.d.	1.98	1.31	2.2	n.d.
	CSP 5	0.77	1.41	2.4	n.d.	1.76	1.26	1.3	n.d.
	CSP 8	0.56	1.63	5.6	n.d.	1.55	1.50	7.4	n.d.
E3, α -Me-DOPA 	CSP 1	0.71	1.53	4.3	D	1.29	1.29	2.0	D
	CSP 2	0.71	1.47	1.0	D	1.81	1.00	0.0	-
	CSP 3	1.26	1.46	3.2	D	2.86	1.22	1.6	D
	CSP 4	1.05	1.52	2.5	D	2.62	1.29	1.7	D
	CSP 5	1.59	1.00	0.0	-	3.38	1.00	0.0	-
	CSP 8	0.66	2.11	3.1	L	1.84	1.85	5.1	L
E4, α -Me-Tryptophan 	CSP 1	0.90	2.64	13.4	n.d.	1.36	2.01	11.1	n.d.
	CSP 2	0.89	3.32	16.8	n.d.	1.55	2.10	10.4	n.d.
	CSP 3	1.47	3.40	20.6	n.d.	2.98	2.14	13.3	n.d.
	CSP 4	1.35	3.56	20.5	n.d.	2.94	2.07	13.3	n.d.
	CSP 5	1.21	3.06	14.6	n.d.	2.46	1.95	8.0	n.d.
	CSP 8	0.83	3.04	11.1	n.d.	1.94	1.91	7.0	n.d.
E5, α -Me-Leucine 	CSP 1	0.30	1.15	0.5	n.d.	0.66	1.09	0.9	n.d.
	CSP 2	0.33	1.00	0.0	-	0.81	1.00	0.0	-
	CSP 3	0.63	1.00	0.0	-	1.50	1.12	1.0	n.d.
	CSP 4	0.44	1.08	0.5	n.d.	1.35	1.18	1.3	n.d.
	CSP 5	0.56	1.00	0.0	-	1.44	1.16	0.8	n.d.
	CSP 8	0.56	1.00	0.0	-	1.44	1.16	0.8	n.d.
E6, α -Me-Serine 	CSP 1	0.56	1.09	0.8	n.d.	1.02	1.07	0.7	n.d.
	CSP 2	0.60	1.00	0.0	-	1.27	1.00	0.0	-
	CSP 3	1.21	1.13	0.8	n.d.	2.89	1.11	0.9	n.d.
	CSP 4	0.94	1.11	0.6	n.d.	2.61	1.08	0.5	n.d.
	CSP 5	1.10	1.00	0.0	-	2.75	1.00	0.0	-
	CSP 8	1.10	1.00	0.0	-	2.75	1.00	0.0	-
E7, 1-Me-Tryptophan 	CSP 1	0.94	1.33	3.4	D	1.30	1.13	2.1	D
	CSP 2	0.98	1.72	6.1	D	1.50	1.32	1.8	D
	CSP 3	2.00	1.33	4.5	D	3.33	1.10	1.3	D
	CSP 4	1.94	1.36	5.0	D	3.68	1.12	1.6	D
	CSP 5	1.78	1.28	1.6	D	3.51	1.00	0.0	-
	CSP 8	1.69	1.14	1.8	L	3.42	1.06	0.6	D
E8, N-Me-Leucine 	CSP 1	0.35	1.00	0.0	-	0.55	1.00	0.0	-
	CSP 2	0.34	1.06	0.4	n.d.	0.62	1.07	0.4	n.d.
	CSP 3	0.66	1.09	0.5	D	1.08	1.18	1.0	D
	CSP 4	0.55	1.01	0.9	D	0.95	1.28	1.9	D
	CSP 5	0.63	1.10	0.5	D	1.15	1.18	1.0	D
	CSP 8	0.63	1.10	0.5	D	1.15	1.18	1.0	D

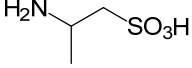
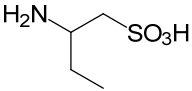
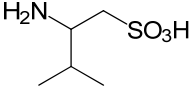
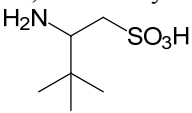
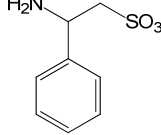
Class F, remaining aliphatic amino acids

		k_1	α	R_s	EO	k_1	α	R_s	EO
F1, Pimelic acid 	CSP 1	0.48	1.07	0.6	L	0.77	1.06	0.6	L
	CSP 2	0.47	1.19	1.0	L	0.88	1.20	1.0	L
	CSP 3	0.92	1.13	0.8	L	1.64	1.12	1.0	L
	CSP 4	0.79	1.18	1.2	L	1.63	1.17	1.3	L

	CSP 5	0.91	1.19	0.9	L	1.73	1.19	1.1	L
	CSP 8	0.65	1.31	1.9	D	1.59	1.36	2.7	D
F2, erythro- β -Me-cyclohexylala	CSP 1	0.57	1.00	0.0	-	1.05	1.06	0.6	n.d.
	CSP 2	0.54	1.19	0.5	n.d.	1.25	1.12	0.5	n.d.
	CSP 3	1.28	1.27	1.9	n.d.	3.17	1.39	2.7	n.d.
	CSP 4	1.11	1.31	2.8	n.d.	3.06	1.36	3.6	n.d.
	CSP 5	1.18	1.39	1.5	n.d.	3.10	1.54	1.7	n.d.
	CSP 8	0.98	1.49	5.1	n.d.	3.41	1.43	6.2	n.d.
F3, threo- β -Me-cyclohexylala	CSP 1	0.54	1.00	0.0	-	0.92	1.06	0.5	n.d.
	CSP 2	0.55	1.00	0.0	-	1.11	1.00	0.0	-
	CSP 3	1.17	1.23	1.6	n.d.	2.74	1.26	2.0	n.d.
	CSP 4	1.00	1.29	2.3	n.d.	2.70	1.22	2.0	n.d.
	CSP 5	1.14	1.29	1.4	n.d.	2.99	1.27	0.8	n.d.
	CSP 8	1.03	1.30	1.5	n.d.	3.49	1.13	0.9	n.d.
F4, allo-Isoleucine	CSP 1	0.43	1.00	0.0	-	0.81	1.05	0.5	L
	CSP 2	0.37	1.00	0.0	-	0.84	1.00	0.0	-
	CSP 3	0.97	1.26	1.6	L	2.26	1.32	2.2	L
	CSP 4	0.76	1.25	1.5	L	2.21	1.22	2.2	L
	CSP 5	0.89	1.28	1.3	L	2.55	1.23	0.6	L
	CSP 8	0.64	1.36	2.1	D	2.26	1.24	2.1	D
F5, Neopentylglycine	CSP 1	0.46	1.09	0.7	L	0.81	1.12	1.1	L
	CSP 2	0.43	1.12	0.6	L	0.95	1.08	0.4	L
	CSP 3	1.18	1.38	3.0	L	2.56	1.40	3.1	L
	CSP 4	0.98	1.38	3.0	L	2.47	1.32	2.8	L
	CSP 5	1.07	1.38	1.7	L	2.66	1.33	0.8	L
	CSP 8	0.87	1.44	3.9	D	2.71	1.31	3.8	D
F6, <i>tert</i> -Leucine	CSP 1	0.41	1.00	0.0	-	0.83	1.07	0.8	L
	CSP 2	0.36	1.00	0.0	-	0.95	1.09	0.3	L
	CSP 3	0.90	1.43	2.6	L	2.14	1.57	4.2	L
	CSP 4	0.73	1.37	2.3	L	2.14	1.43	3.9	L
	CSP 5	0.81	1.40	1.9	L	2.32	1.50	2.2	L
	CSP 8	0.62	1.57	4.1	D	2.22	1.53	5.8	D
F7, Norvaline	CSP 1	0.44	1.00	0.0	-	0.82	1.05	0.5	L
	CSP 2	0.42	1.06	0.4	L	0.95	1.05	0.3	L
	CSP 3	1.00	1.22	1.6	L	2.31	1.27	2.1	L
	CSP 4	0.81	1.21	1.6	L	2.21	1.20	1.9	L
	CSP 5	0.91	1.21	0.9	L	2.36	1.20	0.6	L
	CSP 8	0.63	1.33	1.8	D	2.19	1.28	2.1	D

Class G, remaining aromatic amino acids

		k_1	α	R_s	EO	k_1	α	R_s	EO
G1, Kynurenine	CSP 1	1.02	1.05	0.6	D	1.35	1.00	0.0	-
	CSP 2	1.11	1.00	0.0	-	1.72	1.00	0.0	-
	CSP 3	2.07	1.24	2.6	L	3.54	1.23	1.9	L
	CSP 4	1.98	1.10	1.3	L	3.79	1.12	1.6	L
	CSP 5	1.98	1.00	0.0	-	3.18	1.13	0.5	L
	CSP 8	1.39	1.26	3.3	D	3.13	1.28	4.1	D
G2, 1-Naphthylalanine	CSP 1	0.85	1.00	0.0	-	1.21	1.00	0.0	-
	CSP 2	0.89	1.00	0.0	-	1.42	1.09	0.5	n.d.
	CSP 3	1.68	1.14	1.5	L	3.16	1.16	1.5	L
	CSP 4	1.60	1.12	1.7	L	3.44	1.14	1.7	L
	CSP 5	1.44	1.13	0.6	L	3.22	1.10	0.4	L
	CSP 8	1.20	1.53	5.3	D	3.01	1.56	4.7	D
G3, Tic	CSP 1	0.59	1.11	1.1	S	0.84	1.11	1.3	S
	CSP 2	0.64	1.25	0.6	S	1.06	1.25	0.9	S
	CSP 3	1.13	1.33	2.3	S	1.96	1.29	1.9	S
	CSP 4	1.11	1.32	2.2	S	2.17	1.27	2.1	S
	CSP 5	1.01	1.38	1.4	S	1.99	1.32	1.1	S
	CSP 8	0.91	1.34	4.1	R	1.94	1.32	4.9	R
G4, OMe-Tyrosine	CSP 1	0.63	1.07	0.6	L	0.98	1.00	0.0	-
	CSP 2	0.68	1.00	0.0	-	1.15	1.00	0.0	-
	CSP 3	1.25	1.14	1.2	L	2.54	1.17	1.2	L

	CSP 4	1.21	1.15	1.4	L	2.74	1.19	1.7	L
	CSP 5	1.12	1.16	0.6	L	2.39	1.19	0.8	L
	CSP 8	0.92	1.39	3.9	D	2.38	1.40	5.0	D
Class H, aminosulfonic acids									
		k₁	α	R_s	EO	k₁	α	R_s	EO
H1, 2-Methyltaurine	CSP 1	0.59	1.00	0.0	-	0.52	1.00	0.0	-
	CSP 2	0.52	1.00	0.0	-	0.47	1.25	0.5	n.d.
	CSP 3	3.32	1.08	0.6	R	4.10	1.08	0.5	R
	CSP 4	2.81	1.16	0.8	R	3.65	1.17	0.7	R
	CSP 5	2.44	1.16	0.7	R	3.16	1.22	0.8	R
	CSP 8	1.95	1.00	0.0	-	2.69	1.00	0.0	-
H2, 2-Ethyltaurine	CSP 1	0.55	1.00	0.0	-	0.52	1.00	0.0	-
	CSP 2	0.49	1.29	0.5	n.d.	0.41	1.30	0.5	n.d.
	CSP 3	2.70	1.39	2.3	R	3.18	1.43	2.0	R
	CSP 4	2.27	1.52	2.5	R	2.85	1.54	2.2	R
	CSP 5	2.09	1.50	2.2	R	2.58	1.56	2.0	R
	CSP 8	1.69	1.43	1.3	S	1.97	1.65	1.2	S
H3, 2-Isopropyltaurine	CSP 1	0.53	1.00	0.0	-	0.45	1.00	0.0	-
	CSP 2	0.43	1.00	0.0	-	0.35	1.30	0.4	n.d.
	CSP 3	2.05	1.47	4.4	R	2.54	1.53	4.0	R
	CSP 4	1.91	1.63	3.0	R	2.36	1.67	2.6	R
	CSP 5	1.82	1.60	2.6	R	2.25	1.66	2.2	R
	CSP 8	1.45	1.56	1.6	S	1.86	1.55	0.8	S
H4, 2-tert-Butyltaurine	CSP 1	0.61	1.00	0.0	-	0.36	1.49	0.5	-
	CSP 2	0.35	1.00	0.0	-	0.35	1.00	0.0	-
	CSP 3	1.29	2.46	5.8	R	1.46	2.52	4.3	R
	CSP 4	1.18	2.79	6.5	R	1.52	2.62	5.0	R
	CSP 5	1.25	2.61	5.7	R	1.55	2.51	4.1	R
	CSP 8	1.06	2.27	2.9	S	1.41	2.04	1.7	S
H5, 2-Phenyltaurine	CSP 1	0.53	1.00	0.0	-	0.47	1.00	0.0	-
	CSP 2	0.43	1.00	0.0	-	0.41	1.33	0.5	-
	CSP 3	2.31	1.21	2.6	R	3.21	1.16	1.7	R
	CSP 4	1.91	1.37	2.8	R	2.57	1.31	1.8	R
	CSP 5	1.86	1.27	1.9	R	2.52	1.24	1.4	R
	CSP 8	1.44	1.28	1.2	S	2.57	1.00	0.0	-

425 ^a Conditions: column dimensions 250x3 mm i.d., 3 μm particle size; Mobile phase: 50 mM FA and 25 mM DEA
426 in 100% MeOH (left column) or ACN-MeOH 50/50 v/v (right column); flow rate 0.4 mL/min, 25°C; t₀ = 3.68
427 min; UV detection 254 nm and CAD detection; ^b EO: absolute configuration of the first eluted enantiomer

428

429

430

431

432

433

434 **Table 2.** Enantiomer separation of amino acids on CSP 6 and CSP 7^a

Analyte	CSP 6			CSP 7		
	k_1	α	EO ^b	k_1	α	EO ^b
A6, Pro	0.55	1.32	L	1.24	1.07	L
A8, Trp	0.99	1.81	D	1.57	2.14	D
C2, 5-HTP	0.99	1.88	D	1.92	1.86	D
C3, trans-4-OH-Pro	0.51	2.84	L	1.15	1.53	L
C4, cis-4-OH-Pro	1.45	1.12	D	1.76	1.33	D
D4, Nipe	0.96	1.67	(R)	2.12	1.09	(S)
E3, α -Me-DOPA	0.61	1.50	D	1.25	1.34	D
E7, 1-Me-Trp	1.04	1.42	D	1.38	1.26	D
G3, Tic	0.68	1.21	(S)	0.97	1.13	(S)

435 ^aColumns: CSP 6: 250 x 3 mm i.d., 3 μ m particle size; CSP 7: 150 x 4mm i.d., 5 μ m particle size; Mobile phase:

436 MeOH, 50 mM FA, 25 mM DEA; 25°C; flow rate CSP 6 0.4 mL/min, CSP 7 1.0 mL/min, UV detection 254 nm;

437 ^b EO: absolute configuration of the first eluted enantiomer

Supporting Information:

Mechanistic investigations of cinchona alkaloid-based zwitterionic chiral stationary phases

*Reinhard Pell, Siniša Sić, Wolfgang Lindner**

Department of Analytical Chemistry, University of Vienna, Währinger Strasse 38, 1090 Vienna, Austria

* Author for correspondence:

e-mail: Wolfgang.Lindner@univie.ac.at

Tel.: +431427752300

Fax: +43142779523

1. Discussion on the preparation of CSPs 2 and 4-8

The preparation of the zwitterionic chiral selectors **6-11** was accomplished by fusion of β -aminosulfonic acids **5a-f** and the activated 4-nitrophenyl ester hydrochlorides of quinine **2a** or quinidine **2b**, respectively. The synthesis of **2** and the fusion step to prepare selectors **6-11** followed the procedure reported previously by Hoffmann et al.[1]. The chiral selectors were purified by flash chromatography in order to remove byproducts such as 4-nitrophenol and cinchona-alkaloid derivatives.

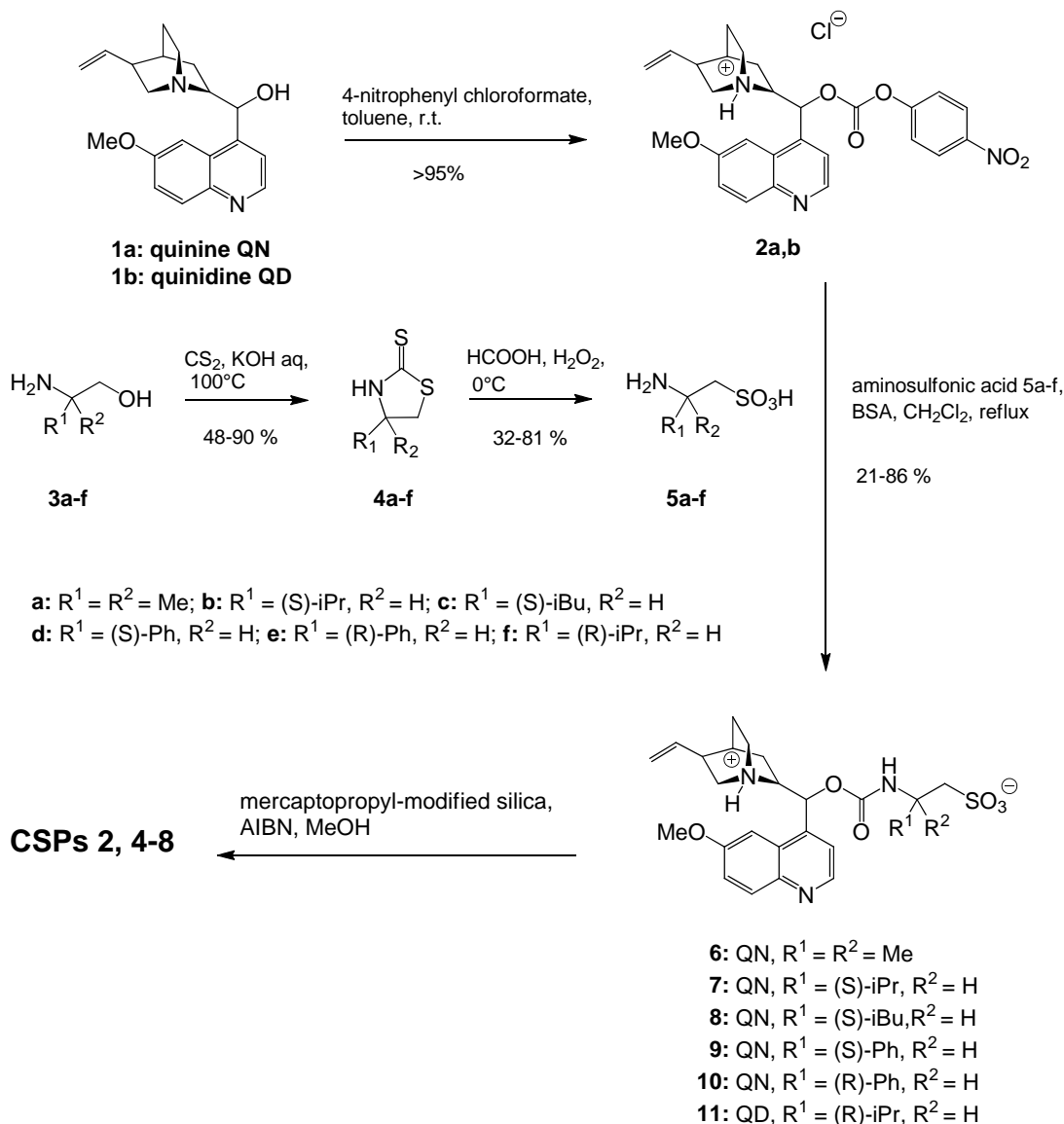


Figure S-1. Synthetic scheme for the preparation of CSPs 2 and 4-8

The chiral and achiral β -aminosulfonic acids **5a-f** were synthesized from corresponding amino alcohols **3a-f** in a two-step synthesis according to a procedure from Xu et al.[2]. In the first step the 4-substituted thiazolidine-2-thiones **4a-f** were prepared by reaction of the corresponding vicinal amino alcohols with carbon disulfide in an aqueous potassium hydroxide solution.

For all six reactions we observed the formation of oxazolidine-2-thione byproducts, which had to be removed by flash chromatography. The second step involved the oxidation of thiazolidine-2-thiones **4** with peroxyformic acid, which was prepared in situ by mixing formic acid with a 30 % aqueous hydrogen peroxide solution. The β -aminosulfonic acids **5a-f** were isolated in moderate yields and high purity after crystallization from the concentrated reaction solution. Furthermore, the synthesis of the chiral β -aminosulfonic acids from the optically active amino alcohols was carried out without any racemization (the enantiomeric purity of **5b-f** was measured by HPLC using CSP 3 and gave enantiomeric excess values >99%).

The silica gel for SO immobilization was mercaptopropyl-modified and trimethylsilyl-encapped in house. The covalent immobilization of the chiral selector onto the 3-mercaptopropyl-modified silica gel was carried out via radical addition reaction[1]. It has to be noted that for immobilization of the quinidine-based SO **11** the ten-fold amount of azobisisobutyronitrile (AIBN) had to be employed to achieve comparable SO coverage. The reason is presumably the less accessible vinyl group of the quinidine-molecule compared to quinine.

2. Experimental part

2.1 General information and materials

All chemical reactions were carried out under anhydrous conditions (nitrogen atmosphere and oven dried glassware) unless otherwise stated. Technical grade solvents, which were used for flash chromatography only, were obtained from VWR (Vienna, Austria) and HPLC grade solvents were obtained from Carl-Roth GmbH (Karlsruhe, Germany). All chemical reagents were purchased from Sigma-Aldrich (synthesis grade or higher purity), except for quinine and quinidine which were obtained from Buchler (Braunschweig, Germany). Flash chromatography was carried out with Silica 60 (0.040-0.063 mm particle size) from Merck (Darmstadt, Germany).

^1H and ^{13}C NMR spectra were acquired on a Bruker DRX 400 MHz or on a Bruker DRX 600 Mhz spectrometer. Chemical shifts are given in ppm. Spectra were recorded in CDCl_3 , CD_3OD or D_2O and the solvent signals were used as reference signals. For data processing Spinworks 2.2.5 software was

used. MS experiments were performed using an ion trap mass spectrometer with an electrospray ionization source (Agilent 1100 series CL/MSD Trap ion-trap MS System).

Silica gel for selector immobilization (Daisogel 120-3P or Daisogel 120-5P, particle size 3 or 5 μm ; pore diameter 12 nm, surface area 300 m^2 / g) was purchased from Daiso Co., Ltd. (Osaka, Japan). Surface coverages of the CSPs were calculated by elemental analysis (CHNS) using an EA 1108 CHNS-O Element analyzer (Carlo Erba, now Thermo Scientific). The SO coverage on the silica was calculated from the nitrogen content (accuracy according to manufacturer specifications: $\pm 8\%$).

The CSP with 5 μm particle size was slurry packed in house into a 150 x 4 mm i.d. stainless steel column. The 3 μm particle size CSPs were packed at Bischoff (Leonberg, Germany) into 250 x 3 mm i.d. stainless steel columns.

2.2 Procedures

2.2.1 Procedures for compounds **2a-b**, **4a-f** and **5a-f**

The synthetic procedure of activated quinine- and quinidine ester **2a** and **2b** including spectroscopic data is described elsewhere[1]. The preparation of aminosulfonic acids **5a-f** from the corresponding amino alcohols **3a-f** via thiazolidine-2-thiones **4a-f** followed strictly the published protocol by Xu et al.[2].

2.2.2 General procedures for zwitterionic SOs **6-11**

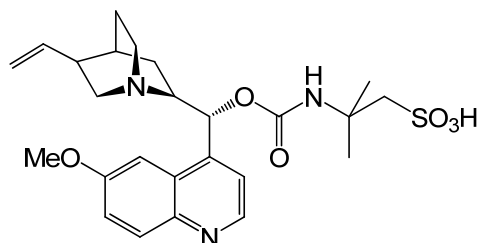
The synthesis followed a protocol already described by Hoffmann et al. [1, 3]. Finely ground aminosulfonic acid **5** (4.0 mmol; **5a** 0.61 g, **5b/5f** 0.67 g, **5c** 0.73 g, **5d/5e** 0.81 g) was suspended in dry CH_2Cl_2 (ca. 100 mL). N,O-bis(trimethylsilyl)acetamide (3.0 mL, 12.0 mmol, 3 equiv.) was added portionwise to the suspension. The resulting solution was refluxed until it became clear (12-24 hours). After cooling to room temperature, activated cinchona alkaloid ester **2** was added portionwise in a counterstream of N_2 . The solution was stirred over night at room temperature turning pale yellow. After quenching with MeOH (5 mL), the reaction mixture was concentrated and purified by flash chromatography (CH_2Cl_2 : MeOH 9:1 to 1:1) yielding the zwitterionic SO.

2.2.3 General procedures for SO immobilization

2.20 g of thiol-modified and endcapped silica (SH-content: 680 $\mu\text{mol} / \text{g}$ silica) were suspended in 10 mL MeOH. The SO (1.0 mmol) was dissolved in 15 mL of MeOH and added to the silica slurry. A methanolic solution of AIBN (60 mg, 0.37 mmol; for quinidine based SO **11**: 600 mg, 3.65 mmol, each in 5 mL) was added in a counterstream of N_2 . The suspension was stirred under reflux for 6 hrs. Then it

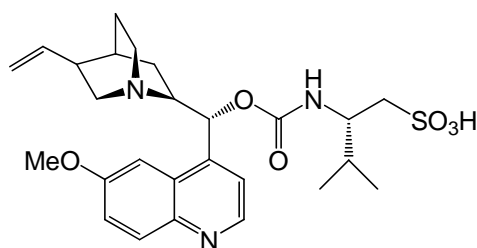
was cooled to ambient temperature, filtered and washed with MeOH (3 x 20 mL) and dichloromethane (2 x 20 mL). The immobilized silica was dried in vacuum at 60°C.

2.3 Analytical data

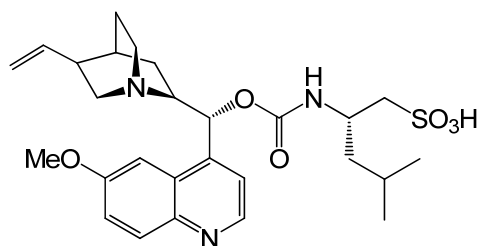


SO 6 (SO for CSP 2): 25 % yield, white crystals. ¹H-NMR [CD₃OD]: δ = 8.71 (d, 1H), 8.00 (d, 1H), 7.62 (d, 1H), 7.50 (dd, 1H), 7.45 (s, 1H), 6.66 (s, 1H), 5.79 (m, 1H), 5.11 (d, 1H), 5.03 (d, 1H), 4.04 (s, 3H), 3.81 (s, 1H), 3.65 (s, 1H), 3.40 (d, 1H), 2.94 (d, 1H), 2.71 (s, 1H), 2.22-2.14 (m, 2H), 1.88 (m, 1H), 1.72 (m, 1H), 1.54 (s, 2H), 1.48 (s, 3H), 1.42 (s, 3H). ¹³C-NMR [CD₃OD]: δ = 160.8 (C_{ar}), 155.3 (C=O), 148.74 (C_{ar}H), 145.5 (C_{ar}), 143.6 (C_{ar}), 138.9 (CH=), 132.3 (C_{ar}H), 128.0 (CH₂=), 127.4 (C_{ar}), 124.3 (C_{ar}H), 120.5 (C_{ar}H), 102.7 (C_{ar}H), 71.1 (CH), 60.6 (CH), 59.4 (CH₂SO₃H), 57.2 (OCH₃), 45.6 (CH₂), 38.3 (CH₂), 38.3 (CH), 28.9 (CH₃), 28.4 (C₄), 28.3 (CH₃), 25.0 (CH₂), 20.7 (CH₂).

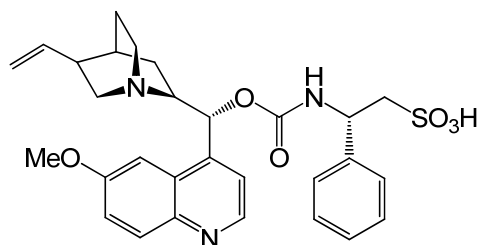
MS (ESI, positive): 504.2 [M + H]⁺.



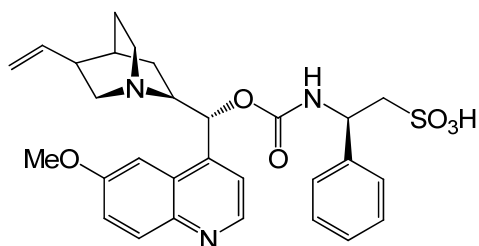
SO 7 (SO for CSP 4): 53 % yield, yellowish crystals. ¹H-NMR [CD₃OD]: δ = 8.86 (d, 1H), 8.06 (d, 1H), 7.89 (d, 1H), 7.64 (d, 1H), 7.60 (dd, 1H), 7.06 (s, 1H), 5.74 (m, 1H), 5.09 (d, 1H), 4.99 (d, 1H), 3.99 (s, 3H), 3.91 (m, 2H), 3.81 (m, 1H), 3.68 (t, 1H), 3.30 (m, 2H), 2.94 (m, 2H), 2.81 (s, 1H), 2.34 (m, 1H), 2.25 (m, 1H), 2.09 (s, 1H), 1.94 (m, 1H), 1.75 (m, 2H), 0.85 (d, 3H), 0.83 (d, 3H). ¹³C-NMR [CD₃OD]: δ = 162.2 (C_{ar}), 156.7 (C=O), 149.9 (C_{ar}), 145.0 (C_{ar}H), 139.8 (C_{ar}), 139.5 (CH=), 128.8 (C_{ar}), 127.9 (C_{ar}H), 127.5 (C_{ar}H), 120.6 (C_{ar}H), 117.8 (CH₂=), 103.7 (C_{ar}H), 71.4 (CH), 60.1 (CH), 58.0 (OCH₃), 56.4 (CH₂SO₃H), 55.8 (CH), 54.5 (CH₂), 46.2 (CH₂), 38.8 (CH), 34.3 (CH), 28.7 (CH), 25.4 (CH₂), 21.0 (CH₂), 20.1 (CH₃), 18.8 (CH₃). MS (ESI, positive): 518.4 [M+H]⁺.



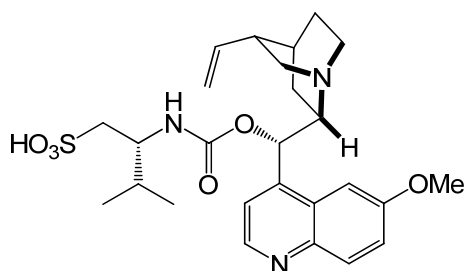
SO 8 (SO for CSP 5): 35 % yield, yellowish crystals. $^1\text{H-NMR}$ [CD_3OD]: δ = 8.59 (m, 1H), 7.86 (d, 1H), 7.47 (d, 1H), 7.40-7.31 (m, 2H), 6.97 (s, 1H), 5.67 (m, 1H), 5.04-4.88 (m, 2H), 3.89 (s, 3H), 3.59 (m, 1H), 3.52 (m, 1H), 3.15 (m, 2H), 3.00 (d, 1H), 2.96 (m, 1H), 2.82 (m, 1H), 2.19-2.02 (m, 2H), 1.96 (m, 1H), 1.63 (m, 2H), 1.51 (m, 3H), 1.40 (m, 1H), 1.25 (m, 1H), 0.87 (dd, 6H). $^{13}\text{C-NMR}$ [CD_3OD]: δ = 160.8 (C_{ar}), 156.5 ($\text{C}=\text{O}$), 148.4 (C_{arH}), 145.4 (C_{ar}), 144.3 (C_{ar}), 140.0 ($\text{CH}=\text{}$), 132.0 (C_{arH}), 127.8 (C_{ar}), 124.5 (C_{arH}), 119.8 (C_{arH}), 117.5 ($\text{CH}_2=\text{}$), 102.6 (C_{arH}), 60.5 (CH), 57.7 (CH_2), 57.5 (CH), 56.6 (CH_2), 53.5 (CH_2), 49.1 (CH), 48.5 (CH), 45.9 (CH_2), 43.1 (CH_2), 39.2 (CH), 28.8 (CH), 26.4 (CH), 25.8 (CH_2), 25.7 (CH), 22.7 (CH_3), 22.5 (CH_3). MS (ESI, positive): 532.2 [$\text{M}+\text{H}$] $^+$.



SO 9 (SO for CSP 6): 50 % yield, brownish crystals. $^1\text{H-NMR}$ [CD_3OD]: δ = 8.88 (d, 1H), 8.12 (d, 1H), 7.97 (d, 1H), 7.75 (dd, 1H), 7.68 (d, 1H), 7.32 (m, 3H), 7.30 (m, 3H), 7.03 (s, 1H), 5.25 (m, 1H), 5.17 (d, 1H), 4.75 (m, 1H), 4.07 (s, 3H), 3.87 - 3.72 (m, 2 H), 3.68 (s, 1H), 3.49 (m, 1H), 3.23 (d, 1H), 3.13 (d, 1H), 2.30 - 2.17 (m, 2H), 2.03 (m, 2H), 1.82 (m, 1H). $^{13}\text{C-NMR}$ [CD_3OD]: δ = 160.3 (C_{ar}), 155.6 ($\text{C}=\text{O}$), 148.3 (C_{arH}), 145.0 (C_{ar}), 143.5 (C_{ar}), 139.5 ($\text{CH}=\text{}$), 131.2 (C_{arH}), 131.0 (C_{arH}), 130.2 (C_{arH}), 128.8 (C_{arH}), 125.6 (C_{ar}), 120.9 (C_{arH}), 119.6 (C_{arH}), 118.1 ($\text{CH}_2=\text{}$), 102.2 (C_{arH}), 71.4 (CH), 60.2 (CH), 58.1 (OCH_3), 55.3 (CH_2), 54.3 (CH), 46.4 (CH_2), 39.6 (CH_2), 38.93 (CH), 35.0 (CH_2), 28.8 (CH), 25.5 (CH_2), 21.7 (CH_2). MS (ESI, positive): 552.4 [$\text{M}+\text{H}$] $^+$.



SO 10 (SO for CSP 7): 86 % yield, colorless crystals. $^1\text{H-NMR}$ [CD_3OD]: δ = 8.63 (d, 1H), 7.85 (d, 1H), 7.72 (d, 1H), 7.31 (m, 2H), 7.27 (d, 2H), 7.20 (t, 2H), 7.11 (t, 1H), 6.87 (s, 1H), 5.58 (m, 1H), 5.09 (d, 1H), 4.95 (d, 1H), 4.87 (d, 1H), 3.78 (s, 3H), 3.68 (t, 1H), 3.47 (t, 1H), 3.40 (t, 1H), 3.33 (dt, 1H), 3.20 (t, 1H), 3.18-3.12 (m, 1H), 3.07-3.01 (m, 1H), 2.53 (s, 1H), 2.14-2.00 (m, 2H), 1.94 (s, 1H), 1.73 (m, 1H), 1.52 (t, 1H). $^{13}\text{C-NMR}$ [CD_3OD]: δ = 161.2 (C_{ar}), 155.9 ($\text{C}=\text{O}$), 147.8 (C_{arH}), 145.0 (C_{ar}), 144.7 (C_{ar}), 143.3 (C_{ar}), 139.3 ($\text{CH}=\text{}$), 131.1 (C_{arH}), 130.8 (C_{arH}), 129.7 (C_{arH}), 129.1 (C_{arH}), 127.9 (C_{ar}), 125.3 (C_{arH}), 121.1 (C_{arH}), 117.8 ($\text{CH}_2=\text{}$), 102.9 (C_{arH}), 71.5 (CH), 60.3 (CH), 58.3 (OCH_3), 56.2 (CH_2), 54.5 (CH), 50.3 (CH), 45.6 (CH_2), 38.6 (CH), 28.4 (CH), 25.2 (CH_2), 21.0 (CH_2). MS (ESI, positive): 552.4 [$\text{M}+\text{H}$] $^+$.



SO 11 (SO for CSP 8): 50 % yield, brownish crystals. $^1\text{H-NMR}$ [CD_3OD]: δ = 8.69 (d, 1H), 7.95 (d, 1H), 7.62 (d, 1H), 7.54 (d, 1H), 7.42 (d, 1H), 7.09 (s, 1H), 6.26 (h, 1H), 5.27 (d, 1H), 3.99 (s, 3H), 3.95 (m, 1H), 3.71 (m, 1H), 3.61 (m, 1H), 3.21-3.14 (m, 2H), 3.01(m, 2H), 2.95(m, 2H), 2.64(dd, 1H), 2.41 (m, 1H), 1.98 (s, 1H), 1.82 (m, 3H), 1.46 (m, 1H), 0.88 (d, 3H), 0.85 (d, 3H). $^{13}\text{C-NMR}$ [CD_3OD]: δ = 160.3 (C_{ar}), 156.9 ($\text{C}=\text{O}$), 147.9 (C_{arH}), 145.0 (C_{ar}), 144.3 (C_{ar}), 139.4 ($\text{CH}=\text{}$), 131.5 (C_{arH}), 127.7 (C_{ar}), 124.2 (C_{arH}), 119.6 (C_{arH}), 117.6 ($\text{CH}_2=\text{}$), 102.3 (C_{arH}), 72.0 (CH), 60.1 (CH), 57.1 ($\text{CH}_2\text{SO}_3\text{H}$), 55.6 (OCH_3), 55.2 (CH), 54.5 (CH_2), 50.8 (2CH_2), 50.4 (CH_2), 39.2 (CH), 33.5 (CH), 29.2 (CH_3), 24.6 (CH_2), 21.2 (CH_2), 19.7 (CH_3), 18.3 (CH_3). MS (ESI, positive): 518.4 [$\text{M}+\text{H}$] $^+$.

3. References

- [1] C.V. Hoffmann, R. Pell, M. Lämmerhofer, W. Lindner, *Anal. Chem.*, 80 (2008) 8780-8789.
- [2] N. Chen, W. Jia, J. Xu, *European Journal of Organic Chemistry*, 2009 (2009) 5841-5846.
- [3] C.V. Hoffmann, R. Reischl, N.M. Maier, M. Lämmerhofer, W. Lindner, *Journal of Chromatography A*, 1216 (2009) 1147-1156.

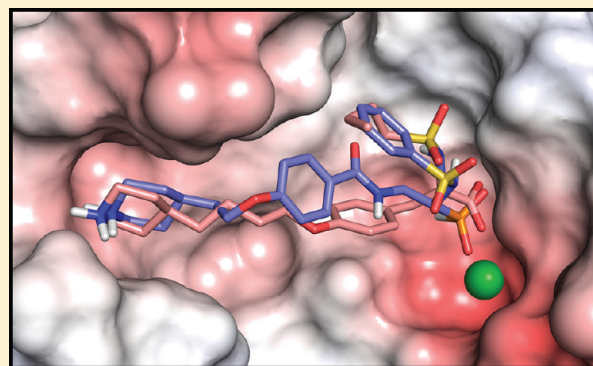
APPENDIX VI

Tailoring of Integrin Ligands: Probing the Charge Capability of the Metal Ion-Dependent Adhesion Site

Markus Bollinger,[†] Florian Manzenrieder,[†] Roman Kolb,[†] Alexander Bochen,[†] Stefanie Neubauer,[†] Luciana Marinelli,[‡] Vittorio Limongelli,[‡] Ettore Novellino,[‡] Georg Moessmer,[§] Reinhard Pell,^{||} Wolfgang Lindner,^{||} Joseph Fanous,[⊥] Amnon Hoffman,[⊥] and Horst Kessler^{*,†,@}[†]Institute for Advanced Study and Center of Integrated Protein Science, Department Chemie, Technische Universität München, Lichtenbergstrasse 4, 85747 Garching, Germany[‡]Dipartimento di Chimica Farmaceutica e Tossicologica, Università di Napoli "Federico II", Via D. Montesano, 49-80131 Napoli, Italy[§]Institut für Klinische Chemie und Pathobiochemie, Klinikum rechts der Isar, Technische Universität München, Ismaninger Strasse 22, 81675 München, Germany^{||}Institute of Analytical Chemistry, University of Vienna, Währinger Strasse 38, A-1090 Vienna, Austria[⊥]School of Pharmacy, Faculty of Medicine, The Hebrew University of Jerusalem, P.O. Box 12065, Jerusalem 91120, Israel[@]Chemistry Department, Faculty of Science, King Abdulaziz University, P.O. Box 80203, Jeddah 21589, Saudi Arabia

Supporting Information

ABSTRACT: Intervention in integrin-mediated cell adhesion and integrin signaling pathways is an ongoing area of research in medicinal chemistry and drug development. One key element in integrin–ligand interaction is the coordination of the bivalent cation at the metal ion-dependent adhesion site (MIDAS) by a carboxylic acid function, a consistent feature of all integrin ligands. With the exception of the recently discovered hydroxamic acids, all bioisosteric attempts to replace the carboxylic acid of integrin ligands failed. We report that phosphinates as well as monomethyl phosphonates represent excellent isosters, when introduced into integrin antagonists for the platelet integrin $\alpha\text{IIb}\beta\text{3}$. The novel inhibitors exhibit *in vitro* and *ex vivo* activities in the low nanomolar range. Steric and charge requirements of the MIDAS region were unraveled, thus paving the way for an *in silico* prediction of ligand activity and in turn the rational design of the next generation of integrin antagonists.



INTRODUCTION

Integrin signaling is profoundly implicated in numerous physiological processes, such as tissue remodeling or angiogenesis, as well as in important pathological disorders such as thrombosis, cancer, osteoporosis, and autoimmune diseases. Because of their biological relevance in many diseases, integrins represent highly important targets for medicinal chemistry.^{1,2} From a structural point of view, integrins are heterodimers of a noncovalently linked α -subunit and a β -subunit. Each domain is composed of an extracellular domain, a single membrane-spanning helical domain, and a short cytoplasmic tail. The β -subunit contains a metal ion-dependent adhesion site (MIDAS) in the ligand binding domain.^{3–5} Among the 24 known integrins, a number of them, known as the RGD-dependent integrins, recognize the tripeptide sequence arginine-glycine-aspartic acid (RGD) of extracellular matrix (ECM) proteins (e.g., fibronectin for $\alpha\text{5}\beta\text{1}$, fibrinogen for platelet integrin $\alpha\text{IIb}\beta\text{3}$, and vitronectin for $\alpha\text{v}\beta\text{3}$ and other αv integrins) or other ligands, such as ADAMs, snake venoms, or viruses

(FMD).^{1,6,7} Constraining and mimicking RGD has successfully been used to develop thousands of integrin ligands, all containing an essential carboxylate moiety as a metal-coordinating group in the MIDAS. Recently, we found hydroxamic acids as a first potent isosteric replacement of the carboxylic group in integrins $\alpha\text{v}\beta\text{3}$ and $\alpha\text{5}\beta\text{1}$.⁸ The known tendency of phosphate groups to coordinate bivalent metal ions (calcium, manganese, or magnesium) prompted us to develop new phosphorus-containing integrin ligands with the aim of unraveling the steric and electrostatic requirements of the MIDAS region and obtaining significant new insights into the binding mode of integrins for further optimizing integrin ligands.

To date, extensive efforts have been made to discover and develop integrin antagonists for clinical applications. However, only for three integrins⁹ ($\alpha\text{IIb}\beta\text{3}$, $\alpha\text{4}\beta\text{1}$, and $\alpha\text{L}\beta\text{2}$), of the 24

Received: October 14, 2011

Published: December 19, 2011

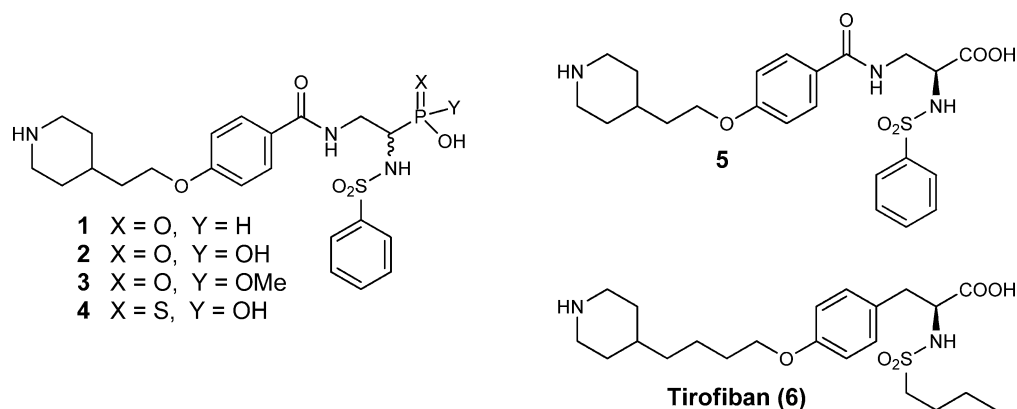
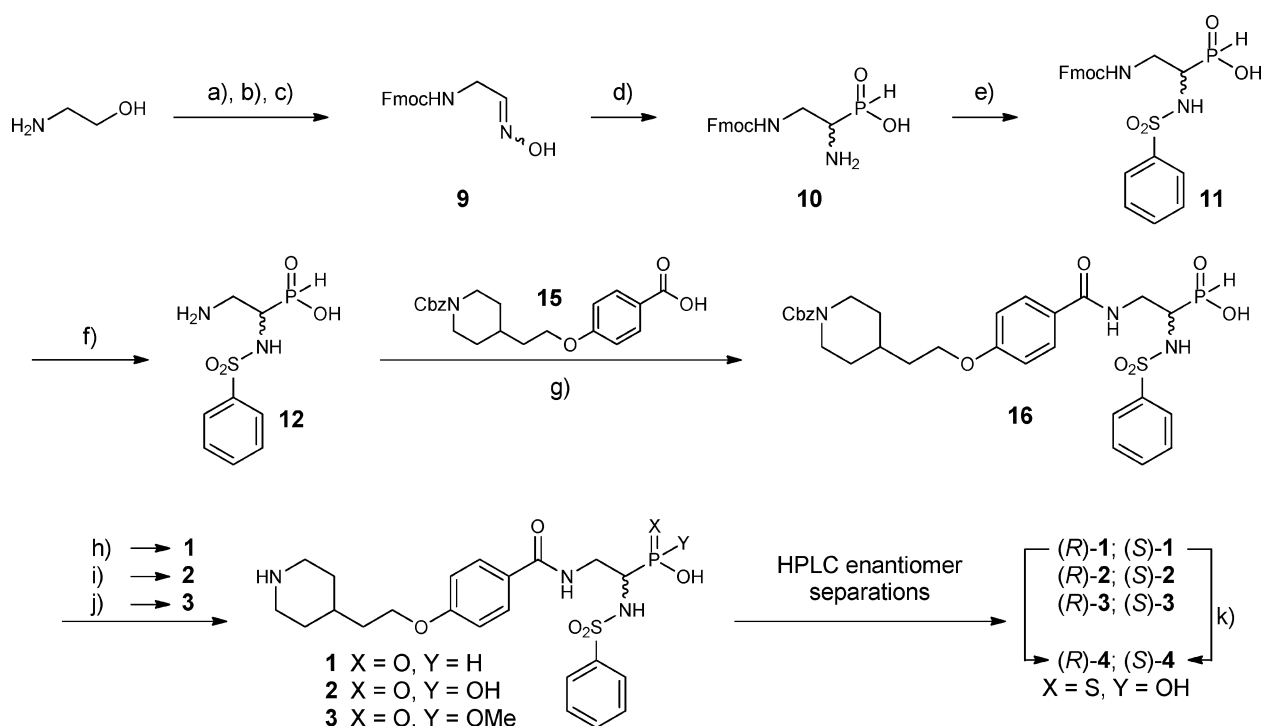


Figure 1. Bioisosteric replacement of the carboxylic MIDAS binding motif for the development of new α IIb β 3 integrin antagonists: phosphonic acid **1**, phosphonic acid **2**, monomethyl phosphonic acid **3**, thiophosphonic acid **4**, tirofiban analogue **5**, and tirofiban **6**.

Scheme 1. Synthesis of Integrin Ligands **1–4**^a

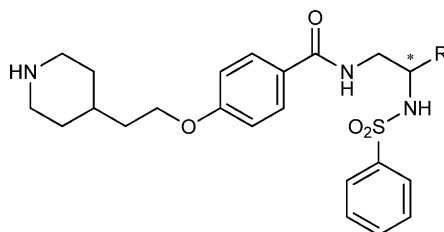


^a(a) Fmoc-Cl, 10% Na₂CO₃, room temperature (RT), 2 h; (b) IBX, DMSO, RT, 16 h; (c) NH₂OH·HCl, DIEA, DCM, RT, 16 h; (d) anhydrous crystalline H₃PO₂, MeOH, reflux, 4 h; (e) PhSO₂Cl, 10% Na₂CO₃, dioxane, RT, 3 h; (f) 20% piperidine/DMF, RT, 2 h; (g) HATU, DIEA, DMF, RT, 16 h; (h) TFA/H₂O/TIPS, RT, 16 h; (i) (1) BSA, air, DCM, RT, 1 h; (2) TFA/H₂O/TIPS, 16 h; (j) (1) BSA, air, DCM, RT, 1 h; (2) EDC·HCl, DMAP, MeOH, RT, 1 h; (3) TFA/H₂O/TIPS, 16 h; (k) BSA, sulfur, DCM, RT, 1 h. All compounds were purified by RP-HPLC (for more details, see the Supporting Information).

known, have small molecular ligands been approved as drugs. Candidates for other integrins, such as α v β 3, are in clinical phase III trials.¹⁰ In contrast, significant advances have been made in targeting platelet integrin α IIb β 3.^{9,11} In fact, the α IIb β 3 integrin inhibitor tirofiban¹² is being successfully used in acute antithrombotic therapy,^{12–14} thus, inhibition of this receptor is now a validated way of inhibiting fibrinogen-dependent platelet aggregation.

In this work, integrin antagonists **1–4** (Figure 1) were developed on the basis of tirofiban analogue **5** (Figure 1) previously described by Duggan et al.¹⁵ Compounds **1–4** allow us to explore the sensitivity of the MIDAS region for coordination of differently charged groups. Synthetic methods

for obtaining the desired compounds **1–4** have been developed (Scheme 1). Enantiomers due to the chiral center in α -position of the phosphorus-containing group were resolved via chromatography on chiral columns and tested independently. The ability of the novel ligands to inhibit the binding of integrin α IIb β 3 to its corresponding ECM protein fibrinogen was tested in a competitive ELISA, and the efficacy of the most active compounds was proven in ex vivo experiments. To understand the dependency of the charge of the metal-coordinating group and the corresponding biological activities, we studied the protonation states of compounds **1–4** by means of extensive theoretical calculations and ³¹P NMR titration experiments. The combination of ab initio calculations and molecular

Table 1. Biological Evaluation of Activities of Ligands 1–6 on Integrin α IIb β 3

compd	R	IC ₅₀ ^a (nM) (α IIb β 3)	EC ₅₀ ^b (nM) (α IIb β 3)
(R)-1	PHOOH	1.2 ± 0.06	7.8 ± 0.9
(S)-1		6.3 ± 0.73	
(R)-2	PO(OH) ₂	22.7 ± 2.7	276 ± 15.6
(S)-2		136 ± 10.7	
(R)-3	PO(OH)(OMe)	3.3 ± 0.4	40.8 ± 1.9
(S)-3		1154 ± 272	
(R)-4	PS(OH) ₂	62.5 ± 6.0	
(S)-4		1322 ± 498	
(S)-5	COOH	0.81 ± 0.05	
(R)-5		4.4 ± 0.3	
6	tirofiban	0.95 ± 0.09	13.6 ± 3.3

^aIC₅₀ values were derived from a competitive ELISA using immobilized fibrinogen and soluble integrin α IIb β 3. ^bEffective concentrations (EC₅₀) of some key compounds for inhibition of platelet aggregation were derived from aggregation measurements using multiple-electrode aggregometry in hirudin-anticoagulated TRAP-6-activated blood.

docking simulations has defined the binding modes of the new ligands **1** and **2** identifying the molecular requisites for achieving a high inhibitory activity, and on the basis of these, a prediction of the activity of **3** and **4** was successfully executed.

CHEMISTRY

To prepare compounds **1**–**4**, two major fragments (**12** and **15**) were connected via an amide bond (Scheme 1). For the synthesis of **12**, commercially available 2-aminoethanol was Fmoc-protected followed by oxidation with IBX.^{16,17} The corresponding aldehyde **8** was converted with hydroxylamine hydrochloride in DCM to oxime **9** in high yield.¹⁸ Refluxing oxime **9** with anhydrous crystalline phosphinic acid in dry methanol resulted in racemic phosphinate intermediate **10**,^{18,19} which was sulfonated upon treatment with phenylsulfonyl chloride in aqueous Na₂CO₃ to provide Fmoc-protected derivative **11**. Fmoc deprotection and purification by reverse-phase high-performance liquid chromatography (RP-HPLC) afforded fragment **12** as a racemic mixture.

The second fragment containing the arginine mimic as a piperidine moiety had already been described by Duggan et al.¹⁵ Herein, Cbz protection was used instead of the more acid labile Boc group, to avoid any deprotection of the secondary amine during synthesis. Furthermore, during purification of **13**, the Cbz group allows UV detection. 2-[N-(Benzyloxycarbonyl)-piperidin-4-yl]ethanol (**13**) was coupled to methyl-4-hydroxybenzoate via Mitsunobu reaction with tributylphosphine and 1,1'-(azodicarbonyl)dipiperidine.^{20,21} Saponification of methyl ester **14** gave benzoic acid derivative **15**. Activation of **15** by use of O-(7-azabenzotriazol-1-yl)-N,N,N',N'-tetramethyluronium hexafluorophosphate (HATU) and subsequent condensation with **12** gave Cbz-protected precursor **16**.

Deprotection of **16** with trifluoroacetic acid yielded molecular probe **1**, while the conversion of phosphinic acid **16** to the bis(trimethylsilyl)phosphonite intermediate, which was oxidized by atmospheric oxygen, afforded after Cbz deprotection phosphonic acid ligand **2** in high yield. When

this process was applied to **1** and an excess of sulfur was added, thiophosphonic acid **4** was obtained. Furthermore, Cbz-protected phosphonic acid **2** undergoes rapid monoesterification at room temperature in the presence of N-[3-(dimethylamino)propyl]-N'-ethylcarbodiimide (EDC) and 2 equiv of 4-dimethylaminopyridine (DMAP) in dry methanol. Without DMAP, the reaction results in exclusive formation of the dimethyl ester and no desired product **3** is observed.

We decided to synthesize all molecular probes as racemic mixtures, as “libraries of enantiomers”. However, for a more detailed biological evaluation, it was necessary to determine the activity of the optically pure compounds.

Enantiomer separation was successfully performed on quinine-based chiral zwitterionic ion-exchange-type stationary phases developed by Hoffmann et al.²² Here, a sulfonic acid derivative of quinine served as a zwitterionic chiral selector.²³ The concept of the resolution of the racemic ampholytes, as compounds **1**–**3** can be classified, is based on a simultaneous ion pair formation of the zwitterionic chiral selector motif of the chiral stationary phase with the individual enantiomers of the analytes. These two diastereomerically behaving selector–(R)-enantiomer and selector–(S)-enantiomer associates are the basis for the enantiomer separations.²² The preference and magnitude of molecular recognition and chiral discrimination are based on the stereochemical properties of the chiral selector and the ampholytes that include additional intermolecular interaction sites like hydrogen bonding and π – π interactions that determine the overall chromatographic enantioselectivity and elution order.

For N-acyl-protected amino acid-type analytes with known absolute configurations, we formulated a general model of intermolecular interactions and chromatographic elution order that correlates with the absolute configuration of the α -carbon of an α -amino acid.^{24,25} Accordingly, we assigned the stereocenter of compounds **1**–**3**, taking into account the isosteric behavior of the analytes and the Cahn–Ingold–Prelog

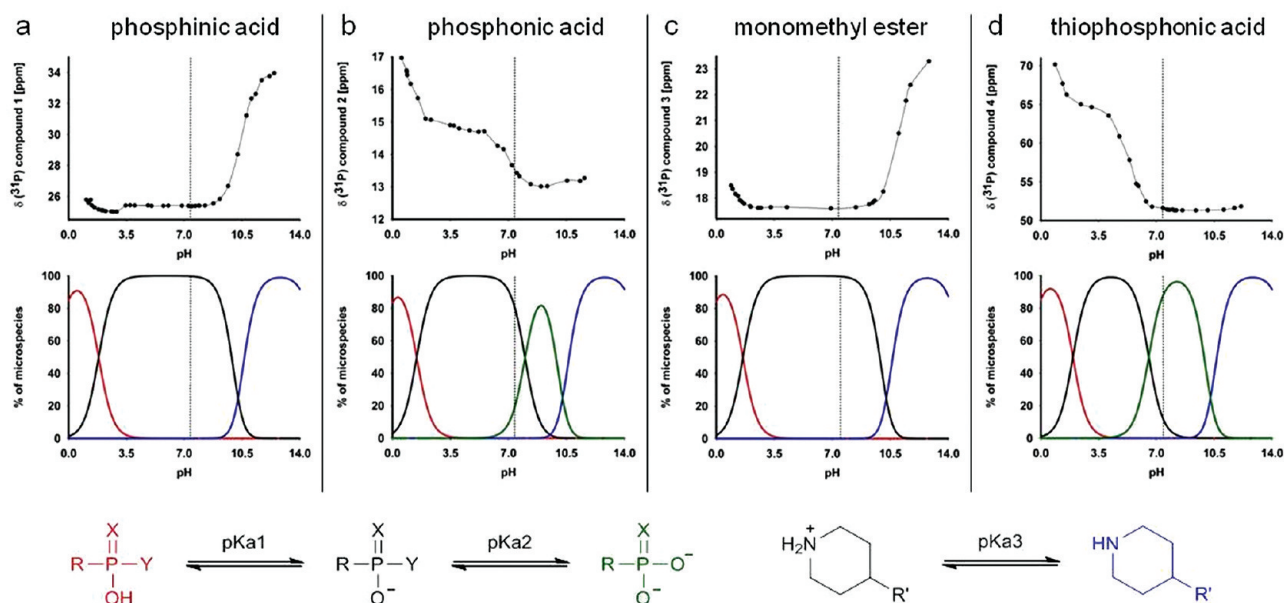


Figure 2. Assessing the protonation state of the molecular probes. Comparison of ^{31}P NMR titration curves (top) and computed microspecies distributions (middle) for molecular probes 1–4 (a–d, respectively). The physiological pH of 7.2 is shown as a dotted line to highlight the presence of either a single protonation state [horizontal line for 1 (a), 3 (c), and 4 (d)] or two protonation states [descending line for 2 (b)]. In the calculated microspecies distribution (bottom), structures of the most dominant protonation states are shown. The dotted line and the intersection with the presentation of microspecies represent the protonation states at the physiological pH of 7.2.

(CIP) convention (for more details, see the Supporting Information).

RESULTS

In Vitro Inhibition of Integrin $\alpha\text{IIb}\beta_3$. To validate the inhibition properties of the compounds against $\alpha\text{IIb}\beta_3$, a competitive ELISA ($\alpha\text{IIb}\beta_3$ fibrinogen assay) was performed using soluble integrin $\alpha\text{IIb}\beta_3$ and the immobilized natural ligand fibrinogen.^{28,27} The clinically used $\alpha\text{IIb}\beta_3$ inhibitor tirofiban was used as an internal control (Table 1, IC_{50}).

Carboxylic acid (S)-5 is similar in potency to tirofiban (6), whereas the (R)-configuration is 6 times less active (0.8 nM vs 4.4 nM). Isosteric replacement of the carboxylic acid with a phosphonic acid results in retained activity depending on its relative configuration [1.2 nM for (R)-1 and 6.3 nM for (S)-1]. However, the phosphonic acid derivatives 2 are 20 times less active [22.7 nM for (R)-2 and 136 nM for (S)-2] than phosphonic acid 1, clearly indicating that additional negative charge is not well tolerated in the MIDAS. Being aware that phosphonic acid 2 might exist in several different protonation states at the given pH, we used thiophosphonic acid 4 as a molecular probe existing only in the double-negative protonation state (Figure 2). The higher IC_{50} of 4 [62.5 nM for (R)-4 and 1322 nM for the less favored (S)-4 enantiomer] indicates that the additional charge in phosphonates and thiophosphonates reduces the binding affinity for the MIDAS. To further prove and underline this concept, we evaluated monomethyl ester 3 of phosphonic acid 2, resulting in the elimination of the additional negative charge. The (R)-3 phosphonic methyl ester regains nearly all of the activity (3.3 nM) compared to the phosphonic acid (R)-1, whereas the (S)-3 methyl ester is far less potent (1154 nM). This could indicate a steric hindrance by the methyl group pointing toward the binding pocket. Similar indications were obtained from the docking calculations (for more details, see the Supporting Information).

Platelet Aggregation in Whole Blood. In an attempt to compare the potencies of binding of various compounds to isolated platelet integrin $\alpha\text{IIb}\beta_3$ (IC_{50}) with their predicted inhibitory potency for the complex biological process of platelet aggregation, the effects of synthetic ligands (R)-1, (R)-2, (R)-3, and tirofiban on ex vivo platelet aggregation were assessed using impedance-based platelet aggregometry^{28,29} in hirudin-anticoagulated TRAP-6-activated whole blood (Table 1, EC_{50}). Phosphonic acid (R)-1 was found to behave like tirofiban in terms of platelet aggregation inhibition, whereas phosphonic acid derivative (R)-2 was ~20 times less potent. Phosphonic methyl ester (R)-3 showed intermediate efficacy. There is a very good correlation between the inhibitory potencies of compounds in the ELISA (IC_{50}) and their inhibitory potencies in the platelet aggregation assay (EC_{50}).

In Vitro Permeability Study. We have tested pharmacokinetic properties (including disposition and membrane permeability) of ligands 1–3 and tirofiban (6) by evaluating their permeability properties with an enterocyte monolayer derived from human colonic carcinoma cells (Caco-2 model).³⁰ This model is commonly used to predict the degree of intestinal permeability of therapeutic compounds as well as to gain a certain indication regarding their likelihood of penetrating the brain. The results could not differentiate between the permeability properties of the four compounds in cases where all of them exhibit poor permeability properties ($P_{\text{app}} < 1 \times 10^{-8}$ cm/s). It should be noted that the permeability of mannitol (positive control) used in this study was 2.4×10^{-6} cm/s. The permeability mechanism of mannitol is paracellular, using the pores between the cells (tight junctions), with no transcellular component. The fact that all of the tested tirofiban analogues had significantly lower permeability values indicates that the charged moiety of these analogues (at physiological pH, 7.2) restricted the paracellular transport properties in an effective manner. However, to validate this argument, we prepared the corresponding dimethyl ester of 2 [inactive in the

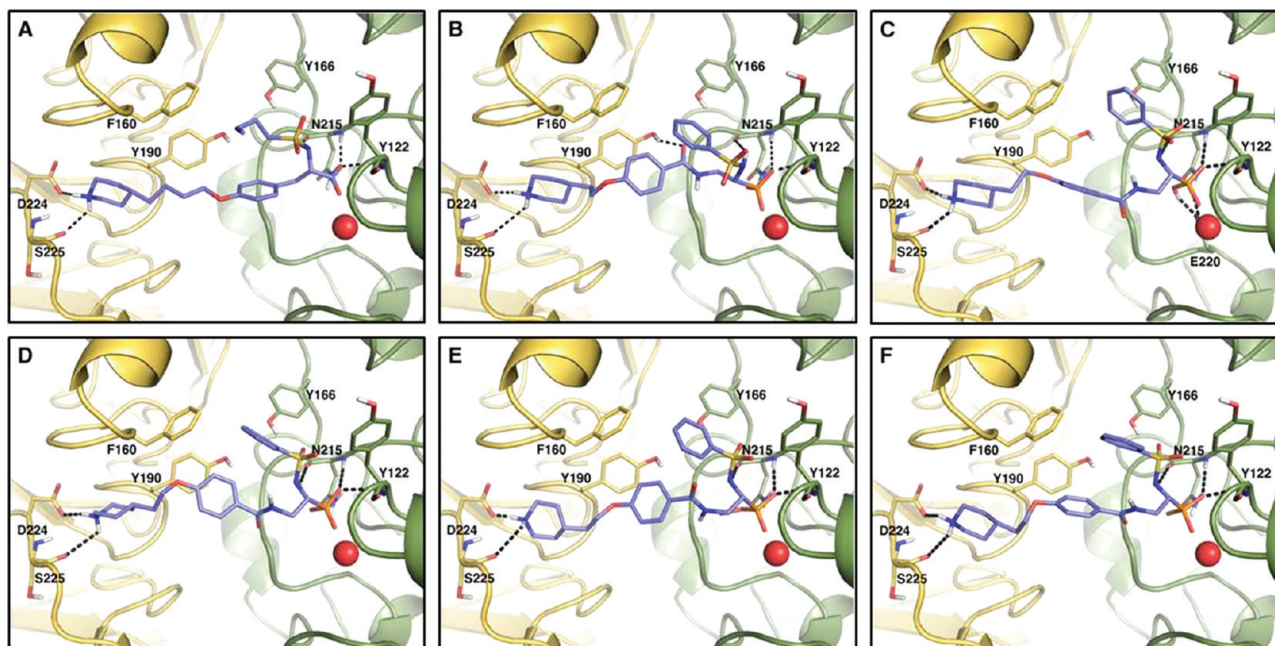


Figure 3. Modes of binding of tirofiban (A), (R)-1 (B), (R)-2 in the overall neutral form (C) and in the overall anionic form (D), (R)-3 (E), and (R)-4 (F). The α IIb domain is displayed as a yellow cartoon, while the β 3 domain is colored green. The interacting residues and the ligands are shown as licorice, while the magnesium ion is represented as a red sphere. For the sake of clarity, only the polar hydrogens are displayed. The stereoview version of each complex is provided in Figure S3 of the Supporting Information.

α IIb/ β 3 fibrinogen assay (data not shown) and tested its permeability. Unfortunately, this compound also exhibited poor permeability.

Assessment of the Protonation State of 1–4. To elucidate the molecular properties responsible for the different activity profiles of the investigated compounds (Table 1) and the mechanism of recognition between the inhibitors and the α IIb/ β 3 integrin receptor (see the docking section), we conducted an extensive computational study. First, the protonation states of compounds 1–4 were computed for each compound, and the distribution of microspecies between pH 0 and 14 was calculated with the Marvin Sketch package. The results were validated via titration experiments monitored by ^{31}P NMR chemical shifts that are very sensitive to ionization state^{31–35} (Figure 2; for more details, see the Supporting Information).

While 1 and 3 are characterized by two pK_a values, corresponding to the acidities of the phosphorus acid moiety (pK_{a1}) and the piperidinium group (pK_{a3}), for 2 and 4 a total of three pK_a values are found [phosphonic and thiophosphonic acid (pK_{a1} and pK_{a2} , respectively) and piperidinium group (pK_{a3})]. The experimental as well as the calculated (in parentheses) pK_a values show that at the physiological pH of 7.2 all piperidine moieties are protonated with pK_{a3} values of 10.44 (10.48) for 1, 10.06 (10.48) for 2, 11.02 (10.57) for 3, and 12.03 (10.58) for 4. Furthermore, the first acid functionality of the phosphorus unit (pK_{a1}) of all compounds 1–4 is present in the completely deprotonated form at pH 7.2 with pK_{a1} values of greater than 1.56 (1.90) for 1, 1.01 (1.63) for 2, 1.13 (1.63) for 3, and 1.27 (1.94) for 4. All in all, we found that the experimental NMR results fully corroborate the trends in the computational calculations.

At the physiological pH of 7.2, the piperidine moiety (pK_{a3}) of 1 is protonated and the phosphinate group (pK_{a1}) is fully deprotonated (Figure 2a). For 2, two microspecies can be

found at physiological pH, both having a protonated piperidine unit; however, in one case, the phosphonic acid is monoanionic ($\sim 86\%$ in silico and 63% in vitro), and in the other case, it is in the dianionic form ($\sim 14\%$ in silico and 37% in vitro) (Figure 2b). To further investigate the effect of the charge of the different substituents on the phosphorus atom, two more molecular probes, 3 and 4, were studied. In particular, the thiophosphonate group of compound 4, like the phosphonate group of 2, coexists at neutral pH as mono- and dianionic species, but a shift toward the dianionic form ($\sim 82\%$ in silico and 99% in vitro) was observed (Figure 2d). The in vitro measurements showed that the second acid functionality (pK_{a2}) of compounds 2 and 4 is more acidic than calculated. For 2 a pK_{a2} of 6.97 (7.99) and for 4 a pK_{a2} of 5.27 (6.53) can be extracted from the obtained data points. Compound 3, like 1, possesses only one single microspecies (Figure 2c).

Molecular Docking and Electrostatic Potential Calculations of 1–4. Compounds 1–4 were docked into the α IIb/ β 3 RGD binding site with the aid of AutoDock version 4.0.^{36,37} Both enantiomers were studied. Results of the (S)-enantiomers are reported in the Supporting Information along with an explanation of the lower inhibitory potency observed for (S)-1, (S)-2, and (S)-3 with respect to those of the corresponding (R)-enantiomers.

As for (R)-1, in accordance with the protonation state assessment (Figure 2a), only the neutral ligand form (piperidine moiety protonated, phosphinate deprotonated) was used for docking simulations. As a result, a binding mode highly similar to that of tirofiban was observed (Figure 3A,B and Figure S2 of the Supporting Information). In fact, the phosphinate group coordinates the magnesium ion occupying in the MIDAS the same region that hosts the carboxylate group of tirofiban. In particular, one of the oxygen atoms coordinates the metal, while the other one engages two H-bonds with the backbone NH groups of (β 3)-Asn215 and (β 3)-Tyr122, like

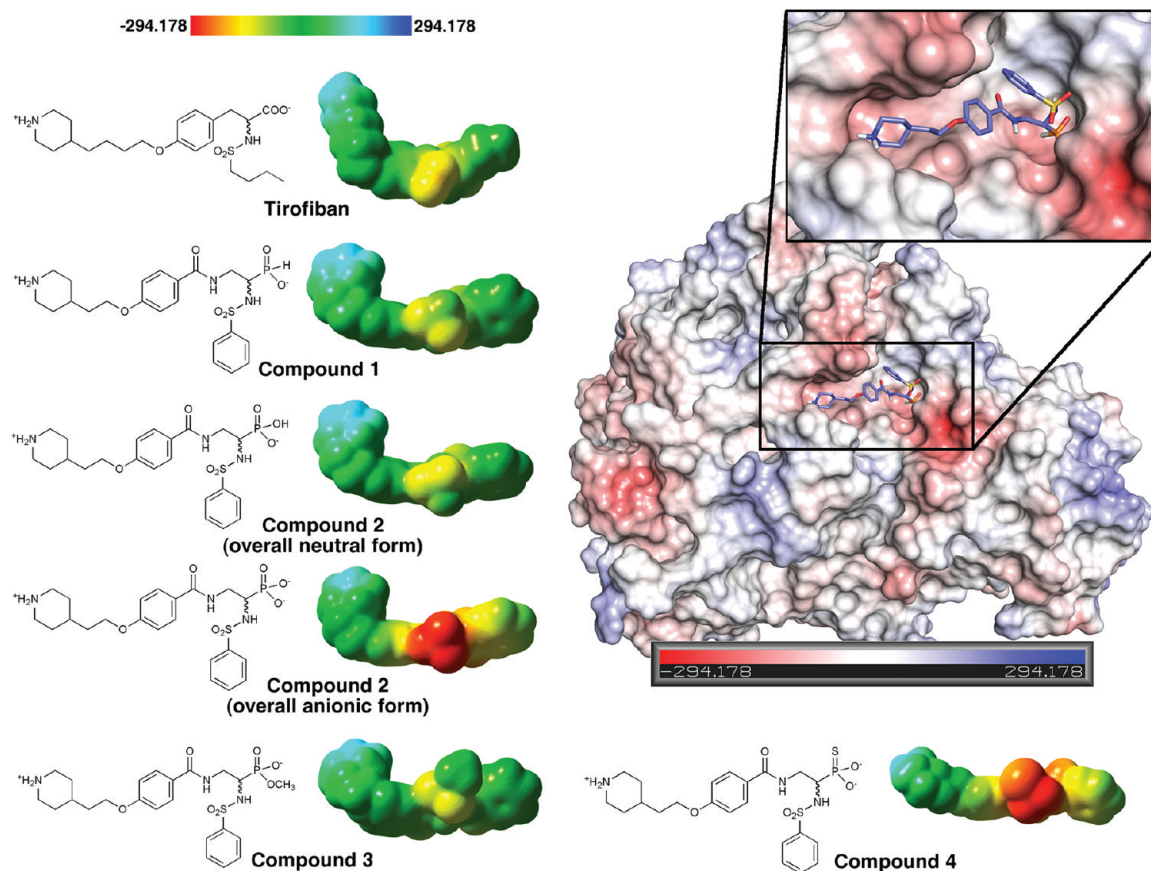


Figure 4. Electrostatic potential mapped onto the molecular surface of tirofiban, 1, 2 in the overall neutral form and in the anionic form, 3, and 4. At the top right, the electrostatic surface of the integrin $\alpha\text{IIb}\beta\text{3}$ binding site complexed with compound (R)-1 is shown. Both for ligands and for the protein, the scale of the electrostatic potential ranges from -294.178 (red) to 294.178 (blue) $k_B T/e_-$.

tirofiban in $\alpha\text{IIb}\beta\text{3}$ and Cilengtide in $\alpha\text{v}\beta\text{3}$ [Protein Data Bank (PDB) entries 2vdm and 1L5G]. The benzenesulfonamide moiety forms H-bonds with the (β3)-Asn215 backbone CO group, while the phenyl ring occupies the aromatic pocket formed by (αIIb)-Phe160, (αIIb)-Tyr190, and (β3)-Tyr166. The aromatic ring of the *p*-hydroxybenzoate scaffold is close enough to form a π - π interaction with (αIIb)-Tyr190, the hydroxyl group of which is involved in an H-bond interaction with the inhibitor amide CO group. This allows the piperidine moiety to point toward the αIIb subunit, where the protonated nitrogen group makes a salt bridge interaction with the (αIIb)-Asp224 side chain and an H-bond with the (αIIb)-Ser225 backbone CO group. All these favorable interactions are certainly responsible for the low nanomolar activity of (R)-1 toward the $\alpha\text{IIb}\beta\text{3}$ receptor.

Because phosphonic acid 2 is present at the physiological pH of 7.2 both in the monoanionic form and in the dianionic form (Figure 2b), docking calculations for (R)-2 were performed for both protonation states, and the results showed a binding conformation similar to that of tirofiban and (R)-1 (Figure 3C,D). This suggests that although the phosphonic group is bulkier than the phosphinate moiety, it can fit in the MIDAS region. Nevertheless, because (R)-2 shows reduced activity compared to that of (R)-1 (Table 1), reasons different from the steric hindrance should be responsible for the experimentally observed lower activity. In this regard, it has to be clarified that all docking algorithms, either based on classical force fields³⁸ or based on empirical free energy scoring functions³⁹ or knowledge-based scoring functions,⁴⁰ cannot accurately predict

properties like the exact metal coordination geometry or particular charge effects. Thus, to overcome this limitation and to shed light on the different activity profiles of (R)-1 and (R)-2, more accurate computational techniques must be used. Recent progress made in the force field parametrization of bivalent ions⁴¹ and some theoretical studies on a Mg^{2+} protein^{42,43} would suggest the use of molecular dynamics-based approaches to sample more accurately the specific ligand-protein interaction of each complex. Another possibility might be to perform QM/MM calculations to accurately describe the ligand-protein interaction at the binding site. Unfortunately, both these approaches are computationally time intensive and are useful for the study of only a few compounds. To perform calculations on most of the ligands of the series in a reasonable computational time, we decided to conduct quantum mechanical calculations only on the ligands, thus elucidating their different electrostatic potential profiles.

Quantum mechanical calculations revealed that (R)-1 has an electrostatic potential profile highly similar to that of tirofiban, particularly with regard to the metal-coordinating group, while (R)-2 is similar to tirofiban only in its neutral form (Figure 4). In fact, with regard to (R)-2, the electrostatic potential of the phosphonate group in the dianionic form, existing at physiological pH, is highly negative. Indeed, if on one hand this improves the coordination of the metal ion, on the other hand, it causes electrostatic repulsion effects with the surrounding atoms in the MIDAS such as the backbone CO groups of (β3)-Asn215 and (β3)-Asp217 or the (β3)-Glu220 side chain (Figures 3D and 4). Thus, our computational study

of (R)-1 and (R)-2 suggests that electrostatic properties, more than steric features, are the crucial factors for the different activities of the two compounds.

Also in the case of (R)-3 and (R)-4, it was not possible to predict the α IIb β 3 activities solely on the basis of the docking calculations (see Figure 3E,F for the predicted binding modes and the Supporting Information for further details about docking). As shown in Figure 4, the electrostatic potential profile calculated for (R)-3 is highly similar to those of tirofiban and (R)-1, while compound (R)-4, like (R)-2, has a highly negative potential localized on the thiophosphonate group (dianionic form). Those results are in perfect line with the ELISA data reported in Table 1. In fact, (R)-4 possesses a reduced activity because of the preponderance (~82% in silico and 99% in vitro) of its dianionic form, which has the less favorable electrostatic profile for its interaction with α IIb β 3. Accordingly, (R)-3 has an electrostatic potential profile and an activity comparable to those of (R)-1.

DISCUSSION

The strong binding affinity of phosphorus ligands for bivalent metal ions stimulated us to investigate those groups as pharmacophores for binding to the MIDAS region of integrins. As a proof of principle, we investigated analogues of α IIb β 3 integrin inhibitor **5**, previously described by Duggan et al.,¹⁵ which is structurally related to the drug tirofiban (**6**) and exhibits a similar binding affinity. The essential carboxyl group of **5** was modified by different phosphorus-containing groups. We found that phosphinate groups as well as a phosphonate monomethyl ester are suitable isosteres for the carboxyl group in integrin ligands while phosphonate and thiophosphonate groups could not be used for this purpose. Docking of ligands **1–4** in the α IIb β 3 receptor did not reveal substantial differences with respect to the tirofiban binding mode (Figure 3 and Figure S2 of the Supporting Information), thus excluding steric effects as a reason for different binding potencies. On the basis of ab initio studies, the high affinity of phosphinate **1** and phosphonate monomethyl ester **3** can be attributed to the lower negative charge of the ligand metal binding groups, if compared to those of **2** and **4** (Figure 4). The differences in charges among compounds **1** and **4** have been investigated both by theoretical calculations and by ³¹P NMR measurements. In phosphonate **2** and thiophosphonate **4** at neutral pH, there are considerable amounts of dianionic species in the equilibrium (Figure 2). Obviously, the high negative charge is not tolerated by the MIDAS region, which is already negatively charged (Figure 4).

The dominating charge effect is accompanied by second-order steric effects induced by substituents in α -position to the phosphorus atom expressed in the different acceptance of stereoisomers. Synthesis and the biological assays of the pure (R)- and (S)-stereoisomers of **5** reveal that the (R)-enantiomer is ~5 times less active than the (S)-enantiomer. The same general trend was found for compounds **1–4**, bearing in mind the fact that according to the CIP rules the notation in the phosphorus compounds is reversed (Table 1). Molecular docking revealed that in the case of compounds **1–4**, although the (S)-enantiomers are also able to bind the receptor, they lose a number of favorable interactions within the binding pocket, particularly in the case of phosphonic compounds (S)-**2** and (S)-**3** (see the Supporting Information for details).

In the biological evaluation of the new α IIb β 3 antagonists, we have shown that the in vitro binding affinity fully correlates

with the ex vivo prevention of platelet aggregation measured by multiple-electrode aggregometry in hirudin-anticoagulated TRAP-6-activated blood. Both assays yield the same order of activities for all tested compounds. Approximately 10-fold higher EC₅₀ values are required compared to inhibition of binding of integrin to fibrinogen (Table 1, IC₅₀).

The pharmacotherapeutic activity of tirofiban is provided following intravenous administration and is confined to the systemic blood circulation. The results of the permeability studies can be regarded as an indication that the new ligands will also be restricted to the central compartment. Thus, once administered by a parenteral route, the molecules will be distributed within the central compartment where they produce their antiplatelet aggregation activity. In case the novel analogues will be further developed for clinical use (e.g., for molecular imaging), the restricted distribution predicted for these analogues ensures minimal side effects that could be derived by interaction with peripheral tissues, including the central nervous system. Thus, the poor membrane permeability contributes to the safety profile of these analogues. Pharmacokinetically wise, the polar moieties of these analogues at the physiological pH of 7.2 did not allow passive diffusion across the biological membrane, like enterocytes. It also inhibited the transport via the tight junctions pores as evidenced by the significantly lower permeability compared to that of mannitol.

In summary, we here report a successful case of drug design on the α IIb β 3 integrin that allowed us to identify the molecular and electrostatic requisites for achieving strong α IIb β 3 inhibition. In particular, we have found that even a space-demanding group such as methyl phosphonate (R)-**3** can bind to the α IIb β 3 MIDAS without strongly affecting the activity. We have found that highly negatively charged metal-coordinating groups are not well tolerated in the α IIb β 3 MIDAS. All these findings, on one hand, are extremely useful for an easy and quick tuning of both the steric and electrostatic features of α IIb β 3 inhibitors; on the other hand, they demonstrate that docking calculations together with more rigorous computational procedures, such as ab initio studies, can be successfully used in rational design of new inhibitors active on integrin receptors different from α IIb β 3.

The modification of the carboxylate group into a phosphinate or a phosphonate monomethyl ester yields an attractive new way of optimizing integrin ligands. The successful design of non-carboxylate-containing ligands as integrin antagonists surely opens a new era in the design and finding of novel integrin ligands.

EXPERIMENTAL SECTION

All technical solvents were distilled prior to use. Dry solvents were purchased from Aldrich, Fluka, or Merck. Reactions sensitive to oxygen or water were performed in flame-dried reaction vessels under an argon atmosphere (99.996%). Fmoc-protected amino acids and coupling reagents were purchased from Novabiochem (Schwalbach, Germany), Iris Biotech GmbH (Marktredwitz, Germany), and Medalchemy (Alicante, Spain). All other chemicals and organic solvents were purchased from commercial suppliers at the highest purity available and used without further purification.

TLC monitoring was performed on Merck DC silica gel plates (60 F-254 on aluminum foil). Spots were detected by UV absorption at 254 nm and/or by staining with a 5% solution of ninhydrine in ethanol or mostain [6.25 g of phosphomolybdic acid, 2.5 g of cerium(IV) sulfate, and 15 mL of sulfuric acid in 235 mL of water] or potassium permanganate (5% in 1 N aqueous NaOH).

Flash column chromatography was performed using silica gel 60 (40–63 μm) from Merck at a pressure of 1–1.5 atm.

Analytical HPLC was performed using Amersham Pharmacia Biotech Äkta Basic 10F equipment, with a P-900 pump system, a reversed-phase YMC-ODS-A C_{18} column (12 nm pore size, 5 μm particle size, 250 mm \times 4.6 mm), and UV detection (UV-900; 220 and 254 nm). The system was run at a flow rate of 1.0 mL/min over 30 min using H_2O (0.1% TFA) and MeCN (0.1% TFA) as solvents.

Semipreparative HPLC was performed using Waters equipment: System Breeze; pump system 1525, UV detector 2487 dual (220 and 254 nm); Driver Software Breeze version 3.20; column material, YMC-ODS-A C_{18} (12 nm pore size, 5 μm particle size, 250 mm \times 20 mm), YMC-ODS-AQ C_{18} (12 nm pore size, 5 μm particle size, 250 mm \times 20 mm), or YMCbasic (proprietary, 5 μm particle size, 250 mm \times 20 mm).

HPLC–ESI-MS analyses were performed on a Hewlett-Packard Series HP 1100 system with a Finnigan LCQ mass spectrometer using a YMC-Hydrosphere C_{18} column (12 nm pore size, 3 μm particle size, 125 mm \times 2.1 mm) or a YMC-Octyl C_8 column (20 nm pore size, 5 μm particle size, 250 mm \times 2.1 mm). The system uses H_2O (0.1% formic acid) and MeCN (0.1% formic acid) as eluents.

High-resolution mass spectrometry was conducted on a Thermo Finnigan LTQ-FT (ESI-ICR) spectrometer.

^1H NMR, ^{13}C NMR, and ^{31}P NMR spectra were recorded at 295 K on 500 MHz Bruker DMX, 360 MHz Bruker AV, and a 250 MHz Bruker AV spectrometers, respectively (Bruker, Karlsruhe, Germany). Chemical shifts (δ) are given in parts per million. The following solvent peaks were used as internal standards: DMSO- d_6 , 2.50 ppm (^1H NMR) and 39.52 ppm (^{13}C NMR); CHCl_3 , 7.26 ppm (^1H NMR) and 77.16 ppm (^{13}C NMR); MeOH- d_3 , 3.31 ppm (^1H NMR) and 49.00 ppm (^{13}C NMR).⁴⁴ With MeOH- d_3 as the solvent, standard pulse sequences provided by Bruker were used to eliminate the solvent peak (watergate, P3919GP; presaturation, ZGPR). For ^{31}P NMR spectra, 85% phosphoric acid was used as an external standard.

Duggan ligand (S)-5 was synthesized according to literature procedures,¹⁵ starting from N^{β} -Fmoc-L-2,3-diaminopropionic acid. Synthesis of the corresponding (R)-enantiomer was conducted as described here, starting from N^{β} -Boc- N^{β} -Fmoc-D-2,3-diaminopropionic acid. Standard peptide coupling techniques were employed.

All yields are not optimized. The analytical data of compounds 7–18 are listed in the Supporting Information. All tested compounds were $\geq 95\%$ pure as determined by RP-HPLC (MS).

1-(Phenylsulfonamido)-2-[4-[2-(piperidin-4-yl)ethoxy]benzamido]ethylphosphonic Acid (1). A mixture of TFA, TIPS, and water [5 mL, 95:2.5:2.5 (v/v/v) TFA/TIPS/ H_2O] was added to 16 (36.0 mg, 0.057 mmol) and the mixture stirred at room temperature (RT) for 16 h. Purification by semi-preparative RP-HPLC and lyophilization gave 1 (23.5 mg, 0.047 mmol, 83%) as a white solid: ^1H NMR (500 MHz, MeOH- d_3 , RT) δ 8.53 (br s, 1 H), 8.24 (br s, 1 H), 8.10 (t, $^3J = 5.0$ Hz, 1 H), 7.83 (d, $^3J = 7.6$ Hz, 2 H), 7.66 (d, $^3J = 9.0$ Hz, 2 H), 7.42 (t, $^3J = 7.3$ Hz, 1 H), 7.37 (t, $^3J = 7.5$ Hz, 2 H), 6.93 (d, $^3J = 9.0$ Hz, 2 H), 6.83 (d, $^1J = 531.3$ Hz, 1 H), 4.11 (t, $^3J = 6.2$ Hz, 2 H), 3.66–3.48 (m, 3 H), 3.43–3.34 (m, 2 H), 3.07–2.87 (m, 2 H), 2.11–1.94 (m, 2 H), 1.96–1.84 (m, 1 H), 1.80 (dt, $^3J = 6.3$ Hz, $^3J = 6.3$ Hz, 2 H), 1.46 (dt, $^3J = 14.9$ Hz, $^3J = 3.9$ Hz, 2 H); ^{13}C NMR (126 MHz, MeOH- d_3 , RT) δ 169.9, 163.2, 142.6, 133.6, 130.4, 130.2, 128.0, 127.5, 115.2, 66.6, 54.9 (d, $^1J_{\text{PC}} = 99$ Hz), 45.5, 39.4 (d, $^2J_{\text{PC}} = 5$ Hz), 36.2, 32.4, 30.1; ^{31}P NMR (101 MHz, $\text{D}_2\text{O}/\text{H}_2\text{O}$, RT) δ 25.4 (pH 7.3); MS (ESI) m/z 430.2 [M – P(OH) $_2$] $^+$, 496.2 [M + H] $^+$, 518.2 [M + Na] $^+$, 991.1 [2M + H] $^+$, 1013 [2M + Na] $^+$, 1029.2 [2M + K] $^+$; RP-HPLC $t_R = 10.5$ min (10–90% in 30 min); HRMS (ESI) m/z calcd for $\text{C}_{22}\text{H}_{31}\text{N}_3\text{O}_6\text{P}^{32}\text{S}$ 496.1671 [M + H] $^+$, found 496.1665.

1-(Phenylsulfonamido)-2-[4-[2-(piperidin-4-yl)ethoxy]benzamido]ethylphosphonic Acid (2). A mixture of TFA, TIPS, and water [5 mL, 95:2.5:2.5 (v/v/v) TFA/TIPS/ H_2O] was added to 17 (24.1 mg, 0.037 mmol) and the mixture stirred at RT for 16 h. Purification by semipreparative RP-HPLC and lyophilization gave 2 (15.0 mg, 0.029 mmol, 79%) as a white solid: ^1H NMR (500 MHz, MeOH- d_3 , RT) δ 8.47 (br s, 1 H), 8.18 (br s, 1 H), 8.12–8.05 (m, 1

H), 7.84 (d, $^3J = 7.4$ Hz, 2 H), 7.70 (d, $^3J = 8.9$ Hz, 2 H), 7.49–7.32 (m, 3 H), 6.95 (d, $^3J = 8.9$ Hz, 2 H), 4.13 (t, $^3J = 6.0$ Hz, 2 H), 3.96–3.85 (m, 1 H), 3.73–3.62 (m, 1 H), 3.55–3.44 (m, 1 H), 3.43–3.35 (m, 2 H), 3.07–2.93 (m, 2 H), 2.08–1.99 (m, 2 H), 1.98–1.87 (m, 1 H), 1.82 (dd, $^3J = 12.4$ Hz, $^3J = 6.1$ Hz, 2 H), 1.51 (m, 2 H); ^{13}C NMR (126 MHz, $\text{D}_2\text{O}/\text{CD}_3\text{CN}/\text{NaOH}$, RT) δ 167.7, 160.9, 141.4, 131.5, 128.6, 128.5, 125.6, 125.2, 113.7, 65.5, 52.1 (d, $^1J = 134$ Hz), 44.8, 41.5 (d, $^2J = 5$ Hz), 35.1, 32.1, 31.8; ^{31}P NMR (101 MHz, $\text{D}_2\text{O}/\text{H}_2\text{O}$, RT) δ 13.7 (pH 7.2); MS (EI) m/z 430.1 [M – PO(OH) $_2$] $^+$, 494.3 [M – OH] $^+$, 512.2 [M + H] $^+$, 1023.1 [2M + H] $^+$, 1045.1 [2M + Na] $^+$; RP-HPLC $t_R = 10.2$ min (10–90% in 30 min); HRMS (ESI) m/z calcd for $\text{C}_{22}\text{H}_{31}\text{N}_3\text{O}_7\text{P}^{32}\text{S}$ 512.1615 [M + H] $^+$, found 512.1616.

Methyl-1-(phenylsulfonamido)-2-[4-[2-(piperidin-4-yl)ethoxy]benzamido]ethylphosphonate (3). A mixture of TFA, TIPS, and water [5 mL, 95:2.5:2.5 (v/v/v) TFA/TIPS/ H_2O] was added to 18 (16.7 mg, 0.025 mmol) and the mixture stirred at RT for 16 h. Purification by semipreparative RP-HPLC and lyophilization gave 3 (10.4 mg, 0.020 mmol, 78%) as a white solid: ^1H NMR (500 MHz, MeOH- d_3 , RT) δ 8.60–8.40 (m, 1 H), 8.18 (t, $^3J = 5.2$ Hz, 1 H), 7.88 (d, $^3J = 8.0$ Hz, 2 H), 7.74 (d, $^3J = 9.0$ Hz, 2 H), 7.49 (t, $^3J = 7.2$ Hz, 1 H), 7.44 (t, $^3J = 7.5$ Hz, 2 H), 7.18–7.11 (m, 1 H), 6.95 (d, $^3J = 9.0$ Hz, 2 H), 4.11 (t, $^3J = 6.2$ Hz, 2 H), 3.73 (ddd, $^3J = 16.8$ Hz, $^3J = 13.3$ Hz, $^3J = 8.1$ Hz, 1 H), 3.65 (ddd, $^2J = 19.2$ Hz, $^3J = 9.8$ Hz, $^3J = 4.9$ Hz, 1 H), 3.53–3.49 (m, 1 H), 3.42–3.35 (m, 2 H), 3.35 (d, $^3J = 10.5$ Hz, 3 H), 3.06–2.32 (m, 2 H), 2.06–1.97 (m, 2 H), 1.97–1.86 (m, 1 H), 1.80 (dt, $^3J = 6.5$ Hz, $^3J = 6.3$ Hz, 2 H), 1.52–1.39 (m, 2 H); ^{13}C NMR (126 MHz, MeOH- d_3 , RT) δ 169.7, 163.1, 142.9, 133.5, 130.3, 130.1, 128.1, 127.7, 115.2, 66.5, 52.7 (d, $^2J = 6.3$ Hz), 50.9 (d, $^1J = 147.1$ Hz), 45.5, 42.4 (d, $^2J = 6.1$ Hz), 36.2, 32.4, 30.1; ^{31}P NMR (101 MHz, $\text{D}_2\text{O}/\text{H}_2\text{O}$, RT) δ 17.6 (pH 6.91); MS (ESI) m/z 494.2 [M – OMe] $^+$, 526.2 [M + H] $^+$, 548.2 [M + Na] $^+$, 1051.1 [2M + H] $^+$, 1073.1 [2M + Na] $^+$, 1576.0 [3M + H] $^+$; RP-HPLC $t_R = 10.8$ min (10–90% in 30 min); HRMS (ESI) m/z calcd for $\text{C}_{23}\text{H}_{33}\text{N}_3\text{O}_7\text{P}^{32}\text{S}$ 526.1777 [M + H] $^+$, found 526.1769.

1-(Phenylsulfonamido)-2-[4-[2-(piperidin-4-yl)ethoxy]benzamido]ethylthiophosphonic Acid (4). *N,O*-Bis-(trimethylsilyl)acetamide (BSA, 18.6 μL , 0.076 mmol) was added to a mixture of 1 (9.60 mg, 0.019 mmol) and sulfur powder (1.86 mg, 0.058 mmol) in DCM (dry, 5 mL) at 0 $^\circ\text{C}$ under an argon atmosphere.³⁴ The mixture was allowed to warm to RT and stirred for 1 h. Concentration in vacuo and purification by semipreparative RP-HPLC gave 4 (7.34 mg, 0.014 mmol, 72%) as a white solid: ^1H NMR (500 MHz, MeOD- d_4 , RT) δ 7.87 (d, $^3J = 7.8$ Hz, 2 H), 7.75 (d, $^3J = 8.6$ Hz, 2 H), 7.46 (dd, $^3J = 8.9$ Hz, $^3J = 15.9$ Hz, 1 H), 7.42 (t, $^3J = 7.4$ Hz, 2 H), 6.96 (d, $^3J = 8.6$ Hz, 2 H), 4.13 (t, $^3J = 6.0$ Hz, 2 H), 3.80 (dt, $^3J = 11.4$ Hz, $^3J = 4.5$ Hz, 2 H), 3.65–3.56 (m, 1 H), 3.42–3.36 (m, 2 H), 3.04–2.95 (m, 2 H), 2.07–1.99 (m, 2 H), 1.98–1.87 (m, 1 H), 1.85–1.79 (m, 1 H), 1.53–1.42 (m, 2 H); ^{13}C NMR (126 MHz, MeOD- d_4 , RT) δ 169.7, 163.1, 142.6, 133.4, 130.3, 129.9, 128.2, 127.7, 115.1, 66.5, 56.8 (d, $^1J = 114.7$ Hz), 45.3, 42.3 (d, $^2J = 11.3$ Hz), 36.2, 32.3, 30.0; ^{31}P NMR (101 MHz, $\text{D}_2\text{O}/\text{H}_2\text{O}$, RT) δ 51.8 (pH 6.73); MS (ESI) m/z 494.2 [M – 2OH] $^+$, 510.2 [M – OH] $^+$, 528.1 [M + H] $^+$, 550.2 [M + Na] $^+$, 1055.0 [2M + H] $^+$; RP-HPLC $t_R = 19.1$ min (10–50% in 30 min); HRMS (ESI) m/z calcd for $\text{C}_{22}\text{H}_{31}\text{N}_3\text{O}_6\text{P}^{32}\text{S}_2$ 528.1392 [M + H] $^+$, found 528.1374.

(9H-Fluoren-9-yl)methyl (2-Hydroxyethyl)carbamate (7). 9-Fluorenylmethoxycarbonyl chloride (Fmoc-Cl, 1.55 g, 6.00 mmol) was added to a solution of 2-aminoethanol (0.330 g, 5.40 mmol) in 10% aqueous Na_2CO_3 (50 mL) and the mixture stirred for 2 h at RT. The reaction mixture was extracted with ethyl acetate (3 \times 50 mL). The organic phases were combined, washed with aqueous HCl (1 M, 2 \times 50 mL) and brine (1 \times 50 mL), and dried over MgSO_4 . Concentration in vacuo and purification by column chromatography (silica gel, 5:1 ethyl acetate/hexane) gave 7 as a white solid (1.48 g, 5.22 mmol, 97%): TLC $R_f = 0.5$ (5:1 ethyl acetate/hexane) (UV). ^1H NMR and ^{13}C NMR spectra were identical to those previously reported.⁴⁵

(9H-Fluoren-9-yl)methyl (2-Oxoethyl)carbamate (8). IBX (7.78 g, 27.8 mmol) was added to a solution of 7 (6.06 g, 21.4 mmol) in DMSO (20 mL) and the mixture stirred at RT for 16 h.¹⁷ DCM (1 L) was added to the reaction mixture, and the resulting white

suspension was stirred for 0.5 h, prior to filtration through Celite. The organic layer was washed with aqueous saturated Na_2CO_3 (3 \times 300 mL) and brine (2 \times 300 mL). Each extraction was followed by filtration through Celite, if necessary. Drying over MgSO_4 and concentration in vacuo resulted in a yellow crude product, which was purified by column chromatography (silica gel, 5:1 ethyl acetate/hexane) to give **8** (4.81 g, 17.1 mmol, 80%) as a white solid: TLC R_f = 0.8 (5:1 ethyl acetate/hexane) (UV). ^1H NMR and ^{13}C NMR spectra were identical to those previously reported.⁴⁵

(9H-Fluoren-9-yl)methyl [2-(Hydroxyimino)ethyl]carbamate (9). DIEA (15.3 mL, 89.7 mmol) was added to a mixture of **8** (4.21 g, 15.0 mmol) and hydroxylammonium chloride (3.12 g, 44.9 mmol) in DCM (dry, 40 mL) and the mixture stirred at RT for 16 h.¹⁸ Concentration in vacuo and purification by column chromatography (silica gel, 3:1 ethyl acetate/hexane) gave **9** (2.45 g, 8.27 mmol, 55%) as a slightly yellow colored solid.

2-[N-[(9H-Fluoren-9-yl)methoxy]carbonylamino]-1-aminoethylphosphonic Acid (10). Commercial 60 wt % aqueous phosphonic acid (40.0 g, 364 mmol) was lyophilized to obtain anhydrous crystalline H_3PO_3 , which was subsequently added to a solution of **9** (2.10 g, 7.09 mmol) in methanol (dry, 100 mL). The reaction mixture was heated to reflux for 4 h and then concentrated in vacuo.^{18,19} The residue was dissolved in aqueous HCl (3 M, 200 mL) and washed with diethyl ether (3 \times 100 mL). The pH was adjusted to 1.5 by addition of solid Na_2CO_3 . The resulting precipitate was isolated and purified by RP-HPLC to give **10** (1.25 g, 3.61 mmol, 51%) as a colorless solid.

2-[N-[(9H-Fluoren-9-yl)methoxy]carbonylamino]-1-(phenylsulfonamido)ethylphosphonic Acid (11). Benzenesulfonyl chloride (0.507 mL, 3.97 mmol) was added to a solution of **10** (0.310 g, 0.895 mmol) in dioxane and aqueous Na_2CO_3 [50 mL, 1:1 dioxane/aqueous Na_2CO_3 (10 wt %)] and stirred at RT for 3 h. The solvent was removed in vacuo and the residue dissolved in water (100 mL). The aqueous phase was acidified (pH 1) by addition of aqueous HCl (3 M) and extracted with ethyl acetate (3 \times 50 mL). The combined organic phases were washed with brine (3 \times 50 mL) and dried over Na_2SO_4 . Concentration in vacuo and lyophilization from dioxane gave **11** (0.382 g, 0.785 mmol, 88%) as a white solid.

2-Amino-1-(phenylsulfonamido)ethylphosphonic Acid (12). A solution of piperidine (20%) in DMF (v/v, 50 mL) was added to **11** (0.672 g, 1.38 mmol) and the mixture stirred at RT for 2 h. Concentration in vacuo and purification by RP-HPLC and lyophilization gave **12** (0.253 g, 0.96 mmol, 69%) as a white solid.

2-[N-(Benzyloxycarbonyl)piperidin-4-yl]ethanol (13). Benzyl chloroformate (Cbz-Cl, 6.05 mL, 42.38 mmol) was added to a solution of 2-(piperidin-4-yl)ethanol (5.00 g, 38.7 mmol) in a dioxane/aqueous 10% Na_2CO_3 mixture (1:1, 250 mL) and the mixture stirred at RT for 1 h. The reaction mixture was concentrated in vacuo and the residue dissolved with ethyl acetate (100 mL). The organic phase was washed with aqueous saturated NaHCO_3 (2 \times 50 mL), aqueous HCl (1 M, 2 \times 50 mL), and brine (1 \times 50 mL). Drying over MgSO_4 was followed by column chromatography (silica gel, 5:1 ethyl acetate/hexane) to give **13** (7.46 g, 28.2 mmol, 73%) as a colorless liquid.

Methyl 4-[2-N-(Benzyloxycarbonyl)piperidin-4-ylethoxy]benzoate (14). **13** (1.17 g, 4.43 mmol) was added to a solution of methyl 4-hydroxybenzoate (0.62 g, 4.08 mmol) and tributylphosphine (1.31 mL, 5.25 mmol) in THF (dry, 40 mL) at 0 °C under an argon atmosphere. A solution of 1,1-(azodicarbonyl)dipiperidine (ADDP, 1.32 g, 5.23 mmol) in THF (dry, 15 mL) was added within 5 h by the help of a syringe pump, and the reaction mixture was stirred at RT for 16 h.^{20,21} The white precipitate was removed by filtration and destroyed. The filtrate was concentrated in vacuo and the residue dissolved in ethyl acetate (100 mL). The organic phase was washed with saturated aqueous Na_2CO_3 (3 \times 50 mL), dried over MgSO_4 , and concentrated in vacuo. Purification by column chromatography (silica gel, 1:2 ethyl acetate/hexane) and crystallization from methanol gave **14** (1.39 g, 3.50 mmol, 86%) as a white solid.¹⁵

4-[2-N-(Benzyloxycarbonyl)piperidin-4-ylethoxy]benzoic Acid (15). Aqueous NaOH (1 M, 100 mL) was added to a solution of **14** (0.50 g, 1.26 mmol) in ethanol (100 mL) and stirred at RT for 16 h. The reaction mixture was concentrated in vacuo, and the residue

was dissolved in water (100 mL) and acidified (pH 1) with HCl (12 M, 10 mL). A white precipitate formed, which was extracted with ethyl acetate (3 \times 100 mL). The combined organic phases were washed with brine (1 \times 100 mL) and dried over MgSO_4 . Concentration in vacuo and lyophilization from dioxane gave **15** (0.47 g, 1.23 mmol, 97%) as a white solid.¹⁵

2-([4-[2-N-(Benzyloxycarbonyl)piperidin-4-yl]ethoxy]benzamido)-1-(phenylsulfonamido)ethylphosphonic Acid (16). HATU (168 mg, 0.442 mmol), **15** (170 mg, 0.443 mmol), and DIEA (452 μL , 2.66 mmol) were dissolved in DMF (dry, 10 mL), and the mixture was stirred at RT for 15 min. A solution of **12** (117 mg, 0.443 mmol) in DMF (dry, 3 mL) was added and the mixture stirred at RT for 16 h. Concentration in vacuo and purification by RP-HPLC gave **16** (234 mg, 0.372 mmol, 84%) as a white solid.

2-([4-[2-N-(Benzyloxycarbonyl)piperidin-4-yl]ethoxy]benzamido)-1-(phenylsulfonamido)ethylphosphonic Acid (17). *N,O*-Bis(trimethylsilyl)acetamide (BSA, 98 μL , 0.400 mmol) was added to a solution of **16** (10.1 mg, 0.016 mmol) in DCM (5 mL) and the mixture stirred at RT for 1 h under an ambient atmosphere. Concentration in vacuo, purification by semipreparative HPLC, and lyophilization gave **17** (9.68 mg, 0.015 mmol, 93%) as a white solid.

Methyl 2-4-[2-[1-(Benzyloxycarbonyl)piperidin-4-yl]ethoxy]benzamido)-1-(phenylsulfonamido)ethylphosphonate (18). EDC-HCl (25.8 mg, 0.134 mmol) and DMAP (8.3 mg, 0.068 mmol) were added to a solution of **17** (21.7 mg, 0.034 mmol) in methanol (dry, 5 mL), and the mixture was stirred at RT for 2 h. Concentration in vacuo and purification via semipreparative RP-HPLC gave **18** (17.4 mg, 0.026 mmol, 78%) as a white solid.

Integrin Binding Assay (Fibrinogen- $\alpha\text{IIb}\beta 3$ Assay). The inhibiting activity of the integrin antagonists was determined in a solid-phase binding assay using coated extracellular matrix protein fibrinogen and soluble $\alpha\text{IIb}\beta 3$ integrin.²⁶ The assay was based on a previously reported method with some modifications.²⁷ Flat-bottom 96-well ELISA plates (BRAND, Wertheim, Germany) were coated overnight at 4 °C with 100 μL of 10 $\mu\text{g}/\text{mL}$ fibrinogen per well (Calbiochem, Darmstadt, Germany) in carbonate buffer [15 mM Na_2CO_3 and 35 mM NaHCO_3 (pH 9.6)]. Wells were then washed three times with PBST buffer [137 mM NaCl, 2.7 mM KCl, 10 mM Na_2HPO_4 , 2 mM KH_2PO_4 , and 0.01% Tween 20 (pH 7.4)] and blocked for 1 h at room temperature with 150 μL of TSB buffer [20 mM Tris-HCl, 150 mM NaCl, 1 mM CaCl_2 , 1 mM MgCl_2 , 1 mM MnCl_2 (pH 7.5), and 1% BSA] per well. After being washed three times with PBST, equal amounts of controls (tirofiban, Sigma-Aldrich) or test compounds were mixed with 5.0 $\mu\text{g}/\text{mL}$ human integrin $\alpha\text{IIb}\beta 3$ (Enzyme Research Laboratory, Swansea, U.K.), resulting in a final TSB buffer dilution of 0.00013 to 10 μM for the inhibitors and 2.5 $\mu\text{g}/\text{mL}$ for integrin $\alpha\text{IIb}\beta 3$; 100 μL of these solutions was incubated per well for 1 h at room temperature. The plate was washed three times with PBST buffer, and 100 μL of 2.0 $\mu\text{g}/\text{mL}$ primary antibody (mouse anti-human CD41b, BD Biosciences, Heidelberg, Germany) per well was added to the plate. After incubation for 1 h at room temperature, the plate was washed three times with PBST, and 100 μL of 1.0 $\mu\text{g}/\text{mL}$ secondary peroxidase-labeled antibody (anti-mouse IgG-POD, Sigma-Aldrich) per well was added to the plate and the plate incubated for 1 h at room temperature. After the plate had been washed three times with PBST, the plate was developed by addition of 50 μL of SeramunBlau fast (Seramun Diagnostic GmbH, Heidesee, Germany) per well and incubated for 5 min at room temperature. The reaction was stopped with 50 μL of 3 M H_2SO_4 per well, and the absorbance was measured at 450 nm with a plate reader (POLARstar Galaxy, BMG Labtechnologies). Each compound concentration was tested in duplicate, and the resulting inhibition curves were analyzed using OriginPro version 7.5G; the inflection point describes the IC_{50} value. Each plate contained tirofiban as an internal control.

In Vitro Permeability Study (Caco-2 test). *Growth and Maintenance of Cells*. Caco-2 cells were obtained from ATCC (Manassas, VA) and then grown in 75 cm^2 flasks with approximately 0.5×10^6 cells/flask at 37 °C in a 5% CO_2 atmosphere at a relative humidity of 95%. The culture growth medium consisted of Dulbecco's modified Eagle's medium (DMEM) supplemented with 10% heat-

inactivated fetal bovine serum (FBS), 1% nonessential amino acids, 2 mM L-glutamine, 2 mM sodium pyruvate, and a 2 mM penicillin/streptomycin solution.

Preparation of Cells. For transport studies, cells in a passage range of 52–60 were seeded at a density of 25×10^5 cells/cm² on untreated culture inserts of a polycarbonate membrane with 0.4 μ m pores and a surface area of 1.1 cm². The culture inserts containing the Caco-2 monolayer were placed in 24 transwell plates (12 mm, Costar). The culture medium was changed every other day. Transport studies were performed 21–23 days after seeding, when the cells were fully differentiated and the TEER values were stable (300–500 Ω cm²).

Caco-2 Assay. The transport study (apical to basolateral, A to B) was initiated by removal of medium from both sides of the monolayer and replacement with apical buffer (600 μ L) and basolateral buffer (1500 μ L), both warmed to 37 °C. The cells were incubated for 30 min at 37 °C with shaking (100 cycles/min). After the incubation period, the buffers were removed and replaced with 1500 μ L of basolateral buffer at the basolateral side. Test solutions were preheated to 37 °C and added (600 μ L) to the apical side of the monolayer; 50 μ L samples were taken from the apical side immediately at the beginning of the experiment, resulting in an apical volume of 550 μ L during the experiment. For the period of the experiment, cells were kept at 37 °C with shaking. At predetermined times (30, 60, 90, 120, and 150 min), 200 μ L samples were taken from the basolateral side and replaced with the same volume of fresh basolateral buffer to maintain a constant volume. A mass balance was performed for each tested compound to detect instability and/or nonspecific binding of the peptides. For the basolateral to apical study (B to A), compounds were placed in the basolateral chamber, followed by sampling of the apical side, in the same manner used for the A to B protocol.

Blood Samples. Venous blood was collected from a healthy volunteer who had refrained from taking any medication affecting platelet function for the two preceding weeks. Blood was drawn by peripheral venipuncture into 4.5 mL plastic tubes containing recombinant hirudin as an anticoagulant (specified final concentration of 25 μ g/mL of blood). Measurements were performed 0.5–4 h after venipuncture.

Platelet Aggregation Assay. Platelet aggregation in hirudin-anticoagulated whole blood with thrombin receptor-activating peptide (TRAP-6, final concentration of 33 μ M) as an activator was measured using an impedance-based multiple-electrode platelet aggregometer (Multiplate, Dynabyte Informationssysteme GmbH, Munich, Germany)^{28,29} according to the manufacturer's instructions, i.e., at 37 °C, minicuvettes with 175 μ L of blood, 175 μ L of isotonic saline, and 12 μ L of TRAP-6 reagent (1 mM). The only modification was the use of a serial saline dilution of integrin inhibitors instead of pure saline. The increase in electrical impedance was recorded for 6 min and transformed into arbitrary aggregation units, and the area under the curve (AUC) was calculated. Reported AUC values represent the average from two electrode pairs per cuvette. Inhibition curves were analyzed using OriginPro version 7.5G; the inflection point indicates the half-maximal effective concentration (EC₅₀).

Protonation State Calculations. The estimation of pK_a values of compounds 1–4 was conducted using the calculator plugin Marvin 5.3, 2010, from ChemAxon (<http://www.chemaxon.com>). The estimation is computed through an algorithm that uses the empirically calculated atomic charges for each protonation state of a subset of molecules.⁴⁶ Each atom of the query molecule is identified in one of the atom's subsets, and via the algorithm, the pK_a is finally calculated. The concentration of the different microspecies formed by a molecule at a given pH is predicted using the distribution coefficient (D), calculated using the previously computed pK_a values.⁴⁷

Molecular Electrostatic Potential Calculations. For tirofiban (6) and compounds 1–4, the electrostatic potential was calculated by means of Gaussian03 and mapped onto the electron density surface for each compound. The isovalue of 0.0004 electron/Bhor³ was chosen for the definition of the density surface, while the electrostatic potential was computed at the Hartree–Fock level of theory using the 6-31G* basis set with a scale of –294.178 (red) to 294.178 (blue) K_BT/e_c. The electrostatic potential of the α IIb β 3 receptor was

calculated using the parm99 Amber force field^{48,49} through apbs, which is an adaptive Poisson–Boltzmann solver.⁵⁰

Docking Simulations. Redocking Experiment. The reliability of AutoDock for this system was assessed through the redocking of the α IIb β 3 cocrystallized ligand, tirofiban (PDB entry 2vdm). The X-ray binding conformation of tirofiban has been clearly predicted by AutoDock among the poses with the best scoring function values (Figure 3A). One may notice that for tirofiban the (S)-enantiomer is the bioactive one, while for the phosphorus-containing compounds, because of the change in priority according to the Cahn–Ingold–Prelog rules, the (R)-enantiomers are the bioactive ones. Molecular docking calculations for tirofiban and compounds 1–4 were conducted using the three-dimensional X-ray structure of α IIb β 3 in the apo form (PDB entry 2vdm) through AutoDock (version 4.0).^{36,37} The apo form of α IIb β 3 was obtained via removal of tirofiban from the X-ray complex.

Ligand Setup. The structures of the inhibitors were first generated using the PRODRG server.⁵¹ Then the ligands and the protein were charged using the Gasteiger partial charge⁵² and converted to AutoDock format files using AutoDockTools (ADT 1.5.4).

Docking Setup. The docking area was defined by a box, centered approximately on the center of mass of tirofiban cocrystallized with the protein. Grid points (60 \times 60 \times 60) with 0.375 Å spacing were calculated around the docking area for all the ligand atom types using AutoGrid4. For each ligand, 100 separate docking calculations were performed. Each docking calculation consisted of 2.5×10^6 energy evaluations using the Lamarckian genetic algorithm local search (GALS) method. Otherwise, default docking parameters were applied. The docking conformations were clustered on the basis of the root-mean-square deviation (rmsd of 2 Å) calculated for the Cartesian coordinates of the ligand atoms and then were ranked on the basis of AutoDock scoring function. The binding mode figures were generated using PyMOL (<http://www.pymol.org>), while the molecular electrostatic potential surfaces were rendered using GaussView.

■ ASSOCIATED CONTENT

Supporting Information

Analytical data of compounds 7–18, HPLC enantiomer separation, ³¹P NMR titration of compounds 1–4, docking of molecular probes (R)-3 and (R)-4, docking of (S)-enantiomers, and supporting figures. This material is available free of charge via the Internet at <http://pubs.acs.org>.

■ AUTHOR INFORMATION

Corresponding Author

*Institute for Advanced Study and Center of Integrated Protein Science, Department Chemie, Technische Universität München, Lichtenbergstrasse 4, 85747 Garching, Germany. Phone: +49 (0) 89 289 13300. Fax: +49 (0) 89 289 13210. E-mail: kessler@tum.de.

■ ACKNOWLEDGMENTS

We gratefully acknowledge financial support from the International Graduate School of Science and Engineering (IGSSE) and from the Studienstiftung des deutschen Volkes, Werner Spahl for recording high-resolution mass spectra, Renate Reher for performing the platelet aggregation measurements, and Timo Huber for initial support.

■ ABBREVIATIONS

ADAMs, disintegrin and metalloprotease; AUC, area under the curve; CIP, Cahn–Ingold–Prelog; DMAP, 4-(dimethylamino)pyridine; ECM, extracellular matrix; EDC, N-[3-(dimethylamino)propyl]-N'-ethylcarbodiimide; ELISA, enzyme-linked immunosorbent assay; FMD, foot-and-mouth disease; HATU, O-(7-azabenzotriazol-1-yl)-N,N,N',N'-tetram-

thyluronium hexafluorophosphate; IBX, *o*-iodoxybenzoic acid; MIDAS, metal ion-dependent adhesion site; RGD, arginine-glycine-aspartic acid

REFERENCES

- (1) Meyer, A.; Auernheimer, J.; Modlinger, A.; Kessler, H. Targeting RGD recognizing integrins: Drug development, biomaterial research, tumor imaging and targeting. *Curr. Pharm. Des.* **2006**, *12*, 2723–2747.
- (2) Mousa, S. A. Anti-integrin as novel drug-discovery targets: Potential therapeutic and diagnostic implications. *Curr. Opin. Chem. Biol.* **2002**, *6*, 534–541.
- (3) Humphries, M. J. Integrin structure. *Biochem. Soc. Trans.* **2000**, *28*, 311–339.
- (4) Arnaout, M. A.; Mahalingam, B.; Xiong, J. P. Integrin structure, allostery, and bidirectional signaling. *Annu. Rev. Cell Dev. Biol.* **2005**, *21*, 381–410.
- (5) Hynes, R. O. Integrins: Bidirectional, allosteric signaling machines. *Cell* **2002**, *110*, 673–687.
- (6) Humphries, J. D.; Byron, A.; Humphries, M. J. Integrin ligands at a glance. *J. Cell Sci.* **2006**, *119*, 3901–3903.
- (7) Ruoslahti, E. RGD and other recognition sequences for integrins. *Annu. Rev. Cell Dev. Biol.* **1996**, *12*, 697–715.
- (8) Heckmann, D.; Laufer, B.; Marinelli, L.; Limongelli, V.; Novellino, E.; Zahn, G.; Stragies, R.; Kessler, H. Breaking the dogma of the metal-coordinating carboxylate group in integrin ligands: Introducing hydroxamic acids to the MIDAS to tune potency and selectivity. *Angew. Chem., Int. Ed.* **2009**, *48*, 4436–4440.
- (9) Cox, D.; Brennan, M.; Moran, N. Integrins as therapeutic targets: Lessons and opportunities. *Nat. Rev. Drug Discovery* **2010**, *9*, 804–820.
- (10) Mas-Moruno, C.; Rechenmacher, F.; Kessler, H. Cilengitide: The first anti-angiogenic small molecule drug candidate. Design, synthesis and clinical evaluation. *Anti-Cancer Agents Med. Chem.* **2011**, *10*, 753–768.
- (11) Shimaoka, M.; Springer, T. A. Therapeutic antagonists and conformational regulation of integrin function. *Nat. Rev. Drug Discovery* **2003**, *2*, 703–716.
- (12) Hartman, G. D.; Egbertson, M. S.; Halczenko, W.; Laswell, W. L.; Duggan, M. E.; Smith, R. L.; Naylor, A. M.; Manno, P. D.; Lynch, R. J.; Zhang, G.; Chang, C. T.-C.; Gould, R. J. Non-peptide fibrinogen receptor antagonists. 1. Discovery and design of exosite inhibitors. *J. Med. Chem.* **1992**, *35*, 4640–4642.
- (13) Topol, E. J.; Moliterno, D. J.; Herrmann, H. C.; Powers, E. R.; Grines, C. L.; Cohen, D. J.; Cohen, E. A.; Bertrand, M.; Neumann, F. J.; Stone, G. W.; DiBattiste, P. M.; Demopoulos, L. Comparison of two platelet glycoprotein IIb/IIIa inhibitors, tirofiban and abciximab, for the prevention of ischemic events with percutaneous coronary revascularization. *N. Engl. J. Med.* **2001**, *344*, 1888–1894.
- (14) Cannon, C. P.; Weintraub, W. S.; Demopoulos, L. A.; Vicari, R.; Frey, M. J.; Lakkis, N.; Neumann, F. J.; Robertson, D. H.; DeLucca, P. T.; DiBattiste, P. M.; Gibson, C. M.; Braunwald, E. Comparison of early invasive and conservative strategies in patients with unstable coronary syndromes treated with the glycoprotein IIb/IIIa inhibitor tirofiban. *N. Engl. J. Med.* **2001**, *344*, 1879–1887.
- (15) Duggan, M. E.; Duong, L. T.; Fisher, J. E.; Hamill, T. G.; Hoffman, W. F.; Huff, J. R.; Ihle, N. C.; Leu, C. T.; Nagy, R. M.; Perkins, J. J.; Rodan, S. B.; Wesolowski, G.; Whitman, D. B.; Zartman, A. E.; Rodan, G. A.; Hartman, G. D. Nonpeptide $\alpha\beta_3$ antagonists. 1. Transformation of a potent, integrin-selective $\alpha_{III}\beta_3$ antagonist into a potent $\alpha\beta_3$ antagonist. *J. Med. Chem.* **2000**, *43*, 3736–3745.
- (16) Frigerio, M.; Santagostino, M.; Sputore, S. A user-friendly entry to 2-iodoxybenzoic acid (IBX). *J. Org. Chem.* **1999**, *64*, 4537–4538.
- (17) Frigerio, M.; Santagostino, M. A mild oxidizing reagent for alcohols and 1,2-diols: *o*-Iodoxybenzoic acid (IBX) in DMSO. *Tetrahedron Lett.* **1994**, *35*, 8019–8022.
- (18) Liboska, R.; Picha, J.; Hanclová, L.; Budesinský, M.; Sanda, M.; Jiráček, J. Synthesis of methionine- and norleucine-derived phosphinopeptides. *Tetrahedron Lett.* **2008**, *49*, 5629–5631.
- (19) Zhukov, Y. N.; Khomutov, A. R.; Osipova, T. I.; Khomutov, R. M. Synthesis of phosphinic analogs of sulfur-containing amino acids. *Russ. Chem. Bull.* **1999**, *48*, 1348–1351.
- (20) Heckmann, D.; Meyer, A.; Laufer, B.; Zahn, G.; Stragies, R.; Kessler, H. Rational design of highly active and selective ligands for the $\alpha_5\beta_1$ integrin receptor. *ChemBioChem* **2008**, *9*, 1397–1407.
- (21) Marugán, J. J.; Manthey, C.; Anaclerio, B.; Lafrance, L.; Lu, T.; Markotan, T.; Leonard, K. A.; Crysler, C.; Eisennagel, S.; Dasgupta, M.; Tomczuk, B. Design, synthesis, and biological evaluation of novel potent and selective $\alpha\beta_3/\alpha\beta_5$ integrin dual inhibitors with improved bioavailability. Selection of the molecular core. *J. Med. Chem.* **2005**, *48*, 926–934.
- (22) Hoffmann, C. V.; Pell, R.; Lämmerhofer, M.; Lindner, W. Synergistic effects on enantioselectivity of zwitterionic chiral stationary phases for separations of chiral acids, bases, and amino acids by HPLC. *Anal. Chem.* **2008**, *80*, 8780–8789.
- (23) Hoffmann, C. V.; Reischl, R.; Maier, N. M.; Lämmerhofer, M.; Lindner, W. Stationary phase-related investigations of quinine-based zwitterionic chiral stationary phases operated in anion-, cation-, and zwitterion-exchange modes. *J. Chromatogr., A* **2009**, *1216*, 1147–1156.
- (24) Maier, N. M.; Schefzick, S.; Lombardo, G. M.; Feliz, M.; Rissanen, K.; Lindner, W.; Lipkowitz, K. B. Elucidation of the chiral recognition mechanism of cinchona alkaloid carbamate-type receptors for 3,5-dinitrobenzoyl amino acids. *J. Am. Chem. Soc.* **2002**, *124*, 8611–8629.
- (25) Lämmerhofer, M.; Hebenstreit, D.; Gavioli, E.; Lindner, W.; Mucha, A.; Kafarski, P.; Wiczorek, P. High-performance liquid chromatographic enantiomer separation and determination of absolute configurations of phosphinic acid analogues of dipeptides and their α -aminophosphinic acid precursors. *Tetrahedron: Asymmetry* **2003**, *14*, 2557–2565.
- (26) Mas-Moruno, C.; Beck, J. G.; Doedens, L.; Frank, A. O.; Marinelli, L.; Cosconati, S.; Novellino, E.; Kessler, H. Increasing $\alpha\beta_3$ selectivity of the anti-angiogenic drug cilengitide by *N*-methylation. *Angew. Chem., Int. Ed.* **2011**, *50*, 9496–9500.
- (27) Chatterjee, J.; Ovadia, O.; Zahn, G.; Marinelli, L.; Hoffman, A.; Gilon, C.; Kessler, H. Multiple *N*-methylation by a designed approach enhances receptor selectivity. *J. Med. Chem.* **2007**, *50*, 5878–5881.
- (28) Tóth, O.; Calatzis, A.; Penz, S.; Losonczy, H.; Siess, W. Multiple electrode aggregometry: A new device to measure platelet aggregation in whole blood. *Thromb. Haemostasis* **2006**, *96*, 781–788.
- (29) Halimeh, S.; Angelis, G.; Sander, A.; Edelbusch, C.; Rott, H.; Thedieck, S.; Mesters, R.; Schlegel, N.; Nowak-Gottl, U. Multiplate whole blood impedance point of care aggregometry: Preliminary reference values in healthy infants, children and adolescents. *Klin. Paediatr.* **2010**, *222*, 158–163.
- (30) Artursson, P.; Karlsson, J. Correlation between oral drug absorption in humans and apparent drug permeability coefficients in human intestinal epithelial (Caco-2) cells. *Biochem. Biophys. Res. Commun.* **1991**, *175*, 880–885.
- (31) Kelley, J. L.; McLean, E. W.; Crouch, R. C.; Averett, D. R.; Tuttle, J. V. [[(Guaninylalkyl)phosphinico]methyl]phosphonic acids. Multisubstrate analogue inhibitors of human erythrocyte purine nucleoside phosphorylase. *J. Med. Chem.* **1995**, *38*, 1005–1014.
- (32) Manzenrieder, F.; Frank, A. O.; Kessler, H. Phosphorus NMR spectroscopy as a versatile tool for compound library screening. *Angew. Chem., Int. Ed.* **2008**, *47*, 2608–2611.
- (33) Stirtan, W. G.; Withers, S. G. Phosphonate and α -fluorophosphonate analogue probes of the ionization state of pyridoxal 5'-phosphate (PLP) in glycogen phosphorylase. *Biochemistry (Moscow, Russ. Fed.)* **1996**, *35*, 15057–15064.
- (34) Selvam, C.; Goudet, C.; Oueslati, N.; Pin, J. P.; Acher, F. C. L-(+)-2-Amino-4-thiophosphonobutyric acid (L-thioAP4), a new potent agonist of group III metabotropic glutamate receptors: Increased distal acidity affords enhanced potency. *J. Med. Chem.* **2007**, *50*, 4656–4664.
- (35) Castellino, S.; Leo, G. C.; Sammons, R. D.; Sikorski, J. A. ³¹P, ¹⁵N, and ¹³C NMR of glyphosate: Comparison of pH titrations to the herbicidal dead-end complex with 5-enolpyruvylshikimate-3-phos-

phate synthase. *Biochemistry (Moscow, Russ. Fed.)* **1989**, *28*, 3856–3868.

(36) Morris, G. M.; Goodsell, D. S.; Halliday, R. S.; Huey, R.; Hart, W. E.; Belew, R. K.; Olson, A. J. Automated docking using a Lamarckian genetic algorithm and an empirical binding free energy function. *J. Comput. Chem.* **1998**, *19*, 1639–1662.

(37) Huey, R.; Morris, G. M.; Olson, A. J.; Goodsell, D. S. A semiempirical free energy force field with charge-based desolvation. *J. Comput. Chem.* **2007**, *28*, 1145–1152.

(38) Jones, G.; Willett, P.; Glen, R. C.; Leach, A. R.; Taylor, R. Development and validation of a genetic algorithm for flexible docking. *J. Mol. Biol.* **1997**, *267*, 727–748.

(39) Rarey, M.; Kramer, B.; Lengauer, T.; Klebe, G. A fast flexible docking method using an incremental construction algorithm. *J. Mol. Biol.* **1996**, *261*, 470–489.

(40) Gohlke, H.; Hendlich, M.; Klebe, G. Knowledge-based scoring function to predict protein-ligand interactions. *J. Mol. Biol.* **2000**, *295*, 337–356.

(41) Oelschlaeger, P.; Klahn, M.; Beard, W. A.; Wilson, S. H.; Warshel, A. Magnesium-cationic dummy atom molecules enhance representation of DNA polymerase β in molecular dynamics simulations: Improved accuracy in studies of structural features and mutational effects. *J. Mol. Biol.* **2007**, *366*, 687–701.

(42) Rucker, R.; Oelschlaeger, P.; Warshel, A. A binding free energy decomposition approach for accurate calculations of the fidelity of DNA polymerases. *Proteins* **2010**, *78*, 671–680.

(43) Xiang, Y.; Oelschlaeger, P.; Florian, J.; Goodman, M. F.; Warshel, A. Simulating the effect of DNA polymerase mutations on transition-state energetics and fidelity: Evaluating amino acid group contribution and allosteric coupling for ionized residues in human Pol β . *Biochemistry (Moscow, Russ. Fed.)* **2006**, *45*, 7036–7048.

(44) Gottlieb, H. E.; Kotlyar, V.; Nudelman, A. NMR chemical shifts of common laboratory solvents as trace impurities. *J. Org. Chem.* **1997**, *62*, 7512–7515.

(45) Porcheddu, A.; Giacomelli, G.; Piredda, I.; Carta, M.; Nieddu, G. A practical and efficient approach to PNA monomers compatible with Fmoc-mediated solid-phase synthesis protocols. *Eur. J. Org. Chem.* **2008**, *2008*, 5786–5797.

(46) Dixon, S. L.; Jurs, P. C. Estimation of pKa for organic oxyacids using calculated atomic charges. *J. Comput. Chem.* **1993**, *14*, 1460–1467.

(47) Csizmadia, F.; Tsantili-Kakoulidou, A.; Panderi, I.; Darvas, F. Prediction of distribution coefficient from structure. I. Estimation method. *J. Pharm. Sci.* **1997**, *86*, 865–871.

(48) Cornell, W. D.; Cieplak, P.; Bayly, C. I.; Gould, I. R.; Merz, K. M.; Ferguson, D. M.; Spellmeyer, D. C.; Fox, T.; Caldwell, J. W.; Kollman, P. A. A second generation force field for the simulation of proteins, nucleic acids, and organic molecules. *J. Am. Chem. Soc.* **1995**, *117*, 5179–5197.

(49) Wang, J.; Cieplak, P.; Kollman, P. A. How well does a restrained electrostatic potential (RESP) model perform in calculating conformational energies of organic and biological molecules? *J. Comput. Chem.* **2000**, *21*, 1049–1074.

(50) Baker, N. A.; Sept, D.; Joseph, S.; Holst, M. J.; McCammon, J. A. Electrostatics of nanosystems: Application to microtubules and the ribosome. *Proc. Natl. Acad. Sci. U.S.A.* **2001**, *98*, 10037–10041.

(51) Schüttelkopf, A. W.; van Aalten, D. M. F. PRODRG: A tool for high-throughput crystallography of protein-ligand complexes. *Acta Crystallogr.* **2004**, *D60*, 1355–1363.

(52) Gasteiger, J.; Marsili, M. Iterative partial equalization of orbital electronegativity: A rapid access to atomic charges. *Tetrahedron* **1980**, *36*, 3219–3228.

Supporting Information

Tailoring of Integrin Ligands: Probing the Charge Capability of the Metal-Ion-Dependent Adhesion Site

Markus Bollinger,¹ Florian Manzenrieder,¹ Roman Kolb,¹ Alexander Bochen,¹ Stefanie Neubauer,¹ Luciana Marinelli,² Vittorio Limongelli,² Ettore Novellino,² Georg Moessmer,³ Reinhard Pell,⁴ Wolfgang Lindner,⁴ Joseph Fanous,⁵ Amnon Hoffman⁵ and Horst Kessler^{1,6*}

¹ *Institute for Advanced Study and Center of Integrated Protein Science, Department Chemie, Technische Universität München, Lichtenbergstrasse 4, 85747 Garching, Germany.*

² *Dipartimento di Chimica Farmaceutica e Tossicologica, Università di Napoli "Federico II", Via D. Montesano, 49-80131 Napoli, Italy.*

³ *Institut für Klinische Chemie und Pathobiochemie, Klinikum rechts der Isar, Technische Universität München, Ismaninger Strasse 22, 81675 München, Germany.*

⁴ *Institute of Analytical Chemistry, University of Vienna, Währinger Strasse 38, A-1090 Vienna, Austria.*

⁵ *School of Pharmacy, Faculty of Medicine, The Hebrew University of Jerusalem, POB 12065, Jerusalem 91120, Israel.*

⁶ *Chemistry Department, Faculty of Science, King Abdulaziz University, P.O. Box 80203, Jeddah 21589, Saudi Arabia.*

Table of Contents

Analytical data of compounds 7-18	S2
HPLC enantiomer separation	S6
³¹ P NMR titration of compounds 1-4	S7
Docking of molecular probes (<i>R</i>)- 3 and (<i>R</i>)- 4	S8
Docking of (<i>S</i>)-enantiomers	S8
Supporting Figures	S10

Analytical data of compounds 7-18

(9H-Fluoren-9-yl)methyl (2-hydroxyethyl)carbamate (7).

MS (ESI): $m/z = 179.2$ [Fmoc-CO₂]⁺, 284.1 [M+H]⁺, 306.2 [M+Na]⁺; RP-HPLC: $t_R = 20.0$ min (10-90% in 30 min); HRMS (ESI): m/z calcd for C₁₇H₁₇NO₃Na: 306.1106 [M+Na]⁺, found: 306.1101.

(9H-Fluoren-9-yl)methyl (2-oxoethyl)carbamate (8).

MS (ESI): $m/z = 179.2$ [Fmoc-CO₂]⁺, 282.0 [M+H]⁺; RP-HPLC: $t_R = 19.57$ min (10-90% in 30 min); HRMS (ESI): m/z calcd for C₁₇H₁₆NO₃: 282.1230 [M+H]⁺, found: 282.1125.

(9H-Fluoren-9-yl)methyl [2-(hydroxyimino)ethyl]carbamate (9).

TLC: $R_f = 0.7$ (ethyl acetate/hexane = 3:1) [UV]; ¹H NMR (500 MHz, DMSO-d₆, RT): δ (ppm) = 11.06 (s, 1 H, CH ^{α E/Z}), 10.73 (s, 1 H, CH ^{α E/Z}), 7.89 (d, ³J = 7.6 Hz, 2 H), 7.69 (d, ³J = 7.6 Hz, 2 H), 7.42 (t, ³J = 7.6 Hz, 2 H), 7.33 (t, ³J = 6.9 Hz, 2 H), 6.58 (t, ³J = 3.9 Hz, 1 H), 4.35 (d, ³J = 6.8 Hz, 1 H), 4.31 (d, ³J = 6.9 Hz, 1 H), 4.23 (m, 1 H), 3.82 (dd, ³J = 5.6 Hz, ³J = 4.0 Hz, 2 H), 3.71 (t, ³J = 5.6 Hz, 2 H), 3.33 (br. s, 1 H); ¹³C NMR (126 MHz, DMSO-d₆, RT): δ (ppm) = 156.2, 149.2, 146.5, 143.8, 140.7, 127.6, 127.0, 125.1, 120.1, 65.5, 46.7, 36.4; MS (ESI): $m/z = 179.2$ [Fmoc-CO₂]⁺, 297.0 [M+H]⁺; RP-HPLC: $t_R = 21.6$ (9), 19.9 (8, decomposition of 9 with TFA) (10-90% in 30 min).

2-[N-((9H-Fluoren-9-yl)methoxy)carbonylamino]-1-aminoethyl phosphinic acid (10).

¹H NMR (500 MHz, DMSO-d₆, RT): δ (ppm) = 8.09 (br. s, 2 H), 7.89 (d, ³J = 7.4 Hz, 2 H), 7.69 (d, ³J = 7.4 Hz, 2 H), 7.42 (t, ³J = 7.4 Hz, 2 H), 7.33 (t, ³J = 7.4 Hz, 2 H), 7.01 (d, ³J = 520 Hz, 1 H), 4.32 (d, ³J = 6.8 Hz, 2 H), 4.23 (d, ³J = 6.8 Hz, 1 H), 3.43 (m, 1 H), 3.32 (m, 1 H), 3.00 (m, 1 H); ¹³C NMR (126 MHz, DMSO-d₆, RT): δ (ppm) = 156.2, 143.8, 140.7, 127.6, 127.1, 125.1, 120.1, 65.7, 49.7 (d, ¹J_{PC} = 83.2 Hz), 46.6, 38.5; ³¹P NMR (101 MHz, DMSO-d₆, RT): δ (ppm) = 12.2; MS (ESI): $m/z = 179.2$ [Fmoc-CO₂]⁺, 347.0 [M+H]⁺, 369.3 [M+Na]⁺, 693.0 [2M+H]⁺, 715.0 [2M+Na]⁺, 731.1 [2M+K]⁺, 1039.0 [3M+H]⁺, 1061.0 [3M+Na]⁺, 1077.0 [3M+K]⁺; RP-HPLC: $t_R = 15.4$ min (10-90% in 30 min); HRMS (ESI): m/z calcd for C₁₇H₂₀N₂O₄P: 347.1161 [M+H]⁺, found: 347.1155.

2-[N-((9H-Fluoren-9-yl)methoxy)carbonylamino]-1-(phenylsulfonamido)ethyl phosphinic acid (11).

¹H NMR (500 MHz, DMSO-d₆, RT): δ (ppm) = 8.03 (br. d, ³J = 7.5 Hz, 1 H), 7.89 (d, ³J = 7.5 Hz, 2 H), 7.81 (d, ³J = 7.5 Hz, 2 H), 7.66 (d, ³J = 7.4 Hz, 2 H), 7.56 (t, ³J = 7.4 Hz, 1 H), 7.50 (t, ³J = 7.4 Hz, 2 H), 7.42 (t, ³J = 7.5 Hz, 2 H), 7.33 (t, ³J = 7.5 Hz, 2 H), 7.01 (t, ³J = 5.3 Hz, 1 H), 6.78 (d, ¹J = 535 Hz, 1 H), 4.17-4.13 (m, 2 H), 4.12-4.05 (m, 1 H), 3.53-3.42 (m, 1 H), 3.29-3.16 (m, 1 H), 3.07-2.96 (m, 1 H); ¹³C NMR (126 MHz, DMSO-d₆, RT): δ (ppm) = 155.6, 143.7, 141.2, 140.6, 132.2, 128.9, 127.5, 127.0, 126.3, 125.1, 119.9, 65.5, 46.5, 38.6 (C ^{α} n.o.); ³¹P NMR (101 MHz, DMSO-d₆, RT): δ (ppm) = 23.9; MS (ESI): m/z = 179.3 [Fmoc-CO₂]⁺, 487.3 [M+H]⁺, 509.4 [M+Na]⁺, 973.1 [2M+H]⁺, 995.0 [2M+Na]⁺, 1011.1 [2M+K]⁺, 1458.7 [3M+H]⁺, 1480.7 [3M+Na]⁺, 1497.8 [3M+K]⁺, 1945.2 [4M+H]⁺, 1967.5 [4M+Na]⁺, 1983.5 [4M+K]⁺; RP-HPLC: t_R = 20.5 min (10-90% in 30 min); HRMS (ESI): m/z calcd for C₂₃H₂₂N₂O₆P³²S: 485.0936 [M-H]⁻, found: 485.0932.

2-Amino-1-(phenylsulfonamido)ethyl phosphinic acid (12).

¹H NMR (500 MHz, MeOD-d₄, RT): δ (ppm) = 7.95 (d, ³J = 7.4 Hz, 2 H), 7.66 (t, ³J = 7.4 Hz, 1 H), 7.59 (t, ³J = 7.4 Hz, 2 H), 6.46 (d, ¹J_{PH} = 530 Hz, 1 H), 3.75-3.70 (m, 1 H), 3.29-3.23 (m, 1 H), 3.09-3.00 (m, 1 H); ¹³C NMR (90 MHz, MeOD-d₄, RT): δ (ppm) = 141.8, 134.2, 130.5, 128.3, 52.5 (d, ¹J = 90.0 Hz), 40.1 (d, ²J = 4.4 Hz); ³¹P NMR (101 MHz, DMSO-d₆, RT): δ (ppm) = 15.9; MS (ESI): m/z = 265.2 [M+H]⁺, 529.1 [2M+H]⁺, 551.1 [2M+Na]⁺, 792.9 [3M+H]⁺, 814.9 [3M+Na]⁺, 1056.8 [4M+H]⁺; RP-HPLC: t_R = 6.1 min (10-90% in 30 min); HRMS (ESI): m/z calcd for C₈H₁₄N₂O₄P³²S: 265.0412 [M+H]⁺, found: 265.0407.

2-[N-(benzyloxycarbonyl)piperidine-4-yl]ethanol (13).

TLC: R_f = 0.5 (ethyl acetate/hexane = 5:1) [UV]; ¹H NMR (360 MHz, CDCl₃, RT): δ (ppm) = 7.34-7.30 (m, 4 H), 7.30-7.25 (m, 1 H), 5.08 (s, 2 H), 4.22-4.02 (m, 2 H), 3.63 (t, ³J = 6.6 Hz, 2 H), 2.83-2.63 (m, 2 H), 2.54 (br. s, 1 H), 1.72-1.61 (m, 2 H), 1.61-1.53 (m, 1 H), 1.46 (dt, ³J = 6.6 Hz, ³J = 6.6 Hz, 2 H), 1.17-1.02 (m, 2 H); ¹³C NMR (91 MHz, CDCl₃, RT): δ (ppm) = 155.4, 136.9, 128.5, 128.0, 127.9, 67.1, 60.0, 44.3, 39.2, 32.5, 32.1; MS (ESI): m/z = 264.1 [M+H]⁺; RP-HPLC: t_R = 18.8 min (10-

90% in 30 min); HRMS (ESI): m/z calcd for $C_{15}H_{22}NO_3$: 264.1600 $[M+H]^+$, found: 264.1595.

Methyl 4-[2-*N*-(benzyloxycarbonyl)piperidine-4-ylethyl-oxy]benzoate (14).

TLC: R_f = 0.4 (ethyl acetate/hexane = 1:2) [UV]; 1H NMR (360 MHz, $CDCl_3$, RT): δ (ppm) = 7.96 (d, 3J = 8.9 Hz, 2 H), 7.36-7.31 (m, 4 H), 7.31-7.26 (m, 1 H), 6.87 (d, 3J = 8.9 Hz, 2 H), 5.11 (s, 2 H), 4.27-4.08 (m, 2 H), 4.02 (t, 3J = 6.0 Hz, 2 H), 3.85 (s, 3 H), 2.87-2.69 (m, 2 H), 1.78-1.65 (m, 5 H), 1.26-1.09 (m, 2 H); ^{13}C NMR (91 MHz, $CDCl_3$, RT): δ (ppm) = 166.9, 162.8, 155.4, 137.0, 131.7, 128.6, 128.1, 128.0, 122.7, 114.1, 67.1, 65.6, 52.0, 44.2, 35.7, 32.9, 32.1; MS (ESI): m/z = 398.2 $[M+H]^+$, 420.4 $[M+Na]^+$, 615.9 $[(3M+K+H)/2]^{2+}$, 1214.0 $[3M+Na]^+$; RP-HPLC: t_R = 29.2 min (10-90% in 30 min); HRMS (ESI): m/z calcd for $C_{23}H_{27}NO_5Na^{23}$: 420.1787 $[M+Na]^+$, found: 420.1781.

4-[2-*N*-(benzyloxycarbonyl)piperidine-4-ylethyloxy]-benzoic acid (15).

TLC: R_f = 0.5 (ethyl acetate/hexane = 1:1 + 1 % AcOH) [UV]; 1H NMR (500 MHz, $DMSO-d_6$, RT): δ (ppm) = 12.62 (s, 1 H), 7.87 (d, 3J = 8.8 Hz, 2 H), 7.40-7.28 (m, 5 H), 7.00 (d, 3J = 8.8 Hz, 2 H), 5.06 (s, 2 H), 4.07 (t, 3J = 5.9 Hz, 2 H), 4.03-3.95 (m, 2 H), 2.92-2.67 (m, 2 H), 1.76-1.60 (m, 5 H), 1.16-1.01 (m, 2 H); ^{13}C NMR (91 MHz, $DMSO-d_6$, RT): δ (ppm) = 167.0, 162.2, 154.3, 137.1, 131.3, 128.4, 127.8, 127.5, 122.8, 114.2, 66.0, 65.5, 43.6, 34.9, 32.2, 31.4; MS (ESI): m/z = 384.0 $[M+H]^+$, 767.0 $[2M+H]^+$, 789.3 $[2M+Na]^+$, 805.2 $[2M+K]^+$, 1171.8 $[3M+Na]^+$; RP-HPLC: t_R = 24.7 min (10-90% in 30 min); HRMS (ESI): m/z calcd for $C_{22}H_{24}NO_5$: 382.1660 $[M-H]^-$, found: 382.1654.

2-{4-[2-*N*-(benzyloxycarbonyl)piperidine-4-yl]ethoxy}-benzamido}-1-(phenylsulfonamido)ethylphosphinic acid (16).

1H NMR (500 MHz, $MeOD-d_4$, RT): δ (ppm) = 7.80 (d, 3J = 6.9 Hz, 2 H), 7.58 (d, 3J = 8.9 Hz, 2 H), 7.39-7.26 (m, 8 H), 6.98 (d, 3J = 567 Hz, 1 H), 6.92 (d, 3J = 8.9 Hz, 2 H), 5.11 (s, 2 H), 4.19-4.12 (m, 2 H), 4.11 (t, 3J = 6.0 Hz, 2 H), 3.89-3.82 (m, 1 H), 3.62 (ddd, 2J = 14.1 Hz, 3J = 5.2 Hz, 3J = 5.2 Hz, 1 H), 3.51 (ddd, 2J = 14.1 Hz, 3J = 9.6 Hz, 3J = 8.5 Hz, 1 H), 3.02-2.70 (m, 2 H), 1.88-1.68 (m, 5 H), 1.27-1.09 (m, 2 H); ^{13}C NMR (126 MHz, $MeOD-d_4$, RT): δ (ppm) = 170.3, 163.6, 157.1, 142.3, 138.4, 133.8, 130.5, 130.3, 129.7, 129.2, 129.0, 128.0, 126.9, 115.3, 68.4, 67.0, 54.0 (d,

$^1J = 106.5$ Hz), 45.5, 38.6 ($^2J = 7.0$ Hz), 36.8, 34.3, 33.3; ^{31}P NMR (101 MHz, MeOD- d_4 , RT): δ (ppm) = 29.1; MS (ESI): $m/z = 630.1$ $[\text{M}+\text{H}]^+$, 652.2 $[2\text{M}+\text{H}]^+$, 668.2 $[\text{M}+\text{K}]^+$, 1259.1 $[2\text{M}+\text{H}]^+$, 1281.1 $[2\text{M}+\text{Na}]^+$, 1297.2 $[2\text{M}+\text{K}]^+$; RP-HPLC: $t_R = 22.3$ min (10-90% in 30 min); HRMS (ESI): m/z calcd for $\text{C}_{30}\text{H}_{37}\text{N}_3\text{O}_8\text{P}^{32}\text{S}$: 630.2039 $[\text{M}+\text{H}]^+$, found: 630.2034.

2-{4-[2-N-(benzyloxycarbonyl)piperidine-4-yl]ethoxy}-benzamido}-1-(phenyl-sulfonamido)ethylphosphonic acid (17).

^1H NMR (500 MHz, MeOH- d_3 , RT): δ (ppm) = 8.11 (t, $^3J = 5.3$ Hz, 2 H), 7.85 (dd, $^3J = 8.2$ Hz, $^3J = 1.2$ Hz, 2 H), 7.68 (d, $^3J = 9.0$ Hz, 2 H), 7.45-7.23 (m, 8 H), 6.93 (d, $^3J = 9.0$ Hz, 2 H), 5.10 (s, 2 H), 4.18-4.11 (m, 2 H), 4.10 (t, $^3J = 6.1$ Hz, 2 H), 3.88-3.74 (m, 1 H), 3.65 (ddd, $^2J = 9.1$ Hz, $^3J = 4.8$ Hz, $^3J = 4.8$ Hz, 1 H), 3.59-3.48 (m, 1 H), 2.95-2.73 (m, 2 H), 1.87-1.66 (m, 5 H), 1.26-1.09 (m, 2 H); ^{13}C NMR (126 MHz, MeOH- d_3 , RT): δ (ppm) = 169.9, 163.3, 157.0, 142.9, 138.3, 133.4, 130.3, 130.0, 129.6, 129.1, 128.9, 128.0, 127.4, 115.2, 68.3, 66.8, 52.5 (d, $^1J = 151.5$ Hz), 45.3, 42.0 (d, $^2J = 6.7$ Hz), 36.7, 34.2, 33.2; ^{31}P NMR (101 MHz, MeOH- d_3 , RT): δ (ppm) = 17.2; MS (EI): $m/z = 646.1$ $[\text{M}+\text{H}]^+$, 668.2 $[\text{M}+\text{Na}]^+$, 684.2 $[\text{M}+\text{K}]^+$, 1291.0 $[2\text{M}+\text{H}]^+$, 1313.1 $[2\text{M}+\text{Na}]^+$, 1329.1 $[2\text{M}+\text{K}]^+$; RP-HPLC: $t_R = 21.4$ min (10-90% in 30 min); HRMS (ESI): m/z calcd for $\text{C}_{30}\text{H}_{37}\text{N}_3\text{O}_9\text{P}^{32}\text{S}$: 646.1988 $[\text{M}+\text{H}]^+$, found: 646.1986.

Methyl 2-{4-[2-(1-(benzyloxycarbonyl)piperidine-4-yl)-ethoxy]benzamido}-1-(phenylsulfonamido)ethyl-phospho-nate (18).

^1H NMR (500 MHz, MeOD- d_4 , RT): δ (ppm) = 7.83 (d, $^3J = 6.8$ Hz, 2 H), 7.66 (d, $^3J = 8.7$ Hz, 2 H), 7.44-7.25 (m, 8 H), 6.93 (d, $^3J = 8.7$ Hz, 2 H), 5.10 (s, 2 H), 4.19-4.12 (m, 2 H), 4.12-4.08 (m, 2 H), 4.08-4.01 (m, 1 H), 3.63 (d, $^3J = 10.7$ Hz, 4 H), 3.51-3.43 (m, 1 H), 2.97-2.73 (m, 2 H), 1.85-1.69 (m, 5 H), 1.26-1.11 (m, 2 H); ^{13}C NMR (126 MHz, MeOD- d_4 , RT): δ (ppm) = 170.1, 163.4, 157.0, 142.9, 138.2, 133.4, 130.4, 130.0, 129.5, 129.1, 128.8, 127.9, 127.1, 115.1, 68.2, 66.8, 53.5 (d, $^2J = 6.5$ Hz), 51.2 (d, $^1J = 156.1$ Hz), 45.3, 41.3 (d, $^2J = 9.1$ Hz), 36.7, 34.2, 33.1; ^{31}P NMR (101 MHz, MeOD- d_4 , RT): δ (ppm) = 21.2; MS (EI): $m/z = 616.2$ $[\text{M}-\text{CO}_2]^+$, 660.1 $[\text{M}+\text{H}]^+$, 682.2 $[\text{M}+\text{Na}]^+$; RP-HPLC: $t_R = 22.5$ min (10-90% in 30 min); HRMS (ESI): m/z calcd for $\text{C}_{30}\text{H}_{37}\text{N}_3\text{O}_9\text{P}^{32}\text{S}$: 660.2145 $[\text{M}+\text{H}]^+$, found: 660.2141.

HPLC enantiomer separation

Isocratic semi-preparative chromatographic resolution of phosphinic acid **1**, phosphonic acid **2** and phosphonic acid monomethylester **3** was performed on a 1100 Series HPLC system from *Agilent Technologies* (Waldbronn, Germany) equipped with an autosampler, binary pump, degasser for the mobile phase, multiple wavelength detector (MWD) and a 6-column switching valve. Due to partial racemization during synthesis of compounds **5** it was also necessary to purify them. For automated fraction collection a 2/10-switching valve from *Agilent Technologies* was connected to the flow path just behind the UV-detector. UV-detection was accomplished at 254 nm.

The employed stationary phases were taurine-based **CSP2**, **CSP A183** and **CSP A185** (120 Å pore size, particle size 5 µm each, see Figure S1), which were packed in-house into stainless steel columns (150 x 4 mm). For separation of the carboxylic acids **5** CSP A185 was used, whereas for the separation of phosphinic- **1** and phosphonic acid **2** CSP A183 was used. Phosphonic acid monomethylester **3** was separated on taurine based CSP 2.

As mobile phase 5 mM HOAc and 5 mM NH₄Ac in MeOH was used (for separation of phosphonic acid **2** 95 mM HOAc and 5 mM NH₄Ac in MeOH was used). MeOH was of HPLC-grade from *Merck* (Darmstadt, Germany), mobile phase additives acetic acid and ammonium acetate were of analytical grade (*Sigma-Aldrich*, Taufkirchen, Germany). The flow rate was set to 1.0 mL/min, column temperature was not thermostat-controlled and therefore varied between 25°C and 34°C.

Phosphinic acid **1** was dissolved in a acetonitrile/water/2,5% TFA mixture at a concentration of 16 mg/mL. Phosphonic acid **2** was dissolved in a acetonitrile/water/methanol/2,5% TFA mixture at a concentration of 9 mg/mL and phosphonic acid monomethylester **3** was dissolved in a acetonitrile/water/0,5% TFA mixture at a concentration of 18 mg/mL.

In a series of injections, the enantiomers were separated and collected in two fractions, which were concentrated in vacuum. The purity of the collected enantiomers was assessed analytically using the same conditions as for the semi-preparative separation. The following enantiomeric excess was determined:

(<i>R</i>)- 1 : ≥96% ee	(<i>R</i>)- 2 : ≥90% ee	(<i>R</i>)- 3 : ≥97% ee	(<i>S</i>)- 5 : ≥97% ee
(<i>S</i>)- 1 : ≥92% ee	(<i>S</i>)- 2 : ≥85% ee	(<i>S</i>)- 3 : ≥96% ee	(<i>R</i>)- 5 : ≥97% ee

³¹P NMR titration of compounds 1-4

For each data point an individual ³¹P NMR spectra was recorded at 295 K on a 250 MHz *Bruker AV* spectrometer. Compounds **1-4** (each about 2 mg) were dissolved in H₂O (0.5 mL) including 10% D₂O. Adjustment of the pH of the solution was achieved with small volumes aqueous NaOH (1.0 M) and HCl (1.0 M) solutions. The ³¹P NMR chemical shifts of each compound were plotted against the measured pH. To extract and evaluate the individual pKa values the obtained data points were plotted in *Origin 7.5 SR6* (*OriginLab* Corp., Northampton, MA). The appropriate intervals for each pKa transition were selected and plotted in individual graphs. A sigmoidal fit was applied and the inflection point calculated giving the corresponding pKa value. In case of pKa1 of compound **1** an additional data point had to be set (pH = -2.0/ $\delta(^{31}\text{P}) = 25.5932$; $\delta(^{31}\text{P}) = 25.5932$ represents the highest measured value for pH = 1.2), due to unsatisfactory data points in the pH range of 0 to 1.2. The resulted pKa1 for compound **1** represents the lower limit for the real pKa1 and is therefore written as pKa1 > 1.56.

Thereby, the set of molecular probes used in this study gradually shifts from mono anionic (**1**, **2**) to almost dianionic form (**4**) as regards the metal-coordinating group. Conversely, **3** is a probe for the steric influence on the MIDAS binding, due to the single negative charge and a methoxy substituent.

Docking of molecular probes (*R*)-3 and (*R*)-4

In one of the best scored binding conformations calculated by the docking program, compound (*R*)-4 binds to the MIDAS similar to Tirofiban with the sulfur atom pointing inner in the binding site and the two oxygens involved one in the metal coordination and the other in the H-bond interactions with (β 3)-Asn215 and (β 3)-Tyr122. All the other main interactions between the ligand and the receptor are conserved like those involving the phenylsulphonamide moiety in the β 3 region and those of the piperidine ring in the α IIb subunit (see Figure 3).

A binding conformation similar to that of (*R*)-4 was found among the best solutions also in the case of (*R*)-3. In this binding pose the methylphosphonic group coordinates the magnesium with one oxygen while the other H-bonds with (β 3)-Asn215 and (β 3)-Tyr122. The ester group points in the inner part of the binding pocket similar to what was found for the sulfur atom of (*R*)-4. The benzenesulfonamide moiety fills properly the β 3 region with the sulfonamide group H-bonding with the backbone CO of (β 3)-Asn215 (see Figure 3). On the other side, the *para*-hydroxybenzoate scaffold of (*R*)-3 engages π - π interactions with (α IIb)-Tyr190 and the piperidine moiety is able to form in the α IIb domain the strong interactions with (α IIb)-Asp224 and (α IIb)-Ser225.

Similarly to (*R*)-1 and (*R*)-2, also for (*R*)-3 and (*R*)-4 the docking calculations did not provide significant differences in the binding mode to the α IIb β 3 receptor.

Docking of the (*S*)-enantiomers

In order to understand how the different chirality of the carbon bearing phosphinic/phosphonic group influences the inhibitory activity, docking calculations on the corresponding (*S*)-enantiomers of the most potent compounds of the series, (*R*)-1, (*R*)-2 and (*R*)-3, were performed. The results showed that in the (*S*)-configuration all the three compounds are able to coordinate the metal, however some differences in the binding mode are found if compared with the corresponding (*R*)-enantiomers (see Supporting Figure S4).

In particular, while in the α IIb region the piperidine moiety conserves the interactions with (α IIb)-Asp224 and (α IIb)-Ser225, in the β 3 region a loss of the H-bond between the sulfonamide group and (β 3)-Asn215 is observed and the benzenesulfonamide moiety is not located in the α IIb/ β 3 aromatic pocket. Moreover, while in (*S*)-1, one oxygen of the phosphinate group coordinates the metal and the other H-bonds with

(β 3)-Asn215 and (β 3)-Tyr122 as usual, in (*S*)-**2** the (*S*) configuration induces a change in the metal coordination geometry with a consequent loss and weakening of the H-bonds formed with (β 3)-Asn215 and (β 3)-Tyr122, respectively. Differently, in case of (*S*)-**3**, due to the (*S*) configuration and the bulkiness of the methylester group, all the favorable interactions established with the β 3 region by (*R*)-**3** are lost except for the metal-coordination (see Supporting Figure S4D). Thus, the loss of one [(*S*)-**1**] or more interactions [(*S*)-**3**] is the reason behind the lower inhibitory potency of (*S*)-compounds if compared with the (*R*)-enantiomers (see Table 1).

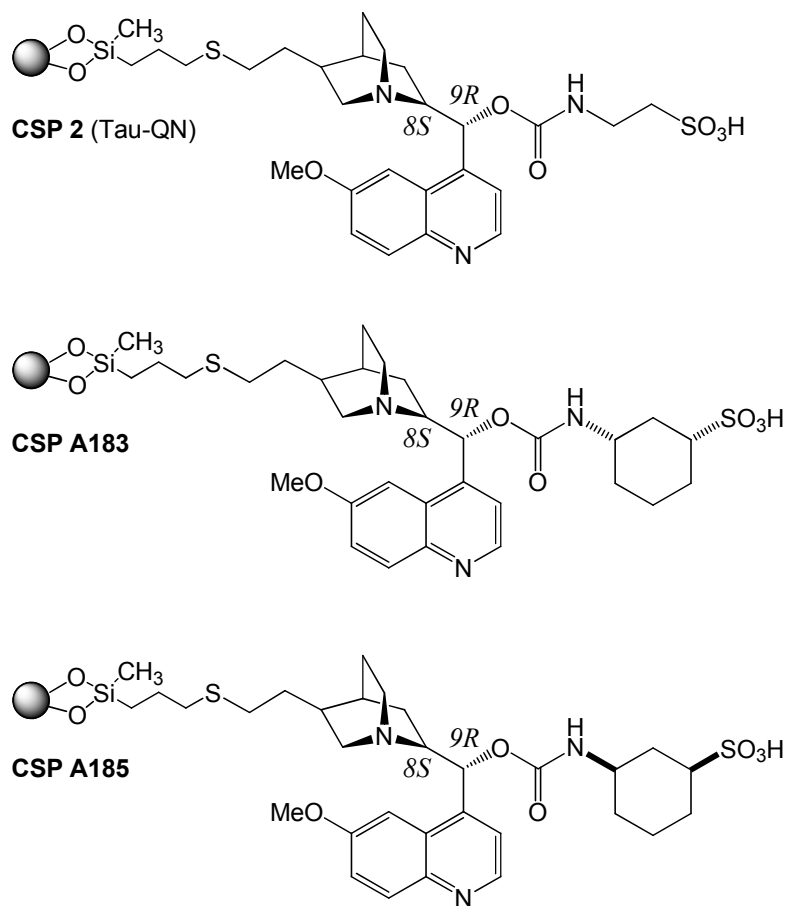


Figure S1. Chemical structures of the quinine based chiral zwitterionic ion-exchange-type stationary phases **CSP 2** (Tau-QN), **CSP A183** and **CSP A185**. Stereoconfiguration at the cyclohexan moiety of **CSP A183** and **CSP A185** has not yet determined.

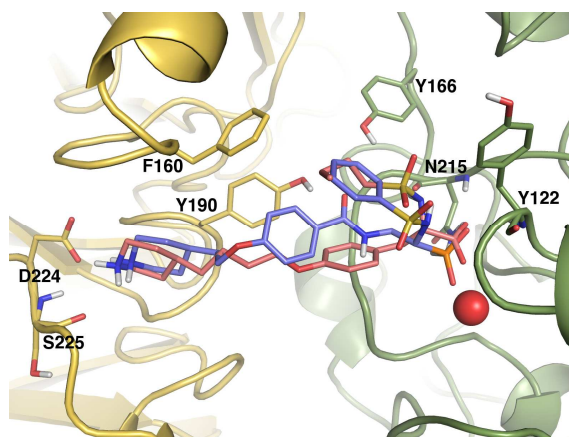
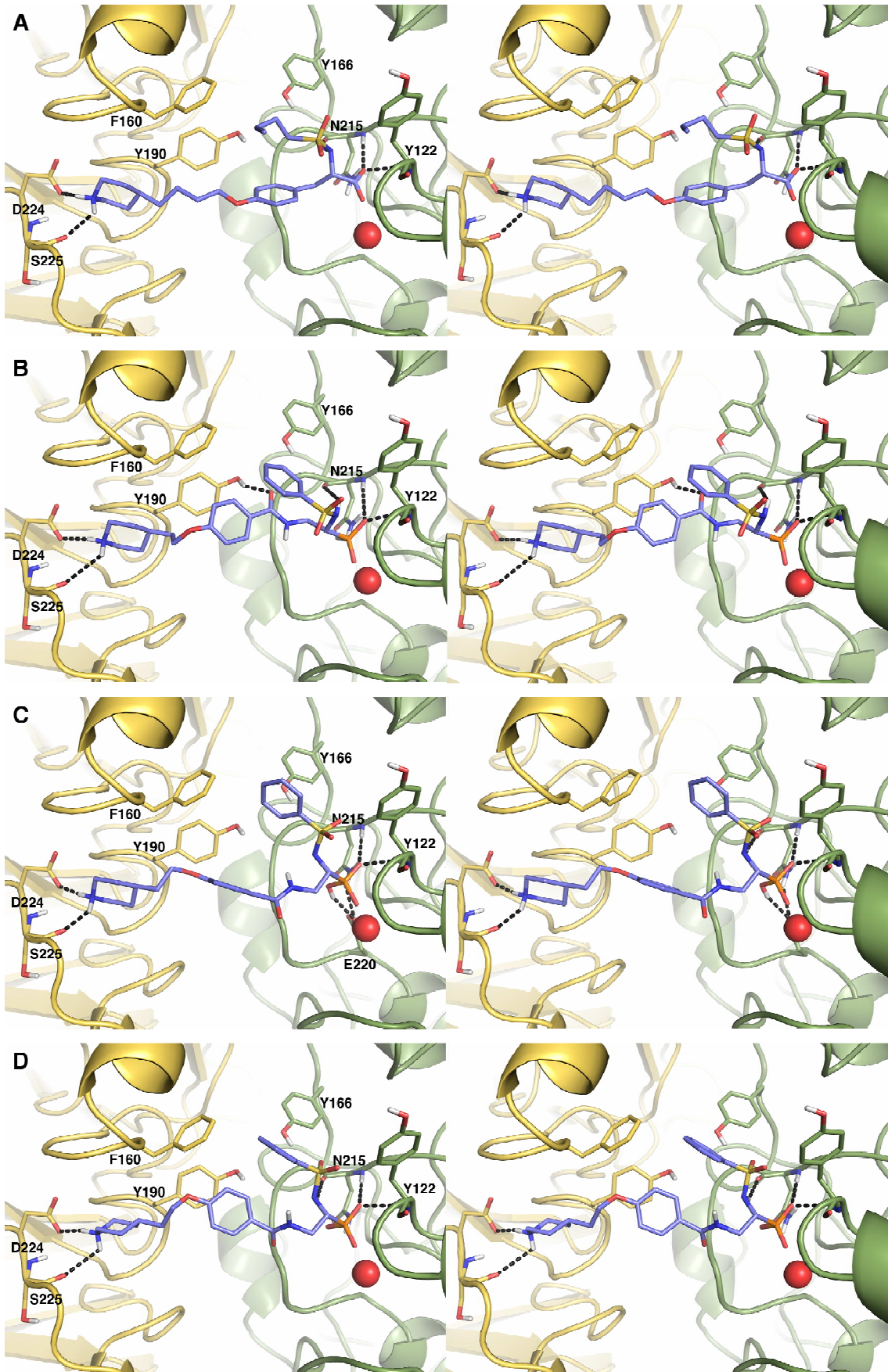


Figure S2. Superimposition of the X-ray binding conformation of Tirofiban (pink) and the binding mode of (*R*)-1 (blue) derived from the docking calculations. The α IIb domain is displayed as yellow cartoon while the β 3 subunit in green. The interacting residues and the ligands are in licorice while the magnesium ion is represented as red sphere. For the sake of clarity only the polar hydrogens are displayed.



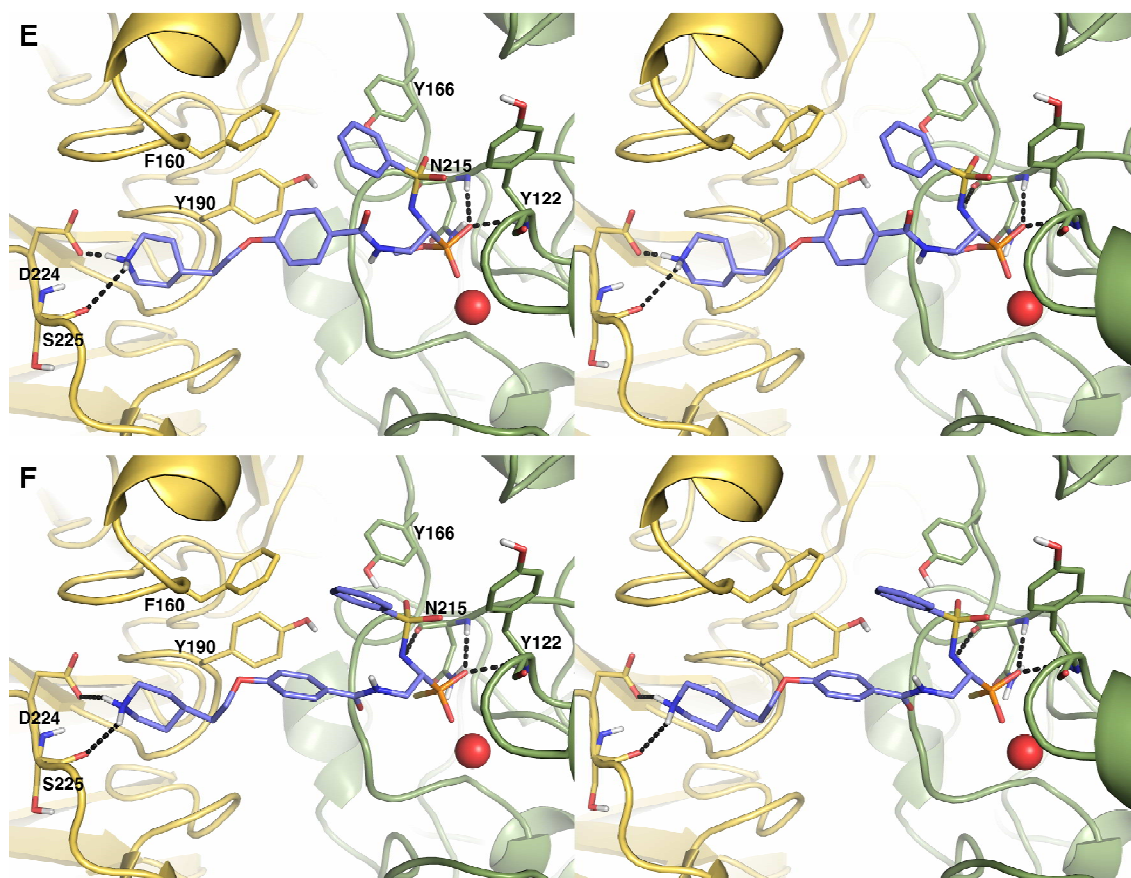
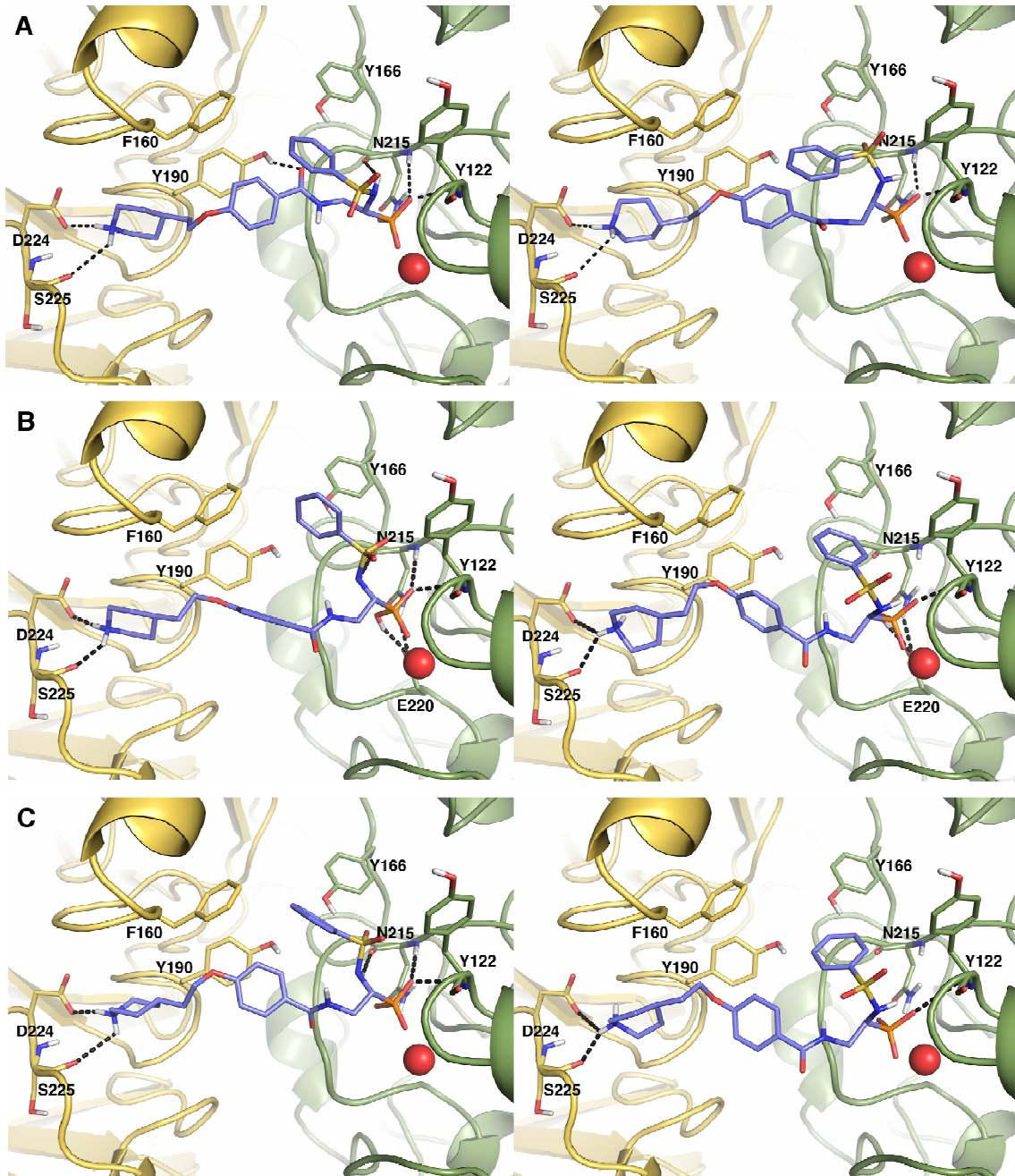


Figure S3. Stereoview of the binding mode of Tirofiban (A), (*R*)-1 (B), (*R*)-2 in the overall neutral form (C) and in the overall anionic form (D), (*R*)-3 (E), and (*R*)-4 (F). The α IIb domain is displayed as yellow cartoon while the β 3 one in green. The magnesium ion is represented as red sphere. For the sake of clarity only the polar hydrogens are displayed.



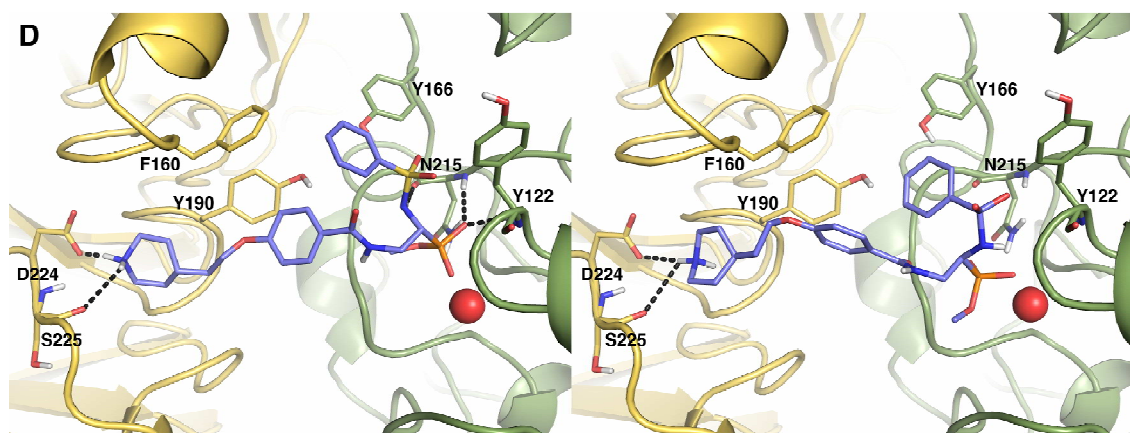


Figure S4. Comparison between the binding mode of the (*R*)-enantiomers (left) and (*S*)-enantiomers (right) of **1** (A), **2** in the overall neutral form (B) and in the overall anionic form (C), and **3** (D). The α IIb domain is displayed as yellow cartoon while the β 3 one in green. The interacting residues and the ligands are in licorice while the magnesium ion is represented as red sphere. For the sake of clarity only the polar hydrogens are displayed.

Abstract

High Performance Liquid Chromatography (HPLC) using chiral stationary phases (CSPs) is of central importance in both industry and academia for either analysis of enantiomeric purity of chiral molecules or (preparative) separation of enantiomers to obtain enantiomerically pure compounds.

The present dissertation describes the preparation of low molecular weight ion exchange-type CSPs and their evaluation using HPLC and Supercritical (or Subcritical) Fluid Chromatography (SFC). The research carried out in the thesis can be divided into two projects.

The first part of the thesis presents a comprehensive evaluation of quinine- and quinidine-based chiral anion exchanger stationary phases (QN-AX- or QD-AX CSPs, respectively) for SFC. Both CSPs proved to be fully applicable in SFC which was manifested in similar enantioseparation properties for chiral acids as compared to HPLC. The retention mechanism was found to be ion exchange dominated and thermodynamic analysis revealed an enthalpically controlled chiral recognition mechanism, thus resembling HPLC behaviour. Additionally, we could chromatographically confirm the *in situ* formation of methylcarbonic acid (and its dissociated species methylcarbonate, respectively) in supercritical CO₂-based methanolic fluids. This phenomenon enables salt free chiral anion exchange chromatography by merely applying super(sub)critical CO₂-methanolic mobile phases, because the *in situ* formed methylcarbonate functions as a counterion and thus enables elution of the acidic analytes. This finding opens up new possibilities for preparative separations of chiral acids, as troublesome mobile phase additives, such as salts or acids, can be avoided.

Furthermore, QN-AX and QD-AX CSPs were applied for enantioseparation of novel chiral sulfonic acids with HPLC and SFC. We could establish a straightforward method for baseline resolving all of the investigated chiral sulfonic acids (or their sulfonate salts, respectively). In another application study, the absolute configuration of structurally related chiral acidic drug compounds was indirectly assigned by means of chiral HPLC using QN-AX and QD-AX CSPs.

The second part of the thesis deals with the synthesis of cinchona alkaloid-based zwitterionic chiral selectors (ZWIX-SOs) and their immobilization onto silica gel to yield the corresponding zwitterionic chiral stationary phases (ZWIX-CSPs). The ZWIX-CSPs provided three modes of ion exchange, namely weak anion exchange mode for separation of chiral acids, strong cation exchange mode for resolving chiral bases (amines) and, most importantly,

zwitterion exchange mode for the separation of amphoteric solutes, such as underivatized amino acids and small peptides.

The synthesis followed a semi-synthetic approach using quinine or quinidine as starting materials, which were then derivatized with structurally different sulfonate group containing moieties (via a carbamate bond at the C9 position of the cinchona alkaloid). A small library of either quinine- or quinidine-based ZWIX-CSPs was prepared to carry out structure - enantioselectivity relationship studies for zwitterionic analytes by means of chromatography.

In short, ZWIX-CSPs with chiral moieties in vicinity to their strong cation exchanger sites exhibited the broadest scope of application for the enantioseparation of amino acids, whereas dipeptides could be well resolved on all ZWIX-CSP independently from the chiral or achiral nature of the strong cation exchange subunit. A special benefit of ZWIX-CSPs is their ability to invert elution orders of amino acid enantiomers, which is easily accomplished by switching from a quinine-based to a pseudoenantiomeric quinidine-based ZWIX-CSP.

Zusammenfassung

Hochleistungsflüssigchromatographie (HPLC) unter Verwendung von chiralen stationären Phasen (CSPs) ist in der Enantiomerenanalytik und in den enantioselektiven Trenntechniken von größter Bedeutung. So wird diese Technik im universitären Bereich und vor allem in der (pharmazeutischen) Industrie massiv eingesetzt, um chirale Verbindungen in enantiomerenreiner Form zu gewinnen.

In der vorliegenden Arbeit wird die Herstellung von CSPs auf Ionenaustauscherbasis beschrieben, welche mittels HPLC und Superkritischer (Subkritischer) Fluid Chromatographie (SFC) auf ihre chiralen Trenneigenschaften hin evaluiert wurden. Im Allgemeinen können die in dieser Dissertation durchgeführten Forschungen auf zwei Bereiche aufgeteilt werden:

Der erste Teil beschreibt eine umfassende Evaluierung von Chinin- und Chinidin-basierten Anionenaustauschern (QN-AX – und QD-AX CSP), welche mittels SFC betrieben wurden. Die chiralen Anionenaustauscher erwiesen sich als vollkommen SFC tauglich, da die Trenneigenschaften im Hinblick auf chirale Säuren vergleichbar waren mit den Ergebnissen aus bereits bekannten HPLC Messungen. Weiters konnte festgestellt werden, dass auch in der SFC ein ionenaustausch-dominiertes Retentionsmechanismus vorliegt und dass die chirale Erkennung enthalpisch kontrolliert ist. Des Weiteren konnte chromatographisch die *in situ* Bildung von Methylnkohensäure (und deren dissoziierte Form, nämlich Methylcarbonat) in super(sub)kritischen CO₂ – Methanol Mischungen festgestellt werden. Dieses chemische Phänomen ermöglicht Anionenaustauschchromatographie ohne Zugabe von (Puffer)Salzen, da die *in situ* gebildete Methylnkohensäure als Gegenion fungiert und somit Elution der sauren Analytmoleküle ermöglicht. Diese Erkenntnisse eröffnen neue Möglichkeiten und Wege für präparative Trennungen von chiralen Säuren, da unerwünschte Salzadditiva in der mobilen Phase vermieden werden können.

Ferner wurden die QN-AX und QD-AX CSPs zur Enantiomerentrennung von neuartigen chiralen Sulfonsäuren (bzw. deren Sulfonatsalzen) mittels HPLC und SFC verwendet. Es konnte eine unkomplizierte Methode erstellt werden, welche die Basislinientrennung aller applizierten Sulfonsäureanalyte ermöglichte. In einer weiteren Applikationsstudie wurden beide vorher genannten Säulen zur indirekten Bestimmung der Absolutkonfiguration einer Reihe von chiralen sauren Wirkstoffen verwendet.

Der zweite Teil der vorliegenden Dissertation beschreibt die Synthese von neuartigen Cinchona-Alkaloid-basierten zwitterionischen chiralen Selektoren (ZWIX-SOs). Durch nachfolgende Immobilisierung der SOs auf Kieselgel wurden zwitterionische chirale

stationäre Phasen (ZWIX-CSPs) erhalten. Diese ZWIX-CSPs ermöglichten alle drei Arten von Ionenaustauschmodi, nämlich den schwachen Anionenaustauschmodus zur Trennung von chiralen Säuren, den starken Kationenaustauschmodus zur Trennung von chiralen Basen (Aminen) und, am wichtigsten, den Zwitterionenaustauschmodus zur Enantiomerentrennung von amphoteren Verbindungen wie freien Aminosäuren und kurzkettigen Peptiden.

Bei der Synthese dieser ZWIX-SOs wurden Chinin oder Chinidin als Edukte verwendet, welche dann mit strukturell unterschiedlichen, sulfonsäuregruppen-enthaltenden Resten derivatisiert wurden (jeweils über eine Carbamatbindung an der C9-Position). Auf diese Art und Weise konnte ein kleines Set an Chinin- oder Chinidin-basierten ZWIX-CSPs hergestellt werden, welche nachfolgend für Studien der Struktur – Enantioselektivitäts-Beziehungen mittels HPLC verwendet wurden.

ZWIX-CSPs mit chiralen Substituenten in Nachbarschaftsstellung zur Sulfonsäuregruppe waren ihren Analoga mit achiralen Seitenketten auf der Kationenaustauscherseite bezüglich Trennleistungen überlegen. Sie zeigten die größte Anwendungsbreite für Aminosäure-Enantiomerentrennungen, wohingegen Dipeptid-Analyte auf allen ZWIX-CSPs ähnlich gut getrennt werden konnten. Eine weitere vorteilhafte Eigenschaft bei Verwendung dieser ZWIX-CSPs war die Möglichkeit zur Umkehr der Elutionsreihenfolge der Aminosäure-Enantiomere, welche durch ein Wechseln von der Chinin-basierten zur pseudoenantiomeren Chinidin-basierten ZWIX-CSP realisiert werden konnte.

Curriculum Vitae

Name: Mag. Franz Reinhard Pell
Adresse: Bogenhofen 12,
4963 St.Peter am Hart
E-Mail: Reinhard.Pell@univie.ac.at
Staatsbürgerschaft: Österreich
Geboren am: 21.06.1983
Familienstand: ledig
Präsenzdienst: abgeleistet

UNIVERSITÄRE AUSBILDUNG:

10/08-06/12 **Universität Wien**
Doktoratsstudium der Chemie am Institut für Analytische Chemie bei
Prof. Dr. Wolfgang Lindner

10/02-10/08 **Universität Wien**
Studium der Chemie
Schwerpunkt im 2. Studienabschnitt: Analytische Chemie
Diplomarbeit mit dem Thema: „Development and Evaluation of
Zwitterionic Chiral Stationary Phases“
Abschluss: 06.10.2008 (Diplomprüfung mit Auszeichnung)
Erlangung des Titels: *Mag. rer. nat.*

SCHULBILDUNG:

09/93-06/01 **Bundesgymnasium Braunau am Inn**
(Matura mit gutem Erfolg)

STUDIENBEGLEITENDE BERUFSTÄTIGKEIT:

07/04-08/04 **Wacker Chemie AG**
07/06-08/06 Arbeit als Werksstudent in der Abteilung für Herstellung und
Bearbeitung von Reinstsilicium

10/08-01/12 **Universität Wien**
Universitätsassistent am Institut für Analytische Chemie:
Praktikumsaufsicht und Studierendenbetreuung

AUSLANDSAUFENTHALTE:

- 01/07-06/07 Erasmus Auslandssemester in Lund, Schweden
Forschungsaufenthalt am Institut für Organische Chemie der
Universität Lund. Thema der Forschungsarbeit:
„Synthesis of Benzodiazepine Analogues“
- 03/11-04/11 Forschungsaufenthalt bei AstraZeneca R&D Mölndal, Schweden

KOMPETENZEN:

- Sprachen:** Englisch verhandlungssicher
 Schwedisch fließend in Wort und Schrift
 Spanisch Grundkenntnisse
 Französisch Grundkenntnisse
- EDV:** gute Computerkenntnisse: Windows, MS Office, CS ChemOffice

AUSZEICHNUNG:

- Diplomarbeitspreis der Gesellschaft Österreichischer Chemiker (GÖCH):
Beste Diplomarbeit Österreichs des Jahres 2009 in Analytischer Chemie

PUBLIKATIONEN:

- R. Pell, S. Sić, W. Lindner. *Mechanistic investigations of cinchona alkaloid-based zwitterionic chiral stationary phases*
Journal of Chromatography A, submitted
- R. Pell, G. Schuster, M. Lämmerhofer, W. Lindner. *Enantioseparation of Chiral Sulfonates by Liquid Chromatography and Subcritical Fluid Chromatography*
Journal of Separation Science, accepted
- R. Pell, W. Lindner. *Potential of Chiral Anion-Exchangers Operated in Various Subcritical Fluid Chromatography Modes for Resolution of Chiral Acids*
Reinhard Pell, Wolfgang Lindner
Journal of Chromatography A, in press
- S. Wernisch, R. Pell, W. Lindner. *Increments to Chiral Recognition Facilitating Enantiomer Separations of Chiral Acids, Bases and Ampholytes Using Cinchona-based Zwitterion Exchanger Chiral Stationary Phases*
Journal of Separation Science, in press

M. Bollinger, F. Manzenrieder, R. Kolb, A. Bochen, S. Neubauer, L. Marinelli, V. Limongelli, E. Novellino, G. Moessmer, R. Pell, W. Lindner, J. Fanous, A. Hoffman, and H. Kessler *Tailoring of Integrin Ligands: Probing the Charge Capability of the Metal Ion Dependent Adhesion Site*

***Journal of Medicinal Chemistry* (2012), 55, 871-882**

M. Lämmerhofer, R. Pell, M. Mahut, M. Richter, S. Schiesel, H. Zettl, M. Dittrich, M. Schubert-Zsilavec, W. Lindner. *Enantiomer separation and indirect chromatographic absolute configuration prediction of chiral pirinixic acid derivatives: Limitations of polysaccharide-type chiral stationary phases in comparison to chiral anion-exchangers*

***Journal of Chromatography A* (2010), 1217, 1033-1040**

C.V. Hoffmann, R. Pell, M. Lämmerhofer, W. Lindner. *Synergistic Effects on Enantioselectivity of Zwitterionic Chiral Stationary Phases for Separations of Chiral Acids, Bases, and Amino Acids by HPLC*

***Analytical Chemistry* (2008), 80, 8780–8789**

WISSENSCHAFTLICHE VORTRÄGE:

“Novel Zwitterionic Chiral Ion Exchangers for HPLC Enantioseparation of free Amino Acids and Peptides”

6. ASAC JunganalytikerInnen Forum, Wien, Juni 2010

POSTERBEITRÄGE:

“Novel Zwitterionic Chiral Ion Exchangers for HPLC - Enantioseparation of free Amino Acids”

Reinhard Pell, Sinisa Sic, Wolfgang Lindner

23rd International Symposium on Chirality (ISCD23), Juli 2011, Liverpool

“Novel Zwitterionic Chiral Ion Exchangers for HPLC Enantioseparation of Amino Acids and Small Peptides”

Reinhard Pell, Stefanie Wernisch, Wolfgang Lindner

35th International Symposium on High Performance Liquid Phase Separations & Related Techniques, Juni 2010, Boston, MA

“Novel Zwitterionic Chiral Ion Exchangers for HPLC-Enantioseparation of Chiral Acids, Amino Acids and Peptides”

Reinhard Pell, Stefanie Wernisch, Dario Bianchi, Wolfgang Lindner

Euroanalysis, September 2009, Innsbruck